Master's thesis

NTNU
Norwegian University of Science and Technology
Faculty of Engineering
Department of Structural Engineering

Anne Øksnes Aal

Development and Validation of a Hemodynamic Model for Varying Exercise Intensity

Master's thesis in Civil and Environmental Engineering
Supervisor: Leif Rune Hellevik
Co-supervisor: Jacob Sturdy and Nikolai L. Bjørdalsbakke
June 2022

NTNU
Kunnskap for en bedre verden

Anne Øksnes Aal

Development and Validation of a Hemodynamic Model for Varying Exercise Intensity

Master's thesis in Civil and Environmental Engineering
Supervisor: Leif Rune Hellevik
Co-supervisor: Jacob Sturdy and Nikolai L. Bjørdalsbakke
June 2022

Norwegian University of Science and Technology
Faculty of Engineering
Department of Structural Engineering

NTNU
Norwegian University of
Science and Technology

Department of Structural Engineering
Faculty of Engineering
NTNU- Norwegian University of Science and Technology

ACCESSIBILITY

Open

MASTER THESIS 2022

SUBJECT AREA:	DATE:	NO. OF PAGES:
Biomechanics	11.06.2022	13+126+46 Appendix

TITLE:

Development and Validation of a Hemodynamic Model for Varying Exercise Intensity

Utvikling og Validering av en Hemodynamisk Modell for Varierende Treningsintensitet

BY:

Anne Øksnes Aal

SUMMARY:
A lumped parameter model representing the systemic circuit of the cardiovascular system and its acute response to exercise is under development as a part of the NTNU project “My Medical Digital Twin” (MyMDT). MyMDT aims to create a digital clinical tool to radically improve the currently uncertain and inefficient procedures of treating hypertension. The MyMDT hemodynamic model integrates a time-varying elastance representing cardiac function into a closed-loop circulation consisting of an arterial and a venous compartment. Personalized model baseline parameters are estimated by a numerical optimization procedure that bases on arterial data for blood pressure and flow during rest. Exercise state is implemented as heart rate-based parameter shifts. This master’s thesis performs an extensive evaluation of the current MyMDT model against cardiovascular data collected in a clinical exercise trial. Six participants are used to examine multiple configurations of the procedures for estimating baseline parameters and simulating exercise state to obtain predictions of stroke volume, systolic and diastolic blood pressures that are consistent with data, without increasing the model complexity. It is found that accurate simulations of the arterial system during rest are obtainable through multiple baseline configurations. Exercise state is in general prone to more uncertainty regarding both data and modelling principles. Predictions of stroke volume, systolic and diastolic blood pressures that simultaneously fulfill clinical criteria of accuracy are not achieved. Together with a brief model validation performed on five new participants, the results indicate a necessity of greater structural interventions beyond adjusting the current procedures for parameter estimation and exercise simulation. Preliminary pilot experiments highlight several issues related to physiologically implausible model representations of the ventricular and venous system. More research, preferably including quality assured data for all trial participants, is indispensable for the model to reach its clinical ambition.

RESPONSIBLE TEACHER:
Leif Rune Hellevik, NTNU

SUPERVISORS:
Leif Rune Hellevik, NTNU
Jacob Sturdy, NTNU
Nikolai Lid Bjørdalsbakke, NTNU

CARRIED OUT AT:
Department of Structural Engineering, NTNU

Preface

This report is a master's thesis in the course TKT4950 - Structural Engineering, Master's Thesis, conducted as a completion of the study program Civil and Environmental Engineering at the Norwegian University of Science and Technology (NTNU). The work was carried out at the Department of Structural Engineering, Faculty of Engineering. Prior to the autumn semester in 2021, i.e. the 9^{th} semester of my master's program, I chose Biomechanics as specialization within the preselected field of Structural Engineering. At NTNU, the Division of Biomechanics is participating in the interdisciplinary research project "My Medical Digital Twin" (MyMDT). A collaboration with the MyMDT project motivated the choice of hemodynamic modelling as topic for this master's thesis.

Trondheim, 11-06-2022

Anne Øksnes Aal

Acknowledgements

I would like to thank my supervisors Prof. Leif Rune Hellevik, Ph.D., and Jacob T. Sturdy, Ph.D., for providing me the opportunity to write my master's thesis within their subject area, which is essentially quite distant to my study program in Civil and Environmental Engineering. I wanted to use the master's project to immerse myself in new areas of engineering, while also participating and contributing in actual, meaningful and innovative research. My supervisors have facilitated my ambitions by letting me be a part of the Biomechanics group and their work within the MyMDT research project, for which I am very grateful.

Further, I want to express my gratitude towards Ph.D. Candidate Nikolai L. Bjørdalsbakke for letting me assist in his research. The continuous support from both Nikolai and Jacob has been invaluable for my progress in this project.

A final thank you to Hilke Straatman at Eindhoven University of Technology for valuable discussions and clarifications on concepts that only a year ago were unknown to me.

Anne Øksnes Aal

Abstract

A lumped parameter model representing the systemic circuit of the cardiovascular system and its acute response to exercise is under development as a part of the NTNU project “My Medical Digital Twin” (MyMDT). MyMDT aims to create a digital clinical tool to radically improve the currently uncertain and inefficient procedures of treating hypertension. The MyMDT hemodynamic model integrates a time-varying elastance representing cardiac function into a closed-loop circulation consisting of an arterial and a venous compartment. Personalized model baseline parameters are estimated by a numerical optimization procedure that bases on arterial data for blood pressure and flow during rest. Exercise state is implemented as heart rate-based parameter shifts. This master’s thesis performs an extensive evaluation of the current MyMDT model against cardiovascular data collected in a clinical exercise trial. Six participants are used to examine multiple configurations of the procedures for estimating baseline parameters and simulating exercise state to obtain predictions of stroke volume, systolic and diastolic blood pressures that are consistent with data, without increasing the model complexity. It is found that accurate simulations of the arterial system during rest are obtainable through multiple baseline configurations. Exercise state is in general prone to more uncertainty regarding both data and modelling principles. Predictions of stroke volume, systolic and diastolic blood pressures that simultaneously fulfill clinical criteria of accuracy are not achieved. Together with a brief model validation performed on five new participants, the results indicate a necessity of greater structural interventions beyond adjusting the current procedures for parameter estimation and exercise simulation. Preliminary pilot experiments highlight several issues related to physiologically implausible model representations of the ventricular and venous system. More research, preferably including quality assured data for all trial participants, is indispensable for the model to reach its clinical ambition.

Sammendrag

En diskret parametermodell som representerer den systemiske kretsen av det kardiovaskulære systemet og dens umiddelbare respons til trening er under utvikling som en del av NTNU prosjektet «My Medical Digital Twin» (MyMDT). MyMDT vil skape et digitalt klinisk verktøy for å radikalt forbedre det som for tiden er usikre og ineffektive prosedyrer innen blodtrykksbehandling. MyMDT sin hemodynamiske modell integrerer en tidsvarierende elastans som representerer hjertefunksjon i et lukket kretsløp som består av et arterielt og et venøst segment. Modellens personaliserte inngangsparametere blir estimert ved hjelp av en numerisk optimaliseringsprosedyre basert på arteriell data for blodtrykk og strømning i hviletilstand. Treningstilstand implementeres som pulsavhengige parameterforskyvninger. Denne masteravhandlingen gjennomfører en omfattende evaluering av den nåværende MyMDT-modellen mot kardiovaskulær data hentet fra en klinisk treningsstudie. Seks deltakere blir brukt for å undersøke flere mulige oppsett av prosedyrene for parameterestimering og treningssimulering for å oppnå prediksjoner av slagvolum, systolisk og diastolisk blodtrykk under trening som er i overenstemmelse med data, uten å øke modellens kompleksitet. Det avdekkes at det gjennom flere inngangsparametere er mulig å oppnå korrekte simuleringer av det arterielle systemet i hviletilstand. Treningstilstand er generelt utsatt for større usikkerhet i både data og modelleringsprinsipper. Prediksjoner av slagvolum, systolisk og diastolisk blodtrykk som samtidig oppfyller kliniske nøyaktighetskriterier oppnås ikke. Sammen med en kort modellvalidering utført på fem nye deltakere, indikerer resultatene at det er nødvendig med større strukturelle tiltak utover å tilpasse prosedyrene for parameterestimering og treningssimulering. Innledende pilotеksperimenter belyser flere problemer relatert til fysiologisk lite troverdige modellrepresentasjoner av ventrikkel- og venesystemet. Ytterligere forskning, fortrinnsvis inkludert kvalitetssikret data for alle studiedeltakerne, er uunnværlig for at modellen skal oppnå sin kliniske målsetning.

Contents

List of Tables

List of Figures

List of Abbreviations

Abbreviation	Explanation
BP	**B**lood **P**ressure
CAP	**C**entral **A**ortic **P**ressure
CO	**C**ardiac **O**utput
CVP	**C**entral **V**enous **P**ressure
CVS	**C**ardio**v**ascular **S**ystem
DP	**D**iastolic **P**ressure
ECG	**E**lectro**c**ardio**g**ram
ED	**E**nd-**D**iastole
EDPVR	**E**nd-**D**iastolic **P**ressure **V**olume **R**elationship
EDV	**E**nd-**D**iastolic **V**olume
EF	**E**jection **F**raction
ES	**E**nd-**S**ystole
ESPVR	**E**nd-**S**ystolic **P**ressure **V**olume **R**elationship
ESV	**E**nd-**S**ystolic **V**olume
HR	**H**eart **R**ate
HRR	**H**eart **R**ate **R**eserve
LVET	**L**eft **V**entricular **E**jection **T**ime
LVOT	**L**eft **V**entricular **O**utflow **T**ract
MAE	**M**ean **A**bsolute **E**rror
MAP	**M**ean **A**rterial **P**ressure
MVP	**M**ean **V**enous **P**ressure
MyMDT	**My** **M**edical **D**igital **T**win
NTNU	**N**orges **T**eknisk- **N**aturvitenskapelige **U**niversitet (Norwegian: Norwegian University of Science and Technology)
ODE	**O**rdinary **D**ifferential **E**quation
PCG	**P**hono**c**ardio**g**ram
PP	**P**ulse **P**ressure
SA	**S**ensitivity **A**nalysis
SP	**S**ystolic **P**ressure
SV	**S**troke **V**olume
VR	**V**enous **R**eturn

Chapter 1

Introduction

Chronically elevated blood pressure is a serious medical condition referred to as *hypertension*, and it constitutes a major public-health problem. World Health Organization (WHO) estimates 1.13 billion people worldwide to be hypertensive [1]. Hypertension is not a disease itself, but a significant contributor to multiple leading causes of disease, disability and death. Its presence increases the risk of a number of serious medical conditions such as hearth disease, atherosclerosis, kidney damage and stroke [2]. High blood pressure that is directly related to specific and identifiable causes is by definition diagnosed as *secondary* hypertension, which is not considered in this thesis. However, the causes are usually unidentifiable, in which case the diagnosis is *primary* hypertension. The causes of primary hypertension are thus by definition unknown, though an extensive number of factors related to genetic and environmental conditions are assumed to be involved [2]. Studies show that environmental risk factors include obesity, excessive salt intake, smoking, exaggerated alcohol consumption, nutrient deficiency, chronic stress and lack of exercise. The extensivity of these factors and their combined impact on the cardiovascular system (CVS) make hypertension a complicated condition to treat. Management of high blood pressure commonly involves medications in combination with exercise and other lifestyle changes. A number of cardiovascular effects can potentially lower blood pressure, meaning that many categories of medications and lifestyle interventions can be prescribed to a hypertensive patient. However, the effects of medications, exercise and other interventions are highly dependent on overall health status. Consequently, the identification of optimal treatment for an individual suffering from hypertension is often an ineffective procedure characterized by trial and error.

1.1 Hemodynamic Modelling

As indicated by the title, the topic for this master's thesis is hemodynamic modelling. The current section introduces this concept and its relation to hypertension and the MyMDT project.

1.1.1 Motivation and Background

As stated above, the procedures for treating hypertension are currently inflicted by inefficiency and uncertainty. A personalized way of predicting how the CVS will respond to various hypertension managing interventions is therefore desired, which is a motivating factor for *hemodynamic modelling*. In this context, hemodynamic modelling refers to the development of computational models that based on a set of patient-specific parameters can simulate the CVS under given conditions. This is the essence of the research project "My Medical Digital Twin" (MyMDT) that is currently carried out at NTNU [3]. The ambition of MyMDT is to develop a clinical digital tool that provides information about the blood pressure status in an individual and targeted advice on how it can most efficiently be improved. Central in this work is the development of a hemodynamic *exercise model*, which is a mathematical model of the CVS and its acute response to exercise at a given intensity. Biological systems are intrinsically variable and remodel over time, and long-term effects are therefore more complicated to predict than short-term fluctuations. This master's project is conducted on the current MyMDT model, which concerns exclusively acute exercise response. By analyzing short-term mechanisms, the ambition is to enhance the understanding of and eventually the ability to predict also long-term effects.

1.1.2 Related Work

The MyMDT hemodynamic model is still in its early stages, and requires more research on several levels to achieve its ambition of being a clinical tool. At the time of writing, one paper has been published on the model, with emphasis on the procedure for estimating resting state (baseline) parameters [4]. This procedure and the model implementation itself are developed through collaboration in the MyMDT project by Dr. Jacob Sturdy and Ph.D. Candidate Nikolai L. Bjørdalsbakke at the Division of Biomechanics. Equations concerning the exercise model are adapted from an unpublished internal note on acute exercise simulation [5]. This master's project builds further on code constituting the hemodynamic exercise model and the corresponding parameter estimation procedure. The methodological basis for progressing the original code is described throughout the report. The hemodynamic model itself and extracts of the estimation procedure are reproduced in Section A.3 along with additions and amendments developed in this work.

During the fall of 2021, I conducted another project on the model through the course TKT4550- Structural Engineering, Specialization Project, which resulted in an unpublished report titled "Sensitivity Analysis of a Hemodynamic Model for Varying Exercise Intensity" [6]. Here, model behaviour was investigated within a statistical framework with emphasis on the input parameters and aspects of exercise intensity. Resulting sensitivities and insights contribute as motivation and background for this master's

project. Parallel to the Specialization Project, medical engineering student Hilke Straatman from Eindhoven University of Technology worked on the MyMDT model through an internship at NTNU, which resulted in an unpublished report [7] and a set of preliminary processed cardiovascular data that is used in this project.

1.1.3 A Clinical Exercise Trial

Studies performed to evaluate any new drug or treatment are denoted *clinical trials*, and they are necessary to obtain clinical approval [8]. As a medical tool, this applies also for the MyMDT model. Cardiovascular data obtained in a clinical trial is in this project used to evaluate the hemodynamic model and its ability to simulate exercise at different intensities. The trial, titled "Mapping of Cardiac Power in Healthy Humans and Testing of a New Blood Pressure Sensor-a Pilot Study", was conducted with ethics approval during the fall of 2021 [9], and will in this report be referred to as "the clinical exercise trial" or simply "the trial". Details concerning the usage of trial data for this project are found in Section 4.1.

1.2 Problem Description

This master's thesis is motivated by the possibility of contributing to the further development of the MyMDT hemodynamic model towards its clinical ambition. Cardiovascular data is used to evaluate and develop the model, with emphasis on aspects of parameter personalization and exercise simulations. The purpose is to investigate how and if structural adjustments can improve the predictive accuracy and physiological consistency of the model, without increasing its level of complexity. In silico experiments, literature research, data analyses and physiological considerations constitute the project methodology. A brief validation is performed to evaluate the current state and status of the model in relation to its intended usage.

1.2.1 Objectives

Development and validation of the hemodynamic model constitute two distinct parts of this project, whose objectives are:

I **Model calibration and development.**
Use data to identify model configurations that yield the most accurate and reliable personalized predictions of pressure and flow during exercise, which implies analyzing the following procedures:

i Estimation of model parameters. Investigate how the parameter estimation procedure should be structured to obtain a baseline that accurately simulates the hemodynamic resting state, in addition to facilitating physiologically plausible simulations of exercise state.

ii Simulation of exercise state. Given a set of baseline parameters, identify how the hemodynamic exercise state should be simulated to be most consistent with data.

II **Model validation.**

Using the most reliable and accurate configurations from the first part, perform a validation of the hemodynamic model, i.e.:

- Quantify individual and average errors.
- Evaluate the level of accuracy in relation to clinical criteria.
- Address potential issues with the current model and whether greater structural modifications beyond altering the procedures in part I are necessary to achieve the clinical ambition of MyMDT.

1.2.2 Outline

The report is organized into seven chapters including this introductory chapter. Chapter 2 introduces the overall anatomy and physiology of the CVS, its exercise response and methods of measurement that are relevant for the clinical trial. Furthermore, the chapter contains a brief introduction to conceptual and statistical aspects of the framework used to evaluate a predictive model. Chapter 3 is dedicated to the hemodynamic model itself, including its mathematical structure, numerical solution method and procedure for parameter estimation. Chapter 4 presents the project methodology for approaching the objectives stated above. It is introduced with a description of the trial that constitutes the project database, followed by a presentation of the model aspects that are subjected to investigation. Further, the premises for evaluating model performance are defined. The chapter concludes with an overall summary of the project procedures, constituting the steps from which the results presented in Chapter 5 are generated. Chapter 6 discusses the results in relation to model aspects presented in Chapter 4. Chapter 7 closes the report with a conclusion based on the preceding discussion, before suggesting how further research may pursue and enhance insights and knowledge obtained in this master's thesis.

Chapter 2

Theory

This chapter is primarily an introduction to the anatomy and physiology of the cardiovascular system (CVS). Furthermore, a section is dedicated to the explanation of central statistical and conceptual aspects within the frameworks of model evaluation and validation.

2.1 Cardiovascular Physiology

In the following, anatomic and physiological properties of the CVS are reviewed. The majority of the theory is based on chapters on cardiovascular physiology found in "Vander's Human Physiology: The Mechanisms of Body Function" by Widmaier et al. [2] and "Medical Physiology: Principles for Clinical Medicine" by Rhoades et al. [10].

2.1.1 Overview of the CVS

Adequate blood flow is essential to supply cells in the body with oxygen, nutrients and hormonal signals, and to remove metabolic and cellular waste products such as carbon dioxide. This is achieved by the CVS, which consists of the heart, the blood and the interconnected set of blood vessels, the latter collectively referred to as the *vascular system*. Blood flow is generated by pressure gradients created by the pumping action of the heart. The CVS forms a closed loop consisting of two distinct circuits that both originate and terminate in the heart. The *pulmonary circulation* includes blood pumped from the right ventricle through the lungs and further to the left atrium. From the left atrium the blood enters the *systemic circulation*, where blood is pumped from the left ventricle through all body tissue and organs except from the lungs, and then back into the right atrium [2].

Blood is pumped out of the heart through one set of vessels and is returned to the heart by a different set. In both the systemic and pulmonary circuits, vessels carrying blood away from the heart are named

arteries, while the blood is transported back towards the heart through *veins*. In the systemic circuit, oxygen-rich blood leaves the left ventricle through a single large artery; the *aorta*. Aorta branches into smaller vessels called arterioles and finally into capillaries. The capillaries exchange oxygen for carbon dioxide by diffusion with the underlying body fluid before veins transport the blood through the body to the *vena cava* and finally back into the right atrium. The pulmonary circulation is similarly composed. Deoxygenated blood leaves the right ventricle via a large artery, namely the *pulmonary trunk*. The trunk branches of into two pulmonary arteries that transport blood to each of the lungs, which are supplied with oxygen by breathing. As blood flows through the lung capillaries, carbon dioxide is exchanged for oxygen by gas diffusion. Oxygenated blood leaves the lungs via the pulmonary veins, which are emptied into the left atrium [2].

Hemodynamics

Physical properties and factors governing blood flow are collectively referred to as *hemodynamics* [2]. As all fluids, blood exerts a *hydrostatic pressure*, resulting in a force on the walls of the blood vessels. In general, blood flows from regions of higher to lower pressures, making the pressure gradient (ΔP) between two regions an important determinant of the corresponding blood flow (Q). To know the flow at a given pressure gradient, one also needs to know the flow *resistance* (R), which is a measure of the friction that impedes flow [2]. Three central determinants of resistance are blood viscosity (μ), vessel length (L) and radius (r). Under idealized flow conditions in a perfect tube, the contributions to R from these factors are defined as follows [2]:

$$R = \frac{8L\mu}{\pi r^4} \tag{2.1}$$

Further, pressure (P), flow (Q) and resistance (R) are related by the following important relation [2]:

$$Q = \frac{\Delta P}{R} \tag{2.2}$$

which is a general equation that governs all systems in which a fluid moves by bulk flow, i.e. flow where all components move together [2]. Note that the magnitude of blood pressure varies throughout the CVS for reasons that are explained in Section 2.1.3.

2.1.2 The Heart

The heart is a muscular organ whose function is to provide the driving force for the circulation. The wall of the heart is named the *myocardium*, and is primarily made up by cardiac muscle cells [2]. Functionally, the heart consists of two vertically separated halves. Each half contains two chambers: An upper chamber named the *atrium* and a lower called the *ventricle*. Blood empties from the atrium into the

ventricle on its respective side. Together, the two halves can be viewed as two pumps in series that separately and simultaneously pump blood into the systemic and pulmonary arteries. The right ventricle and right atrium are the pumping chambers for the pulmonary circulation, while the left ventricle and left atrium support the systemic circulation [2].

To ensure correct direction of blood flow, the heart has four *valves*. The two *atrioventricular (AV) valves* allow blood to flow from an atrium to a ventricle, but not in the reversed direction. The right AV-valve is named the *tricupsid valve*, while the left is commonly known as the *mitral valve*. Pressure differences across the AV-valves leads them to open and close. When atrial pressure exceeds corresponding ventricular pressure, the intermediate valve is pushed open. On the contrary, a valve is forced closed when the pressure in a contracting ventricle becomes greater than that in its respective atrium. Another valve is located in the connection between the left ventricle and the aorta; the *aortic valve*, and one between the right ventricle and the pulmonary trunk; the *pulmonary valve*. These two valves are open during ventricular contraction, when blood flows from the ventricles into the arteries. They close during ventricular relaxation to prevent blood from flowing in the opposite direction. Similarly to the AV-valves, they open and close depending on the pressure gradient across them [2].
Like blood flow through vessels, the relation between flow, pressure and resistance (2.2) also applies to flow between the various cardiac chambers through the valves. Thus, the resistance of a valve regulates the flow at a given pressure gradient. However, in a healthy state, an open heart valve provides little resistance to blood flow, causing small pressure gradients to produce large flows [2].

The Cardiac Cycle

The muscular heart wall, the myocardium, is contracting and relaxing in a cyclic manner. The *cardiac cycle* is the sequence of mechanical, acoustic and electrical events that occurs between two following heartbeats. A cardiac cycle is commonly represented graphically by time-dependent variations in left ventricular and aortic pressures, left ventricular volume and blood flow. These variations are often represented along with tracings of the electrical activity (ECG) and heart sounds (PCG). Mechanical events of the cardiac cycle are emphasized in this paragraph, while electrical and acoustic properties are briefly reviewed in Section 2.1.4.

A cardiac cycle consists of two major phases: The period of ventricular contraction and blood ejection is named *systole*, while *diastole* refers to the period of ventricular relaxation and blood filling. For a typical heart period of $T = 0.8$ s, approximately 0.3 s are in systole, while 0.5 s are in diastole [2]. These two phases can further be subdivided into two periods in the following manner [2]:

- **Systole**

    1. *Isovolumetric Ventricular Contraction*: This is the first part of systole. The ventricles are contracting, but no blood is ejected due to closed valves.

    2. *Ventricular Ejection*: This period is introduced once ventricular pressures rises above the pressures in the aorta and the pulmonary trunk, causing the aortic and pulmonary valves to open. Aortic and ventricular pressures are increasing in the *rapid ejection phase*, during which approximately 70% of the blood to be ejected exits the ventricles [10]. The remaining is ejected with declining pressures during the *reduced ejection phase*.

- **Diastole**

    1. *Isovolumetric Ventricular Relaxation*: This is the first part of diastole. The ventricles begin to relax and the aortic and pulmonary valves close. The AV-valves are also closed, which means that ventricular volumes are unchanged.

    2. *Ventricular Filling*: This period is introduced once the AV-valves open. The ventricles are filled with blood flowing from the atria.

A cardiac cycle is typically represented by a plot of left ventricular pressure against corresponding volume, commonly known as a PV-loop, which is illustrated in Figure 2.1.

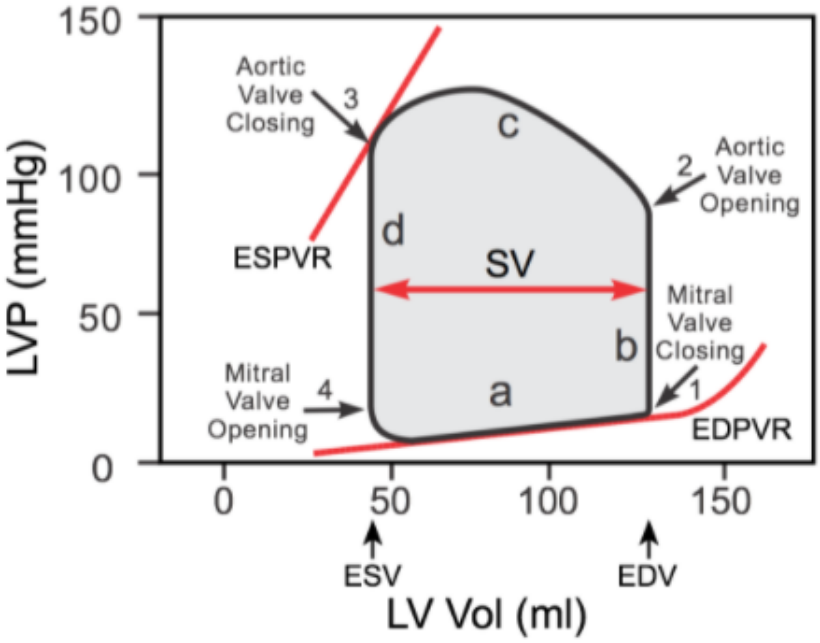

Figure 2.1: A pressure-volume (PV) representation of the cardiac cycle. Letters a-d indicate the current phase of the cardiac cycle. Here, a and d are diastole, while b and c are systole. The parts of each phase are introduced and terminated by the opening or closure of a valve, marked by numbers 1-4. Point 1 represents the end of ventricular filling. Systole is initiated with the isovolumetric contraction phase (b) that terminates in point 2; opening of the aortic valve. Ventricular ejection (c) concludes in point 3 with the closure of the aortic valve and thus the end of systole. Diastole is introduced with the isovolumetric relaxation period (d) followed by the opening of the mitral valve (4) and the ventricular filling phase (a). Left ventricular pressure (LVP) is plotted against left ventricular volume (LV Vol). ESV and EDV refer to the amounts of blood present in the left ventricle at end-systole and end-diastole, respectively. The stroke volume (SV=EDV-ESV) is illustrated as the width of the PV-loop (red arrow). ESPVR and EPVRP are end-systolic and end-diastolic pressure-volume relationships, respectively. Figure obtained from [11] and used with permission from Richard Klabunde. The same illustration was also reused in [6].

The Cardiac Output

The blood volume ejected from each ventricle during systole is the *stroke volume* (SV):

$$\mathrm{SV} = \mathrm{EDV} - \mathrm{ESV} \tag{2.3}$$

where EDV and ESV are end-diastolic and end-systolic ventricular blood volumes, respectively. A resting, average sized adult will typically have SV ≈ 70 $^{\mathrm{mL}}/_{\mathrm{beat}}$ [2]. Note that both ventricles have the same SV. The ratio of SV to EDV is the *ejection fraction* (EF) [2]:

$$\mathrm{EF}[\%] = \frac{\mathrm{SV}}{\mathrm{EDV}} \times 100\% \tag{2.4}$$

The blood volume pumped by each ventricle as a function of time is the *cardiac output* (CO) [2]:

$$\mathrm{CO} = \mathrm{SV} \times \mathrm{HR} \tag{2.5}$$

where heart rate (HR) [bpm] is the number of heartbeats per minute (bpm=beats per minute). CO ≈5.0 $^{mL}/_{min}$ is normal for a resting adult [2]. Knowing the total blood volume, CO can tell the frequency by which the entire blood volume is pumped around the CVS.

Determinants of Cardiac Output

As can be read from Equation (2.5), cardiac output is determined by heart rate (HR) and stroke volume (SV). These quantities are further regulated as follows [2]:

I Heart rate: Inherent autonomous and nervous activation mechanisms determine HR.

II Stroke volume: SV is determined by the force of cardiac contraction, which is affected by a variety of factors, including:

1. Preload: The initial stretch of the cardiac muscle prior to contraction, which is determined by EDV. Tension in the cardiac muscle fibres is proportional to fiber length. Therefore, a greater EDV will generate a greater stretch of the muscular fibres, and consequently a more forceful contraction. This effect is commonly known as the *Frank-Starling Mechanism*. Interrelations between diastolic filling, preload and SV in the context of cardiovascular exercise response are further elaborated on in Section 2.1.5.

2. Afterload: When the ventricle ejects a given blood volume, the contracting muscle must work against a load generated mainly by arterial pressure. Elevated arterial pressure means that ventricular pressure must increase accordingly for the valves to open and induce ventricular ejection. In general, muscles contraction is slower when working against a greater load. Hence, a reduced muscle fiber shortening rate due to increased afterload results in a lower velocity at which the blood is ejected, and consequently a reduced SV [2].

3. Contracility: The innate ability of the myocardium to contract. Ventricular contractility is the strength of contraction at any given EDV. Note that a change in contraction force due to increased EDV (preload) does not reflect increased contractility.

The end-systolic pressure-volume relationship (ESPVR) in Figure 2.1 represents various combinations of preload (volume) and afterload (pressure). By determining the pressure that the ventricle can generate at a given preload, ESPR defines a mechanical limit for how much blood can be ejected by a single ventricular contraction. The slope of this line is a mechanical cardiac parameter named *maximum left ventricular elastance* (E_{max}), and it is a clinical measure of cardiac contractility [12]. Similarly, the slope of EDPVR is *minimum left ventricular elastance* (E_{min}), which characterizes the pressure-volume rela-

tion during the filling phase, i.e. the passive state of the ventricle. Elastance (E) is in general a measure of the expected change in shape of a hollow structure given a change in loading, mathematically defined as [12]:

$$E = \frac{\Delta P}{\Delta V} \tag{2.6}$$

where ΔP and ΔV are differences in pressure and volume, respectively.

2.1.3 The Vascular System

The vascular system refers to the interconnected set of blood vessels in the CVS. While the muscular effects of the heart provide the driving force for blood flow in the CVS, the vascular system has a major function in the regulation of blood pressure and the distribution of blood throughout the body according to metabolic demands [2].

Compliance

A central mechanical property of a blood vessel is *compliance*. Compliance (C) is a measure of how easily a structure stretches at a given pressure [2]:

$$C = \frac{\Delta V}{\Delta P} \tag{2.7}$$

Compliance is an important determinant of pressure in a given region of the CVS. The compliance of a given blood vessel varies by location in the body. Arterial compliance decreases throughout the arterial tree; a structure that originates in the compliant aorta and branches of into stiffer peripheral arteries. Note that veins are in general much more compliant than arteries.

Blood Pressure

Blood pressure (BP) is the force exerted by the blood against the vessel walls. It is traditionally reported in units of mmHg (millimetres of mercury). BP varies by location in the CSV. Since veins are overall much more compliant than arteries, they can store large amounts of blood at a low pressure. Approximately 60% of the blood volume is present in the systemic veins, but venous pressure is on average only ≈10-15 mmHg [2]. Similarly, the pulmonary circulation is also a low-resistance, low-pressure circuit. Consequently, if not stated otherwise, "blood pressure" refers to *systemic arterial* blood pressure, as this is in general of main clinical interest. Maximum systemic arterial pressure during a cardiac cycle is named *systolic pressure* (SP or P_{sys}). *Diastolic pressure* (DP or P_{dia}) is the minimum pressure value, and it is reached just before ventricular ejection. BP is commonly reported as the range of systemic ar-

terial pressure bounded by SP and DP, formulated as $^{\mathrm{SP}}/_{\mathrm{DP}}$. A BP of $^{120}/_{80}$ mmHg is considered normal in resting state for an average young male adult [2]. However, multiple factors such as age, sex, diet and body weight all affect the range of arterial pressure. If the pressure chronically exceeds $^{140}/_{90}$ mmHg, the individual is by definition suffering from *hypertension* [2]. The left ventricle in a hypertensive individual must consistently pump against increased arterial pressure (afterload). This leads to an adaptive increase in cardiac muscle mass that over time alters the properties of the myocardial cells, resulting in diminished contractile function and potentially heart failure [2]. As stated in Chapter 1, the presence of hypertension also enhances the risk of developing kidney damage, stroke, atherosclerosis and heart attacks. For every 20 and 10 mmHg increase in P_{sys} and P_{dia}, respectively, the risk of heart disease and stroke doubles [2].

The difference between SP and DP is the *pulse pressure* (PP).

$$\mathrm{PP} = \mathrm{SP} - \mathrm{DP} \tag{2.8}$$

By substituting PP for ΔP in Equation (2.7) and utilizing that the change in volume during a cardiac cycle is due to blood ejected from the left ventricle (SV), pulse pressure can be approximated as:

$$\mathrm{PP} \approx \frac{\mathrm{SV}}{C_a} \tag{2.9}$$

where C_a is total arterial compliance.

Arterial pressure (P_a) changes continuously through the cardiac cycle. The average pressure value during a cycle lasting between t_1 and t_2, i.e. *mean arterial pressure* (MAP or P_{map}), is defined and commonly approximated as [10]:

$$\mathrm{MAP} = \frac{\int_{t_1}^{t_2} P_a \, dt}{t_2 - t_1} \approx \frac{2}{3}\mathrm{DP} + \frac{1}{3}\mathrm{SP} \tag{2.10}$$

where the factors $^2/_3$ and $^1/_3$ follows that diastole lasts approximately twice as long as systole in resting state. Substituting Q, R and ΔP in Equation (2.2) by cardiac output (CO), total peripheral resistance (TPR) and MAP-P_{ra} yields the following [2]:

$$\mathrm{MAP} = \mathrm{CO} \times \mathrm{TPR} \tag{2.11}$$

where P_{ra} is right atrial pressure, which is normally close to zero [2]. Hypertension will be reflected in an increased MAP, which can theoretically result from both an increase in CO and TPR. However, in most cases of primary hypertension, the most significant factor is increased resistance (TPR) caused by reduced vessel radius in the arterioles [2]. The vast effect of vessel radius on resistance is apparent from Equation (2.1), where radius (r) is a determinant of R in 4^{th} power.

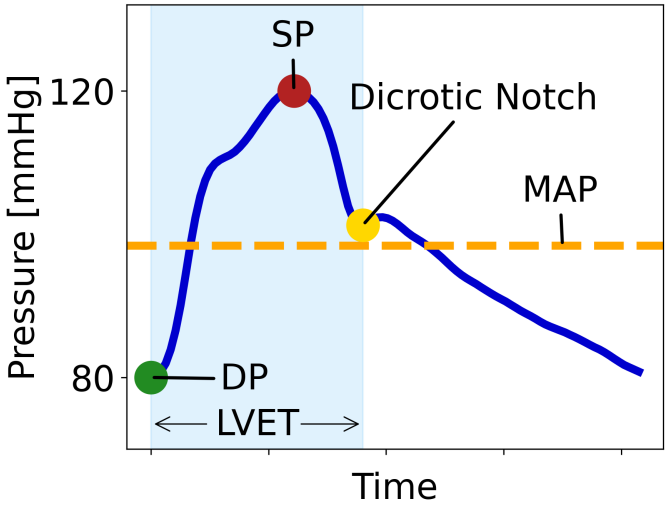

Figure 2.2: A typical arterial pressure waveform during a cardiac cycle for an average young male adult. SP, DP and MAP are systolic, diastolic and mean arterial pressures, respectively. The point named *dicrotic notch* represents the closure of the aortic valve. LVET is left ventricular ejection time. Illustration inspired by Figure 12.34 in [2].

Figure 2.2 shows an arterial pressure wave that is typical for the pressure changes that occur over a cardiac cycle in all of the large systemic arteries. Diastolic, systolic and mean arterial pressures are all important characteristics of the arterial pressure waveform. The beginning of upstroke coincides with diastolic pressure. The *dicrotic notch* is the prominent secondary upstroke in the descending part of the aortic pressure wave, which occurs due to the closure of the aortic valve at the end of systole. The time interval between the beginning of upstroke and the dicrotic notch is the *left ventricular ejection time* (LVET), i.e. the total period during which blood is ejected from the ventricles. By utilizing that left ventricular and arterial pressures are approximately equal at the end of systole, maximum left ventricular elastance (E_{max}) can be expressed as:

$$E_{\text{max}} \approx \frac{P_{\text{dn}}}{\text{ESV}} \tag{2.12}$$

where P_{dn} is the pressure at the time of the dicrotic notch, i.e. representing end-systolic pressure in the left ventricle, and ESV is end-systolic volume.

2.1.4 Cardiovascular Measurements

This section emphasizes relevant methods of cardiovascular measurements in the context of the exercise trial as well as clinical applications.

Electrical and Acoustic Activity

Electrocardiography is the process by which an electrocardiogram (ECG) of the electrical activity of the heart is produced. *Phonocardiography* is the tracing of heart sounds during a cardiac cycle, and a phonocardiogram (PCG) is commonly depicted along with an ECG. Together with tracings of ventricular and aortic pressures and volumes, ECG and PCG represent important characteristic events of a cardiac cycle. Intervals between waves in the ECG and/or PCG are of physiological and clinical importance [10]. Particularly relevant for this project are the various measurements of systolic time intervals. Therefore, this section elaborates on features of the ECG and PCG used to quantify the duration of systole.

Electrical systole (QT) is the the total duration of ventricular activation. QT is read directly from the ECG as the time between the initiation of the QRS-complex and the end of the T-wave [10]. *Electromechanical systole* (QS_2) is the time between the onset of the QRS-complex and the first high frequency vibration in the second heart sound of the aortic compartment (S_2) [13]. The QRS-complex, T-wave and S_2 are depicted in Figure 2.3

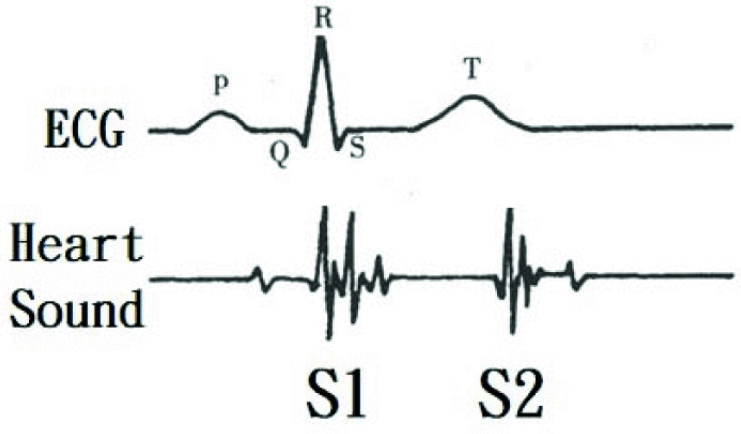

Figure 2.3: Tracing of heart sounds (PCG) mapped to an electrocardiogram (ECG). The QRS-complex represents electrical activation of the ventricles at the onset of systole (isovolumetric contraction). The T-wave occurs when the ventricles are ejecting blood under declining aortic and ventricular pressures (reduced ejection phase). The second heart sound (S_2) is created by the termination of ventricular outflow caused by valve closure [10]. Figure obtained from [14], ©[2019], IEEE. Used with permission.

Blood Pressure

Blood pressure (BP) is a cardiovascular measurement of tremendous clinical interest. In general, the ideal is to measure the BP exerted on the aorta directly, but because this is in most cases impractical, BP is instead obtained in various other arteries depending on situation and available equipment. However, neither pressure waveform nor values of P_{sys} and P_{dia} are constant across the arterial tree. BP depends on the site of measurement due to a redistribution of blood when it branches off from the aorta into progressively smaller arteries, and because of varying vessel stiffness throughout the arterial tree [15].

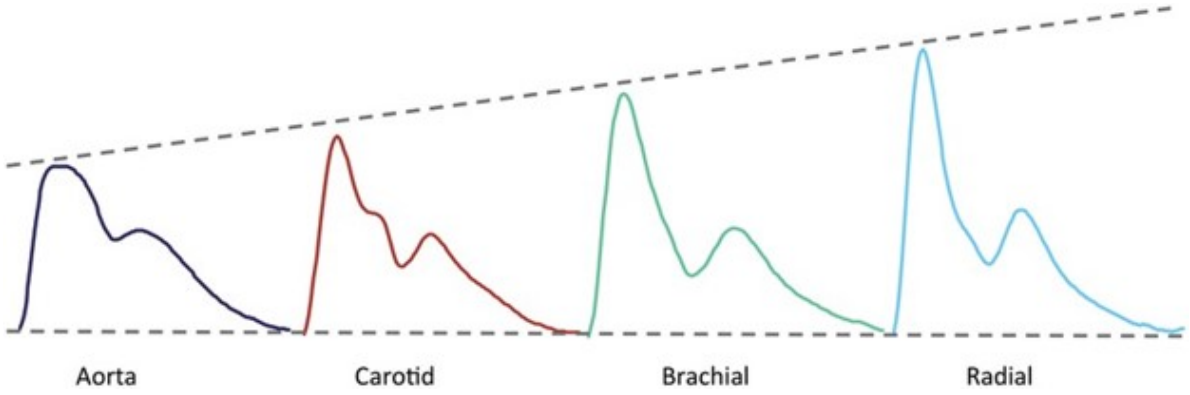

Figure 2.4: Amplification of the BP-waveform between the aorta and the carotid, brachial and radial arteries. Figure obtained from [15], ©[2022] Oxford University Press. Used with permission.

Aorta is a more compliant blood vessel than the stiffer peripheral arteries. This leads the upper section of the BP-wave to become more narrow and the peaks more prominent in accordance with increasing distance to the heart [15]. The consequence is progressive amplification of the pressure waveform, as illustrated in Figure 2.4. In the following, the clinical interpretation and methods of measurement for aortic, carotid, brachial and radial blood pressures are explained. These concepts and their differences are highly important for the usage of clinical data to evaluate the hemodynamic model.

Aortic BP

Blood is pumped from the left ventricle through the left ventricular outflow tract (LVOT) into the aorta, which is the largest artery. Aortic BP is the pressure at the root of the aorta, i.e. in the section of the aorta attached to the heart. Therefore, aortic BP is also denoted central BP, or central aortic BP (CAP). CAP is considered the most significant indicator of the pressure experienced by the heart and other vital organs [16]. The BP represented by the hemodynamic model is CAP. However, obtaining direct measurements of CAP is cumbersome, commonly involving the complicated procedure *cardiac catheterization* [15]. This is clearly an unsuitable method for routine screenings as well as for experimental testing of the hemodynamic model. Hence, peripheral measurements of BP are more frequently chosen for clinical applications, and they were also used in the exercise trial.

Carotid BP

The carotid arteries supply the head and brain with blood, and are located on both sides of the neck [10]. Carotid pressure waveforms were in the exercise trial recorded by applying the noninvasive method *applanation tonometry* over the carotid artery. As illustrated in Figure 2.4, carotid BP is expected to provide a better representation of aortic BP compared to more distal waveforms [15]. However, as this method does not yield explicit pressure values, systolic and diastolic BP were recorded at the *brachial* artery.

Brachial BP

Brachial cuff *sphygmomanometry* is the method most commonly used to record BP due to its ease of measurement as well as suitability for assessing values of systolic and diastolic pressures (SP and DP). The sphygmomanometer uses a cuff that is wrapped around the arm of an individual and inflated to a pressure exceeding SP before it is released to obtain values for SP and DP. For details concerning this method, the reader is referred to [10].

Radial BP

The clinical exercise trial introduced in Section 1.1.3 collected radial pressures invasively by catheterization of the radial artery. Radial pressures were in contrast to carotid and brachial BP collected during exercise in the clinical trial. The various pressure measurements obtained in the trial and how they are used in this project are further elaborated on in Section 4.1.

Blood Flow

Doppler ultrasounds are often used to detect blood flow in vessels and across heart valves. A Doppler instrument determines flow velocity by measuring the change in frequency (the Doppler shift) that occurs when the produced ultrasound wave is reflected by circulating red blood cells [10]. The clinical exercise trial recorded Doppler flow velocity in the left ventricular outflow tract (LVOT).

2.1.5 Cardiovascular Exercise Response

Exercise generates a physiological response in the body to adapt to increased demands in respiratory, metabolic and cardiovascular activity. The response includes elevated body temperature, higher oxygen consumption and increased skeletal muscle blood flow [2]. *Exercise* refers in this context to cyclic contraction and relaxation of muscles over a period of time, such as cycling or jogging. From the view of exercise physiology, exercise is by definition planned, structured and with a clear purpose, while *physical activity* refers to any event involving skeletal muscle use [17]. In the context of this project, exercise refers to also events of general physical activity that do not necessarily fulfill the criteria of structure and purpose. The essence is that the activity endures for some time. A single, intense muscle contraction will generate a very different response and is less relevant for this work. In the following, central physiological changes in cardiovascular variables generated by exercise are reviewed, with emphasis on response mechanisms considered most relevant in the context of modelling hemodynamic exercise state. The arrow depicted along with each variable denotes change during exercise ($\rightarrow\Rightarrow$unvarying, $\uparrow\Rightarrow$increase, $\downarrow\Rightarrow$reduction).

- ↑ Heart rate: Neural mechanisms stimulate the electrical system in the heart, causing heart rate (HR) to increase during exercise within a range from < 50 bpm in a fit individual to > 200 bpm during maximum effort [10]. The duration of the cardiac cycle, i.e. the heart period ($T = {}^{60}/_{\mathrm{HR}}$), is consequently reduced.

- ↑ End-diastolic ventricular volume: Diastolic filling time is decreased due to increased heart rate, which if not counteracted would decrease end-diastolic volume (EDV). However, multiple factors promoting *venous return* (VR), i.e. blood flow from the peripheral veins to the right atrium, more than compensate for the reduced filling time [2]. Using Equation (2.2), VR is expressed as [18]:

$$\mathrm{VR} = \frac{P_v - P_{\mathrm{ra}}}{R_v} \tag{2.13}$$

  where P_v and P_{ra} are venous and right atrial pressures, respectively, and R_v is venous resistance. Therefore, increasing P_v (or decreasing P_{ra} or R_v) increases VR. Central factors promoting VR during exercise are [2]:

  1. Skeletal muscle pump: Muscle contractions compress the veins, increase venous pressure, and force more blood back to the heart.

  2. Respiratory pump: Inspiration of air causes the chest wall to expand and the diaphragm, i.e. the muscle separating the thorax (chest cavity) from the abdomen, to descend. This increases abdominal pressure, and thoracic pressure becomes more negative. Expansion of the chest cavity causes the right atrial pressure to decrease [19]. The net effect is an increased pressure gradient between the heart and peripheral veins and thereby VR, which promotes flow of more blood towards the heart [2].

- ↑ Stroke Volume: The total effect of exercise on SV depends on simultaneous effects that impact ventricular systolic function and diastolic filling time, but the net effect is in general increased SV. Important factors facilitating this are:

  1. Preload: Increased VR and EDV during exercise result in increased cardiac preload, which by the Frank-Starling mechanism described in Section 2.1.2 makes the heart contract with more force, thereby increasing SV [2].

  2. Contractility: Myocardial contractility increases during exercise, generating a larger force independent of preload [2].

  3. Lusitropy: Refers the rate of myocardial relaxation, which is faster at increased HR [13]. This mechanism is elaborated on in the following paragraph.

- $\Uparrow$ Cardiac output: HR and SV increase, the former to the largest extent. The net effect is by Equation (2.5) increased CO.
- $\Uparrow$ Systolic pressure: SP increases due to an increase in both SV and the speed at witch the blood is ejected from the ventricles.
- $\downarrow$ Total peripheral resistance: TPR decreases due to a greater reduction in resistance in the heart and skeletal muscles than the increase present in non-active organs [2].
- $\downarrow$ Arterial compliance: C_a decreases as arterial pressure increases [10].
- $\rightarrow$ Diastolic pressure: No significant fluctuations or tendencies.
- $\uparrow$ Mean arterial pressure: CO increases more than TPR decreases, resulting in increased MAP (2.11).

The Lusitropy Mechanism

Contractile forces in the heart are generated in the myocardium by a type of cells named cardiomyocytes that work in a contraction-relaxation cycle [20]. This process is controlled by highly complex electrophysiological processes, which are beyond the scope of this report. During exercise, the demand for increased cardiac output requires a change in the rate of contraction of the cardiomyocytes [20]. The mechanism that refers to the accelerated relaxation of cardiomyocytes at increased heart rate is known as *lusitropy*. The heart period is reduced during exercise, and consequently also the time available for diastolic filling of the ventricles. If not counteracted, shortened filling time would have decreased end-diastolic volume (preload) and by the Frank-Starling Mechanism also stroke volume (Section 2.1.2). By increasing the rate of myocardial relaxation, the lusitropy mechanism reduces systolic activation time, thus indirectly contributing to the preservation of diastolic filling during exercise.

2.2 Framework for Evaluation and Validation of a Model

Model *evaluation* refers to the part of the development process where statistical metrics are used to understand model performance. *Validation* is essentially the comparison of measured behaviour of a given system to predictions yielded by a mathematical model. This section emphasizes central practical and theoretical aspects of model evaluation and validation. First a conceptual summary of relevant background from the Specialization Project [6] introduced in Section 1.1.2 is provided. Further, important statistical definitions and selected error metrics used for evaluation and validation purposes in this work are presented. The section concludes with a summary of important, general principles of model validation, which as stated in the objectives (Section 1.2.1) is a part of this project.

2.2.1 Uncertainty and Sensitivity

The topics for the Specialization Project [6] were model uncertainty and sensitivity, applied on the hemodynamic model. In the following, the concepts of uncertainty and sensitivity are briefly reviewed to provide a base for interpreting and understanding results from [6] that are referred to in the current work.

Two central challenges related to model uncertainty impact the translation of a mathematical model into a clinical tool [21]. Firstly, model personalization requires patient-specific parameters, whose assessment can be prone to many sources of errors. Biological and time-dependent variations and instrumental inaccuracies impact the majority of clinical measurements. Neither are measurements available for all model parameters. Secondly, capturing all relevant physics and physiology requires a certain level of model complexity. However, increased complexity means more implemented mechanisms that are followed by an increased number of parameters, introducing more uncertainty into the model. An optimal level of accuracy requires balance between the uncertainty associated with the number of parameters and the uncertainty resulting from model simplifications. This balance is illustrated in Figure 2.5.

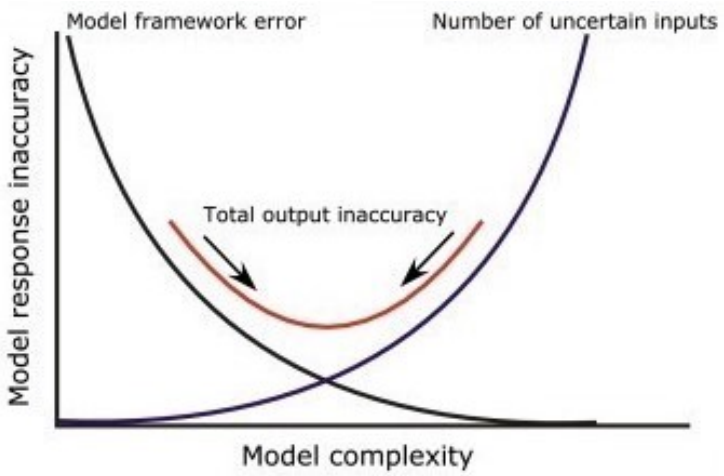

Figure 2.5: Output uncertainty as a function of model complexity. Image obtained from [21] ©[2022] John Wiley & Sons, Inc. Used with permission. The same illustration was also reused in [6].

Some parameters impact model behaviour more than others, and it is beneficial that these are identified. If a parameter is discovered to be particularly influential on exhibited system behaviour, its determination and/or tuning may be essential to model performance. It can also be desirable to target specific model outputs that exhibit implausible behaviour without altering those that already behave adequately. Such insights can be obtained by a *sensitivity analysis* (SA). SA quantifies the contributions to the variance of a model output Y_j from each model input Z_i and their interactions [21]. The Spe-

cialization Project calculated *total, global, variance-based Sobol* sensitivity indices for selected model outputs to each input parameter. The following understandings of the descriptive properties of this type of sensitivity index are obtained from Saltelli et al. [22]: A *global* index is computed across the entire input space and not only at the point of evaluation, which is the case for local methods. *Variance based* refers to the decomposition of output variance into fractions assignable to input parameters and their interactions. *Total sensitivity* refers to the contribution of input parameter Z_i to output variance $\mathbb{V}[Y]$ including interactions of arbitrary order with any other input, in contrast to 1st order indices that only measure the direct contribution of Z_i to $\mathbb{V}[Y]$. The total sensitivity index, $S_{\mathrm{T},i}$, is given as [21]:

$$S_{\mathrm{T},i} = \frac{\mathbb{E}[\mathbb{V}[Y \mid Z_{-i}]]}{\mathbb{V}[Y]} = \frac{\mathbb{V}[Y] - \mathbb{V}[\mathbb{E}[Y \mid Z_{-i}]]}{\mathbb{V}[Y]} = 1 - \frac{\mathbb{V}[\mathbb{E}[Y \mid Z_{-i}]]}{\mathbb{V}[Y]} \tag{2.14}$$

where Z_{-i} is the set of all uncertain inputs, excluded Z_i [21]. $\mathbb{E}[\mathbb{V}[Y \mid Z_{-i}]]$ is the expected variance remaining after all parameters except Z_i have been fixed, and is therefore analogous to the total sensitivity to Z_i. An interpretation of $S_{T,i}$ is expected reduction in the variance of Y if there was no uncertainty related to Z_i [22].

2.2.2 Statistical Description of Data

Treatment of experimental data requires knowledge about some central statistical metrics.

Mean Value

The *mean value*, also known as the average value, is calculated from N measured data points y^m as:

$$\overline{Y} = \mu_Y = \frac{1}{N}\sum_{i=1}^{N} y^m_{(i)} \tag{2.15}$$

Standard Deviation

Standard deviation measures average deviation between data points and their corresponding mean:

$$\sigma_Y = \sqrt{\sigma_Y^2} = \sqrt{\frac{1}{N-1}\sum_{s=1}^{N}\left(y^{(s)} - \mu_Y\right)^2} \tag{2.16}$$

where σ_Y^2 denotes variance, which is the square of the standard deviation (σ_Y). Because the unit of σ_Y is the same as $[Y]$, σ_Y is often preferred over σ_Y^2 to quantify the amount of variability in a dataset. Whether deviations between measurements and model predictions are a consequence of model inaccuracy or data variability is important when evaluating and/or validating a model.

2.2.3 Error Metrics

Performance of a forecasting model can be quantified by a number of error metrics. This section presents the metrics chosen in this project to evaluate and validate the predictions made by the hemodynamic exercise model against data collected in the clinical exercise trial.

Mean Absolute Error

Deviations between measured and predicted values are frequently quantified by the *mean absolute error* (MAE). This is the average of the absolute errors, and is calculated from model predictions ($y_i(\boldsymbol{\theta})$) and corresponding measurements y_i^m as:

$$\frac{1}{N}\sum_{i=1}^{N}\left|y_i^m - y_i(\boldsymbol{\theta})\right| \tag{2.17}$$

Bias

In cases where the sign of the error is of interest, the *bias* is preferable to MAE. Bias is calculated as:

$$\frac{1}{N}\sum_{i=1}^{N}\left(y_i^m - y_i(\boldsymbol{\theta})\right) \tag{2.18}$$

Note that bias must be treated with caution, as it can show misleadingly low errors if deviations are symmetrically distributed around zero.

2.2.4 Performing a Model Validation

As stated in Section 1.2.1, a part of this project is to validate the hemodynamic model against experimental data. In general, validations are performed to assess whether the quality and accuracy of model predictions are adequate in relation to intended purpose. According to Saltelli et al. [22], a validated model can be defined as having undergone a series of extensive experimental tests that have confirmed its ability to adequately predict the behaviour of a given system. Model validation is conditional upon current knowledge. Because the model is subjected to new assumptions, data and structural adjustment, its development is an iterative procedure [23]. A validation process includes the following steps, which are based on the works on introduction to model validation by Paez [24] and Collier & Lambert [23]:

1. Clarify the intended purpose and area of application for the model.
2. Describe the validation experiments.
3. Specify the conceptual model, i.e. assumptions and physical processes from which the mathematical model is constructed.
4. Describe the mathematical model, including equations, initial and boundary conditions.
5. Describe the computational model, i.e. the numerical implementation of the mathematical model.
6. Specify the quantities of interest in the physical system.
7. Specify the validation metrics against which model performance are to be evaluated.
8. Describe the calibration experiments, i.e. the process from which model parameters and other settings are obtained to improve the agreement between experimental data and predictions.
9. Define the validation criteria the model needs to meet to be considered sufficiently accurate in perspective of its intended purpose.

Chapter 3

A Hemodynamic Model For Varying Exercise Intensity

This chapter presents the numerical structure and algorithmic technicalities of the hemodynamic exercise model under development in the MyMDT project. Connections between the physiological quantities presented in Section 2.1 and model implementations are particularly emphasized. First, the equations constituting the model are presented along with their physiological origin, followed by a description of input parameters and the procedure from which they are determined. Further, the numerical solution procedure for the model is explained, and output quantities of interest presented. The chapter concludes with a section on simulation of hemodynamic exercise state.

3.1 Conceptual Summary

Hemodynamics are the dynamics of blood flow. Simulated blood flow in a hemodynamic model is governed by physical factors such as vessel stiffness (compliance), volume and heart rate. Laws of conservation of mass and momentum are lumped over the heart, arteries and veins, which in the the MyMDT model are modelled as separate compartments embedded in a closed circuit. This simplification yields a behaviour of simulated pressure and flow that is found transferable to voltage and current in electric circuit theory. Some mechanisms are very complicated to describe mathematically, such as the variation of certain cardiovascular parameters during exercise. Thus, population-based curve fits constitute a complementary tool when modelling a hemodynamic exercise state.

The purpose of the MyMDT model is to produce realistic predictions of pressure and flow during rest and exercise conditions, while respecting key principles of personalizability, simplicity and computational efficiency. Hence, all model parameters need to be relatively easily determined or approximated on

an individual level. The model under development is a minimal, 0-dimensional, lumped parameter hemodynamic model formulated in global systemic quantities. The term *0-dimensional* implies that wave properties are excluded. *Lumped* means that the behaviour of the distributed system, which in this case is the systemic CVS, is approximated by discrete model compartments, i.e. the arteries, veins and the left ventricle. The compartments are embedded in a closed loop with constant total volume. Mathematical descriptions of the discrete model compartments are presented in the following sections. The presentation builds further on descriptions also provided in [6], and was originally inspired by the structuring found in [25].

3.2 Modelling Cardiac Function

Cardiac function refers to the description and quantification of how the pumping action of the heart interacts with the vascular system. As described in Section 2.1.2, blood is pumped into the systemic circulation from the left ventricle. Because the hemodynamic model exclusively describes the systemic circuit of the CVS, cardiac function is modelled as the pumping action generated by the left ventricle. Many aspects of cardiac behaviour are described by considering the left ventricular pressure–volume relationship, as illustrated in Figure 2.1. The slope of the end-systolic pressure–volume relationship (ESPVR) is an important mechanical cardiac parameter denoted E_{max}; maximum left ventricular elastance, which clinically represents cardiac contractility [12]. Elastance was mathematically defined in Equation (2.6), and its physiological meaning described in Section 2.1.2. In the model, E_{max} and E_{min} are important parameters for describing cardiac function in the active (contractile) and passive (filling) state, respectively. Two model parameters determine times of occurrence of events in a simulated cardiac cycle; the duration of a cycle is defined by the heart period (T), and the parameter t_{peak} represents the time at which E_{max} occurs. Hence, T and $t_{\text{peak}}$are denoted *timing parameters*. The set of parameters and equations that describe the cardiac function constitute a *time-varying elastance model*.

3.2.1 Time-Varying Elastance Model

The pumping action of the left ventricle, i.e. the cardiac function, is represented by a time-varying elastance model [25]. The hemodynamic model uses a time-varying elastance ($E(t)$) to link the cyclic activation and relaxation behaviour of cardiac muscle fibres in the myocardium to the pressure exerted on the blood by the heart (P_{lv}), which ultimately drives the fluid. This is achieved by setting the magnitude of $E(t)$ to vary periodically between E_{max} and E_{min}; $E_{\text{min}} \leq E(t) \leq E_{\text{max}}$. In total, the equations that

constitute the time-varying elastance model are:

$$\begin{aligned} P_{\text{lv}}(t) &= E(t) \times V_{\text{lv}} + P_{\text{th}} \\ E(t) &= (E_{\text{max}} - E_{\text{min}}) \times e(t) + E_{\text{min}} \end{aligned} \tag{3.1}$$

where $e(t)$ is a dimensionless activation function that varies in magnitude from 0 in the passive (relaxed) state to 1 in the active (contracted) state [25], and its shape is determined mainly by t_{peak}. The explicit expression for $e(t)$ is stated in Equation (A.3). Further, P_{lv} and V_{lv} are left ventricular pressure and volume, respectively, while P_{th} is the intrathoracic pressure function representing external pressure effects on the cardiac muscle. In the hemodynamic model, this effect is simply defined as a constant; P_{th}=-4 mmHg. Finally, $E(t)$ is the elastance function, with a period of $T = {}^{60}/_{\text{HR}}$, where T [s] is the heart period, and HR [bpm] is the heart rate.

3.3 Modelling Vascular Function

As stated in Section 2.1.3, the vascular system is the interconnected set of blood vessels in the CVS. Two central functions of the blood vessels are to store and to transport blood, which are modeled separately in this lumped parameter model. Compliance, explained in Section 2.1.3 and defined in Equation (2.7), is used to represent storage capacity. Resistance governs blood flow as described in Section 2.1.1 and defined in Equation (2.2). In the context of exercise physiology, the pulmonary circulation and the lung function are also relevant for cardiovascular exercise response. Nevertheless, the MyMDT hemodynamic exercise model takes account of the systemic circulation only. A central argument for not adding lung function and a pulmonary circuit to the model is to keep the level of complexity and the number of patient-specific parameters to a minimum. As shown in Figure 2.5, this principle of minimization is beneficial for limiting the amount of model uncertainty. Furthermore, measurements related to the heart and large arteries are more frequently collected in clinical settings. Respiratory function, commonly quantified by maximal oxygen uptake ($V0_2$-max), is considered of less interest in the context of hypertension, and MyMDT aims to use a minimal selection of personal input data to calibrate the model into simulating and predicting blood pressure. Hence, all vascular quantities treated by the model represent the systemic circulation, which consists of the systemic arteries and systemic veins. In short, the model is a closed circuit representing the systemic circulation, including a time-varying elastance model to represent left ventricular function.

3.3.1 Three-Element Windkessel Model

The arterial compartment of the model is described with a three-element Windkessel model (3WK) [25]. Here, *three-element* refers to the three mechanical vascular parameters; systemic resistance (R_{sys}), arterial compliance (C_a) and aortic impedance (Z_{ao}). Systemic resistance refers to the resistance offered by the entire systemic vasculature. Arterial compliance represents the total compliance (stiffness) of the large systemic arteries, and the term is often used interchangeably with *aortic* compliance. Similarly, the use of the terms *arterial* pressure (P_a) and *aortic* pressure (P_{ao}) is often inconsistent. As aorta is the largest contributor to arterial compliance and pressure, simplifications and practical limitations in measurements make separating aortic from arterial properties impractical from a modelling perspective. Thus, *aortic* and *arterial* are used somewhat interchangeably also in this work.

The third element in 3WK is *impedance*. Aortic characteristic impedance (Z_{ao}) is defined as the ratio between the forward propagating pressure and the corresponding flow in the aorta [26]. However, the MyMDT model is 0-dimensional, meaning that wave propagation is not considered. Therefore, impedance relates aortic pressure to flow in addition to capturing aortic valve resistance. Note that aortic valve resistance is important for the ejection phase of systole, but its impact is included in Z_{ao} instead of an independent parameter in this model.

3.3.2 The Venous Compartment

As described in Section 2.1.3, veins are very compliant vessels, and highly important in the storage of blood. Note that veins are of less importance compared to arteries in relation to blood pressure due to their inherent low pressure properties. In the model, the storage capacity of the venous compartment is represented by a venous compliance (C_{sv}). Regarding flow properties, blood flows between the venous side and the heart in the course of the diastolic filling phase, during which resistance is offered by the mitral valve. This resistance is captured by the parameter R_{mv}, which represents the force that opposes blood flow between the venous side and the heart. Thus, R_{mv} is an *effective* resistance, as it does not only represent the resistance in the mitral valve alone.

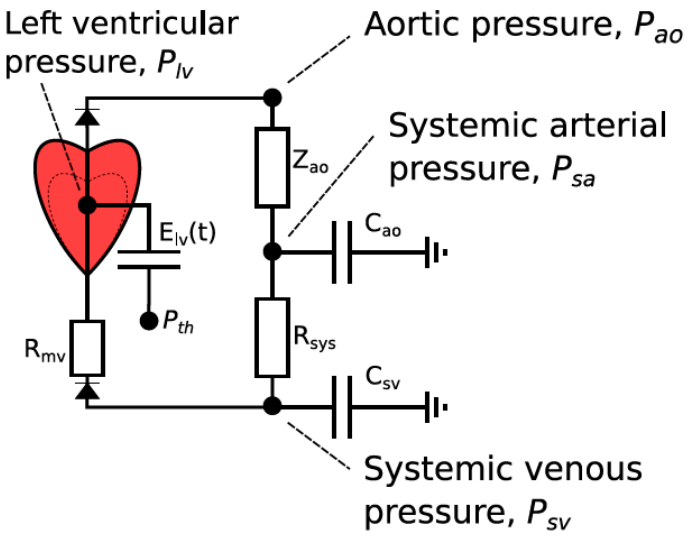

Figure 3.1: Schematic illustration of the closed-loop model used in the MyMDT project. Depicted are the tree model compartments left ventricle, arterial and venous vasculature. Mechanical circulation parameters are presented in its corresponding compartment. Systemic resistance (R_{sys}), aortic compliance (C_{ao}), and aortic impedance (Z_{ao}) describe the arterial compartment, while venous compliance (C_{sv}) and mitral valve resistance (R_{mv}) represent venous function. Further, P denotes pressure, and subscripts sa and sv denote systemic arteries and veins, respectively. The external intrathoracic pressure (P_{th}) is indicated next to the heart. Pumping function is represented by left ventricular pressure (P_{lv}) and time-varying elastance $E_{\text{lv}}(t)$. Finally, V_{tot} determines the total amount of blood volume in the closed-loop. The same illustration was also reused in [6]. Figure originally obtained from [4], licensed under CC BY 4.0 [27].

3.3.3 Conservation of Mass

The governing differential equations (ODEs) for the lumped parameter model are based on the law of mass conservation applied on the systemic circulation. The parameter V_{tot} defines the total amount of volume present in the closed-loop illustrated in Figure 3.1. Note that only *stressed* blood volume is taken into account, i.e. the amount of blood that generates a stretch in the vessel walls. Physiological blood volume also includes an unstressed part (V_0). This volume is present in a compartment without exerting pressure on its walls, and is not considered by the model. Potential issues regarding this feature are discussed in Section 6.1.2.

Circulation in the model is closed, hence total (stressed) blood volume (V_{tot}) is conserved:

$$V_{\text{tot}} = V_{\text{lv}} + V_{\text{sa}} + V_{\text{sv}} \tag{3.2}$$

where subscripts lv, sa and sv denote left ventricle, systemic arteries and systemic veins, respectively. The volumes V_{lv}, V_{sa} and V_{sv} are state variables for each respective model compartment. Note that the blood volume contained in the pulmonary circulation and the right ventricle are unstressed, and

therefore not treated by the model.

According to the law of mass conservation, volume change in any model compartment can be expressed using the following ODE [26]:

$$\frac{dV}{dt} = Q_{\text{in}} - Q_{\text{out}} \tag{3.3}$$

where Q_{in} and Q_{out} are, respectively, blood flow in and out of any model compartment, which in this context is the arterial vasculature, venous vasculature and the left ventricle. Section 3.5 describes explicitly how Equation (3.3) is used in the numerical composition of the ODEs constituting the hemodynamic model.

3.4 Personalized Estimation of Model Input Parameters

This section describes the model input parameters and reviews the numerical estimation procedure from which they are determined. A more elaborate explanation of this method is found in [4].

3.4.1 Model Input Parameters

There are ten individual baseline parameters in the hemodynamic model, excluding exercise and intensity describing parameters. Within these ten, seven parameters describe mechanical properties; E_{max}, E_{min}, C_{ao}, C_{sv}, Z_{ao}, R_{sys} and R_{mv}, two are timing parameters; t_{peak} and T, and the final parameter $V_{\text{tot}}$is the total amount of stressed blood volume in the system. Sections 3.2 and 3.3 described how each of these ten parameters represent a property of either the left ventricular, arterial, or venous model compartments, or the system as a whole (V_{tot}). For a physiological explanation of the parameters, the reader is referred to Section 2.1. A recapitulation of the parameters and their function in the hemodynamic model is presented in Table 3.1.

Parameter (θ)	Unit	Compartment	Type
$E_{\max}$	mmHg/mL	LV	Mechanical
$E_{\min}$	mmHg/mL	LV	Mechanical
C_{ao}	mL/mmHg	Arteries	Mechanical
R_{sys}	mmHg$\times s$/mL	Arteries	Mechanical
Z_{ao}	mmHg$\times s$/mL	Arteries	Mechanical
R_{mv}	mmHg$\times s$/mL	Veins	Mechanical
C_{sv}	mL/mmHg	Veins	Mechanical
V_{tot}	mL	Total vasculature	State-determining
t_{peak}	s	LV	Timing
T	s	LV	Timing

Table 3.1: Input parameters for the hemodynamic model. Column *Compartment* specifies whether the parameter describes a left ventricular (LV), arterial or a venous property. Column *Type* describes the function of the parameter in the model. Parameters representing stiffness (compliance or elastance) or resistance/impedance are mechanical system properties. As stated in Equation (3.2), V_{tot} limits the compartmental state variables V_{lv}, V_{sv} and V_{sa}, thus it is defined as state-determining. Parameters categorized as timing parameters influence times of occurrence of model events.

3.4.2 Numerical Estimation Procedure

The parameter estimation procedure is based on minimizing the deviation between measured data (y_k^m) and model prediction $y(t_k, \boldsymbol{\theta}_{\text{true}})$. The following relation is assumed [4]:

$$y_k^m = y(t_k, \boldsymbol{\theta}) + E_k \tag{3.4}$$

where superscript m denotes measurement and subscript k specifies the timing. Note that the inclusion of k in Equation (3.4) is necessary when comparing two time series, but not for scalar predictions. The purpose of the estimation procedure is to determine the set of model parameters ($\boldsymbol{\theta}$) that minimizes the deviation E_k. Since there are multiple model predictions of interest, a quantification of the overall level of agreement between model fit and data is needed. This is achieved by the *cost function*:

$$\begin{aligned} J(\boldsymbol{\theta}) = &\left(\frac{P_{\text{sys}}(\boldsymbol{\theta}) - P_{\text{sys}}^m}{K_{P_{\text{sys}}}}\right)^2 \times W_Y + \left(\frac{P_{\text{dia}}(\boldsymbol{\theta}) - P_{\text{dia}}^m}{K_{P_{\text{dia}}}}\right)^2 \times W_Y + \left(\frac{SV(\boldsymbol{\theta}) - SV^m}{K_{\text{SV}}}\right)^2 \times W_Y \\ &+ \sum_k^N \left(\frac{Q_{\text{lvao}}(\boldsymbol{\theta}) - Q_{\text{lvao,k}}^m}{K_{Q_{\text{lvao}}}}\right)^2 + \sum_k^N \left(\frac{P_{\text{ao}}(\boldsymbol{\theta}) - P_{\text{ao,k}}^m}{K_{P_{\text{ao}}}}\right)^2 + \left(\frac{\text{MVP}(\boldsymbol{\theta}) - \text{MVP}^f}{K_{\text{MVP}}}\right) \times W_Y \end{aligned} \tag{3.5}$$

where the K_y are scaling factors included to ensure that contributions to $J(\boldsymbol{\theta})$ are weighted approximately equally across all types of predictions [4]. Explicit values of K_y are found in Table A.1. The full implementation of $J(\boldsymbol{\theta})$ in `Python` as developed by Dr. Sturdy and Ph.D. Candidate Bjørdalsbakke

through the MyMDT project is included in Section A.3.2, along with modifications and amendments developed through this work (Section 4.2).

As implied by $J(\boldsymbol{\theta})$ in Equation (3.5), the estimation procedure is based on minimizing the residual between simulated pressure and flow waveforms (P_{ao} and Q_{lvao}), and corresponding continuous measurements, which are collected in resting state. The residuals for the waveforms are summed over N points in time (k). Furthermore, the hemodynamic scalar quantities P_{sys}, P_{dia}, SV and MVP are included in $J(\boldsymbol{\theta})$, because they are considered important in the context of diagnosing hypertension as well as being frequently measured in clinical settings. As waveforms contribute to the residual vector with many more points compared to the scalars, scalar contributions are multiplied with a factor (W_Y) depending on their considered importance and the length of the pressure waveform. The weighs are explicitly stated in Equation (A.5). Mean venous pressure (MVP) is weighted less than P_{sys}, P_{dia} and SV, because it is not considered equally important, and its reference value is very generally defined. Note that there are no available measurements for venous pressures from the trial, but MVP ($\overline{P_{\text{sv}}}$) is still included in $J(\boldsymbol{\theta})$ to ensure a realistic effect of the venous compartment on the remaining system. As stated in Section 2.1.3, venous pressure is commonly 10-15 mmHg, while the pressure in the right atrium is normally ≈0 mmHg [2]. Reported values for central venous pressure (CVP) vary down to 0, where CVP is the pressure in the vena cava, near the right atrium. As it is ambiguous which value is the most correct to use for diastolic filling, the reference value is chosen as MVP^f=6 mmHg, which is located in the middle range of [0–15] mmHg. The cost function may be adjusted to include or exclude model outputs. This project primarily considers the version stated in Equation (3.5), with the exception of experiments where $J(\boldsymbol{\theta})$ is penalized if the resulting ejection fraction (2.4) falls outside a preset range (Section 4.2.6).

After having defined the cost function, personalized parameters ($\boldsymbol{\theta}$) are estimated by solving the minimization problem:

$$\underset{\boldsymbol{\theta}\in\boldsymbol{\Theta}}{\arg\min} J(\boldsymbol{\theta}) \tag{3.6}$$

where $\boldsymbol{\Theta}$ represents predefined parameter bounds, whose purpose is ensuring that parameters are estimated within physiologically reasonable ranges, which are explicitly stated in Section 4.2.5. The minimization problem (3.6) is solved by a numerical optimization procedure. For this project, an implementation available through `scipy.optimize` is chosen for this purpose (`scipy` version no. 1.7.3 [28]). The cost function $J(\boldsymbol{\theta})$ and the bounds ($\boldsymbol{\Theta}$) are passed to the function `least_squares()`, which finds a local minima on the cost function [28]. Argument *method* is set to use the trust region reflective algorithm ("trf") to perform the minimization. "Trf" is a robust algorithm that is also suitable for solving bounded problems [28]. Advantages and disadvantages associated with constraints in the context of estimating parameters for the hemodynamic model are discussed in Section 6.1.3. Note that the cost function is

passed as a vector of residuals, i.e. $J(\boldsymbol{\theta})$ without the squares, as calculation of squared residuals is done in `scipy.optimize.least_squares()` [28]. Explicit implementations of $J(\boldsymbol{\theta})$ and extracts of the optimization procedure are included in Section A.3.2.

3.5 Numerical Solution Procedure

This section describes the mathematical structure of the hemodynamic model along with its prerequisites and limitations. It is shown how model ODEs are solved and relevant cardiovascular predictions extracted from these solutions. The equations and the numerical solution procedure is originally obtained from [4], and the following description builds further on a similar presentation provided in [6].

3.5.1 Model Equations

The hemodynamic model contains a set of nonlinear ordinary differential equations (ODEs) that describe the stressed blood volumes of its three compartments; systemic arteries (V_{sa}), systemic veins (V_{sv}) and left ventricle (V_{lv}), and also corresponding flows and pressures [4]:

$$\begin{aligned}
\frac{dV_{\text{ao}}}{dt} &= C_{\text{ao}}\frac{dP_{\text{ao}}}{dt} = Q_{\text{lvao}} - Q_{\text{aosv}} \iff \frac{dP_{\text{ao}}}{dt} = \frac{Q_{\text{lvao}} - Q_{\text{aosv}}}{C_{\text{ao}}} \\
\frac{dV_{\text{sv}}}{dt} &= C_{\text{sv}}\frac{dP_{\text{sv}}}{dt} = Q_{\text{aosv}} - Q_{\text{svlv}} \iff \frac{dP_{\text{sv}}}{dt} = \frac{Q_{\text{aosv}} - Q_{\text{svlv}}}{C_{\text{sv}}} \\
\frac{dV_{\text{lv}}}{dt} &= Q_{\text{svlv}} - Q_{\text{lvao}}
\end{aligned} \tag{3.7}$$

which is a result of the law of mass balance (3.3) applied on the model compartments. Subscripts ao and sv refer to the aorta and systemic veins, respectively. Note that all properties related to the total systemic arterial vasculature are lumped to the aorta as a part of model simplifications, meaning that there is no practical difference in the model between the arterial system and the aorta ($C_{\text{sa}} \Leftrightarrow C_{\text{ao}}$). As before, C refers to compliance and P is blood pressure. Further, Q_{lvao} is the flow from the left ventricle (LV) to the aorta (systemic arteries), Q_{aosv} is flow from the aorta to the systemic veins and Q_{svlv} is flow from the systemic veins to the LV. Arterial and venous volumes are additionally modelled as linear functions of corresponding pressure based on Equation (2.7), i.e. $V = C \times P$, where C is respective compartmental compliance. Furthermore, blood flow between compartments is governed by corresponding pressure gradient and respective resistance according to the linear relation $Q = {}^{\Delta P}/_{R}$, which is Equation (2.2) rewritten. An additional effect is present in left ventricular flow, namely the effect of valves. As described in Section 2.1.2, valves ensure that the direction and timing of the flow are in accordance with the cardiac cycle, and they are therefore modelled as diodes. Consequently, LV-flow is linearly related to negative

pressure gradients, and 0 when $\Delta P > 0$ [4]. LV-pressure (P_{lv}) is approximated as linearly related to V_{lv}, i.e. $P_{lv} = E_{lv}(t) \times V_{lv}$, where $E_{lv}(t)$ is the time-varying elastance function (3.1). The complete system of equations and additional relations that constitute the hemodynamic model are found in Section A.1.1, and the computational implementation in Section A.3.1.

3.5.2 Numerical Scheme

The model ODEs (3.7) are solved by a 4^{th}-order Runge-Kutta scheme [4], as implemented in the python module `scipy.integrate`. The right hand side of the equation system is passed to the function `solve_ivp()`, with *method* = "RK45", *rtol* = 1×10^{-9} and *atol* = 1×10^{-10} as arguments. "RK45" implies that the error is controlled assuming accuracy of the 4^{th}-order method, but steps are taken using the 5^{th}-order accurate formulation [29]. Relative tolerance (*rtol*) controls the relative accuracy , i.e. the number of correct digits, while absolute tolerance (*atol*) controls absolute accuracy, i.e. the number of correct decimal places [29]. Remaining model outputs are further calculated directly based on ODE solutions of $P_{ao}(t)$, $P_{sv}(t)$ and $V_{lv}(t)$ by a set of algebraic equations (A.2).

3.5.3 Model States

The hemodynamic model simulates the CVS in either resting or exercise state. When model equations are solved for resting parameter values and heart rate (HR) equal to its resting value, $HR_{rest} = {}^{60}/_{T}$, the model is simulating *resting state*. *Exercise state* is simulated by setting model parameter $T = {}^{60}/_{HR}$ equal to the instantaneous exercise value and shifting certain baseline parameters, which is further described in Section 3.6.

The shifted parameters replace the initial (resting) values using the model function `set_pars()` (Section A.3.1), before the equations are solved as before. Now, the model is simulating exercise response at a constant intensity. Note that neither the physiological presence of beat-to-beat variations nor transitions between intensity levels are considered.

3.5.4 Initial Conditions

An initial value problem solver-algorithm such as `scipy.integrate.solve_ivp()` requires initial conditions. In general, solutions to ODEs are dependent on initial conditions. However, in this system, initial conditions are only partly adjusted to match different sets of inputs. Initial aortic pressure ($P_{ao,0}$) and left ventricular volume ($V_{lv,0}$) are, regardless of the baseline parameters, set to 100 mmHg and 100 mL, respectively [4]. Initial venous pressure ($P_{sv,0}$) depends on the resting parameters V_{tot}, C_{ao} and C_{sv},

and the initial aortic pressure and left ventricular volume, $P_{ao,0}$ and $V_{lv,0}$, according to Equation (A.4). This is to ensure that compliance-pressure-volume relations are not violated, and ensure that the sum of initial compartmental volumes equals V_{tot}. The initial conditions do not influence the outcome of the simulations beyond these considerations, because the ODEs are always solved over a time span that yields a converged, periodic solution, referred to as *steady-state*. The model does not consider the transient (short-term) part of the solution.

3.5.5 Time Interval

To reach steady-state, the ODEs must be solved over a time span that covers an adequate number of heart cycles. Here, 10 cycles are considered acceptable in resting state, when the heart period is at its maximum. Exercise reduces heart period, hence 40 cycles are chosen in exercise state to ensure that the final solution has converged to steady-state. In practice, this means passing a time span of *t_span* = $(0, \text{num}_{\text{cycles}} \times T)$ to `scipy.integrate.solve_ivp()`, where T is the heart period in the given model state.

3.5.6 Model Outputs

The model ODEs yields a continuous steady-state behaviour of left ventricular volume $V_{lv}(t)$, aortic pressure $P_{ao}(t)$ and systemic venous pressure $P_{sv}(t)$ over a cardiac cycle. From these solutions, waveforms of left ventricular pressure $P_{lv}(t)$ and flows between the left ventricle (lv), aorta (ao) and systemic veins (sv) are determined, denoted $Q_{lvao}(t)$, $Q_{aosv}(t)$ and $Q_{svlv}(t)$. A number of hemodynamic scalar properties are further derived from the waveform solutions, where systolic and diastolic pressures (P_{sys} and P_{dia}), stroke volume (SV) and cardiac output (CO) are the most important to capture accurately in a clinical setting. Monitoring SV and CO can reveal diseases and serious conditions such as heart failure [2]. The importance of the model capturing P_{sys} and P_{dia} is understood directly from the clinical ambition of the MyMDT model as a tool for managing hypertension, as stated in Chapter 1. An overview of the waveforms and properties that constitute a simulated cardiac cycle is provided in Table 3.2. The physiological understanding of these quantities were reviewed in Section 2.1.

Waveform ($y(t)$)	Unit	Equation
V_{lv}	mL	(3.7)
P_{ao}	mmHg	(3.7)
P_{sv}	mmHg	(3.7)
P_{lv}	mmHg	(3.1)
Q_{lvao}	mL/s	(A.2)
Q_{aosv}	mL/s	(A.2)
Q_{svlv}	mL/s	(A.2)

(a) Simulated waveforms of volume (V), pressure (P) and flow (Q).

Scalar (y)	unit	Calculation
P_{sys}	mmHg	$\max(P_{ao})$
P_{dia}	mmHg	$\min(P_{ao})$
P_{map}	mmHg	$\overline{P_{ao}}$
PP	mmHg	P_{sys} - P_{dia}
MVP	mmHg	$\overline{P_{sv}}$
V_{sys}	mL	$\min(V_{lv})$
V_{dia}	mL	$\max(V_{lv})$
SV	mL	V_{dia} - V_{sys}
CO	mL/min	SV×HR

(b) Scalar quantities describing a simulated cardiac cycle.

Table 3.2: Hemodynamic model outputs divided into simulated waveforms (3.2a) and scalars (3.2b).

3.6 Modelling Exercise State

This section emphasizes the mathematically treatment and implementation of exercise in the hemodynamic model. Simulation of hemodynamic exercise state is a distinct part of the model that to a less extent can rely on well established principles compared to resting state. Exercise state differs from rest in that certain model parameters are adjusted or shifted from their resting (baseline) value prior to solving the model equations. As stated in Section 1.2.1, a project objective is to investigate whether the current treatment of exercise yields reliable simulations. Potential adjustments regarding exercise state are suggested in Section 4.3. This section presents how exercise is treated in the model based on the internal description of the exercise model by Bjørdalsbakke [5]. Note that an additional exercise mechanism named *lusitropy* was established as necessary during the work on the Specialization Project in 2021 [6]. Lusitropy is not treated in [5], and is therefore not presented here, but instead elaborated on in Section 4.3.2 as a part of the investigation of exercise simulation conducted in this project.

3.6.1 Exercise Shifts

As described in Section 2.1.5, exercise generates a physiological response in the body that consequently changes the hemodynamic conditions in the CVS. To preserve adequate cardiac output during exercise, certain parameters must be shifted from their resting (initial) values. However, it is problematic to directly quantify and mathematically describe the acute impact of exercise on cardiovascular model

parameters compared to resting state, with the exception of heart period (T). In the exercise model [5], this issue is handled as follows: The load exerted on the CVS of an individual during exercise is quantified through the concept of exercise intensity (I). Thus, given a state of intensity in an individual, the exercise shift of a resting parameter $\theta \in [R_{\text{sys}}, E_{\max}, C_{\text{ao}}]$ is calculated by the means of a population-based curve fit. There is available literature on measured values of $R_{\text{sys}}, E_{\max}$ and C_{ao}during exercise, while it is less obvious how the behaviour of other, more model-specific parameters such as V_{tot} could be physiologically obtained or mathematically described, hence they are kept constant during exercise. The parameter shifts of $\theta \in [R_{\text{sys}}, E_{\max}, C_{\text{ao}}]$ are implemented as follows:

$$\theta_{\text{pers}}(I) = \theta_{\text{pers, rest}} \times \frac{\theta_{\text{pop}}(I)}{\theta_{\text{pop, rest}}}. \tag{3.8}$$

where subscript pers denotes a patient-specific value, while pop is a population average for the parameter at a given intensity. For the exercise model, the population averages are based on data reported by Chantler et al. [30], who measured a number of hemodynamic quantities across multiple heart rates in normotensive and hypertensive men and women. Thus, the exercise model takes account of sex and whether the individual is hypertensive or normotensive. Note that only normotensive settings are used in this project, as the clinical exercise trial was conducted on healthy participants. Reported values of $E_{\max}$ and C_{ao} are fitted to a quadratic polynomial $ax^2 + bx + c$, and R_{sys} to an exponential function in the form $a \times \exp\left(-\frac{(x-c)}{b}\right) + d$. Exercise intensity ($I$) can be defined in multiple ways depending on setting, purpose and available data. The following describes how the concept of intensity is currently treated in the MyMDT model [5].

3.6.2 Exercise Intensity

The clinical exercise trial reported intensities as the resistances in Watts against which the participants were cycling; $I \in [0,50,100,150]$ W. However, since the loading exhibited by the CVS due to cycling against a given resistance is highly individual, a more personal definition of intensity is used to simulate the hemodynamic exercise response. For this purpose, heart rate (HR) is often taken as a starting point. Because the heart constitutes the force that drives the cardiovascular circulation, instantaneous HR is an important hemodynamic parameter. In some contexts, HR is used directly to describe exercise intensity. However, to objectively compare the cardiovascular loading yielded by an increased HR across individuals, a normalized version of exercise intensity is beneficial. Resting heart rate ($\text{HR}_{\text{rest}} = {}^{60}/_{T}$, where T is resting heart period) is commonly accepted as an important parameter in quantifying exercise intensity, because in contrast to maximum heart rate ($\text{HR}_{\max}$), HR_{rest} is often related to fitness level. $\text{HR}_{\max}$ is on the other hand descriptive for how demanding maintenance of a given HR is for a specific indi-

vidual. The hemodynamic model defines exercise intensity as the difference between HR and HR_{rest}, normalized by the *heart rate reserve*; HRR=$HR_{max} - HR_{rest}$.

$$I_{HRR} = \frac{HR - HR_{rest}}{HRR} = \frac{HR - HR_{rest}}{HR_{max} - HR_{rest}} \tag{3.9}$$

R_{sys}, E_{max} and C_{ao} are scaled depending on I_{HRR} according to Equation (3.8).

HR_{rest} can be collected in a clinical setting by minimal effort, and there are several possible sources from which it can be determined, which is discussed in further detail in Section 4.3.4. It has been shown, e.g. by Quan et.al [31], that HR_{rest} is correlated with both cardiorespiratory fitness level and arterial stiffness, as illustrated in Figure 3.2. Arterial stiffness is in the hemodynamic model represented by aortic compliance (C_{ao}). Because compliance is directly related to blood pressure ($P = V/C$), it can be argued that including HR_{rest} in the definition of exercise intensity facilities personalized predictions of blood pressure during exercise.

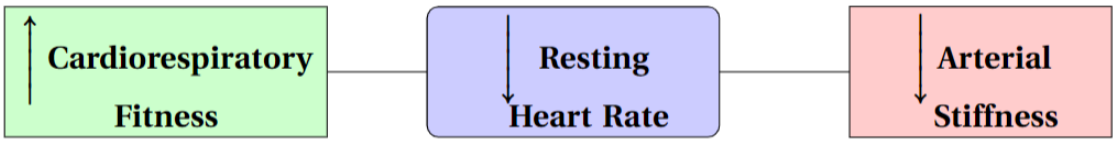

Figure 3.2: Pathways that illustrate the correlation between cardiorespiratory fitness, resting heart rate and arterial stiffness. Inspired by Figure 1 in [31].

Measuring maximum heart rate (HR_{max}) is exceedingly more cumbersome compared to HR_{rest}. Hence, for future practical applications of the hemodynamic model, it is more convenient that this parameter is estimated rather than measured. It is generally accepted that HR_{max} is primarily associated with age, and approximately unaffected by fitness level. The model uses the following simple and frequently used estimate:

$$HR_{max} = 220 - \text{age} \tag{3.10}$$

Chapter 4

Methodology for Development and Validation of the Hemodynamic Model

This chapter presents the project methodology for investigating selected aspects of the hemodynamic model (Chapter 3) according to the objectives stated in Section 1.2.1. Because preserving model simplicity is an important principle in MyMDT, this project aims to improve model performance by primarily adjusting previously implemented mechanisms and parameters, i.e. without increasing the level of complexity. As stated in Section 1.1.3, the majority of this work is based on data collected in a clinical exercise trial, hence the chapter is introduced with a brief review of this study. Particularly emphasized is how trial data is used in various parts of the project. Further, the model aspects that are subjected to investigation are presented in two parts; Section 4.2 elaborates on the parameter estimation procedure, while alternatives for the exercise simulation procedure are suggested in Section 4.3. Conditions and criteria against which model performance is evaluated are defined in Section 4.4. Finally, the chapter concludes with a summary of the procedures that constitute the methodological basis for the results presented in Chapter 5.

4.1 The Clinical Exercise Trial

This section describes the clinical trial "Mapping of Cardiac Power in Healthy Humans and Testing of a New Blood Pressure Sensor-a Pilot Study" [9], with emphasis on how preliminary processed data obtained from this study is used to evaluate the hemodynamic exercise model. Note that no direct processing of cardiovascular raw data has been done as a part of this project.

4.1.1 Study Characteristics

Cardiovascular data was collected 24 participants in resting state and while performing exercise on a bike. Exercise was performed at four intensity levels; [0, 50, 100, 150] Watts, and two positions; supine (sup) and semi-recumbent (sr). *Intensity* in this context refers to the resistance against which the participants were cycling, reported in Watts (W). This resistance resulted in an increased heart rate of varying magnitude, depending on the physiological condition of the participant. Clinical characteristics of the study cohort are presented in Table 4.1.

Characteristic	Unit	Total	Men	Women
n	-	24	11	13
Age	years	32.4 ± 6.6	28.5 ± 5.8	35.7 ± 5.8
Weight	kg	69.3 ± 10.5	77.4 ± 6.0	62.5 ± 8.4
Height	cm	172.1 ± 9.6	179.4 ± 6.0	165.9 ± 7.4
BMI	kg/m^2	23.6 ± 2.1	24.0 ± 1.4	22.7 ± 2.3
P_{sys}^{br}	mmHg	122.5 ± 11.3	127.5 ± 9.7	118.2 ± 10.9
P_{dia}^{br}	mmHg	80.3 ± 10.3	79.5 ± 10.5	80.8 ± 10.0

Table 4.1: Characteristics of the trial study cohort. Reported values are $\mu \pm \sigma$, where μ and σ denote mean and standard deviation, respectively. BMI is body mass index (BMI = $^{Weight}/_{Height^2}$). P_{sys}^{br} and P_{dia}^{br} are, respectively, systolic and diastolic pressures as obtained by brachial sphygmomanometry in resting state.

4.1.2 Resting State

Blood Pressure and Heart Rate

In resting state, carotid pressure signals and brachial pressure values were collected by tonometry and sphygmomanometry, respectively. Central aortic pressure (CAP) is in general the desired input for the personalized parameter estimation procedure, but as described in Section 2.1.4, CAP is in practice most commonly represented by peripheral pressure measurements. Carotid BP is in general a more accurate representation of CAP compared to more distal pressures, as shown in Figure 2.4. However, the tonometry method does not provide real pressure values, hence approximation of CAP from recorded data is conducted in two steps: First, the tonometry signal collected over a number of cardiac cycles is used to approximate the shape of the pressure waveform. Each tonometry cycle is interpolated to have the same number of points, and then averaged over the total number of cycles. The average resting heart period ($T = {}^{60}/_{HR}$) is simultaneously obtained as the average cycle period (T) from the tonometry signal. The

interpolated, averaged pressure signal is further normalized to span from 0 at minimum to 1 at maximum. Finally, the normalized carotid waveform (P_{norm}) is scaled to have similar systolic and diastolic magnitudes as obtained by brachial cuff sphygmomanometry:

$$P_{\text{rest}} = \left(\overline{P^{\text{br}}_{\text{sys}}} - \overline{P^{\text{br}}_{\text{dia}}}\right) \times P_{\text{norm}} + \overline{P^{\text{br}}_{\text{dia}}} \tag{4.1}$$

where $\overline{P^{\text{br}}_{\text{sys}}}$ and $\overline{P^{\text{br}}_{\text{dia}}}$ are, respectively, average values of systolic and diastolic pressures as measured by sphygmomanometry. P_{rest} is the resulting averaged, scaled pressure waveform to represent CAP in the participant during rest. Both sphygmomanometry and applanation tonometry are noninvasive methods, and their accuracy depend on the individual being as motionless as possible. Hence, these methods are not well suited for collecting pressures during exercise, and were therefore only conducted in resting condition.

Blood Flow

Blood flow between the left ventricle and the aorta (Q_{lvao}) passes through a tract denoted the left-ventricular outflow tract (LVOT). LVOT flow velocity (v_{lvot}) was recorded by the means of a Doppler ultrasound instrument. In general, Doppler velocity traces require some stages of processing to translate into a time series of actual, measured velocities. This work was initiated by cardiologist Dr. Hans Martin Flade after the trial experiments were conducted, but had unfortunately not finished in time to be included in the current project. Therefore, the following preliminary processed velocity traces are used:

- Semi-manually obtained traces processed by Straatman for six participants during the fall of 2021 [7], as introduced in Section 1.1.2. These participants are used in the primary part of this project, i.e. concerning development of the hemodynamic model.
- Preliminary semi-automatic traces conducted on site for 11 participants with EchoPac, which is a software for processing ECG data [32]. Five of these are used in the model validation experiments, conducted as a secondary part of this project. The remaining six are either already used in the development part, or their tonometry signals are of poor quality.

From the processed LVOT velocity signals, flow between the aorta and the left ventricle (Q_{lvao}) is obtained as

$$Q_{\text{lvao}} = v_{\text{lvot}} \times A_{\text{av}} = v_{\text{lvot}} \times \left(\frac{\pi}{4} \times D^2_{\text{LVOT}}\right) \tag{4.2}$$

where A_{av} is the cross-sectional area of the aortic valve. By approximating this area as circular, A_{av} is calculated from the diameter of the LVOT (D_{LVOT}), also measured by the Doppler instrument. For

each participant, 2–3 values of LVOT are available, hence the average is used. The translation between velocity traces and flow was done explicitly in this project for the EchoPac-processed participants used in the validation part, and by Straatman [7] for the six participants used to perform the development experiments.

From the flow time series, corresponding stroke volume (SV) is obtained as the area under the flow curve, approximated by the trapezoidal rule:

$$\mathrm{SV} = \int_T Q(t)\,dt \approx \frac{1}{2}\sum_{i=1}^{n}(t_i - t_{i-1})(Q_i - Q_{i-1}) \tag{4.3}$$

where t_i and Q_i are time and flow values over a heart cycle of duration T. The trapezoidal integral is calculated by the function `trapz()` implemented in the python module `numpy` (version 12.1.3) [33].

4.1.3 Exercise State

Blood Pressure and Heart Rate

In general, noninvasive measurements of blood pressure (BP) have significantly greater errors than invasive methods [34]. The quality and accuracy of invasive measurements are also expected to be less sensitive to motion, which is an important consideration when collecting BP during exercise. Invasive recordings of radial pressures were chosen as the most appropriate representation of BP in exercise state, as measuring BP invasively in the aorta is associated with greater risks. Therefore, radial measurements form the basis of comparison against which model performance is evaluated during exercise, despite being inherently different from CAP (Fig. 2.4).

BP was registered by invasive measurements in the radial artery synchronously with ECG recordings over a time span of ≈45 s at each intensity level [0,50,100,150] W. Recordings of BP and ECG were processed prior to the initiation of this project using parts of pre-existing software originating from [35]. This process is based on the following steps: The times of occurrence of QRS-complexes in the ECG (Fig. 2.3) are identified by the Pan Tompkins method, implemented as `pan_tompkins()` in `MATLAB` [36]. From this, the signal is split into individual cycles, and heart periods (T=60/HR) are obtained as the cycle lengths. The pressure signal is also split according to the ECG, but the timing of a QRS-complex does not correspond with the time of minimum pressure, so each cycle is further processed to identify the end-diastolic point following the R-peak. As an initial analysis focus, and in the context of this project, systolic and diastolic pressures (SP and DP) are of greater interest than the radial pressure waveform itself. SP and DP are thus obtained from radial raw data as, respectively, maximum and minimum values of each individual cycle. Thus, arrays of ECG heart rates, SP and DP for each participant and intensity

level are the results of interest from this process. Note that the translation from ECG and radial raw data to SP, DP and HR was done prior to the initiation of this project.

An initial examination of the arrays of SP, DP and HR yielded by the above process showed some irregular tendencies with a presence of outliers. Hence, for use in this project, the arrays are subjected to a filtering procedure. This is done by an interquartile range (IQR) method obtained from [37] as follows: A lower/upper limit is defined as the $25^{\text{th}}/75^{\text{th}}$ percentile minus/plus $1.5\times$IQR, where IQR is the interquartile range, i.e., the difference between the 75^{th} and 25^{th} percentile of the data. Outliers falling outside this interval are removed. The percentiles are identified by the function `quantile()` implemented in the python model `pandas` (version 1.3.3) [38]. Each array is filtered independently of the other. This means that values corresponding to the same point as an outlier are not automatically removed from the other arrays, as is it expected that all values significantly affecting the resulting statistical properties of an array will be detected by each respective filter. Implementation of the filtering procedure for this project is included in Section A.3.3.

As described in Section 3.6, the model uses heart rate (HR) as input to simulate exercise state. HRs obtained from ECG signals are used for this purpose to conduct validation experiments. For the six participants used in the development part of the project, HRs during exercise were additionally manually collected from averaged periods of the flow cycles by Straatman [7]. As manually obtained periods are assumed more reliable compared to the automatically collected ECG values, the flow periods are used for exercise simulations in the development experiments. All four intensity levels are simulated using HR as input. However, because the 0 W-intensity is considered a hemodynamic resting state, HR is set according to its instantaneous value, but no exercise shifts are conducted when simulating this state. Note that HR at 0 W might deviate from the resting HR obtained from the tonometry signal, resulting in a potentially non-zero calculated heart rate reserve-based intensity ($I_{\text{HRR}} \neq 0$). However, this is not considered an issue because the discrepancies are expected to be small, and the 0 W-state is in general not of primary interest.

Blood Flow

In addition to radial BP and ECG, Doppler velocity traces were also assessed at each intensity level in a similar procedure as described for resting state. At the time during which this project was conducted, velocity signals during exercise were only available through the six participants preliminary processed by Straatman [7], who also conducted the corresponding calculations from velocity to flow (4.2) and flow to stroke volume (4.3). These six participants are used in the primary part of this project, i.e. concerning model development, which is described in further detail in the remaining of the current chapter.

4.1.4 Summary of Project Database

Flow waves (Q_{lvao}) during rest are averaged over available values of stroke volume (SV), which depends on the number reported cycles. Further, flow and pressures are synchronized by pairing the flow with the pressure wave (P_{rest}), and rescaling the flow time interval to span the tonometry heart period. This project investigates two ways of defining this synchronization procedure (Section 4.2.2). Resulting flow wave (Q_{rest}) represents aortic flow for the participant in resting state. Further, Q_{rest} and P_{rest} are used to estimate a set of personalized resting parameters that forms the baseline for model predictions in exercise state. Exercise performance is compared against radial BP, and also SV when flow during exercise is available. Table 4.2 summarizes how each part of this project uses trial data. All identification numbers for the participants in the clinical trial have been randomly relabeled for use in this report.

Project part	Participants	P_{rest}	P_{ex}	Q_{rest}	Q_{ex}	HR_{ex}
I) Development	[734, 637, 248, 890, 219, 346]	Tonometry signal scaled by $P^{\text{br}}_{\text{sys}}$ and $P^{\text{br}}_{\text{dia}}$	Radial BP	Straatman	Straatman	From Q_{ex}
II) Validation	[745, 827, 241, 993, 722]			EchoPac	—	From ECG

Table 4.2: Summary of the project usage of trial data. Here, P_{rest} and Q_{rest} are used as input for the baseline parameter estimation procedure. Further, HR_{ex} is model input for simulating exercise, while P_{ex} and Q_{ex} are used as basis of comparison for model predictions.

4.2 Configurations for the Estimation of Model Baseline Parameters

As stated in Section 1.2.1, the first project objective is to identify configurations of the parameter estimation procedure that yield stable and accurate optimized waveforms of pressure and flow in resting state, in addition to facilitating reliable predictions of P_{sys}, P_{dia} and SV during exercise. In the following, one subsection is dedicated to each aspect of the estimation procedure (Section 3.4) that is investigated in this work. Suggestions are based on a combination of physiological cardiovascular properties described in Section 2.1, available data and empirical insights obtained throughout the work. Model simulations resulting from a selection of the suggested configurations are presented in Section 5.1.

4.2.1 Determination of Baseline Parameters

The estimation procedure aims to obtain a set of parameters that yields simulated pressure and flow waveforms (P_{ao} and Q_{lvao}) that best fits P_{rest} and Q_{rest} obtained from data collected in the clinical trial (Section 4.1). The accuracy of a given fit is quantified by the cost function defined in Equation (3.5). A total of 50 cycles of the optimization procedure is conducted in two rounds, and the final baseline parameters are obtained from the 20 final estimates as either:

1. Mean parameters:
   Averaged parameter values over the 20 final estimates with a resulting cost function less than the mean value for all 20.

2. Minimum parameters:
   The single set of the 20 final estimates with minimum cost function.

In general, a mean parameter fit will be more robust given that the variability within the 20 estimates is sufficiently low. This is ensured by constraints. When constraints are not applied, the 20 estimates might differ to an extent that makes the resulting average a meaningless fit. In such cases, the minimum parameters can be a more appropriate baseline than the corresponding mean fit.

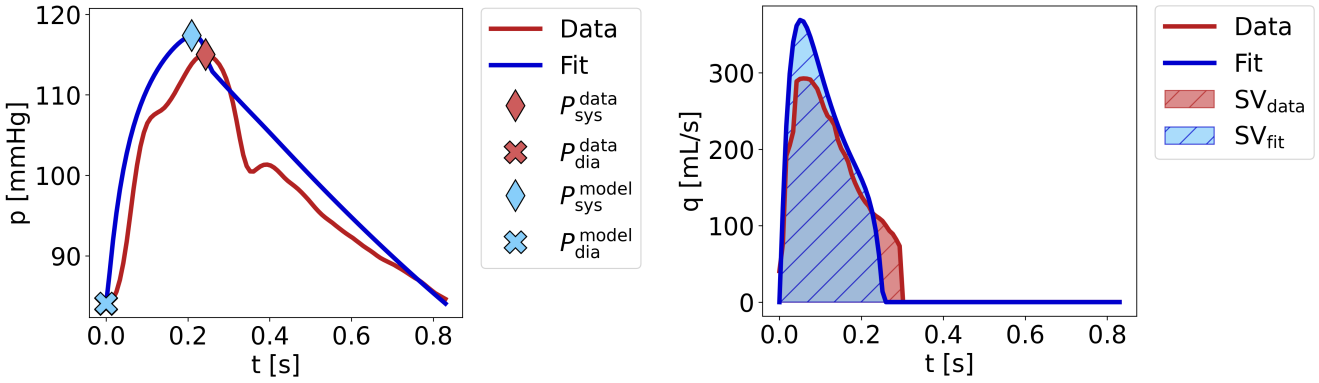

(a) Optimized pressure waveform.

(b) Optimized flow waveform.

Figure 4.1: Example of model fit to waveform data for pressure (4.1a) and flow (4.1b).

Figure 4.1 shows an example of optimized waveforms yielded by the estimation procedure. A resulting parameter fit is evaluated in terms of depicted waveforms and scalar properties P_{sys}, P_{dia} and SV.

4.2.2 Synchronization of Input Data for Pressure and Flow

Before conducting the optimization procedure described in Section 3.4, the pressure and flow data need to be synchronized. Together, they are to constitute correspondingly mapped representations of a single

cardiac cycle that are passed to the cost function (3.5). Ideally, a cardiac cycle presented by a measured flow wave is in unambiguous accordance with corresponding pressure. This implies that the aortic valve opens at the same time that arterial pressure exceeds diastolic pressure, i.e. the systolic phase is introduced simultaneously as read from both signals. Further, diastole begins with the closure of the aortic valve, which remains closed throughout the entire phase. This means that during diastole, there is no flow between the left ventricle and the aorta ($Q_{\text{lvao}} = 0$). The dicrotic notch on the aortic pressure wave is recognized as the closure of the aortic valve, which should therefore ideally correspond to the time at which flow drops to 0. However, when working with clinically measured data, this is often not the case, as can be seen in Figure 4.2. The cycle discrepancies are also natural consequences of the Doppler flows and tonometry pressures not being collected simultaneously in the trial. Therefore, a choice must be made whether to synchronize pressure and flow data according to:

1. Upstroke:

   Both waves defined to begin on upstroke, i.e. with the initiation of systole. Implemented in the original formulation.

2. Aortic valve closure:

   Agreement on timing of valve closure, i.e. the beginning of diastole. This implies using the dicrotic notch from the tonometry signal and the time at which flow drops to 0 as reference points for synchronization. Suggested and tested as a part of the current work.

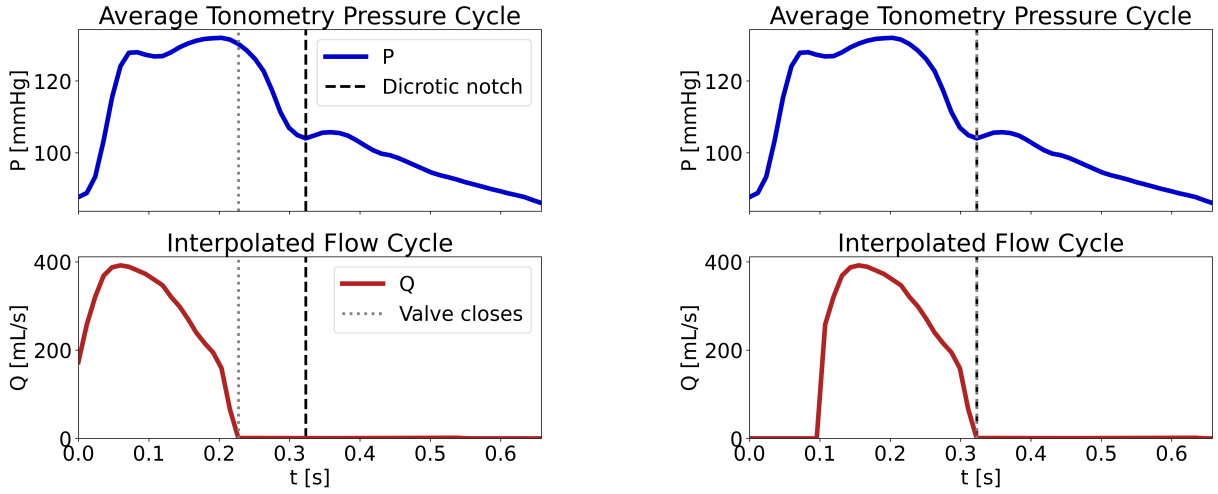

(a) Sync. to upstroke (1).

(b) Sync. to dicrotic notch (2).

Figure 4.2: Example of synchronized pressure (blue lines) and flow (red lines) according to alternative no. 1 (4.2a), i.e. both waves begin on upstroke, and 2 (4.2b), i.e. agreement on timing of valve closure (vertical lines). Potential discrepancy between valve closure read from the flow wave and the pressure signal is indicated by the horizontal space between the vertical dashed lines.

Which alternative appears as the best cycle representation varies across trial participants, as does the deviation between the dicrotic notch and the time of valve closure as read from flow. However, note that the choice of synchronization procedure is not only an issue of determining the most overall consistent representation of a cardiac cycle. It must also be considered how the synchronization coincides with cycle start as defined in the hemodynamic model, and the overall, combined impact on the parameter estimation procedure. This project investigates how cycle timing should be treated to optimize the fitting procedure, and this issue is addressed in Section 6.1.1.

Using the processed and synchronized pressure and flow signals as input, the estimation procedure is executed in three distinct steps: First, a preliminary fitting procedure is conducted to yield an initial estimate of the arterial parameters (R_{sys}, C_{ao} and Z_{ao}). Then, selected parameters are assigned to fixed values based on either literature or data. Finally, the main optimization procedure is executed. The following sections summarize these three steps with emphasis on the selected variations that are investigated in this project.

4.2.3 The Preliminary Fitting Procedure

A preliminary optimization is conducted in a similar manner as the main procedure described in Section 3.4, except that only one iteration is conducted, and it is based exclusively on the three-element Windkessel model, which represents the arterial compartment (Section 3.3.1). Aortic inflow (Q_{lvao}) is a driving function in this model, and venous pressure is neglected, i.e. set to 0. The preliminary fit yields initial estimates of C_{ao}, R_{sys} and Z_{ao} that are used as initial values in the following main optimization. Constraints used in the preliminary part are stated in Table 4.4.

4.2.4 Assignment of Fixed Parameters

Model parameters can be assigned to fixed values based on input data or literature, and are consequently not directly involved in the optimization. Minimum elastance (E_{min}) is fixed based on values reported by Segers et al. [39]. Mitral valve resistance (R_{mv}) has been manually tuned by Bjørdalsbakke et al. [4] based on synthetic test cases, and not further prioritized due to its low rank in sensitivity analyses by Bjørdalsbakke et al. and Aal [6]. Furthermore, T is obtained directly from data as the average value of all heart periods obtained from the tonometry signal ($\overline{T}_{ton}$). It is of interest in this project to investigate the effects of fixing vs. estimating the parameters t_{peak}, Z_{ao} and C_{sv}. For each of these, the following alternatives are evaluated:

- **Time of peak elastance (t_{peak}):**

  1. Estimated:
     Section 4.2.5.

  2. Fixed:
     Relate the determination of t_{peak} directly to the arterial pressure data. The time in the cardiac cycle at which ventricular elastance reaches its maximum (t_{peak}), occurs at the end of the systolic phase, as illustrated in the PV-loop in Figure 2.1. The end of systole is marked by the closure of the aortic valve, recognized as the dicrotic notch on the arterial pressure wave (Fig. 2.2). Fixing t_{peak} implies assigning its value to the time at which the dicrotic notch occurs in the tonometry pressure signal.

- **Aortic impedance (Z_{ao}):**

  1. Estimated:
     Section 4.2.5.

  2. Fixed:
     The preliminary fitting procedure reviewed in Section 4.2.3 yields an initial estimate of Z_{ao} to which the parameter can be fixed before the main optimization is executed.

- **Venous compliance (C_{sv})**

  1. Estimated:
     Section 4.2.5.

  2. Fixed:
     No data is available for the venous compartment from the clinical exercise trial. However, venous compliance is in general within the range of 10 to 20 times greater than arterial compliance [40]. Equation (2.9) yields an approximation of arterial compliance (C_a) from pulse pressure (PP) and stroke volume (SV), where PP and SV are obtained from arterial trial data. By assuming the presence of a pre-determined physiological relation between arterial and venous compliance, C_{sv} can be fixed depending on C_a; $C_{sv}^{fixed} = 10 \times C_a = 10 \times \frac{SV}{PP}$.

All fixed parameters are summarized in Table 4.3 along with their respective values and how these are obtained.

Parameter (θ) [unit]	θ_{fixed}
E_{min} [mmHg/mL]	0.035 [39]
R_{mv} [mmHg×s/mL]	0.006 [4]
T [s]	$\overline{T}(\boldsymbol{P}_{\text{ton}})$
t^*_{peak} [s]	$t\vert_{\text{dicrotic notch}}$
Z^*_{ao} [mmHg×s/mL]	$Z^{\text{prefit}}_{\text{ao}}$
C^*_{sv} [mL/mmHg]	$10 \times \frac{\text{SV}}{\text{PP}}$

Table 4.3: Summary of the fixed model parameters. $^*t_{\text{peak}}$, Z_{ao} and C_{sv} may instead be included in the main estimation procedure (Section 4.2.5).

4.2.5 The Main Estimation Procedure

Parameters that are not fixed according to the previous section are estimated to yield simulated pressure and flow waves optimized against arterial data. Estimated parameters are E_{max}, C_{ao}, R_{sys}, and V_{tot}, plus potentially t_{peak}, Z_{ao}, and C_{sv}. Constraints are included to avoid parameter values exceeding physiologically reasonable ranges. They are set primarily based on values reported in literature, which are extended to allow flexibility with regards to model fits. Empirical insights concerning observed model behaviour have also influenced the bounds. Table 4.4 shows the set of lower and upper bounds passed as constraints to `scipy.optimize.least_squares()` [28] for the estimated parameters. Details concerning how each specific limit has been determined are found in Table A.2. For the preliminary fitting procedure described in Section 4.2.3, constraints are equivalently defined with the exception of the upper bound of Z_{ao}, which is 1.0 $^{\text{mmHg}\times s/\text{mL}}$ in the preliminary optimization compared to 0.2 $^{\text{mmHg}\times s/\text{mL}}$ in the main part.

Param. (θ) [unit]	θ_{lower}	θ_{upper}
E_{max} [mmHg/mL]	0.50	$^{10.84}/_{\text{BSA}}$
C_{ao} [mL/mmHg]	0.148	2.256
R_{sys} [mmHg×s/mL]	$^{0.917}/_{\text{BSA}}$	2.963
V_{tot} [mL]	150	1503
C^*_{sv} [mL/mmHg]	4.44	67.68
Z^*_{ao} [mmHg×s/mL]	0.001	0.2 (1.0 for prefit.)
t^*_{peak} [s]	$\min\{0.15, 0.9 \times T\}$	$\min\{0.442, T\}$

Table 4.4: Constraints used in the numerical optimization. BSA = $\sqrt{\frac{\text{wt}\times\text{ht}}{3600}}$ is body surface area, where wt is weight in kg and ht is height in cm. $^*Z_{\text{ao}}$, t_{peak} and C_{sv} may be fixed according to Table 4.3, in which case the presented constraints are irrelevant.

As described in Section 3.4.2, minimizing the cost function (3.5) yields a set of optimized parameter values. To enhance the understanding of this algorithm and which solutions it searches, another implementation was attempted with $\theta > 0$ as the only constraint for all estimated parameters. Potential advantages and disadvantages associated with constraints are discussed in Section 6.1.3.

4.2.6 Regulation of Ejection Fraction

An issue with the estimation procedure highlighted during this project is that solutions can yield plausible optimized pressure and flow waveforms, while simultaneously displaying nonphysical behaviour in other hemodynamic quantities. This may in turn impede the ability to simulate a physiologically consistent exercise state. Quantities related to blood volume are particularly prone to varying and implausible behaviour. As stated in Section 3.3, the model treats only *stressed* blood volume. Hence, total volume V_{tot} and compartmental volumes of the systemic arteries, veins and the left ventricle (V_{sa}, V_{sv} and V_{lv}) are not explicitly associated with physiological quantities. Consequently, V_{tot} is originally very loosely constrained in the optimization (Table 4.4). An additional issue regarding volumes is that the model is not fitted against any direct ventricular data beyond LVOT-flow (Q_{lvao}), and stroke volume (SV) derived from this flow.

Test cases indicated a tendency of high estimated values of V_{tot} and correspondingly high end-diastolic and end-systolic volumes (EDV and ESV), which still fulfilled the target value of stroke volume (SV=EDV-ESV). This resulted in very low ejection fractions ($\text{EF} = \frac{\text{SV}}{\text{EDV}}$) (2.4). Physiologically, EF is normally 55 to 67% [10], while EF ≤ 40% indicates impaired cardiac performance and possibly heart failure [41], which unlikely was the case during the trial experiments. This project investigates ways of avoiding this improbable behaviour of EF. The direct control of EF is slightly problematic, as the physiological meaning of EF assumes total EDV, while there is no available trial data to calculate the unstressed part (V_0). A suggestion is to implement a penalty on the cost function (3.5) when the resulting parameter fit within an iteration yields an EF falling outside of an expanded physiological range. Two alternatives are investigated, both explicitly included in the implemented cost function provided in Section A.3.2.

I) Step Function

This alternative simply multiplies the cost function by a weight (W_{ef}) when EF exceeds a preset range defined by [EF_{min}, EF_{max}]:

$$J(\boldsymbol{\theta})_{\text{ef}} = \begin{cases} J(\boldsymbol{\theta}) & \text{if } \text{EF}_{\text{min}} \leq EF \leq \text{EF}_{\text{max}} \\ J(\boldsymbol{\theta}) \times W_{\text{ef}} & \text{otherwise} \end{cases} \tag{4.4}$$

where $J(\boldsymbol{\theta})$ is the resulting cost function for a given parameter fit ($\boldsymbol{\theta}$), and $J(\boldsymbol{\theta})_{\text{ef}}$ is the updated value after assessing the estimated EF. $[\text{EF}_{\text{min}}, \text{EF}_{\text{max}}]$ is set to an expanded physiological range of [35,75]%. As this is a very preliminary experiment with this type of intervention, a rather high value of $W_{\text{ef}} = 10^6$ is used to ensure that its effect becomes sufficiently pronounced. A potential problem with a hardmax implementation of this type is whether the stepwise boundary allows the optimization algorithm to search efficiently for solutions along the boundaries of EF. This issue motivated the following alternative.

II) Softmax Function

To avoid problems in the limits of EF, an alternative is to implement a softmax penalty function that progressively increases according to the distance between the boundaries and the estimated EF. This can be achieved with the function:

$$S(x, y) = \frac{1}{1 + \exp(\alpha(y - x))} \tag{4.5}$$

where α determines the smoothness of the transition from 0 to 1, set to 100 in this project. Thus, when x is less than y, the value approaches 0. When x is greater than y, the value approaches 1. The cost function is then updated as

$$J(\boldsymbol{\theta})_{\text{ef}} = J(\boldsymbol{\theta}) + (S(\text{EF}, \text{EF}_{\text{max}}) + S(\text{EF}_{\text{min}}, \text{EF})) \times \left(\text{EF} + \frac{1}{\text{EF}}\right) \times W_{\text{ef}} \tag{4.6}$$

where W_{ef} is a parameter that weights the influence of EF, set to 50 for the purpose of this experiment. Hence, the residual increases progressively if either EF gets too small ($\text{EF} < \text{EF}_{\text{min}}$) or too large ($\text{EF} > \text{EF}_{\text{max}}$). EF_{min} and EF_{max} are set equal to the hardmax limits, i.e. 35 and 75%, respectively. Constants α and W_{ef} were defined based on empirical testing to find a configuration that yielded plausible simulated waveforms, without jeopardizing the functionality of the optimization algorithm.

4.3 Configurations for the Simulation of Hemodynamic Exercise State

This section elaborates on the experimental evaluation of the simulated hemodynamic exercise state, conducted with the purpose of obtaining configurations that improves the reliability of the exercise predictions. Aspects treated are, consecutively, scaling of model pressures, the lusitropy mechanism, parameter shifts and definition of resting heart period. Explicit implementations of algorithms yielded by the methodological basis presented here are found in Section A.3.3.

4.3.1 Scaling of Model Pressures

An issue with using experimental measurements of blood pressure (BP) to evaluate performance of the hemodynamic model is that the exercise data from the clinical trial and the model principally represent BP at different sites in the arterial tree. As explained in Section 2.1.4, the model predicts central aortic BP, while the trial collected BP during exercise at the radial artery. Figure 2.4 illustrates the pressure amplification that is present between aorta and the radial artery. This implies that if the model is directly evaluated against radial measurements, systolic pressures (P_{sys}) will consequently appear underestimated, and diastolic pressures (P_{dia}) overestimated. As brachial measurements are expected to be more representative for aortic pressures compared to radial, a suggestion to remedy the inherent errors caused by amplification is using measurements from the sphygmomanometry to calculate scaling factors for model predictions of BP; one for each of P_{sys} and P_{dia}. The relative deviation between radial and brachial pressures at resting state is calculated as:

$$\epsilon_{\text{BP}} = \frac{\overline{\text{BP}}^{\text{0W}}_{\text{rad}} - \text{BP}^{\text{rest}}_{\text{br}}}{\text{BP}^{\text{rest}}_{\text{br}}} \times 100\% \tag{4.7}$$

where $\overline{\text{BP}}^{\text{0W}}_{\text{rad}}$ is the average radial measurement of P_{sys} or P_{dia} before the participant have begun exercising (i.e. at 0 W intensity). $\text{BP}^{\text{rest}}_{\text{br}}$ is the brachial value of P_{sys} or P_{dia} collected in resting state. By assuming that the relative deviation between radial and brachial BP at rest is representative also in exercise state, model predictions of BP can be scaled to increase the consistency with radial values according to:

$$\widetilde{\text{BP}}_{\text{model}} = \text{BP}_{\text{model}} \times \left(\frac{\epsilon^{\text{rest}}_{\text{BP}}}{100} + 1 \right) \tag{4.8}$$

where BP_{model} and $\widetilde{\text{BP}}_{\text{model}}$ are, respectively, original (aortic) and scaled (radial) model predictions of BP (P_{sys} or P_{dia}) at a given intensity level. An important assumption for this method is that the relative difference between radial and brachial pressures is approximately constant across exercise intensities.

4.3.2 The Lusitropy Mechanism

During the fall of 2021, medical engineering student H. Straatman raised attention to the vast importance of including lusitropy in the model implementation of exercise [7]. As explained in Section 2.1.5, lusitropy describes the relaxation properties of the heart during the diastolic phase. During exercise the heart rate is increased, and the diastolic period reduced. To preserve diastolic filling, the systolic activation period is reduced accordingly. These simultaneous mechanisms are highly involved and a full mathematical representation would require a complexity that is beyond the MyMDT model and its ambition. Essentially, lusitropy affects the timing of cardiac events. In addition to heart period, there is

one timing parameter in the hemodynamic; t_{peak}. Therefore, this section elaborates on how t_{peak} can be modified during exercise to represent the lusitropy mechanism.

Relating t_{peak} to Elecromechanical Systole

There exists scarce literature that quantifies the effect of lusitropy in the context of hemodynamic modelling. A study considered somewhat transferable was carried out in 1968 by Weissler et al. [13], who found a linear relation between the duration of electromechanical systole (QS_2) and heart rate (HR). As shown in Figure 2.3, QS_2 is read from an electrocardiogram (ECG) mapped to a tracing of heart sounds (PCG) as the interval between the initiation of the QRS-complex and the second heart sound (S_2) [13]. The MyMDT model does not have a parameter for QS_2 directly, and it is an important principle to keep the level of complexity and number of parameters to a minimum. However, the behaviour of model parameter t_{peak}, i.e. time of peak ventricular elastance, can be argued to be somewhat transferable to QS_2, as maximum ventricular elastance occurs at the end of systole (Fig. 2.1). Weissler et al. found that the length of QS_2 is inversely proportional to HR, and this effect is adapted to the model by implementing a linear scaling of t_{peak}:

$$\mathrm{t}_{\text{peak}}\,(\mathrm{HR}) = \mathrm{t}_{\text{peak}}^{\text{rest}} + b \times (\mathrm{HR} - \mathrm{HR}_{\text{rest}}) \tag{4.9}$$

which is similar to the relation between HR and the duration of QS_2 obtained by Weissler et al. [13]. As the magnitudes of QS_2 and t_{peak} are different, only the slope represented by the regression coefficient (b) has been adapted from the study. Here, b represents the level of reduction in the contraction phase of the cardiac cycle according to increasing HR, and the value obtained from Weissler et al. is b_{W} = -0.0021 s × min [13]. Lusitropy implemented according to Equation (4.9) with b_{W} was subjected to a sensitivity analysis during the Specialization Project in 2021 [6]. This analysis showed that b is one of the most influential model parameters during exercise, with a sensitivity $S_T(b)$ increasing with intensity.

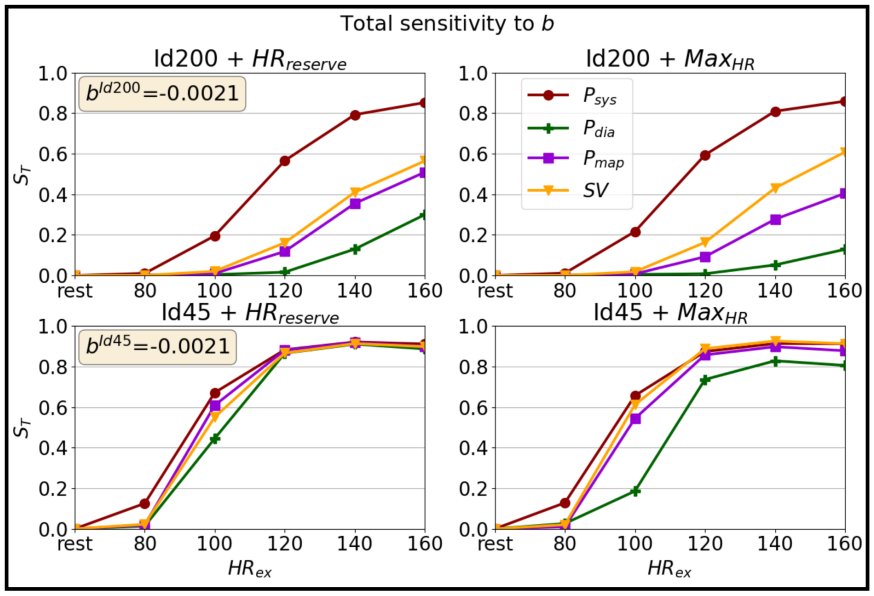

Figure 4.3: Model sensitivity to the lusitropy coefficient (b) resulting from the Specialization Project [6]. Here, b was analyzed as quasi-randomly sampled within an interval of $b_W \pm 50\%$. $HR_{reserve}$ and Max_{HR} refer to different definitions of exercise intensity. Note that the current project only considers intensity defined as I_{HRR}=$HR_{reserve}$. Figure obtained from [6].

Basing the Lusitropy Coefficient on Trial Data

As shown above, the Specialization Project indicated a prominent importance of the lusitropy coefficient (b) for model behaviour during exercise. The current project pursues these results by investigating alternative, trial-based versions of the lusitropy mechanism. A suggestion is to compare the lusitropy coefficient obtained from Weissler et al. with linear regression of systolic periods collected from the clinical exercise trial. Systolic periods in this context refer to left-ventricular ejection times (LVETs), which were obtained by Straatman [7] as the time from the upstroke of the aortic flow until it is zero again. Two alternatives for a trial-based implementation of lusitropy are presented:

1. Personal regression coefficient (b_{pers}):

   An individual coefficient $b = b_{pers}$ for each participant is obtained by linear regression between the points (HR_I,$LVET_I$), where I∈[0,50,100,150] W is intensity level. Outliers deviating from the remaining points are identified by a visual examination and further excluded from the calculation. The linear regression relation is obtained by the function `polyfit()` implemented in the python module `numpy` (version 1.21.3) [33], which yields a slope b_{pers}. Note that this alternative is not relevant for usage in the hemodynamic model, as it requires measurements that are in general unavailable for future MyMDT users. However, it is interesting to investigate whether this highly personalized version of the lusitropy mechanisms significantly improves model predictions.

2. General trial-based regression coefficient (b_{reg}):

   A more general, trial-based coefficient $b = b_{\text{reg}}$ is obtained similarly as presented above, except that all points (HR_I,LVET_I) for each participant and intensity level are included in the linear regression. Using b_{reg}, model predictions are compared against those yielded by b_{W}, i.e. b as reported by Weissler et al. [13]. By assuming a similar quantitative behaviour of QS_2 and t_{peak} across heart rates, this comparison can potentially reveal whether b_{W} represents a change in t_{peak} that facilities model predictions consistent with data. As there are relatively large uncertainties related to the LVETs obtained from the preliminary processed flow data, a brief literature study on systolic periods is further used to evaluate the quality and plausibility of the resulting b_{reg}.

4.3.3 Exercise Shifts of C_{ao}, R_{sys} and E_{max}

At the time at which this project was initiated, the exercise model was implemented with curve fits based on population averages reported by Chantler et al. [30] to shift the parameters E_{max}, R_{sys} and C_{ao} according to Equation (3.8). This implementation is written by Ph.D. Candidate Bjørdalsbakke through collaboration in the MyMDT project as a part of the development of the exercise model [5]. A potential issue regarding this highly general implementation of exercise is insufficiency in the context of predicting individual blood pressures across exercise intensities. Therefore, this project re-evaluates the Chantler-based exercise shifts with the aim of improving the reliability of the personalized model predictions. It is investigated whether alternative, data-based implementations of exercise shifts yield more accurate predictions of pressures and stroke volumes compared to the Chantler-based shifts. Note that because Chantler et al. [30] report sex-specific quantities, values of the population averages used in Equation (3.8) are determined by the sex of a participant. This is not accounted for in the trial-based shifts, as a cohort of six participants is considered too small for capturing variations yielded exclusively by sex. Further, as no data on the ventricular compartment is available from the clinical exercise trial, alternatives for shifting maximum elastance (E_{max}) are not investigated in this project. Note that remaining model parameters, i.e. C_{sv}, V_{tot}, R_{mv}, E_{min} and Z_{ao} are kept constant during exercise.

Aortic Compliance (C_{ao})

Arterial compliance decreases during exercise, which is related to the increase in arterial pressure [10]. Four alternatives a-d for modelling this reduction in C_{ao} during exercise are presented. Alternatives a. and d. are evaluated and compared in Section 5.2.3, where they are referred to as C1 and C2, respectively.

a. Chantler Shift:

This refers to the implementation developed by Bjørdalsbakke [5]. As described in Section 3.6.1, values of arterial elastance [30] are fitted to a quadratic polynomial, and shifted parameter values are yielded by Equation (3.8). During the fall of 2021, attention was raised to a potential error related to using arterial elastance from [30] to shift C_{ao} during exercise. Since compliance mathematically is the inverse of elastance, the approximation $C_{\text{ao}}^{\text{pop}} = \frac{1}{E_a}$ is taken as population data to use as input for the curve fit. However, E_a is defined by Chantler et al. as an *effective* elastance that incorporates peripheral vascular resistance, characteristic impedance, systolic and diastolic time intervals, as well as total lumped arterial compliance [30], while only the latter is included in the model parameter C_{ao}. This motivated the investigation of alternative implementations.

b. Personal Physiological Shift:

Arterial data is available through the clinical exercise trial, hence the physiological relation between arterial compliance (C_a), pulse pressure (PP) and stroke volume (SV) defined in Equation (2.9) is used to yield approximations of C_{ao} at each intensity level I$\in$[0,50,100,150] W. However, since PP is only available from radial measurements, values of C_a obtained in this way are not directly comparable to C_{ao} due to pressure amplification, as discussed in Section 4.3.1. Therefore, a shift is implemented where the percentage of change in SV/PP from the 0 W-value at each intensity is transferred to C_{ao}^0, i.e. the estimated resting value, which further yields a shifted C_{ao}:

$$\begin{aligned} \Delta_{(\text{SV/PP})} &= \frac{(\text{SV/PP})_I - (\text{SV/PP})_{0W}}{(\text{SV/PP})_{0W}} \\ C_{\text{ao}} &= \left(1 + \Delta_{(\text{SV/PP})}\right) \times C_{\text{ao}}^0 \end{aligned} \tag{4.10}$$

c. Personal Linearized Shift:

A literature search on the effects of heart rate (HR) on arterial compliance revealed a study by Liang et al. [42], reporting C_a in nine men at HR$\in$[56(rest),80,100] bpm. However, this study is not entirely transferable to this project, because HR was increased by atrial pacing instead of exercise, and all experiments were under the influence of *β-adrenoceptor blockade* after intravenous injection of metroprolol [42]. This is a medicine belonging to a group of drugs commonly known as *beta-blockers*. Beta-blockers impact the response to nerve impulses in certain sections of the body, which effectively decreases cardiac output, reduces arterial stiffness and reduces blood pressure [2]. Furthermore, it is probable that atrial pacing as stimulus impacts the CVS differently compared to exercise, as exercise activates several physiological response mechanisms in addition to increased HR. However, by similar argumentation as in the above paragraph, the *change* in compliance may be transferable, even though the specific values are not. Liang et al. [42] found that an increase in HR from 56 to 80 and 100 bpm decreased arterial compliance in an approximately linear manner until 50% of resting value at HR=100 bpm. This is a sig-

nificantly greater relative change compared to the development of $^1/_{E_a}$ reported by Chantler et al. [30], even though 100 bpm is within the range of a normal resting HR for an adult. Motivated by the results from Liang et al., and the physiological shifts obtained in point b., a linear compliance shift based on the relative change of $^{SV}/_{PP}$ from 0 to 150 W is calculated as:

$$\begin{aligned} \Delta_{(\mathrm{SV/PP})} &= \frac{(\mathrm{SV/PP})_{150W} - (\mathrm{SV/PP})_{0W}}{(\mathrm{SV/PP})_{0W}} \\ C_{\mathrm{ao}}^{\mathrm{pred}}(\mathrm{HR}_{150W}) &= \left(1 + \Delta_{(\mathrm{SV/PP})}\right) \times C_{\mathrm{ao}}^{0} \\ \boldsymbol{C}_{\mathrm{ao}} &= [C_{\mathrm{ao}}^{0}, C_{\mathrm{ao}}^{\mathrm{pred}}(\mathrm{HR}_{150W})],\ \mathrm{HR} = [\mathrm{HR}_{0W}, \mathrm{HR}_{150W}] \end{aligned} \tag{4.11}$$

where shifted values of C_{ao} as a function of HR are obtained by linear regression between the two points given by **HR** and $\boldsymbol{C}_{\mathrm{ao}}$ in Equation (4.11). The function `polyfit()` is used for this purpose, which is available through the python module `numpy` (version 1.21.3) [33].

d. Average Trial-Based Semi-Linear Shift:

The highly individual suggestions presented in point b. and c. above are not relevant for usage in the hemodynamic model, as they require measurements that are in general not available for future MyMDT users. These points are included primarily for comparison purposes and to investigate whether more personal shifts of C_{ao} benefits model predictions. This point (d) presents an average shift based on data collected in the exercise trial. Initial analyses of pressure and flow data showed a linear trend in $^{SV}/_{PP}$ across heart rates for most of the six participants used in the development experiments. Combined with the rapid linear decline in C_a reported by Liang et al. [42], this observation motivated the implementation of a semi-linear shift based on the average, relative change in $^{SV}/_{PP}$ between 0 and 150 W. This maximum change was paired with a heart rate reserve-based intensity of $I_{\mathrm{HRR}} = 0.6$. The mathematical implementation is similar to Equation (4.11), except that the relative changes are calculated for all six participants to yield an average value; $\overline{\Delta}_{(\mathrm{SV/PP})}$. Further, the linear regression is conducted between $[0, \overline{\Delta}_{(\mathrm{SV/PP})}]$ and $\boldsymbol{I}_{\mathrm{HRR}} = [0, 0.6]$ instead of C_{ao} and HR directly, as in the personal linearization presented in point c. The resulting relative change as a function of intensity ($\Delta_{(\mathrm{SV/PP})}(I_{\mathrm{HRR}})$), is then applied on the resting compliance (C_{ao}^{0}) in a participant to yield a shifted value at a given intensity:

$$C_{\mathrm{ao}} = \left(1 + \Delta_{(\mathrm{SV/PP})}(I_{\mathrm{HRR}})\right) \times C_{\mathrm{ao}}^{0} \tag{4.12}$$

Note that $C_{\mathrm{ao}}(I_{\mathrm{HRR}} > 0.6) = C_{\mathrm{ao}}(I_{\mathrm{HRR}} = 0.6)$ in this version of compliance shift.

Systemic Resistance (R_{sys})

As stated in Section 2.1.5, vascular resistance decreases during exercise. The issue is, as for arterial compliance, to quantify the personal level of reduction according to exercise intensity. Similar to the comparison of compliance shifts presented above, four alternatives a-d for shifting R_{sys} during exercise are presented. Alternatives a. and d. are evaluated and compared in Section 5.2.3, referred to as R1 and R2, respectively.

a. Chantler Shift

As before, this refers to the procedure developed by Bjørdalsbakke [5]. The resistance shift is based on population averages reported by Chantler et al. [30] fitted to an exponential function (Section 3.6.1). During the fall of 2021, it was problematized whether this implementation represents an optimal level of reduction in R_{sys} for the model. It was raised attention to a tendency of consistent overestimation of diastolic pressure (P_{dia}). The results from the Specialization Project [6] yielded a significantly greater sensitivity to systemic resistance, $S_T(R_{sys})$, for P_{dia} than P_{sys}. Therefore, a suggestion to remedy the overestimation of P_{dia} is to impose a greater reduction in R_{sys} during exercise compared to the shifts based on Chantler et al., which motivated the investigation of alternative implementations.

b. Personal Physiological Shift:

This alternative uses the physiological relation between total peripheral resistance (TPR), mean arterial pressure (MAP) and cardiac output (CO) (2.11) to examine the development of resistance during exercise as read from the trial data (TPR = $^{MAP}/_{CO}$). The approach is similar to point b. on compliance shifts, meaning that radial measurements of MAP yields a TPR calculated from Equation (2.11) that is not qualitatively transferable to the model parameter R_{sys}. Additionally, TPR also includes the resistance effect incorporated in the model parameter aortic impedance (Z_{ao}). Therefore, the relative change from the 0 W-value will be used in a similar manner as presented in Equation (4.10) for shifting arterial compliance.

c. Personal Scaled Chantler Shift:

The majority of the six participants showed a tendency of the relative change from 0 W in $^{MAP}/_{CO}$ being significantly greater than the changes yielded by the Chantler-shifted values of R_{sys}. Because the curve shapes appeared somewhat similar, a scaled version of the Chantler-based shifts is attempted. All resulting Chantler-shifted values, R_{sys}^{Ch}, for $I \in [50, 100, 150]$ W are scaled by a factor (ϕ) that yields identical

relative change between 0 and 150 W as present in $^{MAP}/_{CO}$ for each participant:

$$\begin{aligned}
\Delta_{(MAP/CO)} &= \frac{(MAP/CO)_{150W} - (MAP/CO)_{0W}}{(MAP/CO)_{0W}} \\
R_{sys}^{scaled,150W} &= (\Delta_{(MAP/CO)} + 1) \times R_{sys}^{0} \\
\Delta_{scaled,150W} &= \frac{R_{sys}^{scaled,150W} - R_{sys}^{Ch,150W}}{R_{sys}^{Ch,150W}} \\
\phi &= 1 + \Delta_{scaled,150W}
\end{aligned} \tag{4.13}$$

d. General Trial-Based Exponential Shift:

The personal shifts suggested in point b. and c. are, as discussed in the previous paragraph, primarily relevant for comparison and investigation purposes rather than practical. Thus, a suggestion using trial data to generate an average-based alternative to the Chantler shifts is presented in this point (d). When displaying the change in $^{MAP}/_{CO}$ relative to the 0 W-value against I_{HRR} for all six participants, it was observed that 734, 637, 248 and the 50 W-point for 219 were in prominent accordance with a coinciding exponential fit. The least-squares method `scipy.optimize.curve_fit()` [28] is therefore used to fit the data points of

$$\Delta_{\%}(I) = \frac{(MAP/CO)_{I} - (MAP/CO)_{0W}}{(MAP/CO)_{0W}} \times 100\% \tag{4.14}$$

for 734, 637, 248 and 219(50 W) at I[W]>0 to an exponential function $a \times \exp(-b \times x) + c$, where $x = I_{HRR}$. Since I_{HRR} can deviate from 0 at 0 W-intensity, the zero-points (0,0) are added manually to the arrays prior to the fit. Note that the exponential function has a different form compared to the Chantler-based resistance fit described in Section 3.6.1, but the methodologies differ primarily in the database used to yield the shifts. This trial-based curve fit yields a relative change of R_{sys} at a given I_{HRR}, and a shifted value is calculated from the resting parameter value (R_{sys}^{0}) as:

$$R_{sys} = R_{sys}^{0} \times \left(1 + \frac{\Delta_{\%}(I_{HRR})}{100}\right) \tag{4.15}$$

4.3.4 Resting Heart Period (T)

Resting heart period (T) as a model parameter is originally fixed to the average period extracted from the tonometry pressure signal. Attempts to change this definition of T as a baseline parameter were not prioritized in this project. In addition to this role, resting heart period is also a determinant of the heart rate reserve-based exercise intensity (I_{HRR}), as defined in Equation (3.9), which in turn impacts the magnitude of exercise shifts at a given heart rate. By contributing to the determination of I_{HRR}, $T = {}^{60}/_{HR}$ affects model predictions beyond its influence as a baseline parameter. From data collected in the clinical exercise trial, T as input in (3.9) can be determined as either of the following:

1. $\overline{T}_{\text{ton}}$:

   The trial session began with the extraction of pressure signals by applanation tonometry over a number of heart cycles. Resting heart period is approximated as the average time span for each cycle. This definition of T is equivalent to the fixed value from the parameter estimation procedure (Section 4.2.4).

2. $\overline{T}_{0\text{W}}^{\text{sup}}$:

   The first exercise was performed in a supine (sup) position. As described in Section 4.1, heart periods are available from ECG signals, and in some participants also from Doppler flow traces. Average period obtained at 0 W-intensity, e.g. before performing any actual exercise, is thus a possible candidate to use in the calculation of I_{HRR} (3.9).

3. $\overline{T}_{0\text{W}}^{\text{sr}}$:

   After performing exercise in the sup-position and a following break, the participants exercised in a semi-recumbent (sr) position. Similar to $\overline{T}_{0\text{W}}^{\text{sup}}$, the average heart period extracted at 0 W-intensity in the sr-position ($\overline{T}_{0\text{W}}^{\text{sr}}$) is another alternative value from which I_{HRR} can be calculated.

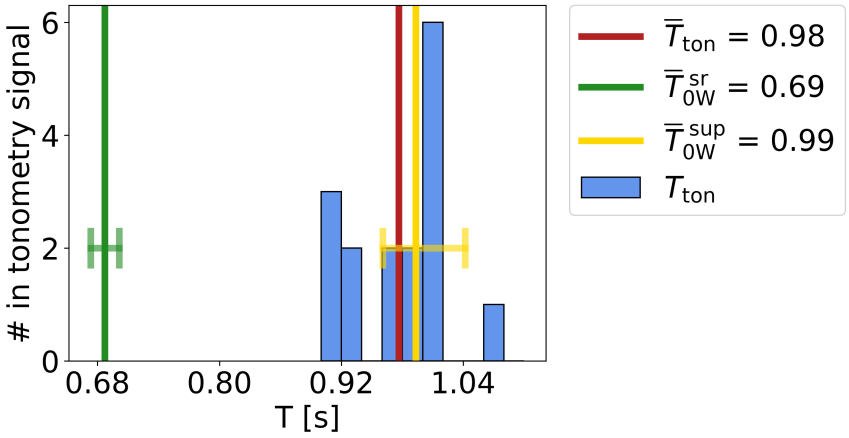

Figure 4.4: Example of how resting heart period varies with data source for one trial participant. The blue histogram shows the distribution of tonometry periods, and the red line is the average value defined as the baseline T. Green and yellow vertical lines represent the average periods collected at 0 W in the sr- and sup-position, respectively. The horizontal lines span between minimum and maximum period obtained from corresponding data source.

Figure 4.4 illustrates how the value of T varies based on data source. Note that no exercise shifts are performed at 0 W-intensity. As previously stated, a reduction in heart period will consequently reduce the diastolic filling. Without any mechanisms implemented to counteract this effect at 0 W, e.g. lusitropy, a potential issue is a diminished cardiac output in this state if $\overline{T}_{0\text{W}}^{\text{sr}} < \overline{T}_{\text{ton}}$, resting period is $\overline{T}_{\text{ton}}$ and sr-data is used. However, this is not considered problematic, as the predictions related to the higher intensities are of primary interest, and not the 0 W resting state itself.

4.4 Evaluation and Validation of Model Performance

This section defines the premises, metrics and requirements against which the performance of the hemodynamic model is evaluated. First, performance measures for the parameter estimation and the exercise simulation procedures are presented separately. Further, error metrics used for evaluation and validation of the model are defined. Validation criteria are suggested at the end of the section.

4.4.1 The Parameter Estimation Procedure

The parameter estimation procedure, whose potential configurations were suggested in Section 4.2, is evaluated based on how the resulting baseline parameters perform against the following measures:

- Deviations between model and data:

  1. Arterial pressures.
     Simulated systolic and diastolic pressures (P_{sys} and P_{dia}) are compared to values obtained by brachial sphygmomanometry in the clinical trial.

  2. Stroke volume (SV).
     Simulated SV are compared to average values of integrated Doppler flow waves (4.3).

  P_{sys}, P_{dia} and SV are the cardiovascular quantities that constitute the most important performance indicators for the hemodynamic model, hence these outputs are heavily weighted when evaluating any model configuration in both resting and exercise state.

- Visual evaluation of optimized waveforms.
  A visual examination of the optimized waveforms of pressure and flow is effective to verify the quality of a given parameter fit. Further, a fitted flow wave can exhibit implausible behaviour despite its area, i.e. estimated SV, being consistent with data.

- The behaviour of non-measured model outputs:

  1. Mean venous pressure (MVP).

  2. End-diastolic and end-systolic volumes (EDV and ESV).

  The model is not specifically constructed to yield physiologically accurate predictions of MVP, EDV and ESV, nor can they be directly fitted or compared against data from the clinical exercise trial. However, as they provide insights into simulated venous return and diastolic filling, important information on model behaviour and limitations can be obtained by evaluating outputs of MVP,

EDV and ESV. EDV is also a determinant of ejection fraction (EF), which is an important measure of cardiac function and its interconnection with the vascular compartments.

- Whether estimated parameters reflect personal cardiovascular properties.
  If a parameter intended to reflect an individual property is estimated equally across participants, there is reason to investigate the impact of constraints on the estimation procedure, and potentially also the entire function of this parameter in the hemodynamic model.

- Parameters R_{sys}, C_{ao} and E_{max} in relation to their direct, data-based approximations.
  As described in Section 2.1.3, these parameters can be directly approximated using arterial data; $R_{sys}=\frac{MAP}{CO}$, $C_{ao}=\frac{SV}{PP}$ and $E_{max}=\frac{P_{dn}}{ESV}$. In general, it is not necessary that these parameters are estimated identical to their physiological equivalents, but a comparison can be useful to evaluate whether the optimization procedure is able to capture physiological differences across participants. Note that a realistic comparison of E_{max} is unobtainable, as there is no data available on ESV. Therefore, this estimate will use Equation (2.4) and an assumed ejection fraction (EF) of 60% to yield an approximated value of ESV.

- Predictive performance during exercise.
  A set of baseline parameters can accurately fit the arterial flow and pressure waveforms in resting state, while simultaneously providing quite disagreeable exercise predictions. Therefore, a preliminary evaluation of the performance of a given baseline set during exercise is an important criteria against which the estimation procedure itself is evaluated. Evaluation criteria concerning exercise state are presented in the following section.

4.4.2 Exercise Simulation Procedure

The aims of investigating both the parameter estimation procedure and the exercise model are coinciding with the ultimate purpose of this project, i.e. improving the predictive performance of the model during exercise on a personal level. This requires both a set of resting (baseline) parameters that captures the necessary properties of an individual CVS, and an exercise model that reflects the hemodynamic response to exercise. A given configuration of the exercise model (Section 4.3) is evaluated based on the following:

- Predictions of the hemodynamic quantities of primary interest in relation to trial data:

  1. Arterial Pressures.

     Model predictions of systolic (P_{sys}) and diastolic (P_{dia}) pressures are evaluated against radial measurements.

  2. Stroke volume (SV).

     Model predictions of SV are compared to values calculated from integrated Doppler velocity signals (4.3). As the uncertainty related to measured SV is quite pronounced, especially at higher intensities, a plot of the stroke volume index (SVI) reported by Chantler et al. [30] is included to verify the plausibility of measured SV. To ease the comparison of SVI to trial data, values of SVI are shifted to start at HR_{0W} and SV_{0W} in accordance with the given participant. This implementation is included in Section A.3.4.

- Simulated behaviour of:

  1. Pulse pressure (PP).

     PP can be read directly from a plot of arterial pressures, but the quantity is extracted separately to explicate the simultaneous variations in P_{sys} and P_{dia} during exercise. Note that the behaviour of PP is related to that of SV through Equation (2.9).

  2. Mean venous pressure (MVP).

     Simulated changes of mean venous pressure (MVP) over heart rates are compared to literature-based data for central venous pressure (CVP), i.e. the pressure in the vena cava. As indicated in Section 2.1.5, the role of the venous compartment and its relation to the arteries and the heart is highly complex, and the hemodynamic model is merely an approximation of some of these central mechanisms. Despite lack of trial data for venous pressures, simulated MVP can be useful to evaluate whether the model is able to capture the physiological increase in cardiac preload during exercise. MVP and CVP are not directly comparable, hence model predictions of MVP during exercise are compared to the development of MVP if the relative changes from the resting value were in accordance with CVP reported by Yoshiga et al. [43]. This study measured CVP using a catheter advanced to the right atrium in male participants performing exercise in the forms of rowing and running. Due to the significant impact of gravity on venous pressure [2], the values collected during rowing is considered most comparable to predictions of MVP made by the model, which does not account for gravitational effects. The implementation of this comparison is included in Section A.3.4.

3. End-systolic and end-diastolic volumes (ESV and EDV).
   Left ventricular volumes ESV and EDV are included in the evaluation of exercise simulations to obtain insights considering distribution of blood during exercise in the closed-loop model. This can potentially indicate structural aspects of the model that make simultaneous physiological behaviour in certain variables numerically impossible, which is discussed in further detail in Section 6.2.6

As stated in Section 4.4.1, PP, MVP, EDV and ESV are quantities that, with the exception of PP, there is no data from the exercise trial against which model predictions can be evaluated. Still, they are considered important in the context of achieving a complete understanding of the hemodynamic exercise model, its limitations and potential for improvement.

4.4.3 Error Metrics

The error metrics used to evaluate and validate the hemodynamic model are mean absolute error (MAE) and bias. The specific way in which these metrics are calculated is highly important in the context of interpreting the resulting values, e.g. the error of the mean does not necessarily equal the mean of the errors, particularly in a nonlinear system such as the hemodynamic model. Thus, the following explicitly states how MAE and bias are calculated from model predictions and data in this project.

1. Mean Absolute Error (MAE):
   For a participant (i) in a given state (intensity and position), MAE is calculated as the absolute deviation between the average model prediction of a quantity (Y^i_{pred}) and the corresponding average measurement $\overline{Y^m}$. Here, Y is either radial systolic or diastolic pressure (P_{sys} or P_{dia}) or stroke volume (SV). For the purpose of evaluating model performance, an average MAE of model outputs Y is calculated across N included participants as:

$$\mu_{\text{MAE}} = \frac{1}{N}\sum_{i=1}^{N}\left|\ \overline{Y^m}^i - Y^i_{\text{pred}}\right| \tag{4.16}$$

   where $\overline{Y^m}^i$ is collected for one participant (i) obtained at an intensity level I$\in$ [0,50,100,150] W. It represents either $\overline{\text{BP}^m_{\text{rad}}}^i$, i.e. the average value of filtered radial pressure measurements of P_{sys} or P_{dia}, or $\overline{\text{SV}^m}^i$, i.e. average SV. Corresponding model prediction (Y^i_{pred}) is calculated using the average heart rate at the given intensity level, collected from data according to Table 4.2. Further, N is the number of participants evaluated, i.e. $N_{\text{I}} = 6$ and $N_{\text{II}} = 5$ for the development (I) and validation (II) parts, respectively. In the latter case, individual errors for each participant are presented in addition to the mean error (μ_{MAE}), which is the only quantity reported from the development experiments.

2. Bias

   Bias (2.18) is calculated similarly as MAE, except that the sign is preserved by not taking the absolute value of the deviation between measurement and model prediction.

MAE summarizes model performance while disregarding the difference between an underprediction and an overprediction. This difference is preserved by bias, which can in contrast to MAE reveal model tendencies of over or underestimation. If errors are approximately symmetric about 0, bias can yield misleadingly low errors, in which case MAE is preferable. In this project, bias is calculated when the model unambiguously either over or underpredicts a certain quantity across all participants. In cases where the configurations subjected to comparison alternates between over and underestimation, MAE is selected as error metric. Note that in practice, the latter appeared as the case during in silico experiments on all configurations with the exception of pressure scaling, which is shown in Section 5.2.1.

4.4.4 Validation Criteria

A reasonable targeted level of accuracy for the hemodynamic model is that errors are kept within the same tolerance as considered acceptable for clinical methods of measurements. Sphygmomanometers, the dominating class of instruments for measuring blood pressure, are identified as inaccurate when the error exceeds ±3 mmHg [44]. Thus, an error of ≤3 mmHg is acceptable also for model predictions of pressure. Stroke volume is in general associated with greater uncertainties than pressures. Trial measurements of SV are based on integrating aortic flow (4.3), which was obtained by a Doppler ultrasound instrument that measured blood velocity in the left ventricular outflow tract. The Doppler method uses an ultrasound probe that is manually placed on the skin of a patient. Hence, deviations in the Doppler angle of the probe may occur, resulting in inaccurate velocities [45]. Inaccuracies are then transmitted directly to SV when solving the integral (4.3). Therefore, a deviation of ±10%, i.e. in the size order of ≈10 mL, is a commonly accepted level of tolerance when measuring SV in clinical settings.

It is noted that these criteria might be somewhat strict for the hemodynamic model. Prediction errors must be evaluated also in the perspective of data variability, especially for higher intensities, hence standard deviations of relevant measurements are tabulated along with resulting errors in Chapter 5. Further, model pressures are evaluated by comparing radial measurements to model predictions scaled to mimic properties of the radial artery, thus the criteria defined for brachial sphygmomanometry might not be suitable for this usage. However, at the current stage of model development, the criteria are considered more as guidelines for targeted accuracy than absolute limits.

4.5 Summary of Project Procedure

To close the current chapter on methodology, this section provides a summary of the procedures from which the results presented in Chapter 5 are generated. One subsection is dedicated to each of the two main parts of the project; I) development and II) validation, and corresponding usage of trial data is found in Table 4.2. All programming is performed in `Python` (version 3.9.6) [46].

4.5.1 Model Calibration and Development (I)

This part of the project is conducted on six participants from the clinical exercise trial; 734 (M29), 637 (F42), 248 (F27), 890 (F29), 219 (M28) and 346 (M35). The sex (M=male and F=female) and age of the participants are indicated in the parenthesis. In accordance with the project objectives stated in Section 1.2.1, this part is investigated in a subdivided manner; i) the parameter estimation procedure and ii) the exercise simulation procedure. Note that the following exclusively describes the simulations conducted to yield the specific results included in Chapter 5, which emphasizes aspects that highlight the project objectives by promoting the identification of implementations beneficial for model improvement. Therefore, the following steps are composed through comprehensive testing in multiple configurations that are not explicitly illustrated, but still included in the discussion (Ch. 6).

i. The Parameter Estimation Procedure:

- Five variants of the parameter estimation procedure are explicitly compared in Chapter 5. Attributes defined equal are stated after the following enumeration, which characterizes the baseline cases and how they differ. The process and reasoning from which these configurations have been determined are elaborated on in Chapter 6.

  1. Full estimation:

     ➢ E_{max}, R_{sys}, C_{ao}, C_{sv} and V_{tot} are estimated with constraints (Table 4.4).

     ➢ Mean parameters are chosen as baseline (Section 4.2.1).

  2. No constraints:

     ➢ E_{max}, R_{sys}, C_{ao}, C_{sv} and V_{tot} are estimated with $\theta > 0$ as only constraints.

     ➢ Minimum parameters are chosen as baseline (Section 4.2.1).

3. Regulate EF:
   - ➢ E_{max}, R_{sys}, C_{ao}, C_{sv} and V_{tot} are estimated with $\theta > 0$ as only constraints.
   - ➢ A penalty is imposed on the cost function if the simulated ejection fraction (EF) $\notin [35, 75]$ %. The step function (4.4) and a weight of $W_{ef} = 10^6$ is used.
   - ➢ Mean parameters are chosen as baseline (Section 4.2.1).
4. Fix C_{sv}:
   - ➢ C_{sv} is fixed to $10 \times \frac{SV}{PP}$ (Section 4.2.4).
   - ➢ E_{max}, R_{sys}, C_{ao}, and V_{tot} are estimated with constraints (Table 4.4).
   - ➢ Mean parameters are chosen as baseline (Section 4.2.1).
5. Fix C_{sv} + regulate EF:
   - ➢ C_{sv} is fixed to $10 \times \frac{SV}{PP}$ (Section 4.2.4).
   - ➢ E_{max}, R_{sys}, C_{ao}, and V_{tot} are estimated with constraints (Table 4.4).
   - ➢ Regulation of EF similarly to case no. 3 (Regulate EF).
   - ➢ Mean parameters are chosen as baseline (Section 4.2.1).

- The following apply for all five configurations:
  - ➢ Pressure and flow waves are synchronized to upstroke (Section 4.2.2).
  - ➢ t_{peak} is fixed to the dicrotic notch (Section 4.2.4).
  - ➢ The preliminary fitting procedure is always performed (Section 4.2.3).
  - ➢ Z_{ao} is fixed to its preliminary estimated value.
  - ➢ E_{min}, R_{mv} and T are fixed according to Table 4.3.
- Results comparing these five configurations are presented in Section 5.1 as follows:
  - ➔ Optimized waveforms of pressure and flow (Section 5.1.1).
  - ➔ Resulting parameter estimates of the ten baseline parameters (Section 5.1.2).
  - ➔ Model outputs of P_{sys}, P_{dia}, SV, MVP, EDV and ESV (Section 5.1.3).
  - ➔ Exercise simulations for participants 734 and 890 and plot of average MAE (Section 5.1.4).

ii. The Exercise Simulation Procedure:

The exercise simulation procedure is evaluated by a stepwise presentation of selected configurations from Section 4.3. Each aspect of the procedure is analyzed with the remaining fixed to one or a selected few configurations. Results from the following simulations are found in Section 5.2

➔ Scaling of model pressures.

Bias of scaled (4.8) vs. non-scaled model predictions of pressure are presented in Section 5.2.1. Parameter case no. 3 (Regulate EF) is used as baseline. Errors are averaged over all six participants.

➔ The lusitropy mechanism.

The effect of the lusitropy mechanism and corresponding value of coefficient b is illustrated in Section 5.2.2. An explicit exercise simulation is depicted for participant 890. Average values of MAE are further presented for P_{sys}, P_{dia} and SV. Parameter case no. 3 (Regulate EF) is used as baseline for comparing the following three values of b:

0. b=0 ⟶ Absence of lusitropy.
1. $b = b_W = -0.0021$ s × min. Implementation according to Equation (4.9) with b as reported by Weissler et al. [13].
2. $b = b_{reg}$. Implementation according to Equation (4.9) with b obtained by linear regression of recorded ejection intervals (LVETs) for six trial participants. An illustration of the general and personal, trial-based regression coefficients is provided (Fig. 5.7), along with a comparison against other literature-based values (Table 5.3).

➔ Exercise shifts of C_{ao} and R_{sys}.

The shifting procedure is presented by explicit exercise simulations for participants 734 and 890 using baseline case nos. 3 (Regulate EF) and 4 (Fix C_{sv}). MAE of P_{sys}, P_{dia} and SV averaged over all six participants are further presented. Four configurations a-d for shifting each of C_{ao} and R_{sys} were presented in Section 4.3.3, and resulting shifted parameter values yielded by each alternative are illustrated in Figure 5.10. However, only the following two alternatives for shifting each parameter are used to yield explicit exercise simulations in Section 5.2.3:

➢ Shift of C_{ao}:

1. Chantler-based shifts (C1). Implemented by Bjørdalsbakke [5] and based on population averages from Chantler et al. [30].

2. Average trial-based semi-linear shift: (C2). Obtained by linear regression of average relative changes in $\frac{SV}{PP}$ from the clinical exercise trial. Corresponding to point d. for compliance shifts in Section 4.3.3.

➢ Shift of R_{sys}:

1. Chantler shifts (R1). Implemented by Bjørdalsbakke [5] and based on population averages from Chantler et al. [30].

2. General trial-based exponential shift (R2). Obtained by exponential regression of relative changes in $\frac{MAP}{CO}$ in selected participants from the clinical exercise trial. Corresponding to point d. for resistance shifts in Section 4.3.3

In the following, attributes that apply for all exercise simulations shown in Chapter 5 are stated. Note that this includes also the preliminary exercise simulations conducted as a part of the evaluation of baseline configurations as well as the model validation (Section 4.5.2).

➢ Shift of maximum elastance (E_{max}) as implemented by Bjørdalsbakke [5], i.e. using Equation (3.8) and population averages reported by Chantler et al. [30].

➢ Unless stated otherwise, Chantler-based exercise shifts of C_{ao} and R_{sys} are used, as this is used in the original formulation of the exercise model [5].

➢ Unless stated otherwise, model pressures are scaled according to Equation (4.8).

➢ Resting heart period used to calculate exercise intensity (3.9) is the same as the baseline parameter ($T = \overline{T}_{ton}$), i.e. obtained from the tonometry pressure signal.

➢ All trial data used is for the semi-recumbent (sr) position only. Data collected in the supine (sup) position is not used in this work.

➢ Unless stated otherwise, the lusitropy mechanism is implemented according to Equation (4.9) with $b = b_{reg}$, i.e. corresponding to point no. 2 in the enumeration of lusitropy coefficients presented above.

4.5.2 Model Validation (II)

Based on part I, a final number of model configuration are selected for the validation experiments, which are performed on five new trial participants; 107 (M39), 359 (F43), 447 (F40), 708 (F38) and 959 (F35). None of these are used for development and calibration purposes, which is an important principle of model validation. Estimation case no. 3 (Regulate EF) is selected to obtain baseline parameters for the validation experiments, and the three exercise configurations enumerated below are compared. The process and reasoning from which these selected configurations were determined are elaborated in Chapter 6. Note that the labels representing exercise shifts in this part, i.e. Cj and Rk, i,k∈[1,2], and the baseline case (no. 3), refer to identical procedures as stated in Section 4.5.1.

1. C1+R1:
   - ➢ C1: Chantler-based shift of C_{ao}.
   - ➢ R1: Chantler-based shift of R_{sys}.
2. C2+R1:
   - ➢ C2: Average trial-based semi-linear shift of C_{ao}.
   - ➢ R1: Chantler-based shift of R_{sys}.
3. C1+R2:
   - ➢ C1: Chantler-based shift of C_{ao}.
   - ➢ R2: General trial-based shift of R_{sys}.

The validation considers the behaviour of simulated blood pressures P_{sys} and P_{dia} during exercise. As stated in Table 4.2, no flow data had been processed for these participants at the time during which this project was conducted, hence stroke volumes are not considered in this part. Results from the validation experiments are presented as individual and average mean absolute errors (MAEs) of P_{sys} and P_{dia}, which are calculated according to Section 4.4.3. Individual MAEs for all five participants are tabulated at each intensity level along with the standard deviation of the respective radial pressure measurement.

For P_{sys}, MAE in a given state is additionally compared to the absolute deviation yielded by a simplified prediction based on end-systolic pressures (ESP) reported by Chantler et al. [30]. Since the heart rates from [30] do not necessarily overlap with those obtained for a given trial participant, the Chantler-based prediction is made by first converting the reported heart rates into heart rate reserve-based intensities using Equation (3.9). Further, the instantaneous intensity in a participant is interpolated to the array

of ESP-values using the function `interpolate()` implemented in the python module `numpy` (version 12.1.3) [33]. Similarly to model predictions of pressures, the Chantler-based predictions are also scaled (4.8) to equate the basis of comparison with radial measurements. Note that this prediction is potentially quite unreliable, as the heart rate used as HR_{max} in (3.9) is taken as the highest reported average heart rate, which does not represent a realistic maximum. Furthermore, ESP is not entirely the same as P_{sys}, as arterial pressure declines between the time at which the peak is reached (P_{sys}) and the aortic valve closes (ESP). Still, this rough comparison is considered an informative tool to investigate whether the personalized and presumably more accurate hemodynamic model actually performs better than average and simplified predictions. The implementation of this comparison is included in Section A.3.4.

Chapter 5

Results

This chapter presents results generated by the methodological basis summarized in Section 4.5, with the purpose of efficiently highlighting the project objectives. Hence, all configurations presented in Chapter 4 are not explicitly illustrated, but empirical insights concerning every suggestion are discussed in the following chapter (Ch. 6). The results are organized in three sections, where the first two contain in silico experiments conducted with the aim of developing the hemodynamic model towards its clinical ambition, i.e. concerning the main part of this project. Section 5.1 compares optimized waveforms, estimated parameters, model outputs, and preliminary exercise simulations across the five baseline configurations presented in Section 4.5.1. Standard deviations of relevant exercise data used for input and comparison purposes are additionally tabulated (Table 5.2). The exercise simulation procedure is emphasized in Section 5.2 by comparing selected variants of pressure scaling, lusitropy and exercise shifts. An exercise simulation visualizes model predictions of systolic and diastolic pressures (P_{sys} and P_{dia}), pulse pressure (PP), end-systolic and diastolic volumes (ESV and EDV), stroke volume (SV) and mean venous pressure (MVP) at each intensity level I$\in$[0,50,100,150] W. A complete simulation is depicted for a selected one or two participants to provide an illustrative supplement to the graphical presentation of errors (MAE or bias) averaged over six participants. Numerical values corresponding to these errors are additionally tabulated in Section A.2. Finally, Section 5.3 concludes the chapter with results from the validation experiments, presented as graphical and tabulated errors of P_{sys} and P_{dia}.

5.1 The Parameter Estimation Procedure

In the following, resulting optimized waveforms of arterial blood pressure and flow, model parameters, outputs, and preliminary exercise simulations are presented to compare the five baseline variants enumerated in Section 4.5.1.

5.1.1 Optimized Waveforms

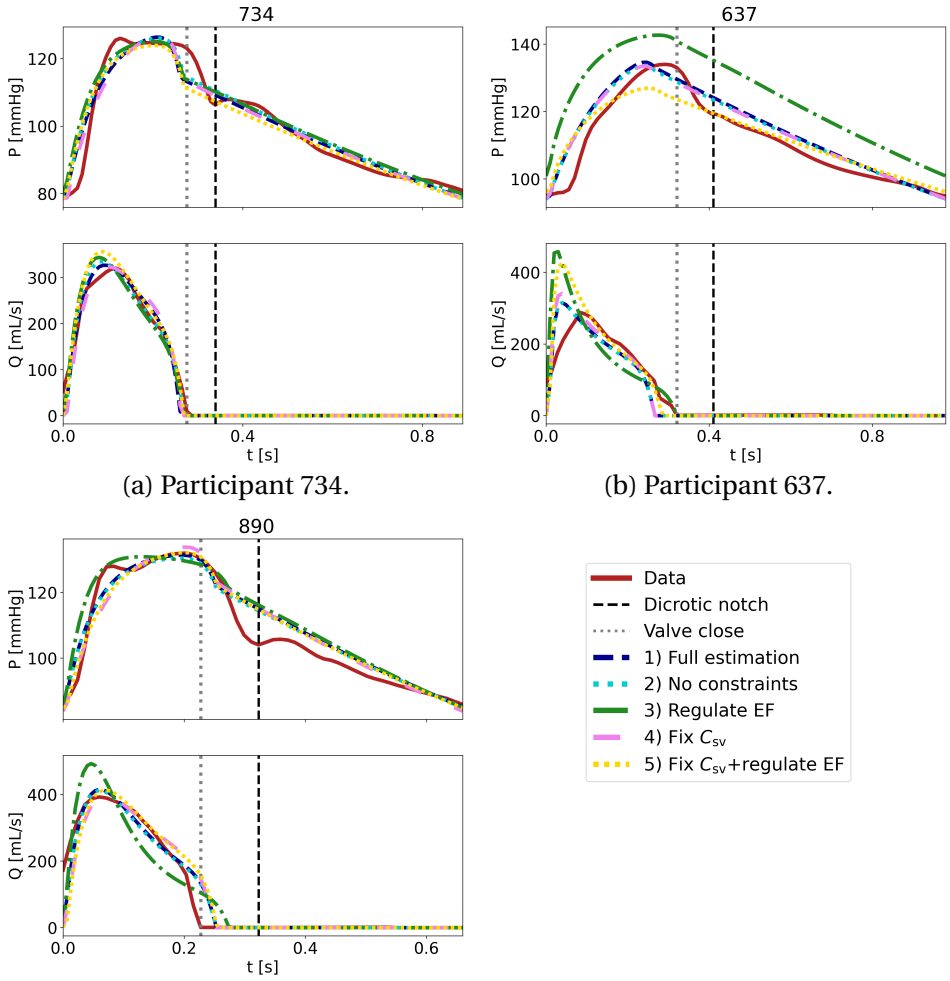

(a) Participant 734.

(b) Participant 637.

(c) Participant 890.

(d) Figure legend.

Figure 5.1: Optimized waveforms of pressure and flow for participants 734 (5.1a), 637 (5.1b) and 890 (5.1c). Red solid lines represent the arterial data that the optimization procedure aims to fit. Coloured lines 1-5 are simulated waveforms for each case enumerated in Section 4.5.1. Times of occurrence of the dicrotic notch and aortic valve closure are indicated by black dashed and grey dotted lines, respectively.

Figure 5.1 shows optimized waveforms for arterial pressure (P) and aortic blood flow (Q) compared to trial data obtained according to Section 4.1. Mean parameter fits are used in all cases with the exception of no. 2 (No constraints). The lack of constraints and regulations in this configuration resulted in a wide span of estimated parameters, and consequently rather meaningless average fits. Therefore, this case is presented with its minimum parameters, i.e. the parameter set with minimum cost function of the 20 last iterations, as described in Section 4.2.1.

It is noted that despite varying conditions for the estimation procedure, most optimized waveforms appear to be consistently in accordance with data. Peak flow (Q_{max}) is more prominent in cases 3 and 5, when ejection fraction (EF) is regulated, particularly in participant 637. Participants 734 and 890

are more robust to choice of estimation procedure compared to 637, where Q_{max}, P_{sys} and P_{dia} deviate from data in timing and/or value for all five estimation configurations. Further, participant 637 have a distinctively more narrow tonometry pressure waveform compared to 734 and 890. Participant 637 is included in Figure 5.1 despite not being explicitly used for exercise visualizations to highlight a potential reason for a more unstable and improbable behaviour exhibited in both this participant and no. 248, who has a similar pressure waveform as 637. This issue is discussed in Section 6.1.5.

5.1.2 Estimated Parameter Values

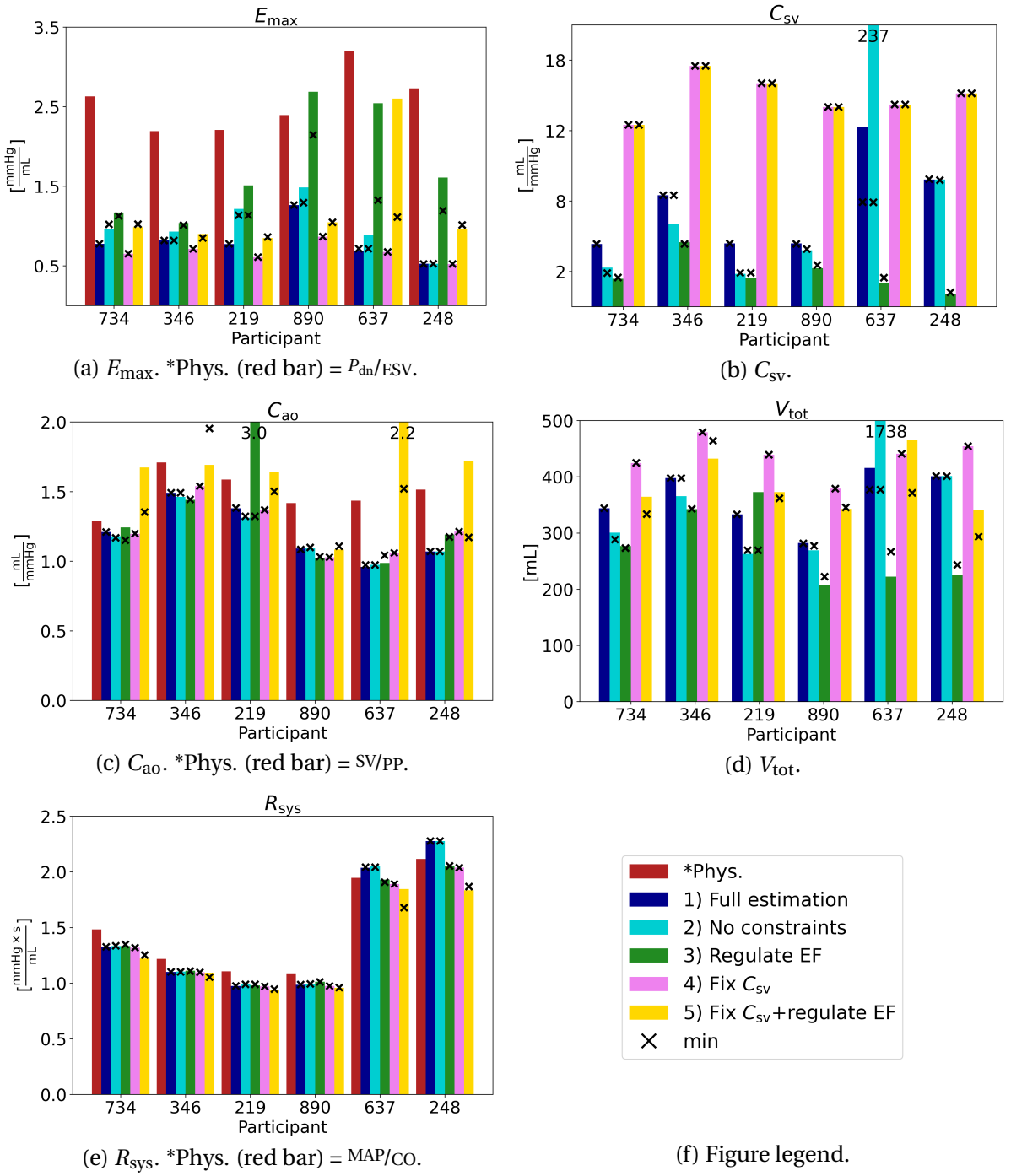

(a) E_{max}. *Phys. (red bar) = $^{P_{dn}}/_{ESV}$.

(b) C_{sv}.

(c) C_{ao}. *Phys. (red bar) = $^{SV}/_{PP}$.

(d) V_{tot}.

(e) R_{sys}. *Phys. (red bar) = $^{MAP}/_{CO}$.

(f) Figure legend.

Figure 5.2: Estimated baseline parameters for participants 734, 346, 219, 890, 637, and 248 in each configuration enumerated in Section 4.5.1. Maximum ventricular elastance (E_{max}; 5.2a), aortic and venous compliances (C_{ao}; 5.2c and C_{sv}; 5.2b), total volume (V_{tot}; 5.2d) and systemic resistance (R_{sys}; 5.2e) are presented to illustrate variation across estimation procedure. Further, E_{max}, C_{ao} and R_{sys} are displayed along with a red bar denoted **Phys* representing their physiological values as approximated from data. Coloured bars 1-5 display resulting mean parameters, while black x-marks show the corresponding minimum values, i.e. from the parameter set with smallest cost function. The values of the remaining five baseline parameters are equal in each configuration, and are presented in Table 5.1.

Figure 5.2 presents parameter values for each participant, compared across the five estimation configurations. It is noted that E_{max} (5.2a) is sensitive to variations in the baseline procedure, and is also frequently estimated as less than the physiological approximations shown as red bars. As no trial data is available for ventricular volumes, ESV was calculated from Equations (2.3) and (2.4) assuming an ejection fraction of 60%. Hence, $^{P_{dn}}/_{ESV}$ does not represent an accurate and personal value of E_{max}. It is nevertheless included to indicate the physiologically inherent individuality in E_{max}, which appears captured only by case no. 3 (Regulate EF). Further, minimum parameters represented by black x-marks show that the cost function reaches its minima for similar or smaller estimates of E_{max} than the corresponding mean values. In most cases, the estimated E_{max} approaches its lower limit of 0.50 $^{mmHg}/_{mL}$. When this boundary was increased to a more physiological value of 1.0 $^{mmHg}/_{mL}$, many test cases in constrained configurations yielded an estimated E_{max} equal to this limit.

Figures 5.2b and 5.2d show that both C_{sv} and V_{tot} vary significantly across the five configurations. It is noted that, with the exception of participant 637, C_{sv} is estimated as less than its fixed and more physiological value regardless of constraints. Total volume (V_{tot}) is interrelated with C_{sv} to maintain a venous pressure (MVP) of 6 mmHg, as targeted by the cost function (3.5). Higher compliance implies that a larger volume is needed to generate a given pressure (2.7). Further, it is noted that C_{ao} (5.2c) and particularly R_{sys} (5.2e) are estimated rather similarly regardless of estimation procedure, and the estimates are also in agreement with the data-based approximations shown as red bars.

Participant (age [yrs])	Z_{ao} [$^{mmHg\times s}/_{mL}$]	t_{peak} [s]	T [s]	E_{min} [$^{mmHg}/_{mL}$]	R_{mv} [$^{mmHg\times s}/_{mL}$]
734 (29)	0.070	0.34	0.89	0.035	0.006
637 (42)	0.013	0.41	0.98		
248 (27)	0.012	0.42	1.28		
890 (29)	0.052	0.32	0.66		
219 (28)	0.051	0.32	0.81		
345 (35)	0.053	0.35	0.88		

Table 5.1: Values of Z_{ao}, t_{peak}, T, E_{min} and R_{mv}, obtained according to Table 4.3. None of these parameters vary across the five baseline cases, and they are therefor not shown in Figure 5.2.

Table 5.1 states the parameter values that are constant across estimation procedure. It is noted that neither T nor t_{peak} vary significantly across the participants, with the exception of participant 248 (T=1.28 s), who exceeds typical values for resting periods [2]. Further, the preliminary fitted impedance is smaller in 248 and 637 ($Z_{ao}\approx$0.01 $^{mmHg\times s}/_{mL}$) than in the remaining participants ($Z_{ao}\approx$0.07–0.05 $^{mmHg\times s}/_{mL}$).

5.1.3 Model Outputs

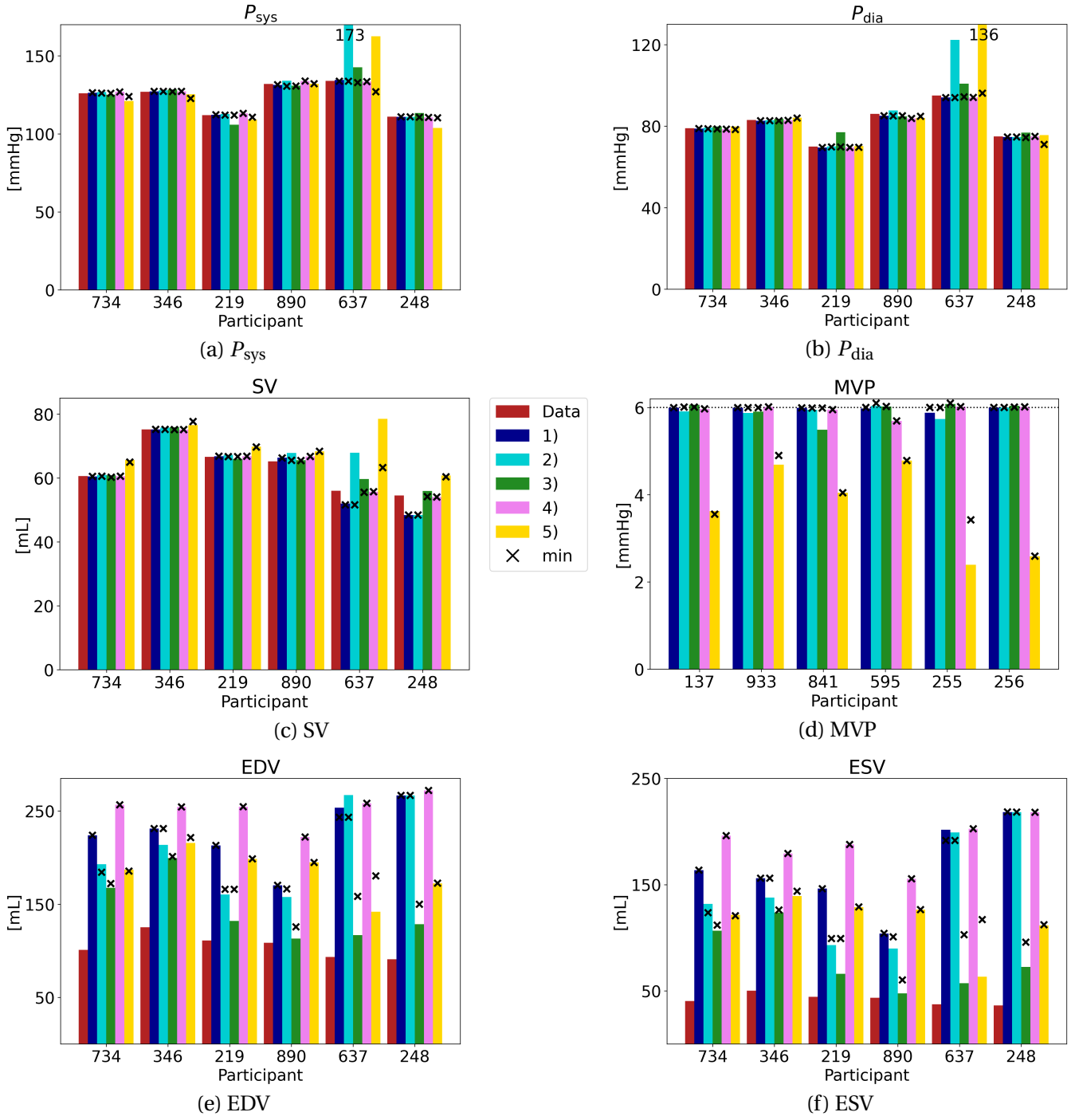

Figure 5.3: Model outputs for participants 734, 346, 219, 890, 637 and 248. Outputs shown are systolic and diastolic pressures (P_{sys} and P_{dia}), stroke volume (SV), mean venous pressure (MVP), and end-diastolic and end-systolic volumes (EDV and ESV). The red bars displayed for P_{sys}, P_{dia}, SV, EDV and ESV represent measured data, where EF=60% is assumed for the last two. Coloured bars 1-5 represent outputs for each baseline case enumerated in Section 4.5.1. Black x-marks represent corresponding outputs for the minimum parameters depicted in Figure 5.2.

Figure 5.3 shows model outputs in resting state for six participants across the five baseline configurations enumerated in Section 4.5.1. Coloured bars 1-5 represent model outputs generated by mean parameter estimates, while black x-marks are the corresponding minimum values. Figures 5.3a, 5.3b and 5.3c show that blood pressures P_{sys} and P_{dia} and stroke volume SV are captured accurately in most of the five baseline cases. This was also indicated by the overall consistent wave fits illustrated in Figure 5.1. The exception is participant 637, for which two of the cases without constraints (2 and 5) yield inaccurate mean results, while the minimum values are in more accordance with data.

As read from the cost function (3.5), P_{sys}, P_{dia} and SV are included in the numerical optimization along with a target value for mean venous pressure (MVP) of 6 mmHg, which as indicated by Figure 5.3d, all cases except no. 5 (Fix C_{sv}+regulate EF) are able to fulfill. It is noted that the combined demands of high C_{sv} (fixed C_{sv}) and low V_{tot} (penalize the cost function for low EF) do not preserve the desired pressure in the venous compartment. Further, Figures 5.3f and 5.3e show that the ventricular volumes (EDV and ESV) vary across the estimation cases, and the values are in general significantly smaller than the corresponding physiological approximations. Note that these are not accurate values, as it is not known whether the assumption of an ejection fraction (EF) of 60% is representative. Additionally, the model only considers *stressed* blood volumes, while EDV and ESV in general represent total (stressed + unstressed) volumes. Combined with the varying and non-physiological estimates of E_{max} in Figure 5.2a, this indicates a tendency of the ventricular system not being represented physiologically by the model.

5.1.4 Preliminary Exercise Simulations

In the following, exercise simulations are presented for the five baseline cases enumerated in Section 4.5.1. Uncertainties in the exercise data used as input (HR) and basis of comparison (P_{sys}, P_{dia} and SV) are initially tabulated, as the variability in this data is highly relevant in the perspective of evaluating errors of model predictions.

Variability in Exercise Data From the Clinical Trial

The following table presents standard deviations (σ) of the data used in the development experiments.

Participant	σ_{0W}	σ_{50W}	σ_{100W}	σ_{150W}
734	3.5	5.1	6.1	6.0
637	2.3	3.2	4.6	7.7
248	4.1	13.2	5.2	8.4
890	2.6	3.7	5.5	8.6
219	4.4	5.6	6.4	9.0
346	3.9	4.0	6.6	6.3
μ_σ	3.5	5.8	5.7	7.7

(a) Standard deviations of radial P_{sys} [mmHg].

Participant	σ_{0W}	σ_{50W}	σ_{100W}	σ_{150W}
734	1.5	2.3	7.8	2.4
637	1.5	2.6	2.7	4.6
248	2.9	8.1	4.0	3.3
890	2.2	2.9	2.6	4.6
219	3.1	2.9	2.7	4.1
346	2.9	3.1	10.8	4.2
μ_σ	2.3	3.7	5.1	3.9

(b) Standard deviations of radial P_{dia} [mmHg].

Participant	σ_{0W}	σ_{50W}	σ_{100W}	σ_{150W}
734	5.5	3.3	7.1	5.2
637	2.0	6.4	6.2	8.3
248	2.9	4.0	3.2	1.5
890	1.0	2.0	1.2	1.9
219	1.1	3.3	6.6	3.4
346	3.0	2.7	1.8	4.6
μ_σ	2.6	3.6	4.4	4.1

(c) Standard deviations of SV [mL].

Participant	σ_{0W}	σ_{50W}	σ_{100W}	σ_{150W}
734	1.7	0.7	1.1	6.6
637	1.5	6.4	2.2	41.3
248	0.3	2.1	1.6	5.1
890	3.0	6.1	11.8	5.6
219	0.9	0.6	2.0	2.2
346	4.5	1.9	1.9	4.6
μ_σ	2.0	3.0	3.4	10.9

(d) Standard deviations of HR [bpm].

Table 5.2: Standard deviations of systolic pressure (5.2a), diastolic pressure (5.2b), stroke volume (5.2c) and heart rate (5.2d) for participants [734, 637, 248, 890, 219, 346] at each intensity level I∈[0,50,100,150] W.

Simulations for Participants 734 (Left Column) and 890 (Right Column)

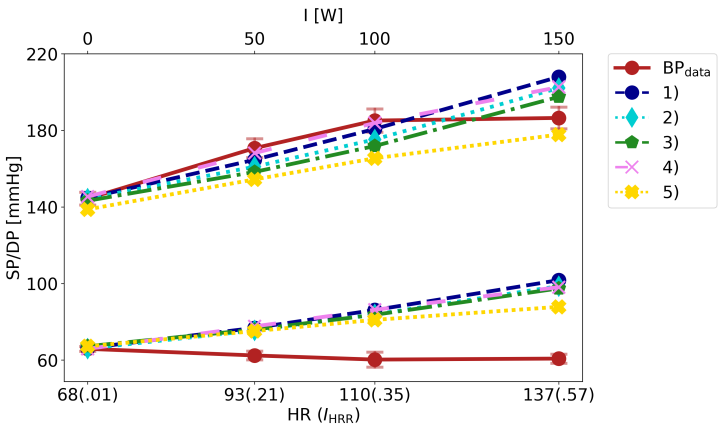

(a) 734: P_{sys} (upper lines) and P_{dia} (lower lines).

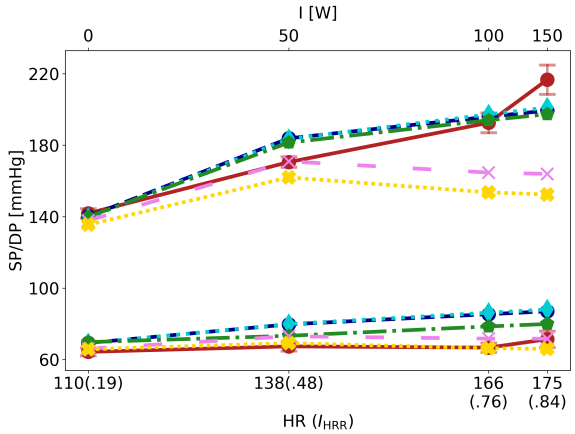

(b) 890: P_{sys} (upper lines) and P_{dia} (lower lines).

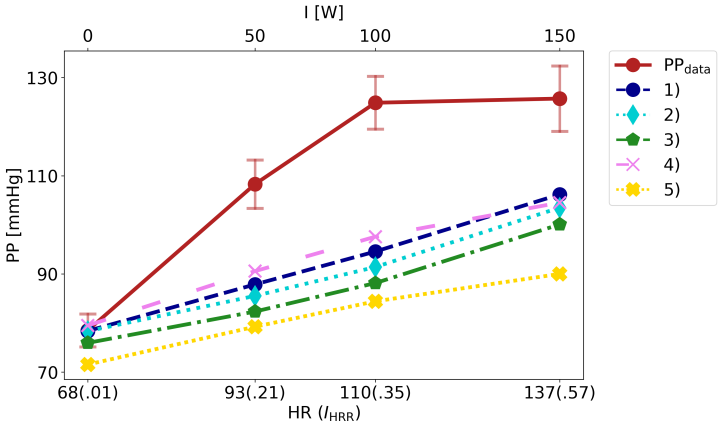

(c) 734: PP.

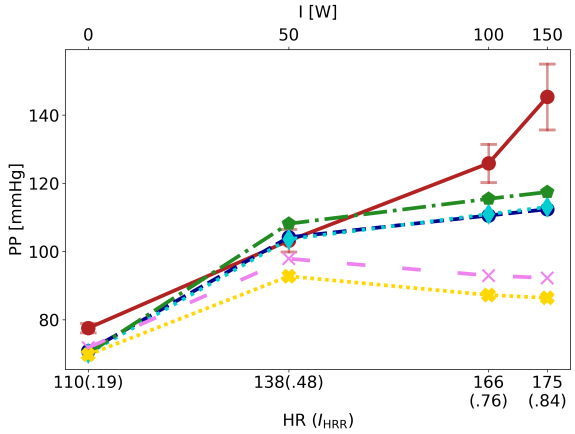

(d) 890: PP.

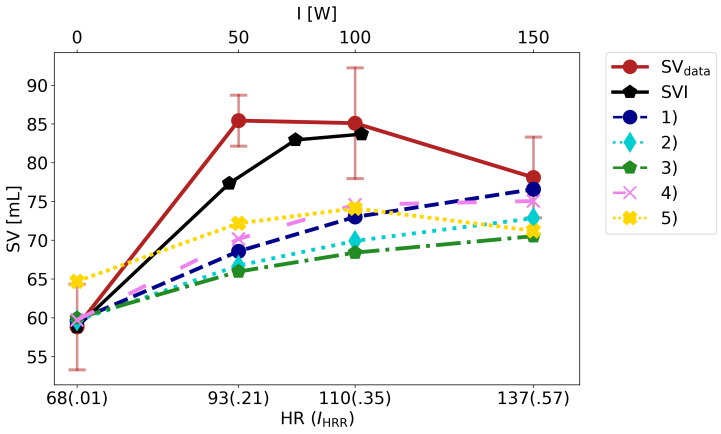

(e) 734: SV.. SVI (black line) is Stroke Volume Index [30].

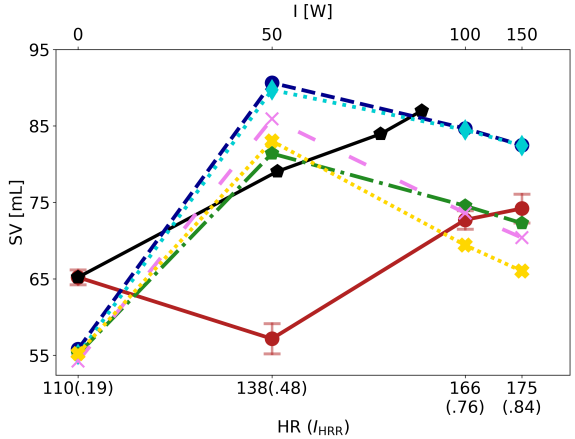

(f) 890: SV.

Figure 5.4: Exercise simulations for participants 734 (left column) and 890 (right column). Coloured lines 1-5 are model predictions given each baseline case enumerated in Section 4.5.1. Red lines represent recorded data marked as $\mu \pm \sigma$ for each intensity level.

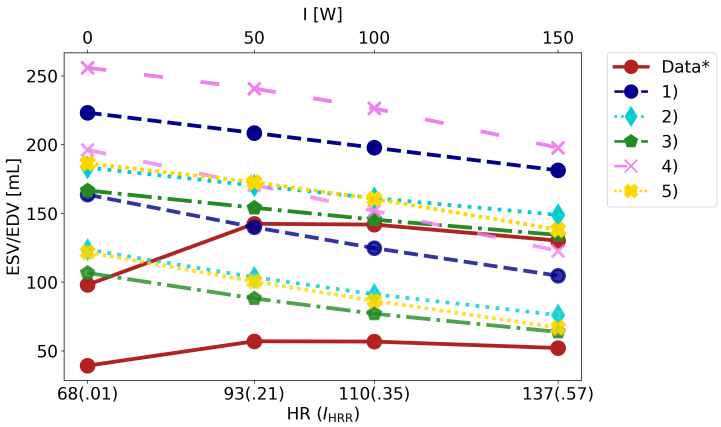

(g) 734: EDV (upper lines) and ESV (lower lines). *Data for ESV and EDV assumes EF=60%.

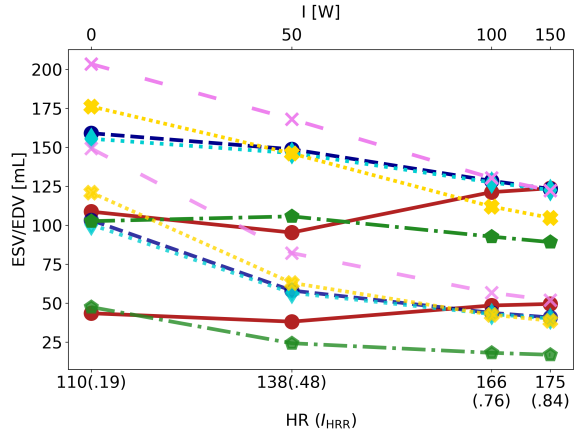

(h) 890: EDV (upper lines) and ESV (lower lines).

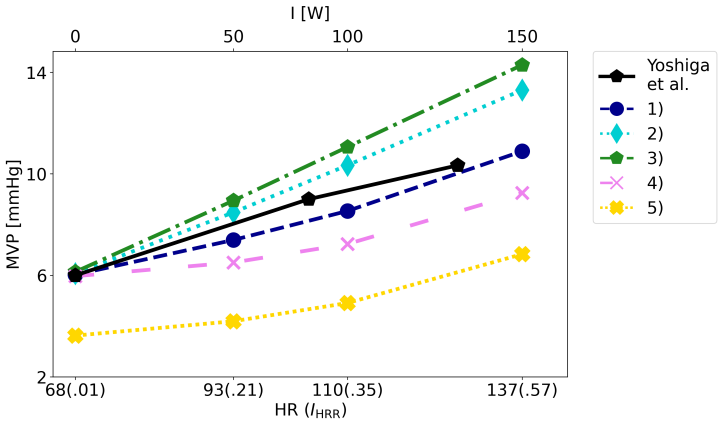

(i) 734: MVP. Simulations (1-5) vs. CVP from[43] (black line).

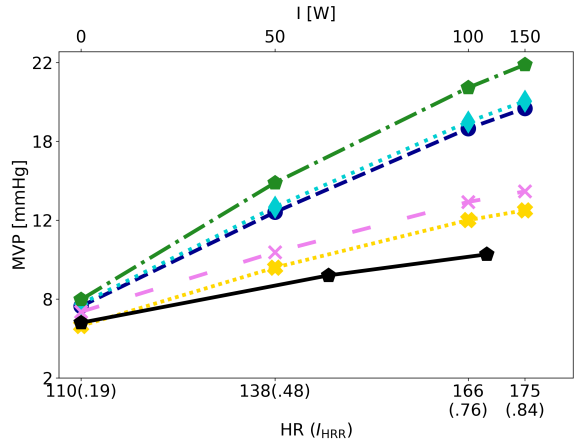

(j) 890: MVP.

Figure 5.4: Exercise simulations for participants 734 (left column) and 890 (right column). Coloured lines 1-5 are model predictions given each baseline case enumerated in Section 4.5.1. Red lines represent recorded data marked as $\mu \pm \sigma$ for each intensity level.

Figure 5.4 illustrates exercise simulations for participants 734 (left column) and 890 (right column) given the five baseline cases enumerated in Section 4.5.1. Model predictions are compared to data when available (arterial pressures and SV) and literature-based values when considered an informative supplement (SV and MVP). Note that the ranges of HR-values on the x-axes are very different for the two participants. At 0 W, participant 734 has a heart period similar to the average tonometry value ($\overline{T}_{0W}$=0.87 s vs. $\overline{T}_{ton}$=0.89 s). Participant 890 begins with a heart period at 0 W of $\overline{T}_{0W}$=0.54 s, while the tonometry heart period is $\overline{T}_{ton}$=0.66 s. Participant 890 also reaches a significantly higher intensity at 150 W (HR_{150W}=175 bpm) compared to 734 (HR_{150W}=137 bpm). A higher HR is in general associated with larger uncertainties in cardiovascular measurements. Systolic (P_{sys}) and diastolic pressure (P_{dia}) (Figs. 5.4a and 5.4b) and pulse pressure (PP) (Figs. 5.4c and 5.4d) are depicted as radial pressures (red lines) compared to scaled model pressures. There are no prominent differences in pressure predictions across the five cases with the exception of nos. 4 and 5 in participant 890, where P_{sys} diminishes at higher intensities.

It is noted that all cases significantly overestimates P_{dia} for participant 734, but captures P_{sys}, which consequently makes PP underestimated (Fig. 5.4c). Overall, PP is predicted more accurately for 890, especially in cases 1–3, where P_{sys} is captured without significantly overestimating P_{dia} (Fig. 5.4d).

From the figures depicting ventricular volumes (5.4g and 5.4h) it is noted that the 0 W-values of end-systolic and diastolic volumes (ESV and EDV) vary significantly across baseline case, which was also observed in Figures 5.3e and 5.3f. However, predicted stroke volume (SV=EDV-ESV) does not vary accordingly, as the developments of EDV and ESV are less varying than their initial values. Figure 5.4e shows that for participant 734, simulated SV is quite similar at each intensity level across the five baseline cases. The consistency between stroke volume index (SVI) reported by Chantler et al. [30] and SV_{data} for participant 734 confirms reliability of this data set. Model predictions are in better accordance with data for intensities 0 and 150 W compared to the intermediate intensities (50 and 100 W) for both 734 and 890. Deviations within SV yielded by the five baseline cases are more pronounced in participant 890 (Fig. 5.4e), but cases 1–2 and 3–5 predict similar behaviours. It is noted that at 50 and 100 W, the data deviates significantly from the development indicated by SVI, with a maximum deviation of 20 mL for 890. As it is implausible that the model will mimic the measured behaviour of SV for 890, SVI can be a more probable and reliable comparison. It is noted that SV at 0 W for participant 890 is underestimated compared to data with a deviation of 8 mL. At 0 W, no exercise shifts are performed to counteract the effect of reduced filling caused by an increased heart rate with resulting shortened diastolic period. Hence, SV predictions are diminished at 0 W for 890 due to $I_{\text{HRR}} = 0.19 > 0$, despite the participant being in a state of rest.

Mean Absolute Error (MAE) of P_{sys}, P_{dia} and SV

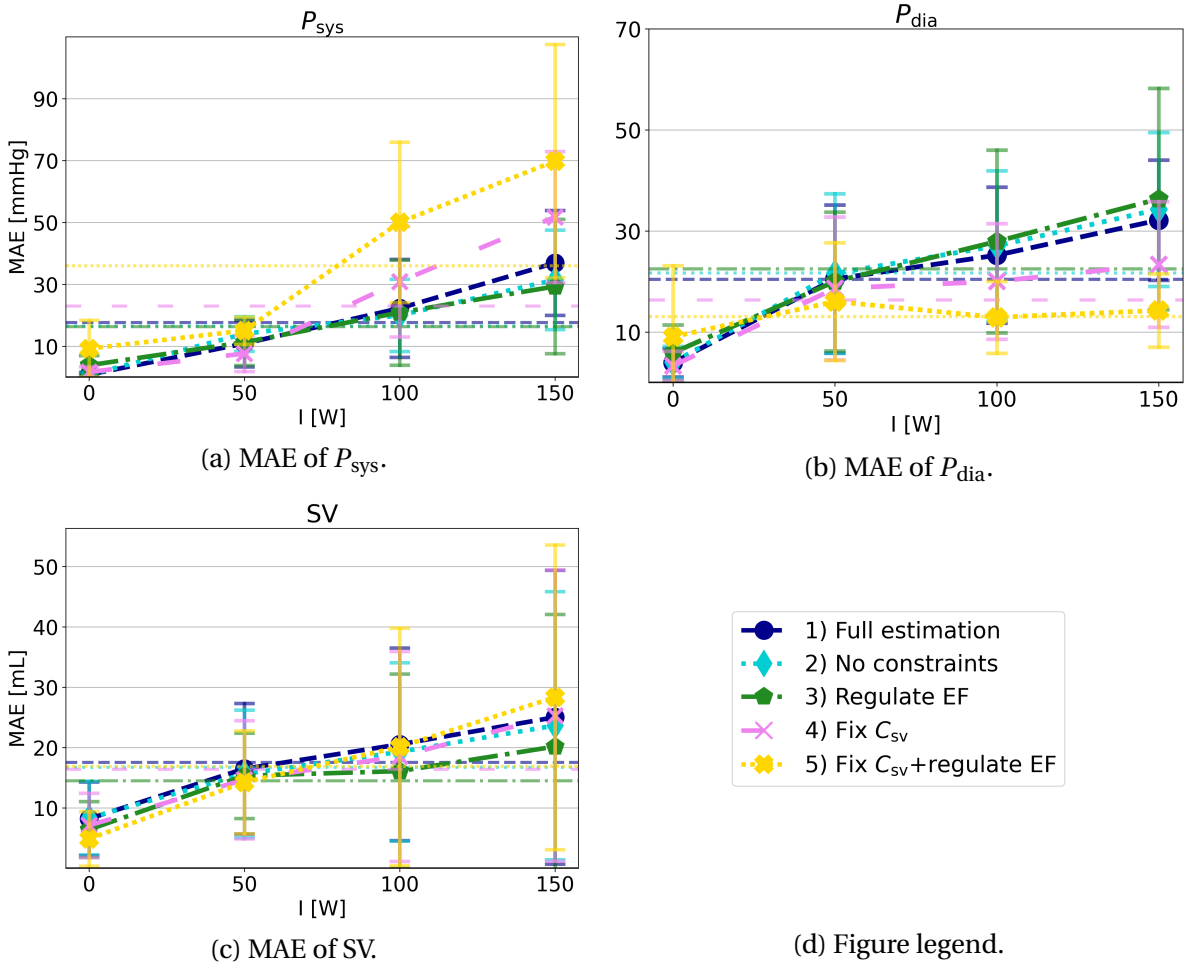

(a) MAE of P_{sys}.

(b) MAE of P_{dia}.

(c) MAE of SV.

(d) Figure legend.

Figure 5.5: MAE of P_{sys} (5.5a), P_{dia} (5.5b) and SV (5.5c) averaged over six trial participants at each intensity level. Cases 1-5 are represented with identical colors and linestyles as in Figure 5.4. Horizontal lines represent mean values across all intensities. All values depicted are explicitly stated in Table A.6.

Figure 5.5 shows MAE of P_{sys}, P_{dia} and SV at each intensity level I$\in$[0,50,100,150] W compared across the five baseline configurations. It is noted that:

- On an average level, cases 1–3 and 4–5 perform similarly in pressure simulations. Cases 4–5 predict lower pressures, yielding a greater MAE of P_{sys}, but smaller errors in P_{dia}.
- Figures 5.5c, 5.4e and 5.4f together indicate a prominent variation between participants regarding which configuration yields the lowest errors in SV. This results in small average differences between the configurations displayed in Figure 5.5c, and also large standard deviations.
- Case no. 3 (Regulate EF) yields the lowest average MAE of SV for higher intensities, but the large standard deviations indicate that a single configuration cannot be defined as more beneficial in predicting SV during exercise for all six participants.

5.2 The Exercise Simulation Procedure

This section emphasizes the exercise simulation procedure by comparing selected implementations of baseline configurations, pressure scaling, lusitropy, and parameter shifts during exercise, as presented in Section 4.5.1. The various effects are highlighted by statistical error presentations as well as explicit exercise simulations for participants 734 and/or 890 when considered an illustrative supplement. Note that the effect of defining resting heart period T (Section 4.3.4) is not shown, as it appeared less influential compared to other variations. However, the aspect is discussed briefly in Section 6.2.5.

5.2.1 Scaling of Model Pressures

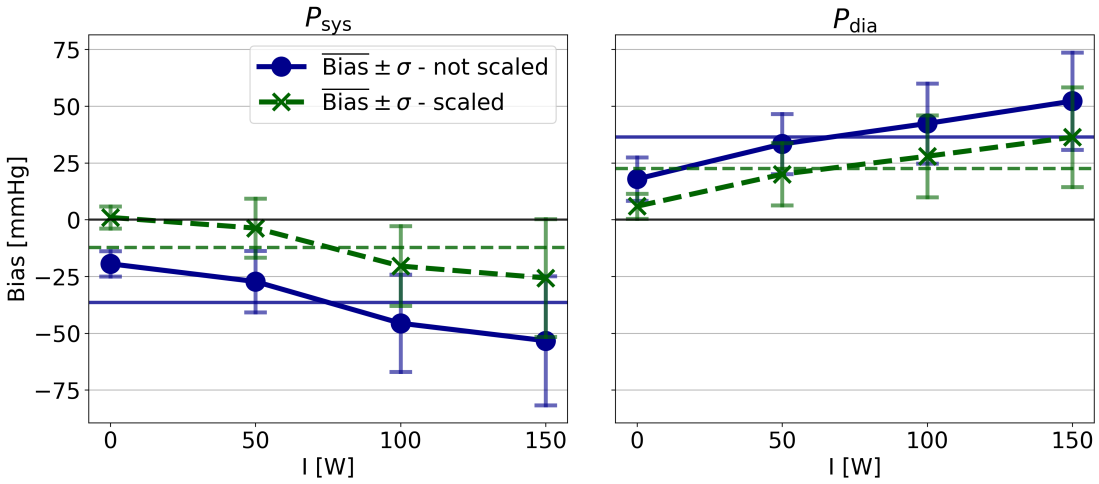

Figure 5.6: Bias of arterial pressures using original model outputs (blue circle-marked lines) vs. scaled outputs (green x-marked lines). Vertical lines represent $\mu \pm \sigma$ averaged over the six participants. Horizontal lines represent mean values across all intensities. All values are explicitly tabulated in Table A.4.

Figure 5.6 illustrates average bias at each intensity level I∈[0,50,100,150] W. The effect of scaling appeared identical across participants, thus no explicit individual simulation is depicted. It is noted that:

- Scaling of model pressures yields smaller errors in both P_{sys} and P_{dia} at all intensities. The magnitude of scaled bias is on average reduced by $^{24}/_{14}$ mmHg for $^{P_{sys}}/_{P_{dia}}$.
- Errors increase in magnitude according to increasing intensity. For the scaled errors, the bias is $^{1}/_{7}$ mmHg at 0 W compared to $^{-26}/_{35}$ mmHg at 150 W for $^{P_{sys}}/_{P_{dia}}$.
- On average, the model underestimates P_{sys} and overestimates P_{dia} in the presented configuration. Mean values of scaled bias across all intensities is $^{-12}/_{23}$ mmHg for $^{P_{sys}}/_{P_{dia}}$.

5.2.2 Implementation of Lusitropy

Lusitropy Coefficient From Clinical Exercise Data

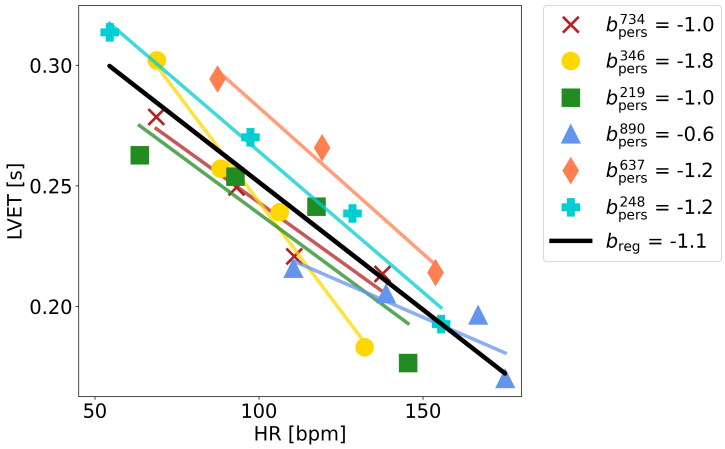

Figure 5.7: Systolic periods as read from left-ventricular ejection times (LVETs), with heart rate on the x-axis. The solid black line represents the general slope (b_{reg}) resulting from linear regression of LVETs for all participants and intensity levels, while the coloured lines have individual slopes for each participants (b_{pers}). Slopes are reported as $b \times 10^3$, and the unit of b is s × min.

It is noted that Weissler et al. report a more rapid decrease in systolic period (b_W=-0.0021 s × min) than read from the trial data ($b_{reg} = -0.0011$ s × min). A more extensive literature search on systolic time intervals during exercise revealed further alternative regression values of both electromechanical systole (QS_2) and LVET. Table 5.3 summarizes the values collected from literature and the trial data.

Source	Slope×10^3 [s × min]	
	QS_2	LVET
Weissler et al. [13]	-2.1	-1.7
Mertens et al. [47]	-1.16	-1.15
Maher et al. (Sub-maximal effort) [48]	-2.1	-1.7
Maher et al. (Maximal effort) [48]	-1.4	-1.4
Exercise trial	—	-1.1

Table 5.3: Regression coefficients for selected measures of systolic period during exercise as obtain by Weissler et al., Mertens et al., Maher et al. and data from the exercise trial. Note that Maher et al. [48] report different values at sub-maximal and maximal exercise. QS_2 is electromechanical systole, while LVET is left-ventricular ejection time.

Exercise Simulation for Participant 890

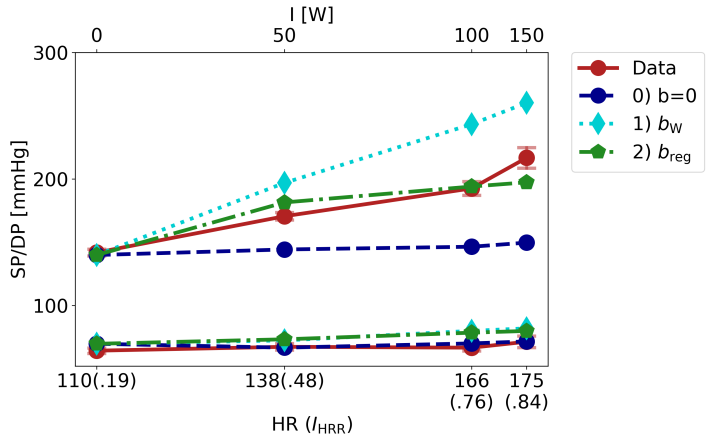

(a) P_{sys} (upper lines) and P_{dia} (lower lines).

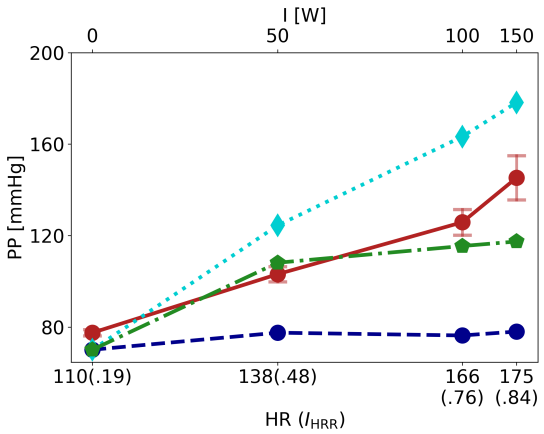

(b) PP.

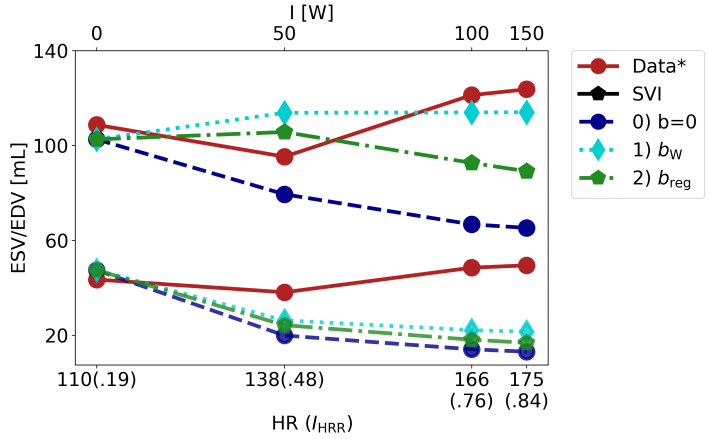

(c) EDV (upper lines) and ESV (lower lines).
*Data for ESV and EDV assumes EF=60%.

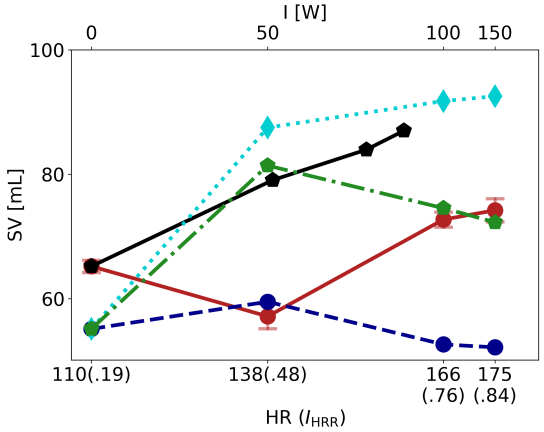

(d) SV.
SVI (black line) is Stroke Volume Index [30].

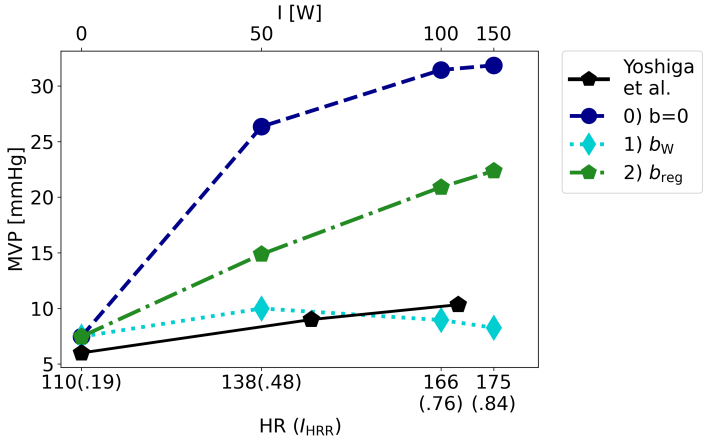

(e) MVP.

Figure 5.8: Exercise simulation for participant 890 given baseline case no. 3 (Regulate EF). Coloured lines 0–3 are resulting model simulations given each value of the lusitropy coefficient enumerated in Section 4.5.1. Red lines report recorded data as $\mu \pm \sigma$.

Mean Absolute Error (MAE) of P_{sys}, P_{dia} and SV

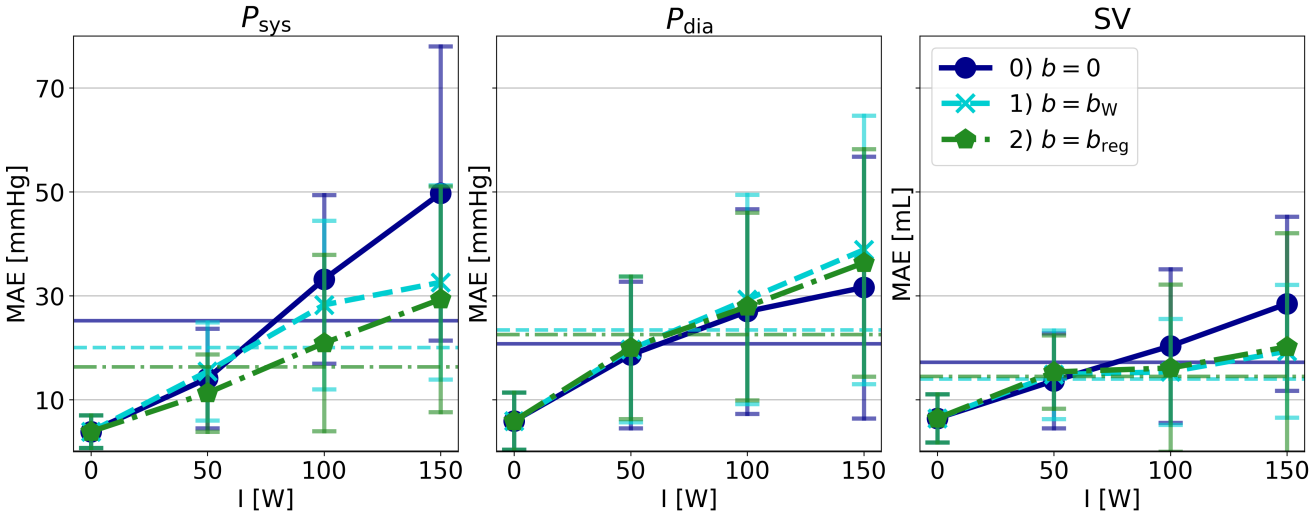

Figure 5.9: MAE of P_{sys}, P_{dia} and SV compared across the three lusitropy coefficients (b) enumerated in Section 4.5.1. Reported values are $\mu \pm \sigma$ averaged over six participants. Horizontal lines represent mean values across all intensities. All values are explicitly stated in Table A.5.

Figure 5.8 illustrates explicitly how the lusitropy coefficient (b) impacts an exercise simulation. It is observed that b significantly affects all hemodynamic quantities except P_{dia}, which is in accordance with results from the sensitivity analysis (Fig. 4.3). Figure 5.9 shows MAE averaged over the six participants. MAE is in this case preferred over bias as error metric, because the value of b did not consistently over or underestimated neither pressures nor SV, resulting in misleadingly small bias. It is noted that:

- The lusitropy mechanism is necessary to preserve diastolic filling during exercise, as it is evident that SV diminishes when lusitropy is absent, i.e. with $b = 0$.
- The largest magnitude of b is present in b_W, which causes greatest systolic pressures (Fig. 5.8a) and SV (Fig. 5.8d).
- From Figure 5.8 it appears as b_{reg} performs best compared to data, but as shown in Figure 5.9, the conclusion is more ambiguous when considering multiple participants.
- On an average level, the differences in MAE of P_{dia} and SV are not significant across the three values of b. For P_{sys}, b_{reg} performs best with a MAE averaged over intensity levels of 16.4 mmHg compared to 25.2 and 20.0 mmHg for $b = 0$ and $b = b_W$, respectively. These averages are recognized as horizontal lines in the left plot of Figure 5.9.

5.2.3 Exercise Shifts of C_{ao} and R_{sys}

Alternative Shifts of C_{ao} and R_{sys}

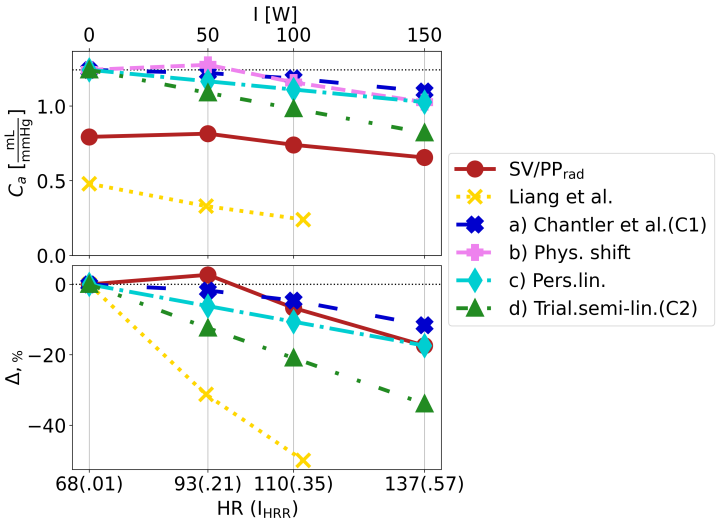

(a) C_{ao} as shifted during exercise (734).

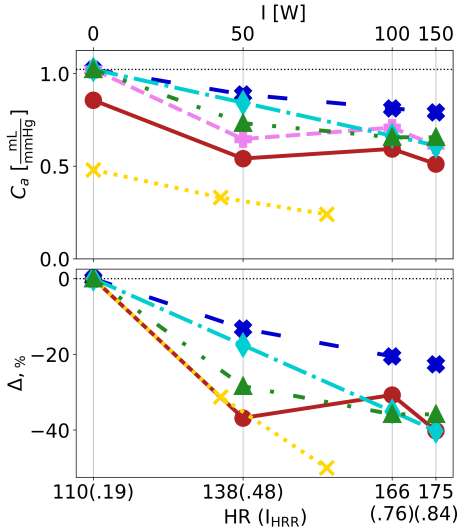

(b) C_{ao} as shifted during exercise (890).

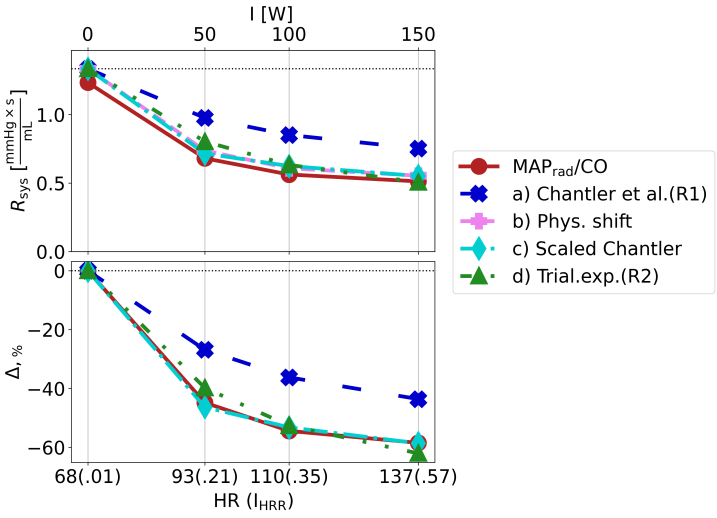

(c) R_{sys} as shifted during exercise (734).

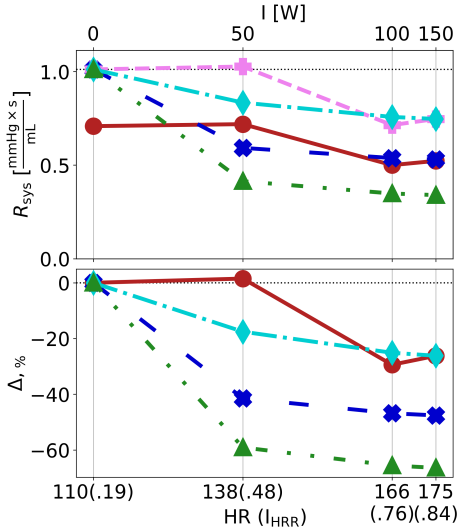

(d) R_{sys} as shifted during exercise (890).

Figure 5.10: Illustration of alternatives a-d for shifting C_{ao} (Figs. 5.10a and 5.10b) and R_{sys} (Figs. 5.10c and 5.10d) for participants 734 (left column) and 890 (right column). Intensity levels in watts $I \in [0, 50, 100, 150]$ W are displayed on the upper x-axes, while corresponding participant-specific heart rates and intensities (HR and I_{HRR}) are presented on the lower x-axes. Upper plot of each subfigure displays specific shifted parameter values, while the lower shows the corresponding changes compared to non-shifted resting value (θ^0) calculated as $\Delta_{\%} = \frac{\theta - \theta^0}{\theta^0} \times 100\%$ for $\theta \in [C_{ao}, R_{sys}]$. Resting values θ^0 are obtained from baseline case no. 3 (Regulate EF). Physiological quantities calculated directly from data are presented along with their respective relative changes as red lines. For compliance, the values reported by Liang et al. [42] are shown as yellow lines. Note that the heart rates from Liang et al. have been shifted to begin at HR_{0W}.

Figure 5.10 illustrates the four alternatives a-d presented in Section 4.3.3 for shifting each of C_{ao} and R_{sys} during exercise. It is noted that the trial-based shifts (C2 and R2) impose greater changes in both C_{ao} and R_{sys} compared to Chantler-based shifts (C1 and R1). The following paragraphs compare model simulations and average errors using alternatives C1, C2, R1 and R2 and baseline cases 3 and 4. Table 5.4 reviews the properties of these configurations.

Shift (Param.)	Source of development	Explanation
C1 (C_{ao}) R1 (R_{sys})	Bjørdalsbakke [5].	Equation (3.8) with population averages from Chantler et al. [30].
C2 (C_{ao}) R2 (R_{sys})	Current work based on clinical exercise trial.	Average trial-based semi-linear shift. General trial-based shift.

(a) Methods for shifting C_{ao} and R_{sys} (Fig. 5.10).

Baseline case (BC)	Features
3	• Estimated E_{max}, R_{sys}, C_{sv}, V_{tot} and C_{ao}. • Fixed t_{peak}, E_{min}, R_{mv}, Z_{ao} and T. • No constraints ($\theta > 0$). • Regulate ejection fraction with hardmax step function (4.4).
4	• Estimated E_{max}, R_{sys}, V_{tot} and C_{ao}. • Fixed C_{sv}, t_{peak}, E_{min}, R_{mv}, Z_{ao} and T. • With constraints (Table 4.4).

(b) Baseline configurations (Section 5.1).

Table 5.4: Review of the features associated with the configurations under investigation (Section 4.5.1).

Exercise Simulations for Participants 734 (Left Column) and 890 (Right Column)

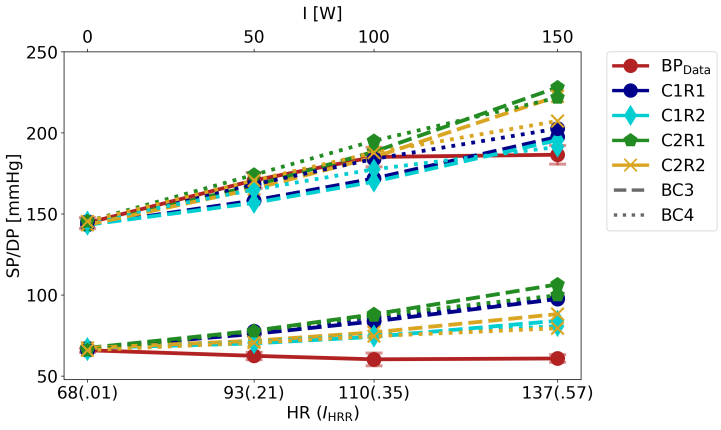

(a) 734: P_{sys} (upper lines) and P_{dia} (lower lines).

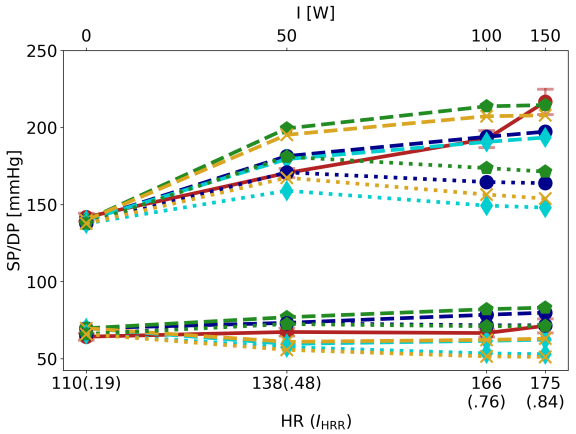

(b) 890: P_{sys} (upper lines) and P_{dia} (lower lines).

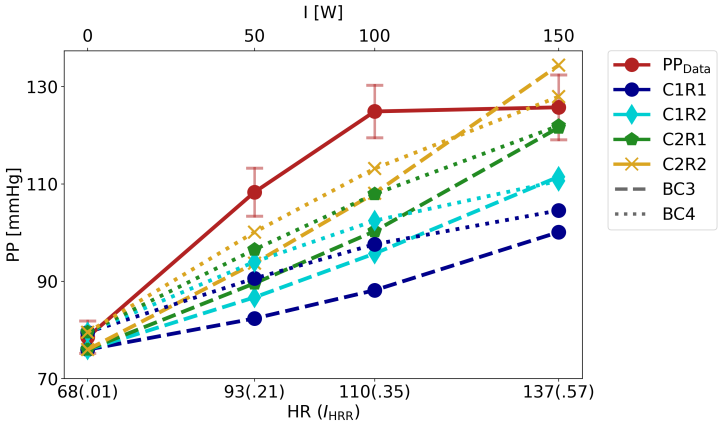

(c) 734: PP.

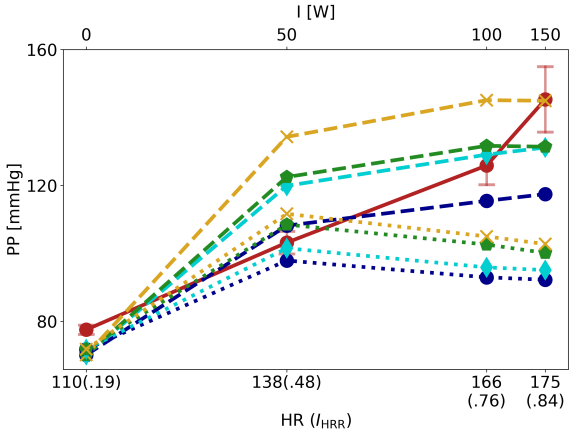

(d) 890: PP.

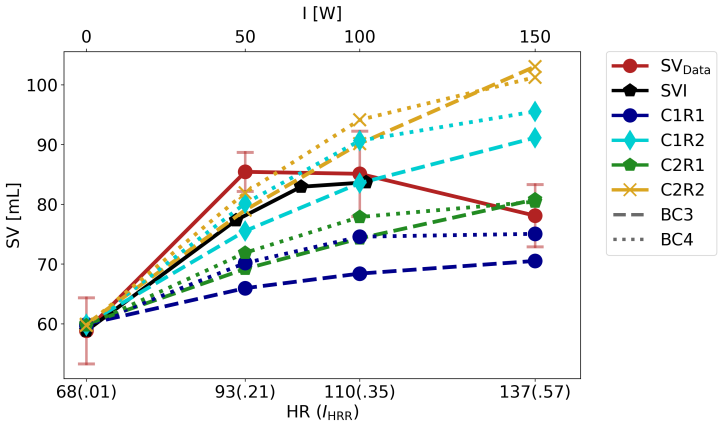

(e) 734: SV. SVI (black line) is Stroke Volume Index [30].

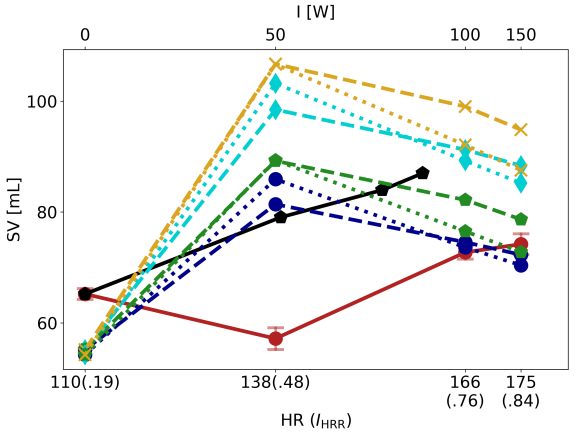

(f) 890: SV

Figure 5.11: Exercise simulations for participants 734 (left column) and 890 (right column). Two baseline cases are depicted; dashed lines represent case no. 3 (Regulate EF), while dotted lines are case no. 4 (Fix C_{sv}). Coloured lines denoted CjRk, j,k$\in$[1,2] are model simulations resulting from combining configurations for shifting C_{ao} and R_{sys} (Table 5.4). Red lines report recorded data as $\mu \pm \sigma$.

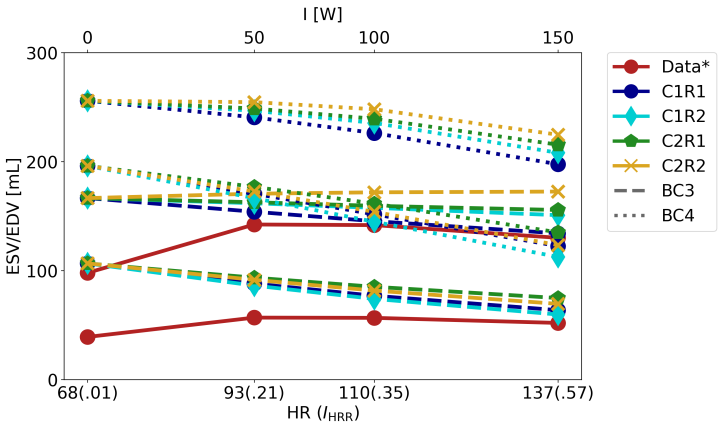

(g) 137: EDV (upper lines) and ESV (lower lines). *Data for ESV and EDV assumes EF=60%.

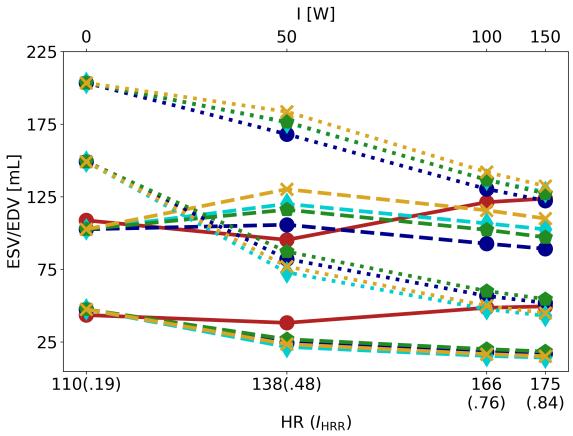

(h) 890: EDV (upper lines) and ESV (lower lines).

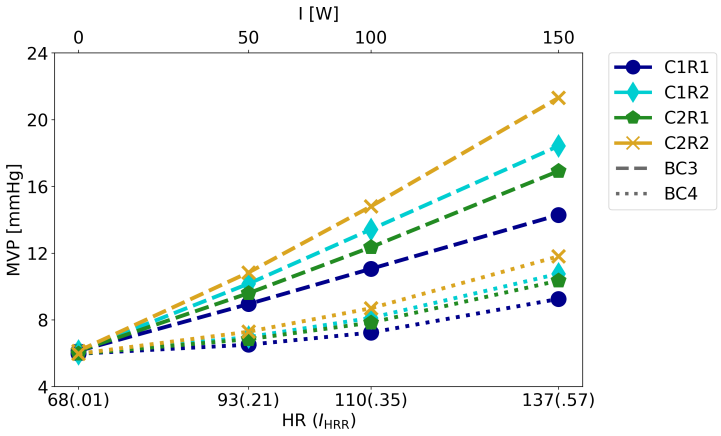

(i) 734: MVP.

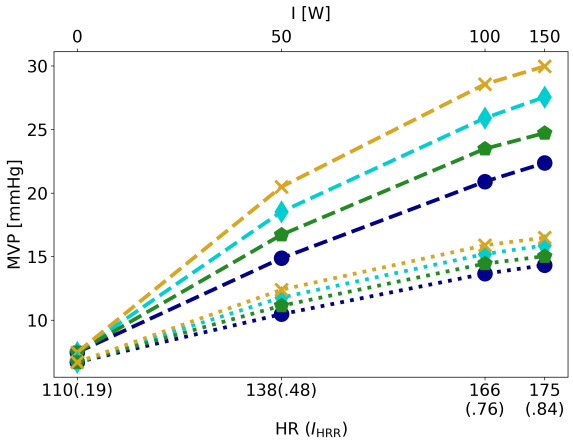

(j) 890: MVP.

Figure 5.11: Exercise simulations for participants 734 (left column) and 890 (right column). Two baseline cases are depicted; dashed lines represent case no. 3 (Regulate EF), while dotted lines are case no. 4 (Fix C_{sv}). Coloured lines denoted CjRk, j,k∈[1,2] are model simulations resulting from combining configurations for shifting C_{ao} and R_{sys} (Table 5.4). Red lines report recorded data as $\mu \pm \sigma$.

Figure 5.11 visualizes the effects of applying selected model configurations on resulting exercise predictions for two participants. The entire left column represents participant no. 734, while the right column is participant no. 890. Both are aged 29 years, 734 is a male, and 890 a female. A total of $2^3 = 8$ configurations are shown; 2 sets of baseline parameters (BC=baseline case) in combination with 2 selected exercise shifts for each of C_{ao} and R_{sys}. Features associated with notations BCi, Cj and Rk, i∈[3,4] and j,k∈[1,2] are summarized in Table 5.4. It is noted that:

- The baseline case (BC3 vs. BC4) greatly impacts the resting values of ventricular volumes EDV and ESV (Figs. 5.11g and 5.11h), and the exercise behaviour of venous pressure (Figs. 5.11i and 5.11j).

- Stroke volume (Figs. 5.11e and 5.11f) and arterial pressures (Figs. 5.11a, 5.11b, 5.11c and 5.11d) appear more sensitive to exercise configuration than baseline case, particularly for participant 734. It is observed that P_{sys} diminishes in participant 890 for higher intensities when baseline case 4 is applied.
- All configurations overestimate P_{dia} for participant 734. Predictions of P_{dia} are more accurate for 890. Choice of baseline case impacts P_{sys} more for 890 than 734.
- The configuration (BC3+C2+R1) yields greatest predictions of both P_{sys} and P_{dia}. It is noted that P_{sys} appears more sensitive to compliance shift (C1 vs. C2) than resistance (R1 vs. R2), while the opposite is the case for P_{dia}.
- Model predictions of SV are not entirely able to capture the shape of the corresponding data in neither of the two participants. Also, there are large variations across intensity levels considering which configuration performs best in predicting SV. The combined effects of large shifts in both compliance and resistance (C2+R2) result in the greatest predictions of SV, while the combination C1+R1 yields the smallest.

Mean Absolute Error (MAE) of P_{sys}, P_{dia} and SV

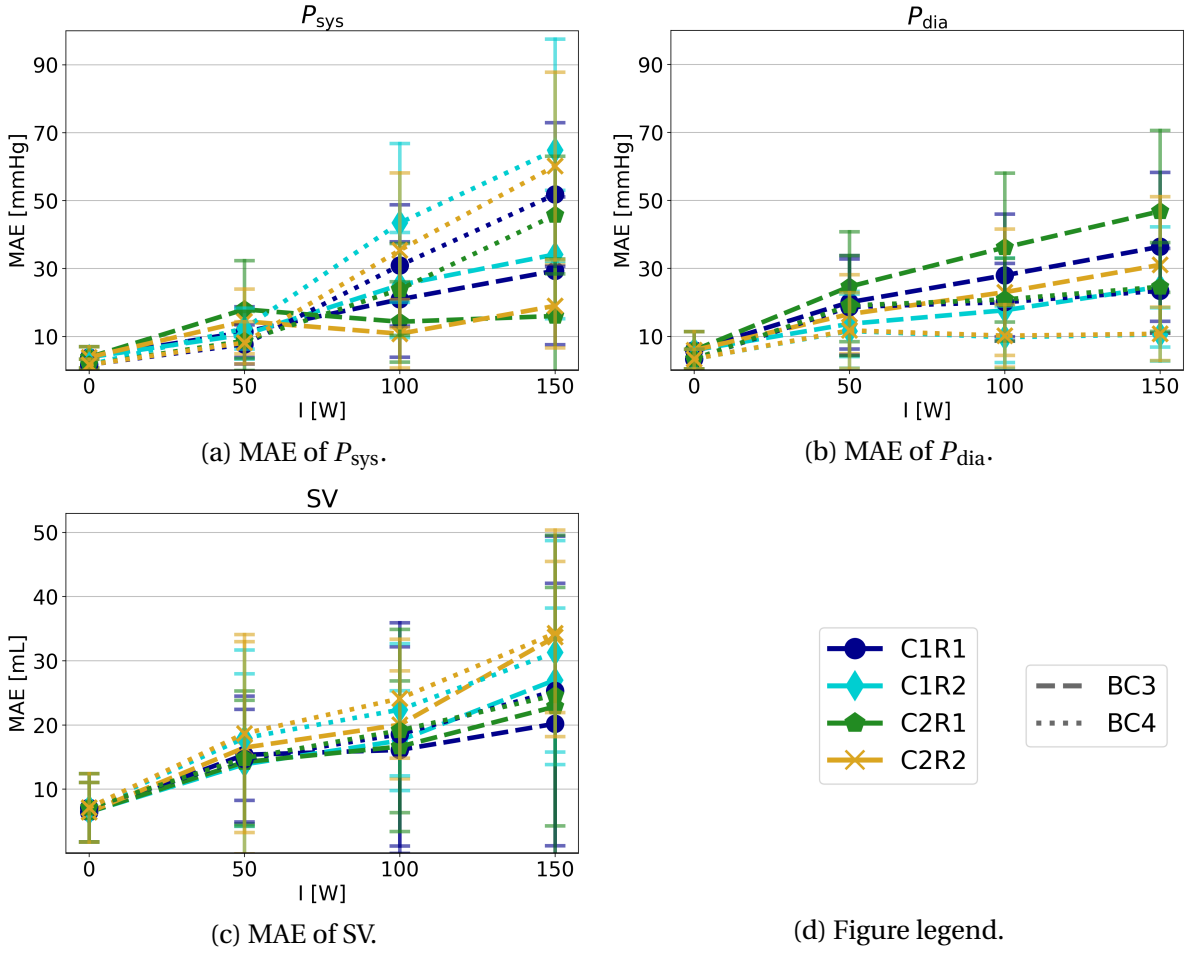

(a) MAE of P_{sys}.

(b) MAE of P_{dia}.

(c) MAE of SV.

(d) Figure legend.

Figure 5.12: MAE of P_{sys} (5.12a), P_{dia} (5.12b) and SV (5.12c) averaged over participants 734, 346, 219, 890, 637 and 248. Lines BCi+CjRk, i∈[3,4] and j,k∈[1,2] represent the same selected configurations as presented in Figure 5.11. Dashed and dotted lines represent baseline cases 3 (BC3) and 4 (BC4), respectively, while the color corresponds to a given combination of exercise shifts. All values are explicitly stated in Table A.6.

Figure 5.12 illustrates the average behaviour of MAE in the same selected configurations as shown in Figure 5.11. The values are reported as $\mu \pm \sigma$ averaged over six participants for each exercise intensity level I∈[0,50,100,150] W. It is observed that:

- For P_{sys} and P_{dia}, the errors appear inversely related. A configuration resulting in small errors in P_{sys}, e.g. BC3+C2R1 (green dashed line) corresponds to greater errors in P_{dia} and vice versa.
- Compared to arterial pressures, MAE of SV varies less across model configurations. It is it observed a slight tendency of R2, the i.e. trial-based resistance shifts, being associated with greater MAE of SV, especially at higher intensities.

5.3 Model Validation

Illustrated Mean Absolute Error (MAE) of P_{sys} and P_{dia}

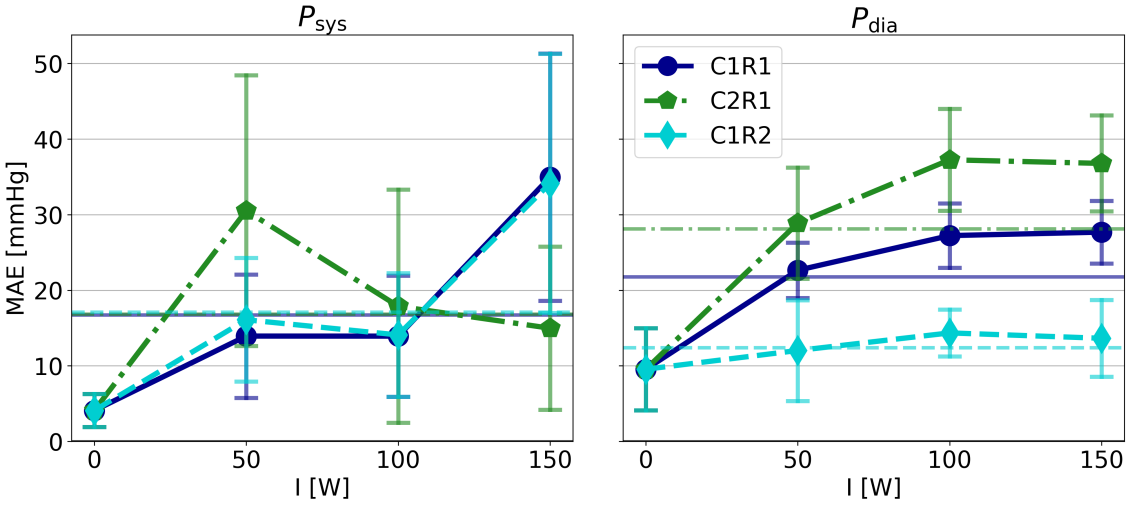

Figure 5.13: MAE of P_{sys} and P_{dia} given the three selected configurations enumerated in Section 4.5.2. Parameter case no. 3 (Regulate EF) is used as baseline. The three exercise configurations CjRk, j,k∈[1,2] are illustrated with each respective colour. Reported values are $\mu \pm \sigma$ averaged over participants 745, 827, 241, 993 and 722 at each intensity level I∈[0,50,100,150] W.

Figure 5.13 illustrates prediction errors over intensity, averaged over the five participants included in the validation experiments. All values are explicitly stated in the bottom rows of Tables 5.6 and 5.7.

Tabulated Individual Errors and Data Variability

Variability in Heart Rates (HR) [bpm] for the Validation Participants:

Participant (age [yrs])	σ_{0W}	σ_{50W}	σ_{100W}	σ_{150W}
745 (39)	4.5	1.2	1.4	1.1
827 (43)	4.3	1.3	0.8	1.1
241 (40)	7.2	12.3	2.4	1.5
*993 (38)	7.7	2.4	1.3	x
722 (35)	4.4	3.2	1.8	1.9
μ_σ	5.6	4.1	1.5	1.4

Table 5.5: Standard deviations of HR [bpm] collected from the clinical exercise trial. The heart rates are used as input for model predictions during exercise, thus their variability is highly relevant in the perspective of validating the hemodynamic exercise model. *No data for no. 993 at 150 W.

Systolic Pressure (P_{sys}) [mmHg]:

Part.	Config.	0 W		50 W		100 W		150 W		μ	
		MAE	σ^m	MAE	σ^m	MAE	σ^m	MAE	σ^m	$\overline{\text{MAE}}$	$\overline{\lvert\Delta_C\rvert}$
745	C1+R1	5.0	4.4	8.6	3.1	20.5	3.8	33.2	5.7	16.8	20.1
	C2+R1			3.8		1.1		0.7		2.7	
	C1+R2			11.6		24.4		37.5		19.6	
827	C1+R1	0.8	6.4	20.8	5.6	0.2	5.9	13.5	7.3	8.8	40.1
	C2+R1			51.2		29.6		10.5		23.0	
	C1+R2			24.0		6.0		6.0		9.2	
241	C1+R1	7.2	5.9	21.1	6.0	23.0	9.4	59.6	9.4	27.7	31.2
	C2+R1			44.8		13.7		30.1		24.0	
	C1+R2			27.0		15.5		52.3		25.5	
993	C1+R1	4.8	8.7	18.8	4.8	11.4	8.2	x	x	11.7	20.1
	C2+R1			36.9		41.3				27.7	
	C1+R2			12.9		3.5				7.1	
722	C1+R1	2.6	5.4	0.4	10.2	14.4	6.1	33.6	5.9	12.7	30.1
	C2+R1			15.9		3.6		18.6		10.2	
	C1+R2			5.0		21.1		40.8		17.4	
$\mu \pm \sigma$	C1+R1	4.1±2.2	6.2±1.4	13.9±8.2	5.9±2.4	13.9±8.0	6.7±1.9	35.0±16.4	7.0±1.5	16.7±11.3	29.8±9.7
	C2+R1			30.5±17.9		17.9±15.4		15.0±10.8		16.9±9.4	
	C1+R2			16.1±8.2		14.1±8.2		34.1±17.1		17.1±10.8	

Table 5.6: MAE of P_{sys} for three configurations applied on the five validation participants. Column σ^m contains standard deviations of the respective pressure measurements against which model predictions are compared. The bottom row reports mean values for each intensity across all participants as $\mu \pm \sigma$, which are illustrated in Figure 5.13. The right column denoted $\overline{\text{MAE}}$ reports averages for each participant across all intensities. Values in the bottom right cell are averaged over μ for each intensity, and represented as horizontal lines in Figure 5.13. Column $\overline{\Delta_C}$ presents errors of the Chantler-based predictions, as described at the end of Section 4.5.2.

Diastolic Pressure (P_{dia}) [mmHg]:

Part.	Config.	0 W		50 W		100 W		150 W		
		MAE	σ^m	MAE	σ^m	MAE	σ^m	MAE	σ^m	$\overline{\text{MAE}}$
745	C1+R1	3.0	3.2	17.5	2.6	23.8	2.7	28.2	7.6	18.1
	C2+R1			19.6		28.6		36.1		21.8
	C1+R2			9.0		11.0		11.9		8.7
827	C1+R1	5.4	3.4	19.8	2.4	32.1	3.2	33.9	6.0	22.8
	C2+R1			26.3		39.2		40.0		27.7
	C1+R2			3.9		13.7		14.0		9.2
241	C1+R1	15.9	4.4	27.6	9.2	22.9	8.7	26.4	13.2	23.2
	C2+R1			41.6		44.9		44.1		36.6
	C1+R2			23.7		18.1		21.4		19.8
993	C1+R1	7.5	7.2	25.4	2.4	32.6	3.0			21.8
	C2+R1			31.1		43.4		x	x	27.4
	C1+R2			14.1		17.8				13.1
722	C1+R1	16.0	3.7	22.9	7.1	24.6	3.3	22.4	3.1	21.5
	C2+R1			25.8		30.1		26.9		24.7
	C1+R2			9.5		11.1		7.3		11.0
$\mu \pm \sigma$	C1+R1	9.5±5.4	4.4±1.5	22.6±3.6	4.7±2.9	27.2±4.2	4.2±2.3	27.7±4.1	7.5±3.7	21.8±7.3
	C2+R1			28.9±7.3		37.3±6.7		36.8±6.4		28.1±11.2
	C1+R2			12.0±6.7		14.4±3.1		13.6±5.1		12.4±1.8

Table 5.7: MAE of P_{dia} for the three selected configurations applied on the five validation participants. The column denoted σ^m contains standard deviations of the respective pressure measurements against which model predictions are compared. Bottom row reports averages for each intensity across all participants as $\mu \pm \sigma$, which are depicted graphically in Figure 5.13. The far right column denoted $\overline{\text{MAE}}$ reports averages for each participant across all intensity levels. Values contained in the bottom right cell are averaged over the mean values (μ) for each intensity, and are represented as horizontal lines in Figure 5.13.

Figure 5.13 illustrates average values of MAE, which are contained in the bottom rows of Tables 5.6 and 5.7. The exercise configurations shown are C1C1, C2R1 and C1R2, all applying baseline case no. 3 (Regulate EF). Table 5.5 presents standard deviations of the exercise measurements from the trial data, along with the ages of the participants. As described in Section 4.1, the heart rates (HR) obtained by ECG and systolic (P_{sys}) and diastolic (P_{dia}) pressures obtained by radial measurements were subjected to an interquartile range filtering procedure prior to being used for model purposes. This has consequently reduced the resulting standard deviations shown in Tables 5.5, 5.6 and 5.7, which were originally greater when calcuated directly from the raw data. It is further noted that the validation participants are on average older than the six used in the development experiments, whose ages are stated in Table 5.1. The validation participants have an average age of 39 years compared to 32 years in the development cohort. Equation (3.10) yields a smaller HR_{max} for a higher age, resulting in a greater heart rate-based intensity (3.9), and consequently greater shifts in E_{max}, R_{sys} and C_{ao} during exercise. The following is observed from the validation experiments:

- Overall, the prediction errors exhibit similar average tendencies as observed in the six development participants (Fig. 5.12). The combinations where semi-linear trial-based compliance shifts are applied (C2) yield the smallest errors in P_{sys}, while the exponential trial-based resistance shifts (R2) are beneficial for reducing errors in P_{dia}.
- A prominent peak in MAE of P_{sys} is observed at 50 W for C2R1 that was not present in Figure 5.12.
- The smallest average errors are 16.7 mmHg for P_{sys} in configuration C1R1 and 12.4 mmHg for P_{dia} in C1R2. For the six development participants, the average errors in the same configurations are 16.4 and 15.5 mmHg, respectively.
- The personalized model predictions of P_{sys} perform better than the ESP-averages, whose errors are contained in the column denoted $|\overline{\Delta_C}|$ in Table 5.6.
- All average errors clearly exceed clinical criteria for blood pressure measurement accuracy of ±3 mmHg (Section 4.4.4). As can be read from Table 5.6, only one participant remains within this criteria across all intensity levels, i.e. 745, whose average MAE is 2.7 mmHg for P_{sys} when configuration C2R1 is applied. Unfortunately, P_{dia} is clearly overestimated in the same case with an average MAE of 21.8 mmHg. The average errors are also too pronounced to be assigned exclusively to uncertainties related to high exercise intensities, as they are relatively greater compared to data variability reported in Table 5.2.
- The validation did not consider SV during exercise, but based on Figure 5.12c it appears improbable that potential predictions would have yielded an accuracy within the criteria of ±10%.

Chapter 6

Discussion

As stated in Section 1.2, this work aims to further develop and validate the MyMDT hemodynamic exercise model against cardiovascular data collected in a clinical exercise trial. First, in silico experiments were conducted to examine model procedures of i) estimating baseline parameters and ii) exercise simulation. The purpose of this primary part of the project was to develop the hemodynamic model by improving its predictive accuracy through structural adjustments, without increasing the level of complexity. As a secondary part, a brief validation was performed on five participants that were not used in the development experiments. In the following, results presented in Chapter 5 are discussed in a consecutive order according to the methods and suggestions stated in Sections 4.2 and 4.3. Insights obtained throughout the work that were not shown in Chapter 5 are also considered, as they explain the process from which the results chosen to highlight were determined. Finally, the chapter concludes with a brief review of three minor pilot experiments motivated by the preceding discussion.

6.1 The Parameter Estimation Procedure

The method based on the work by Bjørdalsbakke et al. [4] concerning the estimation of resting state parameters for the hemodynamic model has been examined. Parameters obtained by this procedure constitute the baseline for following exercise predictions. Section 5.1 compared optimized waveforms (Fig. 5.1) parameter estimates (Fig. 5.2), resting state outputs (Fig. 5.3) and exercise simulations (Fig. 5.4) across five different variants of the baseline procedure.

6.1.1 Synchronization of Input Data and Model Cycle Start

The arterial pressure cycles obtained by tonometry begin on upstroke, i.e. with the initiation of systole, which is the most convenient when splitting a pressure time series into individual cycles. Based on this premise, this project investigated how model cycle start and the synchronization of pressure and flow data should be defined to benefit the optimization procedure. From Figure 4.2, it might be argued that agreement on the timing of valve closure for pressure and flow (Fig. 4.2b) yields a more consistent representation of a cardiac cycle than synchronization to upstroke (Fig. 4.2a). In cases where the deviation was not as prominent as in Figure 4.2, valve closure synchronization appeared to potentially agree better with also the timing of upstroke. However, the alternatives cannot be evaluated without considering also how they facilitate parameter fits in the estimation procedure, which uses flow and pressures waves as input. A potential issue regarding this aspect in the original implementation was discovered early in the current project. Originally, a cardiac cycle as defined by the model begins approximately 0.1 s before systole. It was raised attention to a potential source of optimization problems yielded by lack of consistency between the model and the arterial data it is supposed to fit. This was revealed by inaccurate optimized waveforms with deviating starting points compared to corresponding data. Hence, in collaboration with Ph.D. Candidate Bjørdalsbakke, an additional function was developed to shift model waves of pressure and flow within the cost function to also begin on upstroke (P_{dia} at t=0, and $\dot{Q}_{\text{ao}}, \dot{P}_{\text{ao}}>0$). This change was implemented early in the project and used in all subsequent analyses, as it unambiguously improved the premises for optimizing waveforms. As a consequence of this modification, synchronization to the dicrotic notch became prominently less beneficial compared to upstroke due to discrepancies in cycle start between flow data and the model. Overall, upstroke synchronization for pressure and flow in both model and data yielded significantly more accurate optimized waveforms compared to cases with deviating cycle starts.

6.1.2 Assignment of Fixed and Estimated Parameters

Configurations of the baseline procedure defining t_{peak}, Z_{ao} and C_{sv} as fixed and estimated were investigated. The following paragraphs discuss the overall effect of these alternatives on resulting parameter estimates, exercise predictions and the estimation procedure itself.

Time of Peak Elastance (t_{peak})

All five variations of the baseline procedure presented in Chapter 5 have t_{peak} fixed to the dicrotic notch. It was early observed that the dicrotic notch tends to occur at a time in the cardiac cycle that is significantly less compared to most estimates of t_{peak}. Several test cases estimated t_{peak} to its upper bound of

0.442 s when constraints were applied according to Table 4.4. A parameter estimated to a limit value is an indication that a personal property is not being represented as intended. Further, fixing t_{peak} yielded more physiologically plausible exercise predictions. This is in accordance with observations made during the fall of 2021, where having $t_{\text{peak}} \gtrapprox 0.45$ s indicated inadequate restoration of diastolic filling in combination with the implementation of lusitropy ((4.9) and $b = b_{\text{W}}$) [7]. Overall, no advantages of significance were associated with estimating t_{peak} compared to fixing it to the dicrotic notch, hence the latter alternative was used in all configurations illustrated in Chapter 5.

Aortic Impedance (Z_{ao})

The value of Z_{ao} is affected by adjustments of the parameter estimation procedure if it is included in the main optimization, or if changes impact the preliminary part. However, all five baseline cases presented in Chapter 5 were conducted with preliminary fitted Z_{ao}, and no variations that altered this fit. The inclusion of Z_{ao} in the full estimation procedure was attempted in multiple test cases and configurations throughout. The motivation for this adjustment compared to the original implementation with only preliminary fitted Z_{ao} was the presence of very small values in participants 637 and 248, who also showed prominent peaks in their optimized flow waveforms inconsistent with data (Fig. 5.1b). Since flow is inversely proportional to resistance (2.2), a suggested remedy for this behaviour was to include Z_{ao} in the main estimation procedure. This did indeed result in increased values of Z_{ao} and better flow fits for 637 and 248, but without improved exercise predictions. For the remaining participants, the effect was negligible. Hence, because the inclusion of additional parameters in the optimization also increases the duration of the analysis, it was concluded as advantageous to keep Z_{ao} fixed to its preliminary fitted value.

Venous Compliance (C_{sv})

Estimated values of C_{sv} were sensitive to remaining variations in the baseline procedure, which can be observed in Figure 5.2b. As stated in Table 4.4, C_{sv} is quite loosely constrained, because while there are many studies reporting compliance of particular veins, appropriate values representing a total venous compliance transferable to the model parameter are much scarcer. Furthermore, attempts to model venous function are more commonly done using true blood volumes as opposed to only stressed volumes. However, there is an overall agreement that the compliance of veins is higher than arterial compliance with a factor of roughly ≈10-20 [40]. It was early observed that C_{sv} was estimated significantly less than this approximation in most configurations. Therefore, it was attempted to fix C_{sv} to $10 \times C_a$. The main effect was an overall increase in V_{tot} (Fig. 5.2d), which can be explained by the need for increased volume

to sustain a mean venous pressure (MVP) of 6 mmHg with a higher C_{sv}. Unfortunately, the increased V_{tot} was accompanied by improbably small values of E_{max} (Fig. 5.2a), and very high values of ventricular volumes ESV and EDV (Figs. 5.3f and 5.3e), the latter resulting in small ejection fractions (EF) (2.4).

Blood volume is a complicated issue in the hemodynamic model. In general, EDV and ESV include an unstressed fraction (V_0) that the model does not consider. This means that from a physiological view, V_0 would have to be quite negative to explain the large stressed volumes. As illustrated by the PV-loop (Fig. 2.1), cardiac function is characterized by both ventricular volumes and pressures. Here, V_0 is the reference point from which the slope to end-systole is calculated, which implicitly equals 0 in the model. If the stressed volume becomes larger, the respective slope (E_{max}) must be smaller to produce the same pressure. Hence, slopes E_{max} and E_{min} can be represented despite not assigning a physiological value of V_0, as the inclusion of V_0 simply shifts the PV-loop without affecting the slopes. Although the pumping force of the heart exerted on the arterial compartment can be quantified while considering only stressed volume, the complete behaviour of the heart cannot be physiologically described without V_0. Thus, it is ambiguous based on apparently non-physiological values of ventricular volumes whether fixing or estimating C_{sv} is the most beneficial for the model. Configurations including both alternatives were included in the search for the overall best baseline procedure for accurate exercise simulations.

Two of the five baseline configurations shown in Section 5.1 have fixed C_{sv}; no. 4 (Fix C_{sv}) and 5 (Fix C_{sv}+regulate EF). The latter exhibited an unstable behaviour that differed significantly from the remaining configurations, e.g. with a higher estimate of C_{ao} (Fig. 5.2c) and a mean venous pressure (MVP) lower than the target value of 6 mmHg (Fig. 5.3d). It appears as if the combined demands of high C_{sv} (fixed C_{sv}) and low V_{tot} (penalize the cost function for low EF) are unable to preserve desired venous pressure. In total, this configuration exhibited greatest MAE of P_{sys} and SV (Fig. 5.5). Baseline case no. 4, i.e. with constraints, performed more similarly as the remaining configurations, and more accurately during exercise. Thus, it appears beneficial that the model is allowed to compensate for the large compliance by increasing its volume to maintain physiologically accurate levels of P_{sys} and SV during exercise (Figs. 5.4a and 5.4i). Case no. 4 was further analyzed in Figure 5.12, and yielded overall greater errors in both P_{sys} and SV compared to case no. 3 (Regulate EF), but the errors in P_{dia} were smaller.

The motivation for fixing C_{sv} was to examine whether the model could be forced to contain more volume in the venous compartment to maintain MVP=6 mmHg, particularly when simultaneously penalizing the cost function for small ejection fractions. However, the model appears reluctant to accede to measures implemented to enforce a certain distribution of volume. This behaviour is pursued in Section 6.4.1 with a discussion of an experiment conducted to investigate the interrelations between C_{sv}, V_{tot}, E_{max} and the cost function.

6.1.3 Constraints

Several test experiments in preliminary configurations frequently estimated maximum elastance (E_{max}) to its lower limit value, which was first set to 1.0 $^{mmHg}/_{mL}$ and later adjusted to 0.5 $^{mmHg}/_{mL}$. As can be seen in Figure 5.2a, most estimates of E_{max} are significantly smaller than the physiological, data-based approximation $^{P_{dn}}/_{ESV}$, where P_{dn} is BP at the dicrotic notch (Fig. 2.2). Even though the presented value of $^{P_{dn}}/_{ESV}$ assumes an ejection fraction (EF) defined as 60%, the comparison is useful for investigating whether the estimated E_{max} represents a personal cardiovascular property. Parameters C_{sv} and t_{peak} were also in some preliminary configurations estimated to their lower and upper limits, respectively. A motivation for conducting the estimation procedure without constraints was to investigate why these parameters were estimated to their bounds. A possible explanation is that constraints (Table 4.4) do not allow the optimization algorithm to search efficiently for all possible parameter combinations. As it turned out, t_{peak} was estimated significantly closer to the dicrotic notch when the constraints were removed. In some cases, the lack of constraints yielded very improbable mean parameter fits, recognized e.g. by simulated pressures that were in varying degree shifted above the tonometry waveforms. This unfortunate behaviour was particularly pronounced in participant 637. Therefore, in case no. 2 (No constraints), the minimum parameters, i.e. the parameter set with minimum cost function, are used as basis for comparison with the remaining configurations, where the mean parameters are used as baseline. This resulted in a set of baseline parameters for case no. 2 more similar to case no. 1 (Full estimation), where constraints were applied. Another negative aspect of removing constraints is that the unlimited search range for the numerical optimization showed to significantly increase the duration of the estimation process, which in the slowest cases went from ≈1.5–3.5 hrs for one participant.

6.1.4 Regulation of Ejection Fraction

As described in Section 4.2.6, the motivation for implementing a regulation of ejection fraction (EF) in the estimation procedure was the early observation of estimated high values of V_{tot}. A high V_{tot} is not problematic in itself, as most of the blood should be contained in the venous compartment under low pressure. It can even be beneficial, as a large total volume gives the model more blood to distribute to the ventricles during exercise, thereby facilitating an increased EDV in accordance with physiological theory (Section 2.1.5). However, it was observed that a high V_{tot} was consistently accompanied by high end-diastolic and end-systolic volumes (EDV and ESV). Although the target value of stroke volume (SV=EDV-ESV) could still be fulfilled, this resulted in very low EFs. A suggested remedy for the high volumes was to implement a penalty on the cost function when resulting estimates yielded extreme values of EF. This was attempted in baseline cases 3 (Regulate EF) and 5 (Fix C_{sv}+regulate EF), which essentially differ in

that no. 4 fixes C_{sv}, while no. 3 estimates this parameter.

Overall, ESV and EDV are the least plausible of all predicted quantities, as observed in Figures 5.3f and 5.3e. At the same time, E_{max} is frequently estimated non-physiologically small (Fig. 5.2a). It appears as if the model tends to maintain ventricular pressure by large volumes and a small elastance, while the opposite is desirable from a physiological point of view. Implementing a hardmax regulation of EF (4.4), did indeed increase E_{max} and reduced ventricular volumes. According to Figure 5.5, case no. 3 (Regulate EF) yields the baseline with smallest MAE of P_{sys} and SV during exercise, but unfortunately the greatest errors in P_{dia}.

As stated in Section 4.2.6, it was questioned during the project whether the regulation of EF with a hardmax step function (4.4) perturbates the optimization procedure along the predefined boundaries of $[EF_{min}, EF_{max}]$. Therefore, another version of case no. 3 (Regulate EF) was attempted using the softmax implementation (4.6) with $\alpha = 100$, weight $W_{ef} = 50$, and the same limits $[EF_{min}, EF_{max}] = [35,75]\%$ as used for the step function. Overall, the softmax version found similar parameter fits as hardmax, but the relatively large estimates of E_{max} yielded by hardmax, i.e. in participants 890 and 637, were estimated less with softmax, with correspondingly increased ventricular volumes. Similarly, in cases where E_{max} was estimated small with hardmax, i.e. participants 734 and 346, E_{max} increased, while ventricular volumes decreased. However, the overall difference between penalizing the cost function with hardmax vs. softmax was insignificant when considering the optimized waveforms, model outputs of P_{sys}, P_{dia} and SV, and exercise simulations of these. The softmax implementation thus served as a verification that the solutions obtained by the hardmax step function had not been impeded by algorithmic issues to a level that altered their reliability. Note that these attempts to regulate EF are highly preliminary. The further use of such implementations, determination of boundaries of EF, sensitivity through W_{ef} and the $(1 + 1/EF)$-factor for the softmax version (4.6), would require multiple experiments in various configurations beyond this work.

6.1.5 Remarks on the Baseline Procedure

Of the six participants included in the development experiments, nos. 637 and 248 were associated with overall unstable behaviour. As illustrated in Figure 5.1b, optimized waveforms for 637 and 248 were more sensitive to choice of baseline configuration compared to 734 and 890. 248 yielded a behaviour that was quite similar to 637 in both waveforms and exercise simulations. The simulated behaviour of P_{dia} and SV during exercise in these two participants was very implausible, and did not appear corrigible by adjustments of neither baseline nor exercise simulation procedures. The waveforms depicted in Figure 5.1b reveal a possible explanation for the unstable behaviour exhibited by 637 and 248; the

carotid pressure waveform is quite narrow, lacks a prominent dicrotic notch and is overall more dissimilar to an expected arterial pressure waveform (Fig. 2.2) compared to the remaining four participants. Thus, the individual model simulations for 637 and 248 were decided not to have a direct impact when determining the suitability of a baseline configuration. However, the carotid waveforms were not considered sufficiently nonphysical to exclude 637 and 248 from average error calculations, as the premises for discarding data for model usage are not yet drafted. Furthermore, it is advantageous for model robustness to pursue a wide range of data in a calibration process. Still, the inclusion of these consistently unbehaved simulations may have resulted in average errors that are not necessarily representable for the remaining four, more stable participants.

Based on the exercise simulations depicted in Figure 5.4 and average errors in Figure 5.5, estimation case no. 3 (Regulate EF) was chosen as baseline for the examination of two properties directly related to exercise simulations; pressure amplification and lusitropy. Further, case no. 4 (Fix C_{sv}) was included in the examination of exercise shifts, as this case yielded slightly lower errors in P_{dia} compared to case no. 3. Case 5 (Fix C_{sv}+regulate EF) yielded the lowest errors in P_{dia}, but escalated the errors in P_{sys} and SV, and was therefore not prioritized for further investigations in this project.

The baseline procedure aims to fit a model that includes an arterial, venous and ventricular compartment using flow and pressure data collected only from the arterial circulation. The arterial compartment is represented by the three-element Windkessel model (Section 3.3.1). Figure 5.2 shows negligible deviations between resulting estimates of the Windkessel-related parameters R_{sys} (Fig. 5.3a) and C_{ao} (Fig. 5.3a) across the five baseline configurations for most participants. It is apparent that the arterial part of the hemodynamic model is both more stable and physiologically accurate than the ventricular and venous compartments, reflected by prominent variations in estimates of E_{max}, C_{sv} and V_{tot} in contrast to the stable arterial parameters. This feature can be a consequence of the lack of venous and ventricular data to fit the model against. Another possibility is that the Windkessel model in itself is a better numerical representation of a physiological system than the implementations of cardiac and venous function. It is probable that both factors are contributing to the apparent misbehaviour of the ventricular and venous compartments. This discovery motivated a preliminary pilot experiment using an open-loop model excluding V_{tot} and the venous compartment entirely, which is discussed in Section 6.4.3.

6.2 The Exercise Simulation Procedure

This section discusses aspects of exercise simulation highlighted by the results in Section 5.2 in a stepwise and consecutive order according to the suggestions presented in Section 4.3. Each part is analyzed with the remaining configurations fixed to one or a selected few cases. This is somewhat limiting, as variation in one parameter will in general impact the effect of other. However, the range of possible combinations is too extensive for simultaneous presentation and evaluation. Therefore, a stepwise inspection of the various effects is considered adequate within the limitations of this project. The section is introduced with a brief discussion of the uncertainty and reliability of the project database.

6.2.1 Reliability of the Trial Data

As stated in Section 4.1, model performance during exercise is evaluated against blood pressure (BP) measured at the radial artery, and stroke volume (SV) obtained from integrated Doppler velocity traces. Literature-based values are included as basis of comparison for mean venous pressure (MVP) and SV due to lack of data for the venous compartment and questionable reliability of the preliminary processed flow data, respectively. When measuring SV by a Doppler method, an ultrasound probe is placed manually on the skin of the participant. Resulting velocities are sensitive to motion and angle [45], and are in general prone to more uncertainty compared to pressures. Hence, reliability of these recordings is somewhat limited, especially at higher intensity levels. Greater exercise effort increases the movement under the Doppler ultrasound probe, which can reduce the accuracy of the following semi-manually obtained flow traces. Uncertainties related to higher intensities are reflected by an overall tendency of increased standard deviations of the measurements, although not very pronounced (Table 5.2). The filtering procedure (Section 4.1) ensured a variability of radial pressures within a magnitude of ≈5 mmHg. As SV and HR used in the development experiments had been manually obtained [7], their variability was assumed initially acceptable, and no filtering procedure was applied. The standard deviations of the non-filtered SV and HR are of similar magnitudes as the filtered radial pressures, with the exception of a prominent outlier $\sigma_{150\mathrm{W}}$(HR)=41.3 bpm in participant 637. The method for obtaining preliminary radial systolic and diastolic pressures is considered reasonably accurate. For SV, it was observed some tendencies of prominent, implausible troughs, e.g. in participant 890 at 50 W (Fig. 5.4f). To limit the influence of suspected low-quality data in the development of trial-based exercise configurations, prominent outliers were ignored, e.g. when performing the regression to obtain a general, trial-based b (4.9). Naturally, access to finally processed, quality assured data would have been beneficial. However, the reliability of the preliminary trial data was considered adequate for the scope of this project, confirmed by average model prediction errors (Fig. 5.12) of greater magnitude compared to data variability (Table 5.2).

6.2.2 Scaling of Model Pressures

The direct comparison of predicted BP against experimental measurements from the clinical exercise trial is essentially illogical. The model simulates an aortic pressure wave, which as described in Section 2.1.4 is inherently different from the radial waveform collected in the study (Fig. 2.4). This feature motivated the implementation of a post-processing procedure for the model pressures when comparing against radial data. Figure 5.6 shows that by implementing a scaling factor to adjust for the pressure amplification present between the aorta and the radial artery, model predictions became unambiguously more consistent with data compared to non-scaled predictions. It is apparent that an intervention such as the implemented scaling is necessary for the interpretability and meaning of evaluating and validating the hemodynamic model against exercise data from the trial. Knowledge about physiological relations and properties are important when working with mathematical modelling against clinical applications, which motivated the inclusion of a relatively thorough theoretical review of the cardiovascular system (Section 2.1) in this report.

6.2.3 The Lusitropy Mechanism

The Specialization Project [6] showed that model behaviour is highly sensitive to the lusitropy coefficient (Fig. 4.3), which is supported by results obtained in this project. Figure 5.8 illustrates the vast impact of the lusitropy coefficient (b) on an exercise simulation. The absence of lusitropy is simulated for illustrative purposes by setting $b = 0$. The prominent reduction in EDV (Fig. 5.8c) at higher intensities given $b = 0$ indicates diminished diastolic filling during exercise. ESV is reduced to a near similar degree as EDV, and SV is slightly reduced (Fig. 5.8d). To fulfill its relation to SV (PP$\times C_a$=SV), pulse pressure (PP) tends to stays horizontal (Fig. 5.8b), which corresponds to a flattened P_{sys} (Fig. 5.8a). In general, ESV and E_{max} are major determinants of P_{sys} (2.12), which indicates that when ESV decreases to a level beyond what is compensated by a shifted E_{max}, P_{sys} fails to increase. However, while causing predictions of P_{sys} and SV to behave non-physiologically, the diminished diastolic filling simultaneously counteracts the model tendency of consistently overestimating P_{dia}, thus benefiting these predictions on an average level (Fig. 5.9). Interrelations between model parameters during exercise are further emphasized in Section 6.2.6.

As stated above, $b = 0$ is not an applicable configuration for the model, which was first highlighted by Straatman in 2021 [7]. However, due to the vast importance of lusitropy and the lack of satisfying results obtained with $b = b_{\text{W}} = -2.1 \times 10^{-3}$ s $\times$ min from Weissler et al. [13], this project examined alternative values and increased personalization of lusitropy through the regression coefficient (b). A brief literature study summarized in Table 5.3 revealed the following ranges of experimentally obtained regression

coefficients for two measures of systolic period; electromechanical systolic time intervals (QS_2) $\in$[-2.1,-1.16]$\times 10^{-3}$ s $\times$ min, and left ventricular ejection period (LVET) $\in$[-1.7,-1.15]$\times 10^{-3}$ s $\times$ min. Overall, reported QS_2 are of greater magnitude than LVET. The smallest values of QS_2 and LVET are quite consistent with the regression coefficient of LVET obtained from the trial data ($b_{\text{reg}} = -1.1 \times 10^{-3}$ s $\times$ min). It can be argued that because it incorporates more of the systolic phase, QS_2 is more representative for t_{peak} than LVET, which is why QS_2 collected from Weissler et al. [13] was originally adapted to the hemodynamic model. However, the level of transferability between t_{peak} and physiological systolic period is not yet clarified to an extent that LVET can be unquestionably discarded in favor of QS_2. Therefore, it was chosen to compare model behaviour exhibited with b_{W} to b_{reg}, where the latter has an overall level of agreement with the literature-based LVET-periods, which confirms the reliability of the data used to obtain this value. Overall, simulations based on these two distinct values and $b = 0$ constitute an informative basis of insights about the impact of b.

The explicit exercise simulation in Figure 5.8 shows the impact of lusitropy on diastolic filling. The steepest slope (b_W) yields the greatest reduction in systolic activation time, resulting in high values of EDV (Fig. 5.8c), SV (Fig. 5.8d) and P_{sys} (Fig. 5.8a). In the presented example, P_{sys} and SV are overestimated by b_{W}, while b_{reg} yields model predictions more consistent with data. However, this is more ambiguous when including all six participants (Fig. 5.9). On average, b_{reg} and b_{W} perform similarly for P_{sys}, while b_{reg} clearly benefits the accuracy of the explicit simulation depicted for participant no. 890. It is further noted that the standard deviations of the averaged MAE across participants are relatively large (Fig. 5.9). Therefore, it cannot be concluded which coefficient is the better alternative when simultaneously evaluating P_{sys}, P_{dia} and SV in all participants. Since b_{reg} performed best on average for both P_{sys} and SV, this value was chosen as basis for evaluating the remaining exercise configurations.

A further personalization of the lusitropy implementation was attempted by using personal regression values of LVET for each participant (b_{pers}), as depicted in Figure 5.7. This did not yield significantly better results compared to the average value (b_{reg}), which indicates that increased personalization of the current implementation of lusitropy (4.9) will not radically improve the model. However, the level of influence b clearly has on all aspects of model behaviour during exercise shows that its value should not be defined without caution. Further, the value of b that facilitates most reliable predictions is dependent upon other model configurations. The combined effects of lusitropy and other parameter shifts (E_{max}, C_{ao} and R_{sys}) were not considered in this report, but the impact of b yielded by a pilot experiment with an open-loop model is discussed in Section 6.4.3.

6.2.4 Exercise Shifts of C_{ao} and R_{sys}

The exercise model in its original form, i.e. as developed by Bjørdalsbakke and the MyMDT project [5], is implemented by Equation (3.8) and population averages reported by Chantler et al. [30]. This configuration is referred to as C1R1 in Figures 5.11 and 5.12, where letters C and R refer to compliance and resistance shifts, respectively, and the number 1 denotes Chantler-based shift. This work has experimented with alternative implementations of exercise shifts using values of $^{SV}/_{PP}$ and $^{MAP}/_{CO}$ obtained in the clinical exercise trial to shift C_{ao} and R_{sys}, respectively. Simulations using the more personal alternatives derived in Section 4.3.3 are not depicted, as these implementations rely on data that is in general unavailable for future users of MyMDT. Furthermore, it was observed from test cases that the personalized versions did not result in radically improved predictions compared to the average-based configurations. Another argument is central for not applying trial-data directly on a personal level to shift parameters; the use of data to make predictions that are later compared against the same data is circular logic, and not beneficial for developing a robust and generally applicable model.

Figure 5.10 shows that the data-based shifts of C_{ao} (C2) and R_{sys} (R2) impose greater reductions in the parameter values compared to Chantler-based shifts (C1 and R1). The baseline cases used as basis for examining the exercise shifts are nos. 3 (Regulate EF) and 4 (Fix C_{sv}). From Figures 5.11 and 5.12 it is noted that C2 is associated with the greatest predictions of P_{sys} and minimum MAE when combined with parameter case no. 3. Systolic pressure (P_{sys}) appears more sensitive to compliance than resistance shifts, as C1 and C2 yield approximately equal average errors regardless of resistance shift when baseline case no. 3 is used. The opposite is the case for P_{dia}, where R1 and R2 yield similar errors regardless of compliance shift for both baseline cases. R2 yields smallest predictions of P_{dia}, which corresponds to minimum errors. In total, the tendency previously stated as characterizable for the hemodynamic model is present; diastolic pressures are in general overestimated. Configurations that counteract overestimation the most yield minimum errors. The sign of the bias in P_{sys} varies more across exercise configurations, which is the reason for the choice of MAE as error metric for evaluating the impact of exercise shifts on model performance. Chantler-based shifts are, however, more prone to underestimate P_{sys}. This is recognized in the negative average bias presented in the context of pressure scaling (Fig. 5.6), where Chantler-based shifts in combination with b_{reg} and baseline case 3 were used.

None of the configurations shown predict a physiologically plausible development of ventricular volumes (Figs. 5.11g and 5.11h). As reviewed in Section 2.1.5, cardiovascular theory states that EDV in general increases during exercise. The current model structure is not able to capture this behaviour. It is possible that this property would require implementation of a mechanism representing the redistribution of blood volume in the body during exercise, with more flow to the active tissue. A challenge here

is the scarce availability of mathematical descriptions of how *stressed* volume varies during exercise. However, the implausible behaviour is in itself not a problem, as it is not an ambition for the model to accurately represent ventricular volumes. Furthermore, as observed in Figure 5.11e, the capture of EDV and ESV is not strictly necessary to accurately predict SV, which is a priority for the exercise model. Note that the y-axes on the figures showing EDV and ESV include a much wider range of volumes than the axis related to SV. The baseline case determines the starting value of ventricular volumes, but their development is much more sensitive to the lusitropy coefficient (Fig. 5.8c) than exercise shifts. This indicates that filling time is a greater determinant of ventricular volumes than compliance and resistance. The configuration C2R2 yields greatest predictions of SV, and C1R1 the smallest, and the latter corresponds to minimum average errors in SV (Fig. 5.12c).

In total, baseline case no. 3 (Regulate EF) performed better during exercise compared to no. 4 (Fix C_{sv}). Therefore, it was decided to continue with case no. 3 for the validation experiments. None of the exercise configurations performed convincingly better than the other, hence C1R1, C2R1 and C1R2 are treated in the validation. The combination C2R2 was excluded because it yielded MAE of SV≈30% greater than the other configurations in the development experiments, although pressure predictions were on average more accurate compared to C1C1, C2R1 and C1R1 (Table A.6). Overall, the project part on model development could not obtain any combination of exercise shifts that radically improved the performance on an average level. Remarks on the exercise simulation procedure including a discussion of possible explanations for this revelation are found in Section 6.2.6.

6.2.5 Resting Heart Period (T)

As stated in Section 4.3.4, resting heart period (T) has two roles in the exercise model: First, it is a fixed baseline parameter. Second, it is used in the definition of heart rate reserve-based exercise intensity (3.9), which determines the magnitude of exercise shifts in C_{ao}, R_{sys} and E_{max}. Attempts to change the definition of T as a baseline parameter were not prioritized in this project. This could have been done by e.g. enforcing the tonometry signal to instead span the resting (0 W) heart period from the radial waveform. However, the choice of T is in any case a compromise. Flow was collected simultaneously as radial BP, and is thus better adapted to these heart rates than the tonometry period, which on the other hand is obviously in best accordance with the tonometry pressure signal. Instead, it was raised attention to possible ways of determining T as a exercise-determining quantity based on trial data, but not as a baseline parameter (Section 4.3.4). The following alternatives were presented: 1) Tonometry period ($\overline{T}_{ton}$), 2) 0 W supine period ($\overline{T}_{0W}^{sup}$), and 3) 0 W semi-recumbent period ($\overline{T}_{0W}^{sr}$). Although illustrated for one participant only, Figure 4.4 is representative for a prominent tendency present in the majority of the

six participants evaluated; $\overline{T}_{0W}^{sr} < \overline{T}_{0W}^{sup} \approx \overline{T}_{ton}$. Lack of restitution after exercising in the sup-position may have caused elevated pulse in the sr-position at 0 W.

Only $\overline{T}_{ton}$ was used to produce the results presented in Chapter 5. Several test experiments showed that changing T in the calculation of I_{HRR} was associated with less pronounced variations in predictions compared to other interventions made to improve the quality of the exercise simulations. The effect of changing T in I_{HRR} is also in general more predictable when evaluating the magnitudes of the various periods. A natural consequence of the tendency $\overline{T}_{0W}^{sr} < \overline{T}_{ton}$ is that defining $\overline{T}_{0W}^{sr}$ as resting period results in smaller values of I_{HRR} compared to $\overline{T}_{ton}$ and $\overline{T}_{0W}^{sup}$. This effect appeared the most pronounced at 0 W, and decreased with increasing intensity. A similar tendency was also indicated by the sensitivity analysis in the Specialization Project [6], which yielded small values of $S_T(T)$ in combination with $I = I_{HRR}$ for all quantities at high intensities. Here, T refers to the resting state parameter, and it was also used in the calculation of $I = I_{HRR}$ in [6]. At is was chosen not to perform exercise shifts at 0 W, the total effect of choosing another T than $\overline{T}_{ton}$ in Equation (3.9) did not appear significant. A more thorough investigation of the impact of T might be more appropriate in combination with a study on the effect of alternative definitions of exercise intensity on model behaviour. This work was also initiated in the Specialization Project, but not prioritized to pursue in this work.

6.2.6 Remarks on the Exercise Simulation Procedure

Explaining causalities and correlations between the various model quantities and their behaviour during exercise is challenging, mainly because many variables are extensively interrelated and can vary simultaneously. In the following, simplified versions of some governing principal equations for the model (A.2) are presented and combined. The purpose is investigating whether the overall tendencies indicated by the in silico experiments can be numerically explained by the model structure.

The behaviour of arterial diastolic pressure (P_{dia}) can be analyzed by evaluating the governing differential equation for arterial pressure in the two-element Windkessel model [26]:

$$\frac{dP}{dt} = \frac{1}{C_a}\left(\frac{-P}{R_{sys}} + Q(t)\right). \tag{6.1}$$

By utilizing that there is no inflow from the ventricle ($Q = 0$) during diastole, this reduces to

$$\frac{dP}{dt} = -\frac{P}{R_{sys} \times C_a} \tag{6.2}$$

for the entire diastolic phase. The general solution is:

$$P = P_0 \times \exp\left(-\frac{t - t_0}{R_{sys} \times C_a}\right) \tag{6.3}$$

where P_0 is the arterial pressure at a reference time t_0 during diastole, and $\tau = R_{sys} \times C_a$ is a time constant

that is consequently determining for P_{dia}. By setting time $t = t_{\text{ed}}$ (ed = end-diastole), Equation (6.3) reads:

$$P_{\text{dia}} = P_0 \times \exp\left(-\frac{t_{\text{ed}} - t_0}{R_{\text{sys}}^{\downarrow} \times C_a^{\downarrow}}\right) \tag{6.4}$$

where P_0 and t_0 are often taken at end-systole. The time t_{ed} is mainly determined by heart period (T). Thus, increased reductions in $R_{\text{sys}}(\downarrow)$ and $C_{\text{ao}}(\downarrow)$ during exercise facilitate reduction in P_{dia}.

Arterial systolic pressure (P_{sys}) is an important variable in the hemodynamic model. Its value is governed mainly by the end-systolic pressure in the left ventricle (ESP_{lv}), which is given as:

$$\text{ESP}_{\text{lv}} = \text{ESV} \times E_{\text{max}}^{\uparrow} \tag{6.5}$$

Since systole ends with closure of the aortic valve, marked by the dicrotic notch on the arterial pressure wave, we have that $\text{ESP}_{\text{lv}} \approx P_{\text{ao}}^{\text{dn}}$ at end-systole, where $P_{\text{ao}}^{\text{dn}}$ is aortic pressure at the dicrotic notch. This is similar to the approximation of E_{max} in Equation (2.12). By assuming that $P_{\text{ao}}^{\text{dn}}$ and P_{sys} behave quantitatively similar, it is common to replace ESP_{lv} by P_{sys} in Equation (6.5). The major determinants of systolic pressure during exercise are thus ESV and E_{max}, where the model defines the latter to increase during exercise ($\uparrow$), facilitating an increase in P_{sys}. Additionally, Equations (6.5) and (6.4) explain the observation of P_{dia} being significantly more sensitive to the shifting procedure of R_{sys} (R1 vs. R2 in Fig. 5.11b) compared to P_{sys}, as resistance is not directly a governing determinant of systolic arterial pressure.

Similarly, a relation between E_{min} and EDV can be obtained by applying $Q_{\text{svlv}} = I(P_{\text{sv}} > P_{\text{lv}}) \times \frac{P_{\text{sv}} - P_{\text{lv}}}{R_{\text{mv}}}$ from Equation (A.2), and using that at end-diastole (ED), there is no flow between the systemic veins and the left ventricle ($Q_{\text{svlv}} = 0$) due to the closed mitral valve. I.e., the logical function $I(P_{\text{sv}} > P_{\text{lv}})$ goes from 1 to 0 at ED, and $P_{\text{sv}} \approx P_{\text{lv}}$. Substituting P_{sv} for P_{lv} into the relation $V_{\text{lv}} = {}^{P_{\text{lv}}}/_{E_{\text{lv}}}$ at ED yields the following:

$$\text{EDV} = \frac{P_{\text{sv}}^{\text{dia}}}{E_{\text{min}}}. \tag{6.6}$$

Note that superscript dia in $P_{\text{sv}}^{\text{dia}}$ does not refer to minimum pressure, but the value occurring at the same time as aortic and ventricular diastolic pressures.

Another governing principle for the entire system behaviour is the closed-loop property. To analyze interactions between the three model compartments left ventricle (lv), arteries/aorta (ao) and systemic veins (sv), equations are simplified and presented at two states; end-systole (ES) and end-diastole (ED) and substituted into the closed-loop equation for V_{tot}:

State	E_{lv}	P_{lv}	V_{lv}	$V_{lv}(t) = {}^{P_{lv}}/_{E_{lv}}$	$V_{ao} = P_{ao} \times C_{ao}$	$V_{sv} = P_{sv} \times C_{sv}$
ES	E_{max}	P_{sys}	ESV	ESV=${}^{P_{sys}}/_{E_{max}}$	$P_{sys} \times C_{ao}$	$P_{sv}^{sys} \times C_{sv}$
ED	E_{min}	P_{sv}^{dia}	EDV	EDV=${}^{P_{sv}^{dia}}/_{E_{min}}$	$P_{dia} \times C_{ao}$	$P_{sv}^{dia} \times C_{sv}$=EDV$\times E_{min} \times C_{sv}$

State	V_{tot}=V_{lv} + V_{ao} + V_{sv}
ES	ESV+$P_{sys} \times C_{ao}$+ V_{sv}^{dia}
ED	EDV+$P_{dia} \times C_{ao}$+ EDV$\times E_{min} \times C_{sv}$

Table 6.1: Rearranging and combining model equations presented in Sections 3.2 and 3.3 at end-systole (ES) and end-diastole (ED). Note that superscripts sys and dia for venous pressures (P_{sv}) refer to the pressures occurring at the same time as arterial P_{sys} and P_{dia}, respectively.

This results in the following relations at ES and ED :

$$\begin{aligned} \text{ES} &: V_{tot}^{\rightarrow} = P_{sys} \times \left(\frac{1}{E_{max}^{\uparrow}} + C_{ao}^{\downarrow} \right) + P_{sv}^{sys} \times C_{sv}^{\rightarrow} \\ \text{ED} &: V_{tot}^{\rightarrow} = P_{dia} \times C_{ao}^{\downarrow} + \text{EDV} \times \left(1 + C_{sv}^{\rightarrow} \times E_{min}^{\rightarrow} \right) \end{aligned} \tag{6.7}$$

where the arrows denote change during exercise ($\rightarrow \Rightarrow$constant, $\uparrow \Rightarrow$increase, $\downarrow \Rightarrow$reduction). Quantities without arrows are free to vary. The average model tendency of a nonphysical increase in P_{dia} is indicated by (6.7) at ED. When C_{ao} decreases, either P_{dia} or EDV must increase to keep V_{tot} constant. As shown in multiple examples, the model overall decreases EDV (and ESV) in exercise state. Given this behaviour, P_{dia} must increase to fulfill Equation (6.7) at ED. Note that this contradicts the previous observation in Equation (6.4), where a decrease in C_{ao} indicated a reduction in P_{dia}. This contradiction is a possible explanation for the observed tendency of P_{dia} being more sensitive to resistance shifts than compliance, as the impact of C_{ao} on P_{dia} has opposite signs in two of the governing model equations.

Many configurations, particularly involving Chantler-based shifts and $b = b_{reg} = -0.0011$ s $\times$ min in the lusitropy implementation, have shown to underestimate P_{sys}. This tendency may be recognized by Equation (6.7) at ES. As previously illustrated, mean venous pressure (MVP) increases during exercise. A sufficient increase in MVP may fulfill (6.7) without a proper increase in P_{sys}. A greater increase in arterial compliance allows P_{sys} to increase more without violating the limit of V_{tot}, which corresponds to the observed smaller average errors for C2 compared to C1.

A clear mathematical description and prediction of the chain of events caused by a single parameter adjustment is challenging to obtain from the model equations, as many variables are interrelated and can vary simultaneously. As shown in multiple examples, ventricular volume exhibit non-physiological behaviour in both rest and exercise simulation. In combination with (6.7), this indicates that the en-

forcement of a constant volume may impact arterial pressures in an unfortunate way, because the defined relation between pressure, volume and compliance must be fulfilled without violating V_{tot}. To circumvent these issues, it was attempted in two pilot experiments to increase V_{tot} during exercise and to replace the venous compartment with a constant pressure in an open-loop model (Section 6.4).

6.3 Model Validity

The validation experiments showed similar tendencies as present when the the corresponding configurations were applied on the development participants. In the best configurations, average MAE of P_{sys} and P_{dia} are of orders ≈16 and 12 mmHg, respectively (Fig. 5.13). The pronounced peak in MAE observed at 50 W for compliance shift C2 might be explained by an higher average age in the validation participants, resulting in greater intensities (I_{HRR}) and shifts at the same exercise resistance I [W]. As previously shown, the influence of lusitropy, which is purely heart rate-dependent, increases progressively with higher intensities, diminishing the direct impact of higher age. In general, greater resistance shifts (R2) than yielded by the Chantler-based implementation (R1) appeared beneficial for the accuracy in P_{dia}, and similar for compliance and P_{sys}. However, the combination C2R2 appeared from the development experiments to yield a vast overestimation of SV. The validation experiments did not assess the performance of different lusitropy mechanisms, baseline configurations or the scaling procedure, but it appears improbable that this would have altered the conclusions from the development part. A total of 11 trial participants have been treated in this project. The inclusion of all 24 would naturally have strengthened the resulting observations, as would the the use of quality-assured data processed by a cardiologist. However, it is reasonable to assume that neither of these improvements would have radically altered the results or the conclusions from this project.

As a basis of comparison for model accuracy, radial systolic pressure measurements were additionally evaluated against average end-systolic pressures (ESP) reported by Chantler et al. [30]. The ESP-values were interpolated to heart rate reserve-based intensities and scaled (4.8), before calculating an average deviation between ESP-prediction and data ($|\overline{\Delta_C}|$). MAEs yielded by deviations between model predictions of P_{sys} and data were then compared to corresponding $|\overline{\Delta_C}|$. As can be read from Table 5.6, errors yielded by the rough ESP-predictions are significantly greater than MAE representing deviations between radial data and model pressures. Thus, the model does yield better predictions compared to this version of a purely average-based estimate. Still, the errors are with few exceptions exceeding clinically acceptable levels to an extent that indicates the necessity of greater structural modifications beyond simply adjusting the current procedures for estimating parameters and/or simulating exercise.

6.4 Pilot Experiments on Alternative Model Structures

This section presents three minor pilot experiments motivated by insights discussed in this chapter. The purpose is explicitly highlighting certain observed model tendencies and to motive future research on the hemodynamic model.

6.4.1 Interrelations Between V_{tot}, C_{sv}, E_{max} and Cost Function

It has been shown through multiple experiments that the parameter estimation procedure is able to accurately capture arterial properties, reflected by stable and physiologically consistent estimates of C_{ao} and R_{sys} (Figs 5.2c and 5.2e). However, the venous and ventricular systems are more unstable and non-physiological. As all baseline cases subjected to analysis in this project have been inherently different, an experiment was conducted by fixing C_{sv} to eight values $\in$[1,2,3,4,5,10,15,20] $^{mL}/_{mmHg}$ in the estimation procedure. Resulting values of V_{tot} and E_{max} were then observed, in addition to corresponding cost function value, i.e. the cost function scaled by $^{1}/_{N_{res}}$, where N_{res} is the number of elements in the residual vector. The experiment yielded the following interrelations:

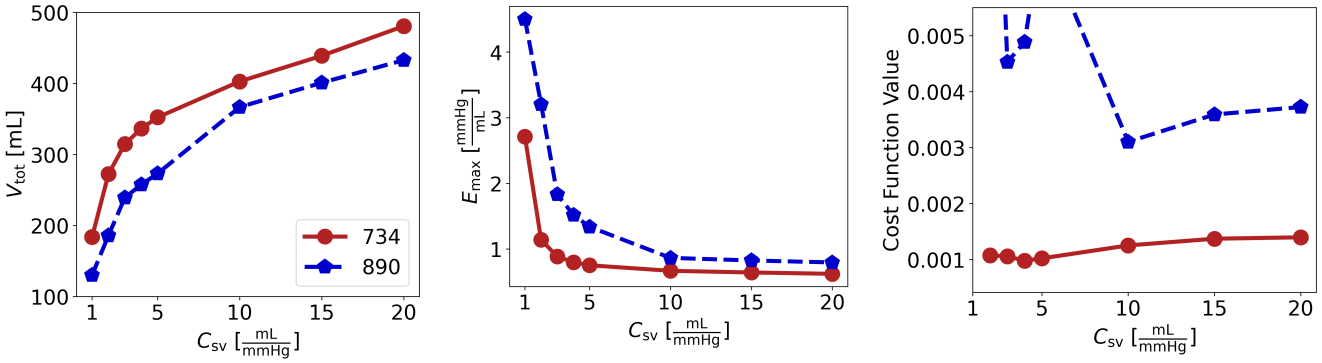

(a) V_{tot} given fixed C_{sv}.

(b) E_{max} given fixed C_{sv}.

(c) Cost function scaled by the number of residual elements.

Figure 6.1: Interrelations between C_{sv}, V_{tot}, E_{max} and cost function value in the parameter estimation procedure for participants 734 (solid red line) and 890 (blue dashed line). Values of C_{sv} were fixed according to the x-axes, which yielded the respective estimates of V_{tot} (Fig. 6.1a), E_{max} (Fig. 6.1b) and a cost function value corresponding to the parameter optimization (Fig. 6.1c). No constraints or regulations were applied in this configuration. Here, V_{tot} and E_{max} are minimum parameters, i.e. obtained from the parameter set with minimum cost function of the 20 last iterations (Section 4.2.1).

This experiment was conducted on two participants to explicitly illustrate how the model fails to simultaneously capture the physiological function of the venous and ventricular compartments. Realistic values of C_{sv} (≈10-20 $^{mL}/_{mmHg}$) resulted in high ventricular volumes and diminished E_{max}, and it is observed that E_{max} is estimated approximately similar in 734 and 890 for higher values of C_{sv}. The model regulates against arterial pressure by instead increasing ventricular volumes, and thus V_{tot}. Ideally, the model would react to the increase in C_{sv} by distributing more of V_{tot} to the veins to maintain MVP=6 mmHg, keeping ventricular volumes small and preserving a physiological value of E_{max}. The model appears reluctant to desired behaviour in the current structure. Because E_{max} and stressed ventricular volume can compensate each other to produce a consistent arterial pressure and stroke volume, there might be insufficient reference points to uniquely identify the stressed volume of the ventricle. Another key challenge is that the volume present in the closed-loop is not distributed to the respective model compartments in a desirable manner, which there are currently no appropriate tools to remedy.

The tendency of the algorithm preferring relatively small values of C_{sv}, $2 \lessapprox C_{sv} \lessapprox 10$ $^{mL}/_{mmHg}$ (Fig. 5.2) is also indicated by Figure 6.1c. A steady increase in residual for greater and more physiological values of C_{sv} confirms that with the exception of participant 637, all attempted configurations that estimated C_{sv} yielded values $\lessapprox 10$ $^{mL}/_{mmHg}$. Participant 734 exhibits a clear minimum in cost function value for C_{sv}=4 $^{mL}/_{mmHg}$ (Fig. 6.1c), while the tendency in 890 is more fluctuating with local minima. Note that the points with minimum residual do not exactly coincide with minimum parameter fits obtained with case no. 2 (No constraints), i.e. with C_{sv} estimated (Fig. 5.2b). Case no. 2 found C_{sv}=2.34 and 4.0 $^{mL}/_{mmHg}$ as minimum values for participants 734 and 890, respectively, hence the tendency of 734 seeking a lower value than 890 is recognized. However, fixing a parameter will impact the cost function and change the starting points for the optimization, causing the algorithm to find slightly different minima. Furthermore, `scipy.optimize.least_squares()` is a local method [28], hence the estimation procedure is based on multiple local optimizations and does not seek global minima. A global method would in some sense be more robust, but also come with a higher cost with respect to time.

6.4.2 Shift V_{tot} in Exercise State

To further investigate the distribution of total blood volume in the closed-loop during exercise, an attempt was made to shift V_{tot} during exercise. This shift was implemented in a preliminary experiment by linear regression between two points; (I_{HRR}=0, V_{tot}=V_{tot}^{rest}) and (I_{HRR}=1, V_{tot}=V_{tot}^{rest} × 150%). The line is thus individual for each participant, yielding shifted values of V_{tot} as a linear function of I_{HRR}. The shift in volume affected all three model compartments. Arterial pressures, ventricular volumes and venous pressure all increased. EDV increased more than ESV, which resulted in a prominent increase in SV. This

was on average beneficial for the accuracy in participant 734, but not 890. In general, the impacts of shifting V_{tot} were pronounced, but it is noted that this test case does not represent a realistic change during exercise as much as an conceptual illustration of its effect. Shifting V_{tot} might be a possibility for tuning model behaviour, but the challenge of not being able to target which model compartment is to be subjected to the potential increase in volume remains a challenge.

6.4.3 Open-Loop Model

The open-loop model differs from the closed-loop in that its entire venous compartment is replaced by a constant pressure of $P_{\text{sv}} = 6$ mmHg. This adjustment removes the closed-loop property, and thus the entire parameter V_{tot} in addition to C_{sv}. An attempt was made to perform the parameter estimation procedure for the two participants 734 and 890 using the open-loop model instead of the closed-loop. The baseline configuration chosen to compare the two models is no. 2 (No constraints), with equal features as stated in Section 4.5.1. As expected, resulting mean estimates of arterial parameters R_{sys}, C_{ao} and Z_{ao} became similar. However, E_{max} went from 0.96 to 0.58 $^{\text{mmHg}}/_{\text{mL}}$ in participant 734, and 1.49 to 0.74 $^{\text{mmHg}}/_{\text{mL}}$ in 890 when replacing the closed-loop with the open-loop version. Resulting fitted flow waves were similar, but the simulated pressure waveforms became more narrow with the open-loop compared to the closed-loop. An exercise simulation of P_{sys}, P_{dia} and SV is illustrated in the following:

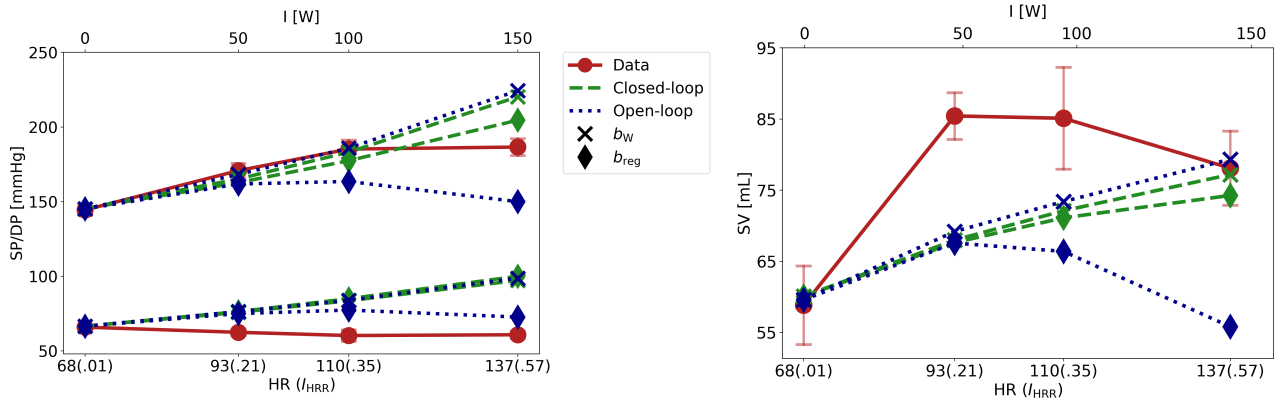

(a) P_{sys} (upper lines) and P_{dia} (lower lines).

(b) SV.

Figure 6.2: Comparison of an exercise simulation when using the closed-loop vs. open-loop model. The simulation is for trial participant 734. No constraints and regulations were applied during the estimation procedure for both models. Green dashed lines are simulations using the closed-loop model as before, while the blue dotted lines represent the open-loop version. X and diamond-shaped markers specifies whether the lusitropy coefficient used is from Weissler et al. [13] or trial data, respectively. As before, red lines represent data.

Figure 6.2 indicates a greater sensitivity to the lusitropy coefficient (b) for the open-loop compared to the closed-loop model. For the two test cases attempted, i.e. participants 734 (Fig. 6.2) and 890, implementing lusitropy with $b = b_W$ was necessary to prevent P_{sys} and SV from collapsing during exercise. It is noted that the venous pressure of 6 mmHg was kept constant in the open-loop simulation, and it is probable that a similar effect as obtained by the change in b could have been achieved by instead increasing venous pressure during exercise. In this preliminary attempt, the open-loop model did not yield a significantly better predictive performance. However, it appears possible to tune the exercise simulation procedure to yield very similar results for the open-loop as produced by the closed-loop. Additionally, the open-loop is a simpler model, hence more computationally efficient. As illustrated in Figure 2.5, there is a trade-off between model complexity and resulting level of uncertainty, as increased complexity means more model parameters. Such considerations are very relevant in this context, as it is known that the additional closed-loop parameters C_{sv} and V_{tot} are associated with a high level of uncertainty. Hence, this pilot experiment indicates that the inclusion of a venous compartment in the model might not improve its predictive performance during exercise to a level that compensates for increased complexity and potential uncertainty. Further, it is noted that the issue of a cardiac function characterized by a small elastance and large ventricular volume remains a challenge also with the open-loop.

Chapter 7

Concluding Remarks

This chapter closes the thesis with concluding remarks on acquired results and insights according to the project objectives (Section 1.2.1). Suggestions on how the work carried out in this project could be augmented are provided in the final section.

7.1 Conclusion

This section consecutively addresses the issues stated in Section 1.2.1.

7.1.1 The Parameter Estimation Procedure

The investigation of the parameter estimation procedure concludes with the following remarks.

- Upstroke synchronization for pressure and flow in both model and data yielded significantly more accurate optimized waveforms compared to cases with deviating cycle starts. The implemented adjustment to shift the arterial model waveforms from their original cycle starts to upstroke in the cost function is considered an improvement of the current estimation procedure.
- Given that a cardiac cycle is represented by synchronized arterial data for pressure and flow in a way that is consistent with model cycle start, the model may accurately fit the given waveforms by a number of baseline configurations.
- Variations in optimized parameters across estimation procedures were dependent upon the participant. It is suspected that narrow pressure waveforms impede the optimization, yielding more sensitive parameter estimates that were also associated with unreliable exercise predictions.
- During exercise, the baseline configuration referred to as no. 3 (Regulate EF) yielded most accurate predictions of P_{sys} and SV, but simultaneously the greatest errors in P_{dia}.

- Overall, the arterial compartment represented by the three-element Windkessel model proved quite stable and probable. The cardiac and venous compartments are less robust, as the estimated parameters related to these systems were more sensitive to the choice of baseline configuration.
- Fixing t_{peak} to the dicrotic notch is beneficial to avoid high parameter values that in combination with lusitropy can cause problems with inadequate diastolic filling during exercise.
- Interventions to regulate the estimated ejection fraction is beneficial to avoid the highest volumes and smallest values of E_{max}, thus facilitating a more physiologically plausible cardiac function.
- Constraints may be eliminated from the estimation procedure to avoid impeding the optimization algorithm and the issue of parameters estimated to their limits. However, in cases without constraints, the determination of mean parameters should be more strictly confined to ensure a representative mean fit.
- Fixing C_{sv} showed that the optimization procedure can efficiently compensate for changes in one variable with another. The enforcement of more plausible values of C_{sv} than resulting from the estimation was consistently overcompensated by an increase in V_{tot}. Thus, making the venous and ventricular compartments simultaneously behave in a physiologically plausible manner appears unachievable in the current model formulation.
- The optimization algorithm appears to prefer small values of C_{sv}. Enforcing a higher value by fixing C_{sv} to $10\times C_a$ resulted in less accurate exercise predictions of P_{sys} and SV compared to configurations with smaller C_{sv}.

7.1.2 Simulation of Exercise State

Mechanisms involved in the simulation of hemodynamic exercise state and their individual effects on model predictions have been investigated in a stepwise manner, concluded with the following remarks.

- More accurate optimized pressure and flow waveforms at rest do not necessarily imply better exercise predictions. This was the case when Z_{ao} was attempted estimated instead of fixed to its preliminary fitted value, which yielded better flow fits for participants with narrow carotid pressure waveforms, but without improved exercise prediction. In general, evaluation of the exercise performance of a given baseline case have showed essential for determining its usability for exercise simulation purposes.

- Post-processing of model outputs in the form of scaling to account for pressure amplification improves the premises for evaluating model behaviour against radial data.
- The lusitropy mechanism is highly influential in the context of regulating diastolic filling in the model. Adjusting the purely literature-based implementation to coincide with the average slope of systolic periods obtained from trial data improved model predictions slightly, but the even more personalized versions yielded negligible average differences. Hence, it appears as if increased personalization of the lusitropy mechanism will not radically improve the model. However, its pronounced level of influence indicates that lusitropy should be implemented with caution, whether a personal or average-based version.
- Overall, the implementation of trial-based exercise shifts of C_{ao} and/or R_{sys} yielded better predictions of P_{sys}, P_{dia} and SV than pure Chantler-based shift when considering these tree quantities separately. However, no shifting procedure providing the best predictions of all quantities of interest simultaneously could be obtained. Overall, the model is prone to overestimate P_{dia}, and the shape of SV is not captured. Errors in P_{sys} are more irregular and dependent upon exercise configuration.
- End-diastolic ventricular volume (EDV) decreased during exercise in every configuration examined. This is in general not physiologically probable, but because the model considers only stressed blood volume, the physiological interpretability of simulated ventricular volume is limited.
- A more combined investigation of baseline parameters, shifting procedures and the lusitropy mechanism may be necessary to optimize the hemodynamic exercise model.

7.1.3 Model Validation and Pilot Experiments

The model validation and the pilot experiments are concluded with the following remarks.

- With the exception of a pronounced peak at 50 W for MAE, similar tendencies were present in the validation experiments as shown in the development part of the project; greater shifts in C_{ao} (C2) remedy for the underestimation of P_{sys} yielded by the Chantler-based shifts (C1). It has been showed that P_{dia} is consistently overestimated, but the errors are smallest when imposing a greater reduction in R_{sys} (R2). The errors in the two pressure measures unfortunately appear somewhat inversely related.
- The model makes better predictions compared to rough ESP-based test estimates, but is overall exceeding clinically acceptable error levels.

- Attempts to enforce a more physiological representation of the venous compartment by fixing C_{sv} are consistently compensated by implausible estimates of V_{tot} and E_{max}. Elastance and stressed ventricular volume can compensate each other to produce a consistent arterial pressure and SV, and it lacks some reference point to uniquely identify the stressed volume of the ventricle.
- This project has revealed that small values of C_{sv} are associated with low residuals. More extensive analyses and investigations of the cost function and the numerical optimization procedure are required to state the exact reason for this behaviour.
- Experiments in various baseline configurations combined with the attempt to increase V_{tot} during exercise have shown that the model distributes the volume present in the closed-loop to its respective compartments in a manner that is hard to predict and control.
- Pilot experiments with an open-loop model resulted in less physiologically accurate shapes of the optimized pressure waveforms than yielded by the closed-loop. However, exercise simulations with the open-loop appeared tunable to similar behaviour as the closed version given different values of the lusitropy coefficient, which could probably also have been achieved by adjusting venous pressure. The open-loop is a simpler model with fewer parameters, making the estimation procedure less computationally expensive and time consuming, which also has the benefit of facilitating more efficient research.
- Parameter optimizations with both the open-loop and the closed-loop model seek small values of E_{max}. More physiological values of E_{max} could be beneficial for the corresponding Chantler-based exercise shifts to have the expected impact on the system, as the shifts are based on greater values than currently yielded by the estimation procedure. However, the issue of making the optimization algorithm seek greater values of E_{max} remains a challenge.

7.2 Recommendations for Future Work

Hemodynamic modelling is a highly multifaceted science, and the consideration of cardiovascular exercise response adds another layer of intricacy. The model itself as well as the procedures for estimating baseline parameters and simulating exercise could be further researched on many levels.

Regarding governing structural features, the primary issue is establishing whether the inclusion of a venous compartment in a closed-loop model is advantageous to an extent that compensates for increased complexity compared to an open-loop with constant venous pressure. It is also possible that other venous mechanisms could enhance model behaviour during exercise, e.g. the skeletal muscle pump could

be attempted implemented in both a closed-loop and an open-loop model. In general, the sufficient level of complexity for the venous function needs to be established. This work has not considered other mechanisms, but a comparison with other, more complex models could be attempted to evaluate the current level of complexity. A suggested model for comparison is one presented by Magosso & Ursino [49] that includes both the heart, the pulmonary and systemic circulations in addition to various neural regulatory mechanisms. Similarly, it must be established whether the current cardiac function that excludes unstressed volumes is adequate for model purposes. One aspect of the cardiac model that has not been considered in this project is the fixed value of E_{min}. More extensive investigation of this parameter and whether it should be estimated, shifted during exercise or in other ways treated differently could be informative in the context of analyzing the cardiac model.

In the context of parameter estimation, more extensive research of a method for regulating ejection fraction (EF) could be beneficial, particularly if found desirable that the model represents the ventricular compartment more physiologically. Determination of boundaries of EF, sensitivity through W_{ef}, and the $(1 + 1/\text{EF})$-factor for a softmax implementation (4.6) could be investigated by multiple experiments in various configurations. Further, to pursue the potential benefits of performing the estimation without constraints, the procedure of determining mean parameters should be more strictly confined than the current version. To ensure the quality of the resulting fit, a suggestion is to perform more than 20 iterations in the final step, and discard parameter sets with a residual exceeding a certain tolerance defined independent of the mean, which may become unreasonably high without constraints. Further, more extensive research is required to reveal why the optimization algorithm prefers low values of C_{sv} and E_{max} and high V_{tot}, particularly if the model is to represent the venous and ventricular compartments in a more physiologically plausible manner.

Regarding the simulation of exercise state, an aspect initiated in the Specialization Project [6] but not pursued in this work is the impact of different definitions of exercise intensity. Other definitions than (3.9) could be attempted, and potentially a combined version consisting of multiple weighted intensity functions. Weights could then be analyzed as uncertain variables in a sensitivity analysis. Further, it has been discovered that some trial participants are more predictable and stable than other. It has been argued that some of the exhibited instability could be caused by narrow carotid pressure waveforms. Another possibility is that stability is related to individual fitness levels. Accounting for fitness beyond resting heart rate could be investigated through a fitness-based scaling factor in the intensity definition. Finally, quality assured data for all 24 trial participants should be included in future research to increase the completeness and reliability of observations and conclusions from this project. It is evident that more research is indispensable for the hemodynamic model to reach its clinical ambition.

Bibliography

[1] World Health Organization (WHO). "Hypertension". [Online], August 2021. URL https://www.who.int/news-room/fact-sheets/detail/hypertension.

[2] E.P. Widmaier, H. Raff, and K.T. Strang. *"Vander's Human Physiology: The Mechanisms of Body Function"*. McGraw-Hill, 14 edition, 2016.

[3] NTNU Cardiac Exercise Research Group (CERG). "My Medical Digital Twin". [Online], 2020. URL https://www.ntnu.no/cerg/mymdt.

[4] N.L. Bjørdalsbakke, J.T. Sturdy, D.R. Hose, and L.R. Hellevik. "Parameter estimation for closed-loop lumped parameter models of the systemic circulation using synthetic data". *Mathematical Biosciences*, 343, jan 2022. doi: https://doi.org/10.1016/j.mbs.2021.108731.

[5] Nikolai Lid Bjørdalsbakke. "Exercise Remodelling". Internal note on the Hemodynamic Exercise Model, 2021.

[6] Anne Øksnes Aal. "Sensitivity Analysis of a Hemodynamic Model for Varying Exercise Intensity". TKT4550; Structural Engineering, Specialization Project, 2021.

[7] Hilke Straatman. "My Medical Digital Twin - Towards personalized blood pressure predictions during exercise using closed-loop lumped parameter models". Internship Report; Department of Structural Engineering, NTNU., 2021.

[8] Norsk Helsenett. "What are clinical trials?", November 2017. URL https://www.helsenorge.no/en/clinical-trials/about/.

[9] Norwegian University of Science and Technology. "Mapping of Cardiac Power in Healthy Humans and Testing of a New Blood Pressure Sensor", 2021. URL https://clinicaltrials.gov/ct2/show/NCT05008133.

[10] R.A. Rhoades and D.R. Bell. *"Medical Physiology: Principles for Clinical Medicine"*. Lippincott Williams & Wilkins, 4 edition, 2013.

[11] R.E Klabunde. "Cardiovascular Physiology Concepts - Ventricular Pressure-Volume Relationship", 2021. URL https://www.cvphysiology.com/CardiacFunction/CF024.

[12] Keith. R Walley. "Left Ventricular Function: Time-Varying Elastance and Left Ventricular Aortic Coupling". *US National Library of Medicine: Critical Care*, 20:270–270, 2016.

[13] A.M. Weissler, W.S. Harris, and C.D Schoenfeld. "Systolic Time Intervals in Heart Failure in Man". *circulation*, 37(2):149–159, 1968. doi: https://doi.org/10.1161/01.CIR.37.2.149.

[14] Y-J. Lin, C-W. Chuang, C-Y. Yen, S-H. Huang, P-W. Huang, J-Y. Chen, and S-Y. Lee. "An Intelligent Stethoscope with ECG and Heart Sound Synchronous Display". In *IEEE International Symposium on Circuits and Systems (ISCAS)*, pages 1–4, 05 2019. doi: 10.1109/ISCAS.2019.8702481.

[15] C.M. McEniery, J.R. Cockcroft, M.J. Roman, S.S. Franklin, and I.B. Wilkinson. "Central blood pressure: current evidence and clinical importance". *European Heart Journal*, 35(26):1719–1725, jan 2014. doi: https://dx.doi.org/10.1093%2Feurheartj%2Feht565.

[16] Y. Yao, L. Wang, L. Hao, L. Xu, S. Zhou, and W. Liu. "The Noninvasive Measurement of Central Aortic Blood Pressure Waveform". *Blood Pressure - From Bench to Bed*, October 2018. doi: DOI: 10.5772/intechopen.76770.

[17] N.A. Dasso. "How is exercise different from physical activity? A concept analysis". *Nurs Forum*, 54 (1):45–52, January 2019. doi: https://doi.org/10.1111/nuf.12296.

[18] R.E. Klabunde. "Cardiovascular Physiology Concepts - Venous Return", 2017. URL https://www.cvphysiology.com/CardiacFunction/CF016.

[19] R.E. Klabunde. "Cardiovascular Physiology Concepts - Factors Promoting Venous Return", 2008. URL https://www.cvphysiology.com/CardiacFunction/CF018.

[20] E.A Woodcocka and S.J. Matkovichb. "Cardiomyocytes structure, function and associated pathologies". *The International Journal of Biochemistry & Cell Biology*, 37(9):1746–1751, May 2005. doi: https://doi.org/10.1016/j.biocel.2005.04.011.

[21] V.G. Eck, W.P. Donders, J. Sturdy, J. Feinberg, T. Delhaas, L.R. Hellevik, and W. Huberts. "A guide to uncertainty quantification and sensitivity analysis for cardiovascular applications".

International Journal For Numerical Methods In Biomedical Engineering, 93:1208–1217, 2015. doi: 10.1002/cnm.2755.

[22] A Saltelli, M Ratto, T Andres, F Campolongo, J Cariboni, D Gatelli, M Saisana, and S Tarantola. *"Global Sensitivity Analysis. The Primer"*. John Wiley & Sons, Ispra, 2008.

[23] Z.A. Collier and J.H. Lampert. "Principles and methods of model validation for model risk reduction". *Environment Systems and Decisions*, 39:146–153, 2019. doi: https://doi.org/10.1007/s10669-019-09723-5.

[24] Thomas L. Paez. "Introduction to Model Validation ", 2009. URL https://www.osti.gov/servlets/purl/1142730.

[25] P.H.H Bovendeerd. "cardiac function - lecture notes 2019". In *department of biomedical engineering — group cardiovascular biomechanics*. Eindhoven University of Technology, 2019.

[26] Leif Rune Hellevik. "Cardiovascular Biomechanics", October 2018.

[27] Creative Commons. "Attribution 4.0 International (CC BY 4.0)", 2022. URL https://creativecommons.org/licenses/by/4.0/.

[28] The SciPy community. "SciPy.optimize", 2022. URL https://docs.scipy.org/doc/scipy/reference/optimize.html.

[29] The SciPy community. "SciPy.Integrate", 2022. URL https://docs.scipy.org/doc/scipy/tutorial/integrate.html.

[30] P.D. Chantler, V. Melenovsky, S.P. Schulman, G. Gerstenblith, L.C. Becker, L. Ferrucci, J.L. Fleg, E.G. Lakatta, and S.S. Najja. "The sex-specific impact of systolic hypertension and systolic blood pressure on arterial-ventricular coupling at rest and during exercise". *American Journal of Physiology- Heart and Circulatory Physiology*, 2008. doi: https://doi.org/10.1152/ajpheart.01179.2007.

[31] H.L Quan, C.L. Blizzard, J.E. Sharman, C.G. Magnussen, T. Dwyer, O. Raitakari, M. Cheung, and A.J. Venn. "Resting Heart Rate and the Association of Physical Fitness With Carotid Artery Stiffness". *American Journal of Hypertension*, 27(1):65–71, September 2012. doi: https://doi.org/10.1093/ajh/hpt161.

[32] GE Healthcare. "EchoPac Software", 2022. URL https://www.gehealthcare.com/products/ultrasound/vivid/echopac.

[33] NumPy Developers. "NumPy", 2022. URL https://numpy.org/doc/stable/index.html#numpy-docs-mainpage.

[34] B. Alexander, M. Cannesson, and T.J. Quill. *"Anesthesia Equipment- Principles and Applications"*, chapter "Chapter 12- Blood Pressure Monitoring", pages 273–282. Saunders, 2 edition, 2013.

[35] T.D. Tannvik, G. Kiss, H. Torp, A.E. Rimehaug, and I. Kirkeby-Garstad. "No evidence of cardiac stunning or decoupling immediatelyafter cardiopulmonary bypass for elective coronary surgery". *Acta Anaesthesiol Scand.*, 64:1128–1135, 2020. doi: https://doi.org/10.1111/aas.13621.

[36] Sankirna D. Joge. "QRS Detection using Pan–Tompkins Algorithm from ECG Signal". Retrieved May 25, 2022., May 2022. URL https://se.mathworks.com/matlabcentral/fileexchange/101078-qrs-detection-using-pan-tompkins-algorithm-from-ecg-signal.

[37] GeeksforGeeks. "How to use Pandas filter with IQR?", 2021. URL https://www.geeksforgeeks.org/how-to-use-pandas-filter-with-iqr/.

[38] The pandas development team. "Pandas Documentation", April 2022. URL https://pandas.pydata.org/docs/index.html.

[39] P. Segers, N. Stergiopolus, and N. Westerhof. "Quantification of the Contribution of Cardiac and Arterial Remodeling to Hypertension". *Hypertension*, 36(5):760–765, November 2000. doi: https://doi.org/10.1161/01.HYP.36.5.760.

[40] Richard E. Klabunde. "Cardiovascular Physiology Concepts - Vascular Compliance", 2016. URL https://www.cvphysiology.com/BloodPressure/BP004.

[41] American Heart Association. "Ejection Fraction Heart Failure Measurement", 2017. URL https://www.heart.org/en/health-topics/heart-failure/diagnosing-heart-failure/ejection-fraction-heart-failure-measurement.

[42] Y-L. Liang, C.D. Gatzka, X-J. Du, J.D. Cameron, and B.A. Kingwell. "Effects Of Heart Rate On Arterial Compliance In Men". *Clinical and Experimental Pharmacology and Physiology*, 26(4):342–346, February 2002. doi: https://doi.org/10.1046/j.1440-1681.1999.03039.x.

[43] C. Yoshiga, E.A. Dawson, S. Voliantitis, J. Warberg, and N.H. SEcher. "Cardiac output during exercise is related to plasma atrial natriuretic peptide but not to central venous pressure in humans". *Experimental Physiology*, 104(3):379–384, March 2019. doi: https://doi.org/10.1113/EP087522.

[44] M. Zuber, H-H. Schafer, W. Kaiser, and P. Erne. Measuring accuracy of sphygmomanometers in the medical practices of swiss primary care physicians. *The European Journal of General Practice*, 19 (4):244–247, July 2013. doi: 10.3109/13814788.2013.779664.

[45] E.Y.L Lui, A.H. Steinmann, R.S.C Cobbold, and K.W. Johnstin. "Human factors as a source of error in peak Doppler velocity measurement". *Journal of Vascular Surgery*, 42(5):972.e1–972.e10, November 2005. doi: https://doi.org/10.1016/j.jvs.2005.07.014.

[46] Python Core Team. *Python: A dynamic, open source programming language*. Python Software Foundation, 2021. URL https://www.python.org/. Python version 3.9.6.

[47] H.M. Mertens, H. Mannebach, G. Trieb, and U. Gleichmann. "Influence of Heart Rate on Systolic Time Intervals: Effects of AtrialPacing versus Dynamic Exercise ". *Clinical Cardiology*, 4:22–27, January 1981. doi: https://doi.org/10.1002/clc.4960040106.

[48] J.T. Maher, G.A. Beller, B.J. Ransil, and L.H. Hartley. "Systolic time intervals during submaximal and maximal exercise in man". *American Heart Journal*, 87(3):334–342, March 1974. doi: https://doi.org/10.1016/0002-8703(74)90075-1.

[49] E. Magosso and M. Ursino. "Cardiovascular response to dynamic aerobic exercise: A mathematical model". *Medical and Biological Engineering and Computing*, 40:660–674, 2002. doi: https://doi.org/10.1007/BF02345305.

[50] N. Stergiopolus, J.J. Meister, and N. Westerhof. "Determinants of stroke volume and systolic and diastolic aortic pressure". *Am J Physiol.*, 270, June 1996. doi: https://doi.org/10.1152/ajpheart.1996.270.6.h2050.

[51] T. Bombardini, L.A. Mulieri, S. Salvardori, M.F. Costantino, M.C. Scali, M. Marzilli, and E. Picano. "Pressure-volume Relationship in the Stress-echocardiography Laboratory: Does (Left Ventricular End-diastolic) Size Matter?" *Rev Esp Cardiol (Engl Ed).*, 70(2):96–104, February 2017. doi: https://doi.org/10.1016/j.rec.2016.04.047.

[52] O. Vardoulis, T.G. Papaioannou, and N. Stergiopulos. "On the estimation of total arterial compliance from aortic pulse wave velocity". *Ann Biomed Eng.*, 40(12):2619–26, December 2012. doi: 10.1007/s10439-012-0600-x.

[53] J. Feldschuh and Y. Enson. "Prediction of the normal blood volume. Relation of blood volume to body habitus". *Circulation*, October 1977. doi: https://doi.org/10.1161/01.cir.56.4.605.

[54] A.L. Colunga, Karam K.G., N.P. Woodall, T.F. Dardas, J.H. Gennari, M.S. Olufsen, and B.E. Carlson. "Deep phenotyping of cardiac function in heart transplant patients using cardiovascular system models". *J Physiol.*, 598(15):3203–3222, August 2020. doi: https://doi.org/10.1113/jp279393.

[55] R. Hainsworth. "The Importance of Vascular Capacitance in Cardiovascular Control". *Physiology*, 5 (6), December 1990. doi: https://doi.org/10.1152/physiologyonline.1990.5.6.250.

Appendix A

Additional Information

A.1 The Hemodynamic Model

A.1.1 Model Equations

The following equations and descriptions are obtained from [4], and were similarly presented in [6].

The model ODEs are are given as:

$$\begin{aligned}
\frac{dV_{\text{ao}}}{dt} &= C_{\text{ao}}\frac{dP_{\text{ao}}}{dt} = Q_{\text{lvao}} - Q_{\text{aosv}} \Longleftrightarrow \frac{dP_{\text{ao}}}{dt} = \frac{Q_{\text{lvao}} - Q_{\text{aosv}}}{C_{\text{ao}}} \\
\frac{dV_{\text{sv}}}{dt} &= C_{\text{sv}}\frac{dP_{\text{sv}}}{dt} = Q_{\text{aosv}} - Q_{\text{svlv}} \Longleftrightarrow \frac{dP_{\text{sv}}}{dt} = \frac{Q_{\text{aosv}} - Q_{\text{svlv}}}{C_{\text{sv}}} \\
\frac{dV_{\text{lv}}}{dt} &= Q_{\text{svlv}} - Q_{\text{lvao}}
\end{aligned} \tag{A.1}$$

where V_{ao} and V_{sv} are the stressed blood volumes of the aorta and veins, respectively, and V_{lv} is the blood volume in the left ventricle (LV). Note that aorta represents the entire systemic arterial vasculature in the model. Further, C_{ao}, C_{sv}, P_{ao} and P_{sv} denote compliance values (C) and pressures (P) of the aorta (ao) and systemic veins (sv). Q_{lvao} is flow from the LV to the systemic arteries (aorta), Q_{aosv} is from the aorta to the veins and Q_{svlv} is flow from the veins to the LV. Remaining quantities are modelled as:

$$
\begin{aligned}
V_{\text{sa}} &= C_{\text{sa}} P_{\text{sa}} \\
V_{\text{sv}} &= C_{\text{sv}} P_{\text{sv}} \\
P_{\text{lv}} &= E_{\text{lv}}(t)\, V_{\text{lv}} + P_{\text{th}}(t) \\
E_{\text{lv}}(t) &= (E_{\max} - E_{\min})\, e(t) + E_{\min} \\
P_{\text{ao}} &= \max\left[P_{\text{ao}}, P_{\text{lv}}\right] \\
Q_{\text{lvao}} &= I\left(P_{\text{lv}} > P_{\text{sa}}\right) \frac{P_{\text{lv}} - P_{\text{sa}}}{Z_{\text{ao}}} \\
Q_{\text{svlv}} &= I\left(P_{\text{sv}} > P_{\text{lv}}\right) \frac{P_{\text{sv}} - P_{\text{lv}}}{R_{\text{mv}}} \\
Q_{\text{aosv}} &= \frac{P_{\text{sa}} - P_{\text{sv}}}{R_{\text{sys}}}.
\end{aligned}
\tag{A.2}
$$

where P_{ao} is aortic pressure, and P_{lv} is the pressure in the LV. Further, Z_{ao} is characteristic aortic impedance, R_{sys} is total systemic resistance, and R_{mv} is (effective) mitral valve resistance. Volumes V_{sa}, V_{sv} and V_{lv} are limited by the parameter V_{tot}, as described in Section 3.3. The logical function I takes the value 1 when the argument is true, and 0 when it is false. The activation function $e(\tau)$ is defined as:

$$
e(\tau) = \alpha \times \frac{(\tau/a_1)^{n_1}}{1 + (\tau/a_1)^{n_1}} \times \frac{1}{1 + (\tau/a_2)^{n_2}} \tag{A.3}
$$

where τ is the position in the cardiac cycle, i.e. between the end of the last and next diastolic period. Parameters a_1 and n_1 influence the shape of the contracting part of the elastance curve. Here, $a1 = 0.708 \times t_{\text{peak}}/T$, where t_{peak} is the time of maximum ventricular elastance. The shape of the relaxing part of the curve is influenced by a_2 and n_2. The values of these shape-determining parameters are originally obtained from [50], and restated in [4].

A.1.2 Initial Conditions

Initial volumes and pressures are set according to [4]:

$$
\begin{aligned}
P_{\text{ao},0} &= 100 \text{ mmHg} \\
V_{\text{lv},0} &= 100 \text{ mL} \\
P_{\text{sv},0} &= \frac{V_{\text{tot}} - V_{\text{ao},0} - V_{\text{sv},0}}{V_{\text{sv}}} \text{ mmmHg} = \frac{V_{\text{tot}} - C_{\text{ao}} \times P_{\text{ao},0} - V_{\text{sv},0}}{V_{\text{sv}}} \text{ mmHg}
\end{aligned}
\tag{A.4}
$$

where $P_{\text{ao},0}$ and $P_{\text{sv},0}$ are initial aortic and venous pressures, respectively. $V_{\text{lv},0}$, $V_{\text{ao},0}$ and $V_{\text{sv},0}$ are the initial stressed volumes of the left ventricle, arterial and venous compartments, respectively. Parameters C_{ao}, C_{sv} and V_{tot} are resting state values for aortic and venous compliance, and total blood volume.

A.1.3 Parameter Estimation Procedure

Scaling Factors Cost Function

Symbol	Unit	Value
$K_{P_{\text{ao}}}$	mmHg	100.0
$K_{Q_{\text{lvao}}}$	mL/s	500.0
$K_{P_{\text{sys}}}$	mmHg	120.0
$K_{P_{\text{dia}}}$	mmHg	80.0
K_{SV}	ml	100.0
K_{MVP}	mmHg	5.0

Table A.1: Scaling factors K_Y used to normalize the terms in the cost function (3.5). Obtained from [4].

Weights for the Scalars Terms in the Cost Function

The scalar quantities included in the cost function, i.e. P_{sys}, P_{dia}, SV and MVP, are weighted to promote approximately equal contributions as the waveform data for pressure and flow, as the time series are arrays with many points contributing to the residual. Weights (W_Y) in the cost function (3.5) for the scalars $Y \in [P_{\text{sys}}, P_{\text{dia}}, \text{SV}, \text{MVP}]$ are calculated as follows:

$$W_Y = \begin{cases} \frac{\text{len}(P_{\text{ao}})}{40} \times 7.5 & \text{if } Y \in [P_{\text{sys}}, P_{\text{dia}}, \text{SV}] \\ \frac{\text{len}(P_{\text{ao}})}{40} \times 2.5 & \text{if } Y = \text{MVP} \end{cases} \tag{A.5}$$

where $\text{len}(P_{\text{ao}})$ is the length of the pressure data array. The weights are defined empirically by Bjørdalsbakke through testing to achieve approximately equal contributions as the waveform data, but also a bit more for P_{sys}, P_{dia} and SV to obtain resting values for these quantities that are as accurate as possible. Explicit use of these weights are shown in the implementation of the cost function included in Section A.3.2.

Constraints for the Numerical Optimization

The following table states how the bounds used as inputs in `scipy.optimize.least_squares()` [28] in the parameter estimation procedure have been determined.

Param. (θ) [unit]	θ_{low}	θ_{up}	Ref.	Remarks
E_{max} [mmHg/mL]	0.50	$\frac{10.84}{\text{BSA}}$	[51]	• Bounds based on reported data set. • Lower bound adjusted throughout the project.
C_{ao} [mL/mmHg]	0.148	2.256	[52]	• Bounds based on 1D model estimates of total C_a.
R_{sys} [mmHg$\times s$/mL]	$\frac{0.917}{\text{BSA}}$	2.963	[30]	• Based on BSA-indexed variations. • Upper bound ignores BSA index to increase limit.
V_{tot}[mL]	150	1503	[53], [54]	• Based on measured total blood volume from [53]. • Method inspired by [54] to estimate stressed V_{tot}. • Observed good fits with low V_{tot} $\Rightarrow \theta_{\text{low}}$ lowered beyond what is realistic based on data.
C^*_{sv} [mL/mmHg]	4.44	67.68	[55]	• Based on reported approx. $C_v \approx [10-30] \times C_a$
Z^*_{ao} [mmHg$\times s$/mL]	0.001	0.2 (prefit 1.0)	[39]	• Covers reported ranges. • Set wider in prefit for free fit to 3WK. • Z_{ao} is typically $< R_{\text{sys}} \Rightarrow$ more narrow bounds.
t^*_{peak} [s]	$\min\{0.15, 0.9 \times T\}$	$\min\{0.442, T\}$	[13], [47]	• Based on variation in reported T_{sys}.

Table A.2: Source of the constraints used in the parameter estimation procedure. BSA = $\sqrt{\frac{\text{wt}\times\text{ht}}{3600}}$ is body surface area, where wt is weight in kg and ht is height in cm. 3WK refers to the three-element Windkessel model. T_{sys} is systolic period. $J(\boldsymbol{\theta})$ is the cost function. $^*Z_{\text{ao}}$, t_{peak} and C_{sv} may be fixed according to Table 4.3, in which case the presented constraints are irrelevant.

A.2 Numerical Error Results in Exercise State

A.2.1 Average MAE in Five Baseline Configurations

Param. [unit]	Config.	$\mu_{MAE} \pm \sigma_{MAE}$				
		0 W	50 W	100 W	150 W	$\overline{MAE}$
P_{sys} [mmHg]	1) Full estimation	0.8±0.8	10.9±7.5	22.3±15.8	36.9±16.9	17.7±13.4
	2) No constraints	0.8±0.9	14.0±5.6	20.0±11.6	31.5±16.1	16.6±11.1
	3) Regulate EF	3.9±3.1	11.3±7.4	20.9±17.0	29.3±21.7	16.4±9.6
	4) Fix C_{sv}	1.7±1.7	7.7±5.8	30.9±17.9	51.8±21.1	23.0±19.9
	5) Fix C_{sv}+regulate EF	9.2±9.2	15.1±4.4	50.1±25.9	69.9±37.7	36.1±25.0
P_{dia} [mmHg]	1) Full estimation	3.9±2.8	20.5±14.6	25.2±13.5	32.2±11.9	20.5±10.4
	2) No constraints	4.0±3.1	21.6±15.8	27.1±14.9	34.3±15.2	21.7±11.2
	3) Regulate EF	5.9±5.5	20.0±13.7	27.9±18.1	36.3±21.9	22.6±11.2
	4) Fix C_{sv}	3.3±2.9	18.6±14.1	20.0±11.5	23.4±12.4	16.4±7.7
	5) Fix C_{sv}+regulate EF	9.1±14.1	16.0±11.6	12.9±7.1	14.3±7.2	13.1±2.6
SV [mL]	1) Full estimation	8.2±6.1	16.5±10.8	20.5±16.0	25.0±24.4	17.6±6.2
	2) No constraints	8.3±6.1	15.6±10.6	19.3±14.8	23.7±22.2	16.7±5.6
	3) Regulate EF	6.4±4.6	15.3±7.1	16.1±16.1	20.2±21.9	14.5±5.0
	4) Fix C_{sv}	7.1±5.3	14.7±9.8	18.5±17.4	25.3±24.1	16.4±6.6
	5) Fix C_{sv}+regulate EF	4.9±4.5	14.3±8.5	20.1±19.7	28.3±25.2	16.9±8.6

Table A.3: Mean absolute error (MAE) of P_{sys}, P_{dia} and SV for five cases of baseline parameter configurations. All reported values are averaged over six trial participants; 734, 219, 346, 890, 637 and 248 for each intensity level I∈[0,50,100,150] W and depicted graphically in Figure 5.9. The far right column denoted $\overline{MAE}$ contains MAEs averaged over all intensity levels for each baseline case, shown as horizontal lines in Figure 5.5.

A.2.2 Average Bias of Scaled vs. Non-Scaled Model Pressures

Param. [unit]	Config.	$\mu_{\text{Bias}} \pm \sigma_{\text{Bias}}$				
		0 W	50 W	100 W	150 W	$\overline{\text{Bias}}$
P_{sys} [mmHg]	Non-scaled	-19.4±5.6	-27.2±13.5	-45.6±21.5	-53.3±28.4	-36.4±13.6
	Scaled	1.0±4.9	-3.7±13.0	-20.4±17.6	-25.7±26.0	-12.2±11.1
P_{dia} [mmHg]	Non-scaled	17.9±9.6	33.3±13.2	42.4±17.6	52.2±21.4	36.6±12.6
	Scaled	5.9±5.5	20.0±13.7	27.9±18.1	36.3±21.9	22.6±11.2

Table A.4: Bias of scaled vs. non-scaled model predictions of P_{sys} and P_{dia}. All reported values are averaged over six trial participants; 734, 219, 346, 890, 637 and 248 for each intensity level I∈[0,50,100,150] W and are depicted graphically in Figure 5.6. The far right column denoted $\overline{\text{MAE}}$ contains MAEs averaged over all intensity levels, shown as horizontal lines in Figure 5.6.

A.2.3 Average MAE for Three Implementations of the Lusitropy Mechanism

Param. [unit]	Config.	$\mu_{\text{MAE}} \pm \sigma_{\text{MAE}}$				
		0 W*	50 W	100 W	150 W	$\overline{\text{MAE}}$
P_{sys} [mmHg]	0) b=0	3.9±3.1	14.1±9.6	33.2±16.2	49.7±28.3	25.2±17.6
	1) $b = b_{\text{Weissler}}$		15.5±9.4	28.3±16.2	32.6±18.7	20.0±11.3
	2) $b = b_{\text{reg}}$		11.3±7.4	20.9±17.0	29.3±21.7	16.4±9.6
P_{dia} [mmHg]	0) b=0	5.9±5.5	18.6±14.1	27.0±19.7	31.6±25.2	20.8±9.8
	1) $b = b_{\text{Weissler}}$		19.7±14.0	29.3±20.2	38.8±25.8	23.4±12.2
	2) $b = b_{\text{reg}}$		20.0±13.7	27.9±18.1	36.3±21.9	22.6±11.2
SV [mL]	0) b=0	6.4±4.6	13.6±9.1	20.3±14.8	28.5±16.7	17.2±8.1
	1) $b = b_{\text{Weissler}}$		14.8±8.5	15.4±10.2	19.3±12.8	14.0±4.7
	2) $b = b_{\text{reg}}$		15.3±7.1	16.1±16.1	20.2±21.9	14.5±5.0

Table A.5: Mean absolute error (MAE) of P_{sys}, P_{dia} and SV for three selected values of the lusitropy coefficient (b). All reported values are averaged over six trial participants; 734, 219, 346, 890, 637 and 248 for each intensity level I∈[0,50,100,150] W and are depicted graphically in Figure 5.9. The far right column denoted $\overline{\text{MAE}}$ contains MAEs averaged over all intensity levels for each lusitropy configuration, shown as horizontal lines in Figure 5.9. *Note that the lusitropy mechanism is not applied on the 0 W-column, as this is considered a hemodynamic resting state.

A.2.4 Average MAE in Selected Exercise Configurations

Param. [unit]	Config.		$\mu_{MAE} \pm \sigma_{MAE}$				
	BC	Ex.shift	0 W*	50 W	100 W	150 W	$\overline{MAE}$
P_{sys} [mmHg]	3	C1+R1	3.9±3.1	11.3±7.4	20.9±17.0	29.3±21.7	16.4±9.6
		C1+R2		10.5±7.2	25.2±15.5	34.1±18.9	18.4±11.9
		C2+R1		18.0±14.4	14.3±11.8	16.0±16.8	13.0±5.4
		C2+R2		14.4±9.5	10.8±10.1	19.0±12.4	12.0±5.5
	4	C1+R1	1.7±1.7	7.7±5.8	30.9±17.9	51.8±21.1	23.0±19.9
		C1+R2		12.3±6.0	43.4±23.4	64.9±32.7	30.6±25.0
		C2+R1		8.7±8.7	23.8±13.5	45.7±17.3	20.0±16.9
		C2+R2		8.2±6.2	35.4±22.8	60.2±27.6	26.3±23.3
P_{dia} [mmHg]	3	C1+R1	5.9±5.5	20.0±13.7	27.9±18.1	36.3±21.9	22.6±11.2
		C1+R2		13.7±9.6	17.7±15.4	24.6±17.7	15.5±6.7
		C2+R1		24.6±16.2	36.1±21.9	46.8±23.8	28.4±15.1
		C2+R2		16.5±11.6	23.0±18.6	31.0±20.1	19.1±9.2
	4	C1+R1	3.3±2.9	18.6±14.1	20.0±11.5	23.4±12.4	16.4±7.7
		C1+R2		11.6±10.9	9.7±9.2	10.6±7.8	8.8±3.2
		C2+R1		19.1±14.7	20.8±12.1	24.6±13.1	17.0±8.1
		C2+R2		11.7±11.1	10.2±9.2	10.7±7.9	9.0±3.3
SV [mL]	3	C1+R1	6.4±4.6	15.3±7.1	16.1±16.1	20.2±21.9	14.5±5.0
		C1+R2		13.9±14.1	17.6±7.8	27.0±11.2	16.2±7.4
		C2+R1		14.2±9.6	16.6±10.3	22.8±18.6	15.0±5.9
		C2+R2		16.5±16.5	20.0±8.4	33.7±11.8	19.2±9.8
	4	C1+R1	7.1±5.3	14.7±9.8	18.5±17.4	25.3±24.1	16.4±6.6
		C1+R2		17.9±13.7	22.4±10.3	31.3±17.4	19.7±8.7
		C2+R1		14.8±10.5	19.1±15.7	24.6±24.9	16.4±6.4
		C2+R2		18.7±15.4	24.1±9.3	34.3±16.1	21.0±9.8

Table A.6: Mean absolute error (MAE) of P_{sys}, P_{dia} and SV during exercise for the selected configurations graphically illustrated in Figure 5.12. A given configuration is subdivided according to the column denoted *Config.* into baseline case (BC) and exercise shift (*Ex.shift*), where the latter describes the shift of aortic compliance (C) and systemic resistance (R) during exercise. The attributes related to each configuration is found in Section 4.5.1. All reported values are averaged over six trial participants; 734, 219, 346, 890, 637 and 248 for each intensity level I∈[0,50,100,150] W and depicted graphically in figure 5.12. The far right column denoted $\overline{MAE}$ contains MAEs averaged over all intensity levels for each configurations. These values are not shown in Figure 5.12 to avoid jeopardizing the readability of the illustration. *Note that no exercise shifts are conducted for the 0 W-column, as this is considered a hemodynamic resting state.

A.3 Python Source Code

All programming related to the model have been performed using `Python` (version 3.9.6) [46]. This section includes extracts of the explicit python code used in this work. The hemodynamic exercise model is presented in its entirety. Further, central functions used for parameter estimation is included. Finally, algorithms developed in this project for exercise simulation purposes and literature-based comparisons are presented. Note that the project database cannot be published due rules of patient confidentiality.

A.3.1 The Hemodynamic Model For Varying Exercise Intensity

The presented implementation only accounts for population-based exercise shifts according to Chantler et al. [30]. This can, however, easily be adjusted by manually setting the parameter to desired value before solving the model by using the class function `set_pars()`. The model can in principle take exercise intensities given in other formats than heart rate. However, as only heart rate is considered in this project, only functionality related to heart rate-based intensity is included in the following implementation. Note that the code is originally written through a collaboration in the MyMDT project by Dr. Jacob Sturdy and Ph.D. Candidate Nikolai L. Bjørdalsbakke, and no direct changes of this implementation have been done in this project beyond adjusting exercise shifts of parameters (Section A.3.3). A review of the content, stating which functions are found on each code line, is found inline in the following code extract.

Listing A.1: The Hemodynamic Exercise Model

```
import scipy
import scipy.integrate
from scipy.optimize import curve_fit
from scipy.integrate import solve_ivp
import numpy as np
"""
The hemodynamic model as written by Dr. Sturdy and
Ph.D. Candidate Bjordalsbakke through a collaboration in
the MyMDT project. The model is used in this master's project.
Includes:
21 : activiation function to define the time-varying elastance.
58 : Class containting parameters and functions to use to solve the model.
182 and 234 : Class functions defining intensity and exercise shifts.
304 : RHS of the ODE system
326 and 382 : calc_all and calc_summary describes how quantities are
```

```
16              derived from the ODE solutions.
17 364 : ODE solver function.
18 """
19 ml_per_sec_to_L_per_min = 60/1000
20
21 def stergiopolous_elastance(self, t):
22     """
23     Computes the normalized elastance at time t,
24     according to the shape parameters given by Stergiopolus 1994.
25     """
26     a1 = 0.708 * self.t_peak/self.T
27     a2 = 1.677 * a1
28     n1 = 1.32
29     n2 = 21.9
30     alpha = 1.672
31     shapeFunction1 = (t/(a1*self.T))**n1 / (1.0 + (t / (a1*self.T)) ** n1)
32     shapeFunction2 = (1.0 + (t/(a2*self.T))**n2)
33     e = alpha * shapeFunction1/shapeFunction2
34     return e
35
36 def lambda_setter(pars, rp, prp):
37     return lambda iy: (pars[0]*(iy**2) + pars[1]*iy + pars[2])/rp * prp
38
39 def lambda_setter_exp(pars, rp, prp):
40     return lambda iy: (pars[0]*np.exp(-1/pars[1]*(iy-pars[2])) + pars[3])/rp *
    prp
41
42 def poly_func(x, a, b, c):
43     return a*(np.array(x)**2) + b*np.array(x) + c
44
45 def poly3_func(x, a, b, c, d):
46     return a*(np.array(x)**3) + b*(np.array(x)**2) + c*np.array(x) + d
47
48 def simple_exp_func(x, a, b, c):
49     return a*np.exp(-np.array(x)/b) + c
50
51 def exp_func(x, a, b, c, d):
52     return a*(np.exp(-(x-c)/b)) + d
53
54 def hrreserve_def(hr, hrmax, hrrest,**kwargs):
55     res_intensity = (hr-hrrest)/(hrmax-hrrest)
```

```
    return res_intensity

class VaryingElastance():
    """
    Class containing parameters and functions for
    the hemodynamic exercise model.
    """
    def __init__(self):

        # 3-element Windkessel pars
        self.Z_ao       = 0.033
        self.C_ao       = 1.5
        self.R_sys      = 0.95
        # Time varying elastance pars
        self.E_max      = 2.34
        self.E_min      = 0.055
        self.t_peak     = 0.3
        self.T          = 0.85
        # Venous compartment pars
        self.C_sv       = 11.0
        self.R_mv       = 0.010
        # Volume determining par
        self.V_tot      = 300
        # Lusitropy par
        self.b          = -2.1/1000

        self.par_dict = self.__dict__.copy()

        # Intrathoracic pressure
        self.pleural_pressure_func = lambda t: -4

        # Elastance function
        self.elastance_fcn = stergiopolous_elastance

        # Basis pars
        self.age = 44 #yrs
        self.wt = 81 #kg
        self.ht = 177 #cm
        self.sex = 'M' # Only M and F are handled

        # Un-exercised parameters
```

```
97          self.E_max_ux = self.E_max
98          self.T_ux = self.T
99          self.C_ao_ux = self.C_ao
100         self.R_sys_ux = self.R_sys
101         # Additional Un-exercised parameters
102         self.V_tot_ux = self.V_tot
103         self.C_sv_ux = self.C_sv
104         self.R_mv_ux = self.R_mv
105         self.E_min_ux = self.E_min
106         self.Z_ao_ux = self.Z_ao
107         self.t_peak_ux = self.t_peak
108
109         self.exercised_flag = False
110
111         # Parameter_functions
112         self.E_max_func = lambda hr: self.E_max
113         self.C_ao_func = lambda hr: self.C_ao
114         self.R_sys_func = lambda hr: self.R_sys
115         # Optional functions
116         self.V_tot_func = lambda hr: self.V_tot
117         self.C_sv_func = lambda hr: self.C_sv
118         self.R_mv_func = lambda hr: self.R_mv
119         self.E_min_func = lambda hr: self.E_min
120         self.Z_ao_func = lambda hr: self.Z_ao
121         self.t_peak_func = lambda hr: self.t_peak
122
123         ##################################################
124         # Lusitropy funtion - Added by Straatman, 2021
125         self.t_peak_func = lambda iy: self.t_peak + self.b*(iy-(60/self.T_ux))
126         ##################################################
127
128         #ChantlerArrays
129         self.HR_pop = np.array([66,89,99,109,146])
130         self.HR_max_pop = self.HR_pop[-1]
131         self.HR_rest_pop = self.HR_pop[0]
132
133         self.T_max = 60./(220-self.age)
134
135         self.set_parameter_response("Nor")
136
137     def set_max_hr_period(self,T_max):
```

```
        self.T_max = T_max

    def set_max_hr(self,HR_max):
        self.T_max = 60./HR_max

    def set_max_workload(self,workload):
        self.Workload_max_pers = workload

    def set_parameter_response(self, disease_state="Nor"):
        BSA_calc = np.sqrt(self.wt*self.ht/3600.0)

        if disease_state == "Nor":
            if self.sex == "M":
                # Normotensive parameter responses for males from Chantler et al.
                self.E_a_pop = np.array([2.32, 2.33, 2.40, 2.57, 3.15])/BSA_calc
                self.C_ao_x_pop = 1./self.E_a_pop
                self.E_max_x_pop = np.array([4.26, 5.66, 6.73, 8.12, 13.21])/
BSA_calc
                self.R_sys_x_pop = np.array([2.405, 1.667, 1.512, 1.431, 1.253])
*0.75/BSA_calc
            elif self.sex == "F":
                # Normotensive parameter responses for males from Chantler et al.
                self.E_a_pop = np.array([2.26, 2.43, 2.54, 2.56, 2.94])/BSA_calc
                self.C_ao_x_pop = 1./self.E_a_pop
                self.E_max_x_pop = np.array([4.73, 7.98, 8.95, 9.77, 15.49])/
BSA_calc
                self.R_sys_x_pop = np.array([2.193, 1.568, 1.369, 1.293, 1.158])
*0.75/BSA_calc
        elif disease_state == "Hyp":
            if self.sex == "M":
                # Hypertensive parameter responses for males from Chantler et al.
                self.E_a_pop = np.array([2.98, 2.84, 2.88, 3.02, 3.52])/BSA_calc
                self.C_ao_x_pop = 1./self.E_a_pop
                self.E_max_x_pop = np.array([6.08, 7.43, 9.13, 10.37, 16.27])/
BSA_calc
                self.R_sys_x_pop = np.array([2.803, 1.964, 1.743, 1.655, 1.444])
*0.75/BSA_calc
            elif self.sex == "F":
                # Hypertensive parameter responses for males from Chantler et al.
                self.E_a_pop = np.array([2.63, 2.52, 2.64, 2.60, 2.86])/BSA_calc
                self.C_ao_x_pop = 1./self.E_a_pop
```

```
173                 self.E_max_x_pop = np.array([7.06, 8.80, 15.35, 12.71, 17.82])/
    BSA_calc
174                 self.R_sys_x_pop = np.array([2.193, 1.568, 1.369, 1.293, 1.158])
    *0.75/BSA_calc
175         else:
176             # Default to male normotensive responses
177             self.E_a_pop = np.array([2.32, 2.33, 2.40, 2.57, 3.15])/BSA_calc
178             self.C_ao_x_pop = 1./self.E_a_pop
179             self.E_max_x_pop = np.array([4.26, 5.66, 6.73, 8.12, 13.21])/BSA_calc
180             self.R_sys_x_pop = np.array([2.405, 1.667, 1.512, 1.431, 1.253])
    *0.75/BSA_calc
181
182     def set_intensity(self,intensity_function, data_type='hr',
183                       max_iy=1., min_iy=0., intensity_list=None,
184                       parameter_change_dict=None, additional_parameters=None):
185         """
186         Function that specifies the input intensity format
187             and fits the parameter scaling functions to the specified intensity
    format
188         It fits the built in or given population data to the intensity
189             to scale parameters with exercise intensity
190
191         intensity_function(intensity, max_intensity, min_intensity, **kwargs)
192             - a function that specifies the intensity given by
193               heart_rate, workload or other intensity measures.
194         Must take arguments intensity_input, max_intensity, and rest_intensity
    and
195         optional keyword arguments or a dictionary of other function arguments.
196         Fits parameter data to intensity and stores parameter
197         scaling functions in the model object
198         """
199
200         if data_type == 'hr':
201
202             intensity_input = np.array(self.HR_pop.copy())
203             intensity_max = self.HR_max_pop
204             intensity_rest = self.HR_rest_pop
205
206             intensity_formatted = intensity_function(intensity_input,
    intensity_max, intensity_rest, **(additional_parameters if
    additional_parameters is not None else {}))
```

```
207             pers_rest_intensity = intensity_function(60./self.T_ux, 60./self.
    T_max, 60./self.T_ux, **(additional_parameters if additional_parameters is not
     None else {}))
208 
209             # Fit R_sys
210             optparsR,_ = curve_fit(exp_func,intensity_formatted,self.R_sys_x_pop,
    bounds=(0, [10000.0, 10000.0, 100.0, 1.5]))
211             dummy_func = lambda iy: optparsR[0]*np.exp(-1/optparsR[1]*(iy-
    optparsR[2])) + optparsR[3]
212             restR = dummy_func(pers_rest_intensity)
213             prpR = self.R_sys_ux
214             self.R_sys_func = lambda_setter_exp(optparsR, restR, prpR)
215 
216             # Fit C_ao
217             optparsC,_ = curve_fit(poly_func,intensity_formatted,self.C_ao_x_pop)
218             dummy_func = lambda iy: optparsC[0]*(iy**2) + optparsC[1]*iy +
    optparsC[2]
219             restC = dummy_func(pers_rest_intensity)
220             prpC = self.C_ao_ux
221             self.C_ao_func = lambda_setter(optparsC, restC, prpC)
222 
223             # Fit E_max
224             optparsE,_ = curve_fit(poly_func,intensity_formatted,self.E_max_x_pop
    )
225             dummy_func = lambda iy: optparsE[0]*(iy**2) + optparsE[1]*iy +
    optparsE[2]
226             restE = dummy_func(pers_rest_intensity)
227             prpE = self.E_max_ux
228             self.E_max_func = lambda_setter(optparsE, restE, prpE)
229 
230         else:
231             raise TypeError("Wrong intensity type entered")
232         return 0
233 
234     def exercise_shift_hr(self,hr,intensity_function,additional_arguments=None):
235         """
236         Takes an intensity as heartrate and the intensity function,
237         translating this to intensity and shifts E_max,R_sys,C_ao and T
238         """
239         #Compute intensity
240         HR_max_pers = 60./self.T_max
```

```
241         HR_rest_pers = 60./self.T_ux
242         intensity_level = intensity_function(hr,HR_max_pers,HR_rest_pers,**(
    additional_arguments if additional_arguments is not None else {}))
243 
244         #Set new HR and set new parameter values
245         self.T = 60./hr
246 
247         self.E_max = self.E_max_func(intensity_level)
248         self.C_ao = self.C_ao_func(intensity_level)
249         self.R_sys = self.R_sys_func(intensity_level)
250         self.par_dict["T"] = self.T
251         self.par_dict["E_max"] = self.E_max
252         self.par_dict["C_ao"] = self.C_ao
253         self.par_dict["R_sys"] = self.R_sys
254 
255         ##################################################
256         # Lusitropy mechanism - Added by Straatman, 2021
257         self.t_peak = self.t_peak_func(60/self.T)
258         self.par_dict["t_peak"] = self.t_peak
259         ##################################################
260 
261     def reset_exercise_shift(self):
262         self.E_max = self.E_max_ux
263         self.T = self.T_ux
264         self.C_ao = self.C_ao_ux
265         self.R_sys = self.R_sys_ux
266         self.par_dict["T"] = self.T_ux
267         self.par_dict["E_max"] = self.E_max_ux
268         self.par_dict["C_ao"] = self.C_ao_ux
269         self.par_dict["R_sys"] = self.R_sys_ux
270 
271     def reset_exercise_shift_all_pars(self):
272         pars = ['E_max', 'E_min', 'V_tot', 'C_ao', 'C_sv', 'R_sys', 'R_mv', 'Z_ao
    ', 't_peak', 'T']
273         for p in pars:
274             p_ux = getattr(self, p+'_ux')
275             setattr(self, p, p_ux)
276             self.par_dict[p] = p_ux
277 
278     def elastance(self, tau):
279         return self.elastance_fcn(self, tau)
```

```
280
281     def set_pars(self, **kwargs):
282         for key, val in kwargs.items():
283             if hasattr(self, key):
284                 self.__setattr__(key, val)
285                 self.__setattr__(key+"_ux", val)
286                 self.par_dict[key] = val
287                 self.par_dict[key+'_ux'] = val
288             else:
289                 print("Warning: object has no attribute %s" % key)
290
291     def set_subject(self, **subjectkwargs):
292         for key, val in subjectkwargs.items():
293             if hasattr(self, key):
294                 self.__setattr__(key, val)
295             else:
296                 print("Warning: object has no attribute %s" % key)
297
298     def calc_consistent_initial_values(self, V_lv_0=100, P_ao_0=100):
299         V_ao_0 = self.C_ao*P_ao_0
300         P_sv_0 = (self.V_tot - V_lv_0 - V_ao_0)/self.C_sv
301         u0 = (V_lv_0, P_ao_0, P_sv_0)
302         return u0
303
304     def rhs(self, t, u):
305         """
306         Right hand side of the ODE system.
307         """
308         V_lv = u[0]
309         P_ao = u[1]
310         P_sv = u[2]
311         tau = np.mod(t, self.T)
312         e_t = self.elastance(tau)
313         E = (self.E_max-self.E_min)*e_t + self.E_min
314         P_lv = E * V_lv + self.pleural_pressure_func(t)
315         Q_lvao = (P_lv > P_ao)*(P_lv - P_ao)/self.Z_ao
316         Q_aosv = (P_ao - P_sv)/self.R_sys
317         Q_svlv = (P_sv > P_lv)*(P_sv - P_lv)/self.R_mv
318
319         der_V_lv = Q_svlv - Q_lvao
320         der_P_ao = (Q_lvao - Q_aosv)/self.C_ao
```

```
321         der_P_sv = (Q_aosv - Q_svlv)/self.C_sv
322         der_u = [der_V_lv, der_P_ao, der_P_sv]
323 
324         return der_u
325 
326     def calc_all(self, t, u):
327         """
328         Calculate all model outputs based on the ODE solutions,
329         and remaning system relations.
330         """
331         V_lv = u[0]
332         P_ao = u[1]
333         P_sv = u[2]
334         tau = np.mod(t, self.T)
335         e_t = self.elastance(tau)
336         E = (self.E_max-self.E_min)*e_t + self.E_min
337         P_lv = E * V_lv + self.pleural_pressure_func(t)
338         Q_lvao = (P_lv - P_ao)/self.Z_ao * (P_lv > P_ao)
339         Q_aosv = (P_ao-P_sv)/self.R_sys
340         Q_svlv = (P_sv - P_lv)/self.R_mv * (P_sv > P_lv)
341         P_meas = np.maximum(P_lv, P_ao)
342         P_ao = P_meas
343         P_sys = np.max(P_ao)
344         P_dia = np.min(P_ao)
345         PP = P_sys - P_dia
346         V_sys = np.min(V_lv)
347         V_dia = np.max(V_lv)
348         SV = V_dia - V_sys
349 
350         all_vars = locals()
351         del all_vars["self"]
352         del all_vars["u"]
353 
354         der_V_lv = Q_svlv - Q_lvao
355         der_P_ao = (Q_lvao - Q_aosv)/self.C_ao
356         der_P_vc = (Q_aosv - Q_svlv)/self.C_sv
357         der_u = [der_V_lv, der_P_ao, der_P_vc]
358 
359         return der_u, all_vars
360     ########################################
361     #### END OF CLASS VaryingElastance ####
```

```
    ########################################

def solve_to_steady_state(model, t_eval=None, n_cycles=5, n_eval_pts=100):
    """
    Numerically solve the model ODEs over a number of cycles,
    until steady state is reached.
    """
    u0 = model.calc_consistent_initial_values()
    t_span = (0, model.T*n_cycles)
    if t_eval is None:
        t_eval = model.T*np.linspace(n_cycles-1, n_cycles, n_eval_pts)
    else:
        t_eval = t_eval + model.T*(n_cycles-1)

    sol = scipy.integrate.solve_ivp(model.rhs, t_span, u0, dense_output=True,
   method="RK45",
            atol=1e-10, rtol=1e-9)
    u_eval = sol.sol(t_eval)
    _, all_vars = model.calc_all(t_eval, u_eval)
    return all_vars, t_eval, sol

def calc_summary(var_dict):
    P_ao = np.maximum(var_dict["P_ao"], var_dict["P_lv"])
    P_sys = np.max(P_ao)
    P_dia = np.min(P_ao)
    P_map = np.mean(P_ao)
    Q_max = np.max(var_dict["Q_lvao"])
    PP = P_sys - P_dia
    V_sys = np.min(var_dict["V_lv"])
    V_dia = np.max(var_dict["V_lv"])
    MVP = np.mean(var_dict["P_sv"]) #Anne
    SV = V_dia - V_sys
    CO = ml_per_sec_to_L_per_min*SV/(var_dict["t"][-1] - var_dict["t"][0])
    ret_dict = locals()
    del ret_dict["var_dict"]
    del ret_dict["P_ao"]
    ret_dict["V_sys"]
    ret_dict["V_dia"]
    return ret_dict
```

A.3.2 Numerical Optimization with the Cost Function

Implementation of the cost function stated in Equation (3.5) and how it is used in a least-squares optimization procedure, partly developed in [4]. Note that the entire estimation procedure is not included, as it is very extensive, and presentation of its details are not considered essential for the purpose of this work. The code is originally written by Dr. Jacob Sturdy and Ph.D. Candidate Nikolai L. Bjørdalsbakke through a collaboration in the MyMDT project. An outline of the content, highlighting the additions developed in this project, is found inline in the following code extract.

Listing A.2: Cost Function

```
import numpy as np
import scipy.optimize as opt
import model as models

"""
Extraction from the code used in the parameter estimation procedure.
Primarly written by Sturdy and Bjordalsbakke through collaboration
    in the MyMDT Project.

Adjustments and additions developed as a part of the master's project
included and highlighted explicitly throughout the code.
Includes:
28 : closed-loop parameters.
      model parameters initialized. Fixed parameters must update this dictionary.
40 : Function to shift model waves to upstroke.
        Developed by Nikolai L. Bjordalsbakke and Anne Aal, 2022.
64 : Cost function.
        Addition to regulate EF developed in this project included in this code.
160 : Run optimization.
        Fit paramters to data.
196 : Outline of the script that executes the parameter estimation procedure.
        Illustrates how fixed vs. estimated parameters are defined,
        and how constraints are included vs. ignored.
"""

# Initializaton of parameters.
# All parameters updated through the procedure with the exception of R_mv and
   E_min.
closed_loop_base_pars ={'C_ao': 1.13,
                        'E_max': 1.5,
```

```
                        'E_min': 0.035,
                        'R_mv': 0.006,
                        'R_sys': 1.11,
                        'T': 0.85,
                        'Z_ao': 0.033,
                        't_peak': 0.32,
                        'C_sv': 11.0,
                        'V_tot': 300
                       }

def shift_minimum(p,q,t):
    """
    Shift the model waves of pressure (p) and flow (q) to start at upstroke.
    Developed by Nikolai L. Bjordalsbakke and Anne Aal
    """
    min_ind = np.argmin(p)
    t_base = t[0]
    t=t-t[0]
    if (t[min_ind] < 0.65*t[-1]):
        p_temp = p.copy()
        q_temp = q.copy()
        p_slope = p[:min_ind]
        p_temp[len(p)-min_ind:] = np.append(p_slope[1:], p[min_ind])
        p_temp[:len(p)-min_ind] = p[min_ind:]

        p = p_temp.copy()
        q_temp[len(q)-min_ind:] = q[:min_ind]
        q_temp[:len(q)-min_ind] = q[min_ind:]
        q = q_temp.copy()

        return p, q, t+t_base
    else:
        return p, q, t+t_base

def data_cost_function(pars, measurements=dict(P_sys=120, P_dia=80), active_pars=
    None, ret_all=False,
                base_pars=dict(closed_loop_base_pars)):
    """
    The data cost function J.
    Originally written by Sturdy and Bjordalsbakke.
    Additions from the current project are stated in the following code.
```

```
    """
    measurement_scales = dict(P_sys=120,
                              P_dia=80,
                              P_meas=100,
                              P_ao=100,
                              Q_lvao=500,
                              Q_aosv=500,
                              Q_svlv=300,
                              SV=100,
                              PP=40,
                              V_lv=100,
                              MVP=5.)

    it_base_pars = dict(base_pars)
    for idx, name in enumerate(active_pars):
        try: #LMFIT
            it_base_pars[name] = pars[name]
        except: #SCIPY
            it_base_pars[name] = pars[idx]

    ve_closed = models.VaryingElastance()
    ve_closed.set_pars(**it_base_pars)
    var_dict, t_eval,_ = models.solve_to_steady_state(ve_closed,n_cycles=10,
                                                      n_eval_pts=len(
measurements["P_ao"]))
    ret_dict = models.calc_summary(var_dict)
    residual = []
    residual_short = []
    for name, val in measurements.items():

        if ((name in ret_dict) and (name == 'MVP')):
            residual_short.append((val - ret_dict[name])*(len(measurements["P_ao"
])/40.)*2.5/(measurement_scales[name]))
        elif ((name in ret_dict) and (ret_dict[name].size == 1)):
            residual_short.append((val - ret_dict[name])*(len(measurements["P_ao"
])/40.)*7.5/(measurement_scales[name]))
        else:
            ######################################################################
            # Shift the model pressure (p) and flow (q) to start at upstroke #
            # Developed by Nikolai L. Bjordalsbakke and
            # Anne Aal, motivated by the master's project ####################
```

```
            pn, qn, tn = shift_minimum(var_dict["P_ao"],
                                       var_dict["Q_lvao"], t_eval)
            ######################################################################
            if name == 'P_ao':
                try:
                    residual.append((val - pn)/measurement_scales[name])
                except KeyError:
                    print("Skipping pressure measurement")
            elif name == 'Q_lvao':
                try:
                    residual.append((val - qn)/measurement_scales[name])
                except KeyError:
                    print("Skipping flow measurement")
            else:
                try:
                    residual.append((val - ret_dict[name])/measurement_scales[
    name])
                except KeyError:
                    residual.append((val - var_dict[name])/measurement_scales[
    name])

     residual = np.array(residual).flatten()
     residual = np.append(residual, residual_short)

######################################################################
###### ADDITIONS FOR REGULATING EF ###################################
######  - DEVELOPED AND TESTED IN THE MASTER'S PROJECT###############
######################################################################

    EF_min = 0.35
    EF_max = 0.75
    EF = var_dict['SV']/var_dict['V_dia']

    # Hardmax version - Written by Anne Aal
    W_ef_hm = 10**6
    if EF > 0.75 or EF < 0.35:
       residual = residual*W_ef_hm

    # Softmax version - Written and tested by
    # Sturdy, Bjordalsbakke and Aal
    alpha = 100.
```

```
147     W_ef_sm = 50
148     weight1 = 1./(1. + np.exp(alpha*(EF-EF_min)))
149     weight2 = 1./(1. + np.exp(alpha*(EF_max-EF)))
150     EF_term = (weight1 + weight2)*(1./EF+EF)*W_ef_sm
151     residual = np.append(residual, EF_term)
152 
153 ##################################################################
154 
155     if ret_all:
156         return residual, var_dict, t_eval, ret_dict
157     else:
158         return residual
159 
160 def run_realdata_measurements(active_params,x0,x_scale,writers,wflag,t_r,p_r,q_r,
    v_r,meas_dict,b_in,b_low):
161     """
162     Fit parameters to data. Written by Sturdy and Bjordalsbakke.
163     meas_dict- the name of measurments to fit against.
164     x0 - initial values
165     b_in and b_low - upper and lower constraints.
166         Examined in this project as both included and excluded.
167     """
168     measurements = meas_dict.copy()
169 
170     residual, var_dict, t_eval, ret_dict = data_cost_function(x0,
171                                                               active_pars=
    active_params,
172                                                               measurements=
    measurements, ret_all=True,
173                                                               base_pars=
    closed_loop_base_pars)
174 
175     resultsR = opt.least_squares(data_cost_function, x0,
176                                  xtol=2.3e-16,ftol=2.3e-16,gtol=2.3e-16,diff_step
    =1e-3,
177                                  bounds=(b_low,b_in),
178                                  kwargs=dict(active_pars=active_params,
    measurements=measurements,base_pars=closed_loop_base_pars))
179 
180     residual, var_dict, t_eval, ret_dict = data_cost_function(resultsR.x,
```

```
                                                                active_pars=
    active_params,
                                                                measurements=
    measurements, ret_all=True,
                                                                base_pars=
    closed_loop_base_pars)

     print("Estimated resting parameters")
     standard_dev_sq = np.sum(residual**2)/len(residual)
     print(active_params)
     estimated_pars = resultsR.x
     print("Measure of residual variance: ", standard_dev_sq)
     print(estimated_pars)

     estimated_pars = np.append(np.round(estimated_pars,4),standard_dev_sq)

     return resultsR.x, standard_dev_sq, residual
########## SCRIPT TO EXECUTE THE ESTIMATION PROCEDURE #################
if __name__ == '__main__':
    # Prefit for arterial parameters in three-element Windkessel model #
    active = ["C_ao", "R_sys", "Z_ao"]
    x0 = np.array([0.436*bsa, 0.91725/bsa, 0.033])
    x_scale = [2.0, 2.0, 0.01]
    b_temp_in = [2.256, 2.963, 1.]
    b_temp_low = [0.148, 0.917/bsa, 0.001]
    try:
        C_ao, R_sys, Z_ao = run_prefit(active, x0, x_scale,None,False,t_r,p_r,
                                       q_r,b_temp_in,b_temp_low)
    except:
        print("Prefit failed!")
        # Use data from Segers et al. if fit fails
        if(np.max(p_r) > 140):
            Z_ao = 0.035
        else:
            Z_ao = 0.033
        _,C_ao,Rpz = volume_initial_guess_estimator(q_r, p_r, t_r)
        R_sys = Rpz-Z_ao
    ######################### End prefit ###################################
    ###################### Update base pars ################################
    closed_loop_base_pars["C_ao"] = C_ao
    closed_loop_base_pars["Z_ao"] = Z_ao
```

```
    closed_loop_base_pars["R_sys"] = R_sys
    print(closed_loop_base_pars["T"])
    ########################################################################
    ############## ADD FIXED PARAMETERS ####################################
    ########################################################################
    # t_peak is fixed to the dicrotic notch in this case
    t_peak_estimate = t_peak_dicrotic(p_r, t_r)
    ########################################################################
    # Fixed parameters are added to closed_loop_base_pars
    closed_loop_base_pars["t_peak"]  = t_peak_estimate

    # Set which values to fit against (include in cost function)
    # p_r and q_r is synchronized input data for pressure and flow
    PPref = np.max(p_r) - np.min(p_r)
    Psys_ref = np.max(p_r)
    Pdia_ref = np.min(p_r)
    SVref = np.trapz(q_r,t_r)
    meas_dict = dict(P_ao=p_r,Q_lvao=q_r, SV=SVref, P_sys=Psys_ref, P_dia=
   Pdia_ref, MVP=6.)
    ############### Set the premises for the main optimization ############
    print("FIVE PARAMETER FITS-------")
    print("---------RESTING----------")
    # Add/remove parameters that are estimated/fixed
    active =         ["E_max", "C_ao", "R_sys", "V_tot", "C_sv"]
    # Intitial guess (x0_0). Resampled for each iteration
    x0_0 = np.array( [7.58/bsa, C_ao, R_sys, TBVS, 13.084])
    x_scale =        [2.0, 2.0, 2.0, 250., 10.0]
    # The constraints. No constraints in this case.
    b_in =           [np.inf, np.inf, np.inf, np.inf, np.inf] # Upper
    b_low = np.array([0, 0, 0, 0, 0]) # Lower

    # multi_sample runs the "run_real_data_measurements" first 30 times,
    # and then another 20 times.
    # Initial guess (x0) is randomly resampled for each iteration.
    multi_sample(active, x0_0, x_scale,None,False,t_r,p_r,q_r,v_r,
    b_in,b_low, meas_dict,30,part_id)
############### END ESTIMATION PROCEDURE ###################################
```

A.3.3 Data-Based Exercise Shifts

Extraction of the code developed during this project for the purpose of obtaining data-based implementations of exercise shifts. In the numerical experiments conducted, algorithms developed to shift R_{sys} and C_{ao} replace the Chantler-based shifts in A.3.1 by the class function `set_pars()` in the hemodynamic model prior to solving the ODEs. Algorithms developed for scaling model pressures and obtaining data-based lusitropy coefficients are also included. An outline of the content is found inline in the following code extract.

Listing A.3: Data-based exercise shifts

```
import matplotlib.pyplot as plt
import numpy as np
# Functions used to read data and extract estimated parameters:
import read_data
# The Hemodynamic Model:
import model
from model import VaryingElastance

"""
Extract from code developed and/or used in the master's project.
Written by Anne Oksnes Aal, 2022.
Includes:
40  : How outliers are removed by an IQR-method [37].
62  : Participant class.
        A class implemented to contain data and
        derived properties for a trial participant.
389 : A model wrapper.
        Code written to solve the hemodynamic model
        and extract quantities of interest.
461 : Tpeak and systolic period.
        Obtain regression values for LVET to use as b in lusitropy.
549 : Linear personal compliance shift (c).
        Obtain a personal linear shift of C_ao based on
        relative changes of SV/PP.
578 : A semi-linear average-based shift of C_ao (d, C2).
608 : Personal resistance scaling factor (R,c).
        Obtain a scaling factor to yield similar relative change
        between 0-150 W in Chantler shifts as trial data.
641 : General trial-based exponential resistance shift (d, R2).
        Use exponential regression on relative changes of MAP/CO
```

```
        in selected participants
674 : Shift Vtot during exercise
        A pilot experiment to shift Vtot in a
        linear manner during exercise
"""

#####################################################
########### INTERQUARTILE RANGE METHOD [37] ########
#####################################################
def removeOutliers(meas):
    """
    Method obtained from [38] (See Bibliography)
    Clean a dict for outliers belove/above 50% of first/fourth quartile.
    meas - dict of measurements (Psys, Pdia, HR, SV etc.)
    """
    cleanedMeas = dict()
    for param, vals in meas.items():
        df = pd.DataFrame.from_dict(meas[param])
        if df.empty:
            continue
        Q1, Q3 = df.quantile(0.25), df.quantile(0.75)
        IQR = Q3 - Q1
        df = df[~((df < (Q1 - 1.5 * IQR)) |(df > (Q3 + 1.5 * IQR))).any(axis=1)]
        list = df[0].tolist()
        cleanedMeas[param] = list
    return cleanedMeas

#####################################################
########### THE PARTICIPANT-CLASS ##################
#####################################################

class Participant():
    """"
    A class to contain relevant data and characteristics
    for a given trial participant.
    Id = participant identification number.
    data_case = 'Straatman', i.e., cardiovascular data pre-processed by
                Hilke Straatman during an internship at NTNU.
                Refers to the use of flow and heart rates
                obtained by Straatman.
              = 'Echopac', i.e., heart periods obtained from ECG,
```

```
72                and semi-automatic flow traces
73                from Echopac as flow during rest.
74    Radial systolic and diastolic pressures used for both data cases.
75    model = The MyMDT hemodynamic model
76    """
77    # Tonometry signal contained in a json-file loaded as CYCLE_DATABASE_FILE
78    CYCLE_DATABASE_FILE
79
80    def __init__(self, Id):
81
82        self.Id = Id
83        self.basis = read_data.getAllCharacteristicParams(self.Id) #
    Characteristics
84        self.sex = self.basis['sex']
85        self.BMI = self.basis['BMI']
86        self.SP = self.basis['SP']
87        self.DP = self.basis['DP']
88        self.age = self.basis['age']
89
90        ## STROKE VOLUME INDEX AND ESP-PREDICTIONS FROM CHANTLER ET AL. [30] ##
91
92        # Stroke Volume Index from Chantler et al. [30] during exercise
93        SVI_M = np.array([48.4, 58.3, 61.3, 61.7, 60.1])
94        SVI_F = np.array([47.9, 56.1, 59.0, 60.8, 60.0])
95
96        # End-Systolic Pressure (ESP) from Chantler et al. [30] during exercise
97        ESP_M = [137, 152, 164, 171, 200]
98        ESP_F = [134, 146, 162, 158, 173]
99
100       # Heart rates during exercise from Chantler et al. [30]
101       HR_M = [66, 89, 99, 109, 146]
102       HR_F = [70, 99, 114, 120, 148]
103
104       if self.sex == 'M':
105           self.SVI = SVI_M*self.BSA_calc
106           self.HR_sex_pop = HR_M
107           self.ESP = ESP_M
108       elif self.sex == 'F':
109           self.SVI = SVI_F*self.BSA_calc
110           self.HR_sex_pop = HR_F
111           self.ESP = ESP_F
```

```
112
113         ##########################################################################
114
115     def getTrest(self, T_rest_case = 'T_tonometry', out_data_case = 'Straatman'):
116         """
117         Get resting heart period obtained either as the average tonometry-period,
118                 or the 0W-period from sr or sup-position.
119         data_case = 'Straatman' or 'ECG'.
120                 Where the 0W-periods shall be obtained from.
121         """
122         if T_rest_case == 'T_tonometry':
123             avg_p,_,_ = self.getTonometryTimes()
124             return avg_p
125
126         elif T_rest_case == 'T_0W_sr':
127             pos = 'sr'
128         elif T_rest_case == 'T_0W_sup':
129             pos = 'sup'
130
131         if out_data_case == 'Straatman':
132             out_data = self.getHilkeOutputsData(0, pos)
133             if not out_data:
134                 raise Exception ('No outputs for Id %.0f, pos: %s' % (self.Id,
    pos))
135             periods = out_data['T']
136         elif out_data_case == 'ECG':
137             out_data = self.getCycleData(0, pos)
138             if not out_data:
139                 raise Exception ('No ECG for Id %.0f, pos: %s' % (self.Id, pos))
140             heart_rates = out_data['HR']
141             periods = []
142             for hr in heart_rates:
143                 periods.append(60/hr)
144
145         return np.nanmean(periods)
146
147     def get_all_0W_periods(self, T_rest_case = 'T_tonometry', out_data_case = '
    Hilke_data'):
148         """
149         Get resting heart period obtained either as the average tonometry-period,
150                 or the 0W-period from sr or sup-position.
```

```
151         data_case = 'Straatman' or 'ECG'.
152                 Where the 0W-periods shall be obtained from.
153         """
154         if T_rest_case == 'T_tonometry':
155             _,periods,_ = self.getTonometryTimes()
156             return periods
157 
158         elif T_rest_case == 'T_0W_sr':
159             pos = 'sr'
160         elif T_rest_case == 'T_0W_sup':
161             pos = 'sup'
162 
163         if out_data_case == 'Straatman':
164             out_data = self.getHilkeOutputsData(0, pos)
165             if not out_data:
166                 raise Exception ('No outputs for Id %.0f, pos: %s' % (self.Id,
    pos))
167             periods = out_data['T']
168         elif out_data_case == 'ECG':
169             out_data = self.getCycleData(0, pos)
170             if not out_data:
171                 raise Exception ('No outputs for Id %.0f, pos: %s' % (self.Id,
    pos))
172             heart_rates = out_data['HR']
173             periods = []
174             for hr in heart_rates:
175                 periods.append(60/hr)
176 
177         return (periods)
178 
179     def convertWattsToIntensity(self, intensity, pos = 'sr', T_rest_case = '
    T_tonometry',
180                                 out_data_case = 'Straatman'):
181         """
182         Takes a participant Id and an intensity in watts.
183         T_rest_case = 'T_tonometry', 'T_0W_sr' or 'T_0W_sup'
184         data_case = 'Straatman' or 'ECG'
185         Returns: The exercise heart rate and intensity
186                     as defined by the HRR-function
187         """
188         out_data = dict()
```

```
189         if out_data_case == 'Straatman':
190             out_data = self.getHilkeOutputsData(intensity, pos)
191             if out_data:
192                 periods = out_data['T']
193                 heart_rates = []
194                 for p in periods:
195                     heart_rates.append(60/p)
196 
197         elif out_data_case == 'ECG':
198             out_data = self.getCycleData(intensity, pos)
199             if out_data:
200                 heart_rates = out_data['HR']
201 
202         if not out_data:
203             return -1,-1
204 
205         HR_ex = np.nanmean(heart_rates)
206         HR_max = 220-self.age
207         T_rest = self.getTrest(T_rest_case, out_data_case = out_data_case)
208         HR_rest = 60/T_rest
209 
210         # The definition of heart-rate based intensity as found in the model
211         I = model.hrreserve_def(HR_ex, HR_max, HR_rest)
212         return HR_ex, I
213 
214     def getBPScalingFactors(self, pos):
215         """
216         Calculate epsilon_SP and epsilon_DP for a participant.
217         I.e., the difference in % between brachial pressures at
218                 resting state and radial pressures at 0 W.
219         """
220 
221         cycle_data = self.getCycleData(0, pos)
222         if not cycle_data:
223             print('No cycle data for this case')
224             return dict()
225 
226         SP_rad, DP_rad = (cycle_data['P_sys']), (cycle_data['P_dia'])
227         diff_SP, diff_DP = np.mean(SP_rad)-self.SP, np.mean(DP_rad)-self.DP
228 
229         eps_SP, eps_DP = diff_SP*100/self.SP, diff_DP*100/self.DP
```

```
230
231         return {'SP_eps': eps_SP, 'DP_eps': eps_DP, 'SP_diff': diff_SP, 'DP_diff'
    : diff_DP}
232
233     def getPersonalB(self, pos = 'sr'):
234         """
235         Linear regression on LVET periods to obtain
236         a personal lusitropy coefficient (b_pers)
237         """
238         HR = []
239         LVET_mean_vals = []
240         intensities = [0, 50, 100, 150]
241         for I in intensities:
242             HR_ex,_ = self.convertWattsToIntensity(I, pos = pos)
243             if HR_ex == -1:
244                 print('No exercise data exist for participant: ' + str(self.Id))
245                 return -1
246             HR.append(HR_ex)
247             out_data = self.getHilkeOutputsData(I)
248             if not out_data:
249                 print('No T_per-data available for participant: ' + str(self.Id))
250             LVET_per_Id = out_data['T_per']
251             LVET_mean_vals.append(np.mean(LVET_per_Id))
252
253         # Remove extreme outliers
254         i = 0
255         for val in LVET_mean_vals:
256             if val > 0.2 and HR[i] > 180:
257                 LVET_mean_vals.remove(val)
258                 HR.remove(HR[i])
259             i += 1
260
261         reglin = np.polyfit(HR, LVET_mean_vals, 1)
262
263         return reglin[0] #b_pers
264
265     def getTonometryTimes(self):
266         """
267         Read the tonometry-file to obtain the resting heart periods.
268         Note: Code based on dataprocessing by Bjordalsbakke.
269         """
```

```
        df = pd.read_json(self.CYCLE_DATABASE_FILE)
        pat_df = df[df['Surname'] == self.Id]
        pat_df = pat_df[pat_df['use_data']  == 'Y']
        avg_p = 0.
        sample_count = 0
        periods = []
        min_len = np.inf
        for idx, row in pat_df.iterrows():
            if row['use_data'] == 'Y':
                times = np.array(row['times'])
                times = times - times[0]
                period = times[-1]
                periods.append(period)
                if len(times) < min_len: min_len = len(times)
                avg_p += period
                sample_count += 1
        avg_p = avg_p/sample_count

        return avg_p, periods, min_len

    def getTonometryPressureWave(self):
        """
        Read the tonometry-file to obtain the average pressure-cycle
             from carotid measurement, scaled to brachial SP and DP
        Note: Code based on dataprocessing by Bjordalsbakke.
        """
        df = pd.read_json(self.CYCLE_DATABASE_FILE)
        pat_df = df[df['Surname'] == self.Id]
        pat_df = pat_df[pat_df['use_data']  == 'Y']
        avg_p,_,min_len = self.getTonometryTimes()

        sample_count = 0
        average_sample = np.zeros(min_len)
        new_time = np.linspace(0., 1., min_len)
        for idx, row in pat_df.iterrows():
            if row['use_data'] == 'Y':
                times = np.array(row['times'])
                times = times - times[0]
                times = times/times[-1]
                samples = np.array(row['samples'])
                new_samples = np.interp(new_time, times, samples)
```

```
                average_sample += new_samples
                sample_count += 1
        average_sample = average_sample/sample_count
        final_time = new_time*avg_p

        # Adjust pressure for SBP and DBP
        average_sample = average_sample - np.min(average_sample)
        average_sample = average_sample/np.max(average_sample)

        Psys_mean = pat_df["SP"].mean()
        Pdia_mean = pat_df["DP"].mean()

        average_sample = (Psys_mean-Pdia_mean)*average_sample + Pdia_mean

        ret = dict()
        ret['p'], ret['t'] = average_sample, final_time
        return ret

    def getPhysicalComplianceAtIntensity(self, intensity, pos = 'sr'):
        """
        Obtain the physical arterial compliance (C_a=SV/PP) at a given intensity.
        """
        hilke_outputs = self.getHilkeOutputsData(intensity, pos)
        if not hilke_outputs:
            print('No SV avaialble for participant: ' + str(self.Id))
            return -1
        SV = np.mean(hilke_outputs['SV'])
        P_sys, P_dia = hilke_outputs['P_sys'], hilke_outputs['P_dia']
        PP = np.mean(np.asarray(P_sys)-np.asarray(P_dia))
        return SV/PP

    def getPhysicalResistanceAtIntensity(self, intensity, pos = 'sr'):
        """
        Obtain the physical systemic resistance (R=MAP/CO) at a given intensity.
        """
        Straatman_outputs = self.getHilkeOutputsData(intensity, pos)
        if not Straatman_outputs:
            print('No SV avaialble for participant: ' + str(self.Id))
            return -1
        SV, P_map = np.mean(Straatman_outputs['SV']), np.mean(Straatman_outputs['
    P_map'])
```

```
351         T = np.mean(Straatman_outputs['T'])
352         HR = 60/T
353         CO = SV*HR/60
354         return P_map/CO
355 
356     def getSVatRest(self):
357         SV = 0
358         # The semi-manually obtained flow, processed by Hilke Straatman
359         if self.Id in support.all_Hilke_participants:
360             q_h = self.getCycleProcessingPickles(flow_case= 'StraatmanDataBased')
    ['q'][0]
361             t_h = self.getCycleProcessingPickles(flow_case= 'StraatmanDataBased')
    ['t'][0]
362             SV = np.trapz(q_h,t_h) # mL
363         # The EchoPac Flow data
364         elif self.Id in support.all_NewData_participants:
365             q_n = self.getCycleProcessingPickles(flow_case= 'StraatmanDataBased')
    ['q'][0]
366             t_n = self.getCycleProcessingPickles(flow_case= 'StraatmanDataBased')
    ['t'][0]
367             SV = np.trapz(q_n,t_n)
368         return SV
369 
370     def getPhysicalComplianceAtRest(self):
371         SV = self.getSVatRest()
372         PP = self.SP - self.DP
373         return SV/PP
374 
375     def getPhysicalResistanceAtRest(self):
376         P_map = np.mean(self.getTonometryPressureWave()['p'])
377         SV = self.getSVatRest()
378         HR = 60/self.getTrest('T_tonometry') # Beats per min
379         CO = SV*HR/60 #mL/min --> mL/s
380         R_sys = P_map/CO
381         return R_sys
382 
383 ############ END PARTICIPANT CLASS ###################
384 
385 ######################################################
386 ############ A MODEL WRAPPER #########################
387 ######################################################
```

```
388
389 def model_wrapper(Id, data_case, param_case, b_case,
390                 T_rest_case, state = 'ex', intensity_watts = 0):
391     """
392     A wrapper for the hemodynamic model used to solve
393             the model and obtain quantities of relevanse for this project.
394     state: 'rest' or 'ex'
395     data_case: 'Straatman' (The six participants processed by Straatman), or
396                 'EchoPach' (EchoPac-processed participants)
397     Parameter case: 'FixTpeak'(1), 'NoConstraintsFixTpeak'(2),
398                     'NoConstraintsFixTpeakBoundEF_HardMax'(3),
399                     'Fix Csv(4), 'NoConstraintsFixCsvBoundEF_HardMax'(5)
400     b_cases: 'b0', 'b_weissler', 'average_Tper_based_b',
401             'personal_Tper_based_b'
402     T_rest_case: 'T_tonometry', 'T_0W_sr', or 'T_0W_sup'
403
404     At 0-intensity: no exercise shifts are conducted
405     """
406
407     vewk3 = VaryingElastance()
408     participant = Participant(Id)
409
410     basis_params = read_data.getBasisParamsFromCharaceristics(Id)
411     if param_case == 'NoConstraintsFixTpeak':
412         input_params = read_data.getResParsMin(Id, data_case = data_case,
413                     param_case = 'NoConstraintsFixTpeak')
414     else:
415         input_params = read_data.getResParsMean(Id, data_case = data_case,
416                     param_case = param_case)
417
418     vewk3.set_pars(**basis_params)
419     vewk3.set_pars(**input_params)
420     vewk3.set_parameter_response(disease_state="Nor")
421
422     b_cases = {'b_weissler': -2.1/1000, 'average_Tper_based_b': -1.1/1000,
423             'b0':0, 'personal_Tper_based_b': participant.getPersonalB()}
424     b = b_cases[b_case]
425     vewk3.set_pars(**{'b':b})
426
427     if data_base_case == 'Straatman':
```

```
428         out_data_case = 'Straatman' # Use heart rates manually obtained by
    Straatman
429     else:
430         out_data_case = 'ECG' # Use ECG heart rates
431 
432     HR_ex,_ = participant.convertWattsToIntensity(intensity_watts, pos = 'sr',
433                 T_rest_case = T_rest_case, out_data_case = out_data_case)
434     if HR_ex == -1:
435         print('No heartrate data for participant no. ' + str(Id) )
436         return dict()
437 
438     if state == 'ex':
439         num_cycles = 40
440         if intensity_watts == 0: # Set heart rate, but do not perform exercies
    shift
441             vewk3.set_pars(**{'T': 60/HR_ex})
442 
443         elif intensity_watts > 0:   # Exercise state-> Perform exercise shift
444             vewk3.set_intensity(model.hrreserve_def, data_type='hr')
445             vewk3.exercise_shift_hr(HR_ex, model.hrreserve_def)
446     else:
447         num_cycles = 10
448 
449     # Solve model
450     all_vars,_,_= model.solve_to_steady_state(vewk3,n_cycles = num_cycles)
451     output_params = model.calc_summary(all_vars)
452     output_params['V_lv'] = all_vars['V_lv']
453     output_params['P_lv'] = all_vars['P_lv']
454 
455     return output_params
456 
457 ##########################################################
458 ############# AVERAGE LUSITROPY COEFFICIENT ###########
459 ##########################################################
460 
461 def TpeakAndSystolicPeriod(Ids, data_base_case, respar_case):
462     """
463     Plots the values of LVET from the data from Hilke Straatman
464     and obtain an average regression line (b_reg).
465     Presented in Sections 4.3.2 and 5.2.2.
466     """
```

```
    intensities = [0,50,100,150]
    colors = ['firebrick','gold' ,'forestgreen', 'cornflowerblue', 'coral', '
darkturquoise']
    markers = ['x', 'o', 's', '^', 'd', 'P']

    all_HR = []
    all_LVET = []
    avg_LVET_0, avg_HR_0, avg_HR_end = 0,0,0
    fig, ax = plt.subplots(figsize = (9,8), dpi = 300)
    out_data_case = 'Straatman'
    for Idx, Id in enumerate(Ids):
        participant = Participant(Id)

        HR, T_per,t_peak,local_I = [],[],[],[]

        for I in intensities:
            vewk3 = VaryingElastance()
            basis_params = read_data.getBasisParamsFromCharaceristics(Id)
            input_params = read_data.getResParsMean(Id, data_case=data_base_case,
                                param_case=respar_case)
            vewk3.set_pars(**basis_params)
            vewk3.set_pars(**input_params)
            vewk3.set_parameter_response(disease_state="Nor")

            HR_ex,_ = participant.convertWattsToIntensity(I, pos = 'sr',
                    T_rest_case='T_tonometry', out_data_case= out_data_case)
            if HR_ex > 180: continue
            HR.append(HR_ex)
            all_HR.append(HR_ex)
            local_I.append(I)
            if HR_ex == -1: print('No heartrate data for participant no. ' + str(
Id))

            if I > 0:
                vewk3.set_intensity(model.hrreserve_def, data_type='hr')
                vewk3.exercise_shift_hr(HR_ex, model.hrreserve_def)
            else:
                vewk3.set_pars(**{'T': 60/HR_ex})

            if out_data_case == 'Straatman':
                outputs = participant.getHilkeOutputsData(I, pos = 'sr')
```

```
            elif out_data_case == 'ECG':
                outputs = participant.getCycleData(I,pos = 'sr')

            T_per_Id = outputs['T_per']
            T_per.append(np.mean(T_per_Id))
            all_LVET.append(np.mean(T_per_Id))

            t_peak.append(vewk3.getShiftedParam('t_peak'))

        avg_LVET_0 += T_per[0]
        avg_HR_0 += HR[0]
        avg_HR_end += HR[-1]
        reglin = np.polyfit(HR, T_per, 1)
        lw_big = 5
        lw_small = 4
        ax.plot(HR, T_per, color = colors[Idx], marker = markers[Idx], linestyle = '',  markersize = 18, markeredgewidth = 3,
                label ='$b_\mathrm{pers}^{%s}$ = %.1f' % (str(support.random_participant_labels[Id]), (reglin[0]*1000)))

        ax.plot(HR, reglin[0]*np.asarray(HR) + reglin[1], linewidth = lw_small,
                    alpha = 0.75, linestyle = '-', color = colors[Idx])

    reglin = np.polyfit(all_HR, all_LVET, 1)
    # b_reg = reglin[0]
    avg_LVET_0 = avg_LVET_0/len(Ids)
    avg_HR_0 = avg_HR_0/len(Ids)
    avg_HR_end = avg_HR_end/len(Ids)

    ax.plot(all_HR, reglin[0]*np.asarray(all_HR) + reglin[1],
            label = '$b_\mathrm{reg}$ = %.1f ' % (reglin[0]*1000), linewidth = lw_big, color = 'k')
    ax.set_xticks([50,100,150])
    ax.set_xlim(45,180)
    ax.set_yticks([0.2,0.25,0.3])
    ax.set_xlabel('HR [bpm]')
    ax.set_ylabel('$T_\mathrm{sys}$ [s]')
    ax.set_ylabel('LVET [s]')
    ax.legend(bbox_to_anchor = (1.05,1), loc = 2, borderaxespad = 0.) # Savefig
    path = folder_path + 'TperRegression.png'
    fig.savefig(path, pad_inches = 0.2, bbox_inches = 'tight')
```

```
544
545 ################################################
546 ####### COMPLIANCE SHIFTS ######################
547 ################################################
548
549 def LinearPersonalCShifts(Id, HR_ev, resParCase):
550     """
551     Use trial data of SV and PP to obtain a
552         personal linear shift of arterial compliance.
553     Id = participant number.
554     HR_ev = instantaneos heart rate.
555     resParCase = resting parameter set.
556     Referred to as compliance shift 'c' in Section 4.3.3.
557     """
558     # A class for each participant Id
559     participant = Participant(Id)
560     # The input parameters obtained from the
561     input_params = read_data.getResParsMean(Id, data_case = 'Straatman',
562                         param_case = resParCase)
563     C_ao_rest = input_params['C_ao']
564     C_0W = participant.getPhysicalComplianceAtIntensity(0)
565     C_150W = participant.getPhysicalComplianceAtIntensity(150)
566     delta_phys_150W = (C_150W - C_0W)/C_0W
567     phys_based_shift_150W = (1+delta_phys_150W)*C_ao_rest
568     C = [C_ao_rest, phys_based_shift_150W]
569     HR_0W,_ = participant.convertWattsToIntensity(0, pos = 'sr',
570                             T_rest_case='T_tonometry')
571     HR_150W,_ = participant.convertWattsToIntensity(150, pos = 'sr',
572                         T_rest_case='T_tonometry')
573     HR = [HR_0W, HR_150W]
574     relation = np.polyfit(HR, C, 1)
575
576     return relation[0]*HR_ev + relation[1]
577
578 def linearAvgPhysBasedCShift(I_hrr, Ids):
579     """
580     Use trial data of SV and PP to obtain a personal linear
581          shift of arterial compliance
582     I_hrr = heart rate reserve-based exercise intensity
583     Ids = participant numbers to include
584     Referred to as compliance shift 'd' in Section 4.3.3.
```

```
    """
    delta_phys_150W = 0
    n = len(Ids)
    for Id in Ids:
        participant = Participant(Id)

        C_0W = participant.getPhysicalComplianceAtIntensity(0)
        C_150W = participant.getPhysicalComplianceAtIntensity(150)
        delta_phys_150W += (C_150W - C_0W)/C_0W*100

    delta_phys_150W = delta_phys_150W/n

    relation = np.polyfit([0, 0.6], [0, delta_phys_150W], 1)

    if I_hrr < 0.6:
        return relation[0]*I_hrr + relation[1]
    elif I_hrr>0.6:
        return delta_phys_150W

############################################################
################### RESISTANCE SHIFTS ######################
############################################################

def getPersonalChantlerScalingFacRestistance(Id, param_case):
    """
    Calculate a personal scaling factor to obtain the same relative change
         between rest and 150 W as yielded by the physiological data.
    Refferred to as resistance shift 'c' in Section 4.3.3.
    Returns: the scaling factor.
    """
    # An object from the model
    vewk = VaryingElastance()

    participant = Participant(Id)
    HR_150W,_ = participant.convertWattsToIntensity(150)
    input_params = read_data.getMeanOutputsRest(Id, data_case = 'Straatman',
                    param_case = param_case)
    basis_params = read_data.getBasisParamsFromCharaceristics(Id)
    vewk.set_pars(**basis_params)
    vewk.set_pars(**input_params)
    vewk.set_parameter_response('Nor')
```

```
    vewk.set_intensity(hrreserve_def, 'hr')
    vewk.exercise_shift_hr(HR_150W, hrreserve_def)

    R_sys_rest = vewk.R_sys_ux
    R_sys_chantler = vewk.R_sys
    R_phys_0 = participant.getPhysicalResistanceAtIntensity(0, pos = 'sr')
    R_phys_150 = participant.getPhysicalResistanceAtIntensity(150, pos = 'sr')
    delta_phys = (R_phys_150-R_phys_0)/R_phys_0

    R_sys_chantler_scaled_150 = delta_phys*R_sys_rest + R_sys_rest
    diff = (R_sys_chantler_scaled_150-R_sys_chantler)/R_sys_chantler

    scale_fac = 1+diff
    return scale_fac

def averageExponentialResistanceShift(Ids):
    """
    Use data of physical resistance for the participants who
    showed an exponential trend and return the fit; "popt".
    Referred to as resistance shift 'd' in Section 4.3.3.
    """
    intensities = [50, 100, 150]
    delta_phys_all, HR, I_hrr_all = [], [], []

    for Id in Ids:
        participant = Participant(Id)
        R_phys_0 = participant.getPhysicalResistanceAtIntensity(0, pos = 'sr')
        delta_phys_p, I_hrr_p = [], []
        for I in intensities:
            HR_ex, I_hrr = participant.convertWattsToIntensity(I, pos = 'sr',
                        T_rest_case = 'T_tonometry', out_data_case='Straatman')
            R_phys = participant.getPhysicalResistanceAtIntensity(I, pos = 'sr')
            delta_phys = (R_phys - R_phys_0)/R_phys_0*100
            if (I_hrr > 0.3 and delta_phys>-40): continue
            delta_phys_p.append(delta_phys)
            I_hrr_p.append(I_hrr)
            delta_phys_all.append(delta_phys)
            I_hrr_all.append(I_hrr)

    I_hrr_all.extend([0,0,0])
    delta_phys_all.extend([0,0,0])
```

```
    popt,_= curve_fit(expFunc, I_hrr_all, delta_phys_all)
    I_hrr_all.sort()

    return popt

######### Shift Vtot - A preliminary experiment #######

def shift_V_tot(Id, intensity_watts, resparCase):
    """
    Discussed in Section 6.4.2
    """
    participant = Participant(Id)
    # Resting parameters
    input_pars = rd.getResParsMean(Id, data_case='Straatman', param_case =
   resparCase)
    V_tot_res = input_pars['V_tot']
    maxShift = 0.5
    V_tot_max = (1+maxShift)*V_tot_res
    I = [0,1]
    V = [V_tot_res, V_tot_max]
    reglin = np.polyfit(I,V,1)
    HR_ex, I_hrr = participant.convertWattsToIntensity(intensity_watts, pos = 'sr
   ',
             T_rest_case='T_tonometry', out_data_case='Straatman')
    V_tot_shifted = reglin[1] + I_hrr*reglin[0]

    return V_tot_shifted
```

A.3.4 Literature-Based Comparisons

Code showing how model predictions of SV, P_{sys} and MVP are compared to literature in this project.

Listing A.4: Model Evaluation Support

```
import matplotlib.pyplot as plt
import numpy as np

"""
20 & 24 : Definitions of bias and mean absolute error (MAE)
32  : Development of C_a by Liang et al. [42]
38  : How stroke volume index (SVI) from Chantler et al. [30]
```

```
        is used as basis of comparison.
54  : How ESP from Chantler is used to calculate the deviations
        between data and an approximate prediction.
100 : How relative changes in central venous pressure (CVP)
        from Yoshiga et al. [43] is used as basis for comparison
        to MVP for the model.
"""

##############################################
##### ERROR CALCULATIONS #####################
##############################################

def bias(x_true, x_pred):
    dev = x_pred - x_true
    return dev

def mean_absolute_error(x_true, x_pred):
    dev = np.abs(x_pred-x_true)
    return dev

##############################################
##### RELATIVE COMPARISONS TO LITERATURE ####
##############################################

## Liang et al. [42] Development of arterial compliance
HR_Liang = [56, 80, 100]
HR_Liang = np.asarray(HR_Liang) - HR_Liang[0]*np.ones(3) + HR[0]*np.ones(3)
C_Liang = [0.48, 0.33, 0.24]
delta_C_Liang = (np.asarray(C_Liang) - np.ones(len(C_Liang))*C_Liang[0])/C_Liang
    [0]*100

## STROKE VOLUME INDEX FROM CHANTLER ET AL. [30] ##

plt.figure()
participant = Participant(Id)
SV_chantler = participant.SVI
HR_pop_chantler = participant.HR_sex_pop
SV_0 = SV_data[0] # SV at 0W
diff = SV_chantler[0] - SV_0
as_SVI = SV_chantler - diff*np.ones(len(SV_chantler))
```

```
x_ax_SVI = HR_pop_chantler-HR_pop_chantler[0]*np.ones(len(HR_pop_chantler)) + HR[0]*np.ones(len(HR_pop_chantler))
as_SVI = np.ma.masked_where(((x_ax_SVI>HR[-1])), as_SVI)
plt.plot(x_ax_SVI, as_SVI, label = 'SVI Chantler', color = 'k', linewidth = 4 ,
        markersize = 15, markeredgewidth = 2.5, linestyle = 'solid', marker = 'p')

#### ESP-PREDICTIONS FROM CHANTLER ET AL.[30] ####

def devChantlerESP():
    """
    Calculate average and individal deviation between
        scaled Chantler-based ESP predictions and radial pressures
    Remaining errors (MAE) are calculated similarly.
    """
    pos = 'sr'
    intensities = [0, 50, 100, 150]
    metrics = dict()
    metric_func = mean_absolute_error

    for idx, I in enumerate(intensities):
        metrics[I] = []
        for Id in Ids:
            participant = Participant(Id)

            cycle_data = participant.getCycleData(I, pos = pos)
            if not cycle_data:
                metrics[I].append(np.nan)
                continue
            param_data = cycle_data['P_sys']

            ESP_chantler = participant.ESP
            epsilon = participant.getBPScalingFactors(pos = pos)
            eps = epsilon['SP_eps']
            ESP_chantler_val = ESP_chantler[idx]*(eps/100+1)
            error = metric_func(np.mean(param_data), ESP_chantler_val)
            metrics[I].append(error)

    metrics['Participant'] = Ids
    df = pd.DataFrame.from_dict(metrics)
    df.set_index('Participant', inplace=True)
```

```
    df.loc['mean_i'] = df.mean()

    df_copy_1 = df
    df_copy_2 = df

    df['mean_p'] = df.mean(numeric_only=True, axis=1)
    df_copy_1.loc['stdev_i'] = df_copy_1.std(numeric_only=True, axis=0)
    df.loc['stdev_i'] = df_copy_1.loc['stdev_i'].tolist()

    df_copy_2['stdev_p'] = df_copy_2.std(numeric_only=True, axis=1)
    df['stdev_p'] = df_copy_2['stdev_p'].tolist()

    return df

########### MVP FROM YOSHIGA ET AL. [43] ###########

plt.figure()
HR_CVP = [79, 115, 138, 159]
CVP = [1.8, 2.7, 3.1, 3.8]
delta_CVP = (np.asarray(CVP) - np.ones(len(CVP))*CVP[0])/CVP[0]
MVP_0 = 6
MVP_row = delta_CVP*MVP_0 + np.ones(len(CVP))*MVP_0
x_ax_CVP = np.asarray(HR_CVP)-HR_CVP[0]*np.ones(len(HR_CVP)) + HR[0]*np.ones(len(
    HR_CVP))
as_MVP_row = np.ma.masked_where(((x_ax_CVP>HR[-1])), MVP_row)
plt.plot(x_ax_CVP, as_MVP_row, label = 'Yoshiga et al.', marker = 'p', linewidth
    = lw,
         color = 'k', markersize = 15, markeredgewidth = 3.5, linestyle = 'solid')
```

Anne Øksnes Aal

Development and Validation of a Hemodynamic Model for Varying Exercise Intensity

NTNU
Kunnskap for en bedre verden